Phase behaviour in water/hydrocarbon mixtures involved in gas production systems

Antonin Chapoy

ECOLE DES MINES
DE PARIS

Collège doctoral

T H E S E

pour obtenir le grade de
Docteur de l'Ecole des Mines de Paris
Spécialité "Génie des Procédés"

présentée et soutenue publiquement par
Antonin CHAPOY

Le 26 Novembre 2004

**PHASE BEHAVIOUR IN WATER/HYDROCARBON MIXTURES
INVOLVED IN GAS PRODUCTION SYSTEMS**

**ETUDE DES EQUILIBRES DES SYSTEMES :
EAU-HYDROCARBURES-GAZ ACIDES DANS LE CADRE DE LA
PRODUCTION DE GAZ**

Directeur de thèse : Dominique RICHON

Jury :

M. Jürgen GMEHLING .... President
M. Jean-Michel HERRI .... Rapporteur
M. Gerhard LAUERMANN ....Examinateur
M. Francois MONTEL ....Examinateur
M. Dominique RICHON ....Examinateur
M. Bahman TOHIDI .... Rapporteur

A ma *Miss*tinguette,

Remerciements

Dans un premier temps, je voudrais exprimer ma sincère gratitude au Professeur Dominique Richon d'avoir été mon Directeur de Thèse durant ces trois années passées au sein du laboratoire TEP et qui m'a fait confiance pour réaliser ce travail.

Ich bin Herrn Jürgen Gmehling außerordentlich dankbar, den Vorsitz des Prüfungsausschusses für diese Dissertation angenommen zu haben.

Je remercie très sincèrement M. Jean-Michel Herri et M. Bahman Tohidi d'avoir accepté d'être rapporteurs de cette thèse et de participer au jury chargé de son examen.

Je tiens également à remercier M. Gerhard Lauermann et M. Francois Montel d'avoir eu la gentillesse de s'intéresser à ce travail et pour leur participation au jury d'examen.

Ce travail est, pour une grande partie un travail expérimental et il matérialise les efforts et la participation de toute l'équipe du laboratoire. Pour cela je tiens à remercier Alain Valtz, Albert Chareton et Pascal Théveneau pour leurs conseils sur le plan expérimental ainsi que David Marques et Hervé Legendre pour leurs aides techniques.

Sans aucun doute, les résultats de ce travail tiennent la marque d'une série de discussions très fructueuses avec l'ensemble des doctorants et post-doctorants. Je garderai également un très bon souvenir des différents membres du laboratoire que j'ai pu côtoyer au cours de ces trois années: Christophe, Fabien, Cathy, Jeannine, Armelle, Vania, Samira, Salim, Wael, Duc.

I also would like to thank Professor Bahman Tohidi from the Centre of Gas Hydrate, for welcoming me in his team. It has been very helpful time to discuss problems with him, during my stay at the Heriot Watt Petroleum Institute. A big thank you goes to his Ph. D. students, A. H. Mohammadi and Zahidah Md Zain for all the help they provided me during my stay, for

Table of Contents

List of Symbols

Abreviations

AAD	Average absolute deviation
AD	Absolute deviation
BIP	Binary interaction parameter
EG	Ethylene glycol
EOR	Enhanced oil recovery
FID	Flame ionization detector
FOB	Objective function
GC	Gas Chromatography
MC	Mathias-Copeman alpha function
MW	Micro wave
NDD	Non density dependent mixing rules
NIR	Near infrared
NRTL	Non random two liquids
PVT	Pressure – volume – temperature
PR - EoS	Peng Robinson equation of state
ppt	Part per trillion
ppm	Part per million
RK- EoS	Redlich and Kwong equation of state
RKS- EoS	Soave modification of Redlich and Kwong equation of state
ROLSI	Rapid online sampler injector
RTD	Resistance Thermometer Devices
TB	Trebble – Bishnoi alpha function
TCD	Thermal conductivity detector
TDLAS	Tunable diode laser absorption spectroscopy
UNIFAC	Universal quasi chemical
UNIQUAC	Universal quasi chemical model Functional activity coefficient model
VHE	Vapour – hydrate equilibrium
VLE	Vapour – liquid equilibrium
VLLE	Vapour – liquid – liquid equilibrium
VSE	Vapour – solid equilibrium
VPT – EoS	Valderrama modification of Patel-Teja equation of state

Latin letter

F	Parameter of the equation of state
G	Gas
H	Henry's constant [Pa]
L	Liquid
M	Number of components
N	Number of experimental points
P	Pressure [Pa]
Q	Quadruple point
R	Universal gas constant [J/(mol K)]
T	Temperature [K]

V	Volume [m^3]
a	Parameter of the equation of state (energy parameter) [Pa.m^6.mol^{-2}]
b	Parameter of the equation of state (co volume parameter) [m^3.mol^{-1}]
c	Parameter of the equation of state [m^3.mol^{-1}]
f	Fugacity
k	Binary interaction parameter for the classical mixing rules
k'	Boltzmann's constant [J/K]
l	Dimensionless constant for binary interaction parameter for the asymmetric term
n	number of moles [mol]
v	Molar volume [m^3/mol]
Z	Compressibility factor
x	Liquid mole fraction
y	Vapour mole fraction

Greek letters:

α_{ij}	NRTL model parameter
τ_{ij}	NRTL model binary interaction parameter [J/mol]
ω	Acentric factor
Δ	Deviation
Ψ	Power parameter in the VPT - EoS
Ω	Numerical constant in the EoS
α	Kihara hard-core radius [Å]
$\alpha(T_r)$	Temperature dependent function
ϕ	Fugacity coefficient
ω	Acentric factor
ε	Kihara energy parameter [J]
σ	Kihara collision diameter [Å]
ΔC_{pw}	Heat capacity difference between the empty hydrate lattice and liquid water [J.mol^{-1}.K^{-1}]
ΔC_{pw}°	Reference heat capacity difference between the empty hydrate lattice and liquid water at 273.15 K [J.mol^{-1}.K^{-1}]
Δh_w^0	Enthalpy difference between the empty hydrate lattice and ice at ice point and zero pressure [J.mol^{-1}]
Δv_w	Molar volume difference between the empty hydrate lattice and ice [m^3/mol]
$\Delta \mu_w^{\circ}$	Chemical potential difference between the empty hydrate lattice and ice at ice point and zero pressure [J.mol^{-1}]

Superscript

E	Excess property
GM	Gas Meter

L	Liquid state
Ref	reference property
V	Vapour state
Sat	Property at saturation
∞	Infinite dilution
A	Asymmetric property
C	Classical property
0	Non-temperature dependent term in NDD mixing rules
1	Temperature dependent term in NDD mixing rules

Subscripts

C	Critical property
cal	Calculated property
exp	Experimental property
i,j	Molecular species
∞	Infinite pressure reference state
T	Total
a	Index for properties
b	Index for properties
c	Critical property
c_*	Index for properties
cal	Calculated property
exp	Experimental property
i, j	Molecular species
p	Polar compound
r	Reduced property
w	Water
0	Reference property
1	First quadruple point
2	Second quadruple point

Introduction

Cette thèse présente des mesures de teneur en eau dans les phases vapeurs de différents hydrocarbures, méthane et éthane, et dans un mélange d'hydrocarbures gazeux (méthane 94%, éthane 4%, n-butane 2%) dans des conditions proches de la formation d'hydrates (de 258.15 à 313.15 K et jusqu'à 34.5 MPa). Des mesures de solubilités de gaz sont aussi tabulées.

Ce chapitre expose la technique expérimentale mise en œuvre pour déterminer ces propriétés, ainsi que les difficultés rencontrées lors de l'étude, notamment dues à l'analyse des traces d'eau.

Les résultats expérimentaux ont été modélisés en utilisant différentes approches pour la représentation des équilibres entre phases.

1. Introduction and Industrial Context

The worldwide demand for primary energy continues to rise. The energy resources of the earth may be classified into two categories, fossil fuels and geophysical energy. Fossil fuels (crude oil, natural gas and coal) currently provide 90 % of primary energy [1]. Crude oil is a finite resource but the question of how long reserves will last is difficult to answer. Based on current trends, half of the proven reserves of crude oil will be consumed by 2020. In 1994 30 % of crude oil reserves had been consumed compared to only 15 % of proven natural gas reserves [2]. At the end of 1999 the proven world gas reserves were estimated to be 146.43 trillion cubic meters, which corresponds to 131.79 thousand million tonnes oil-equivalent (mtoe) (Proven oil reserves at the end of 1999 are estimated to be 140.4 thousand million tonnes) [3]. By the end of 2001, the proven world gas reserves were estimated to be 153.08 trillion cubic meters, which corresponds to 137.8 thousand million tonnes oil-equivalent (mtoe) (Compared to 143 thousand million tonnes of oil reserves) [4]. By comparison, the reserves/production (R/P) ratio of the proven world reserves of gas is higher than oil's R/P ratio (Figure 1.1).
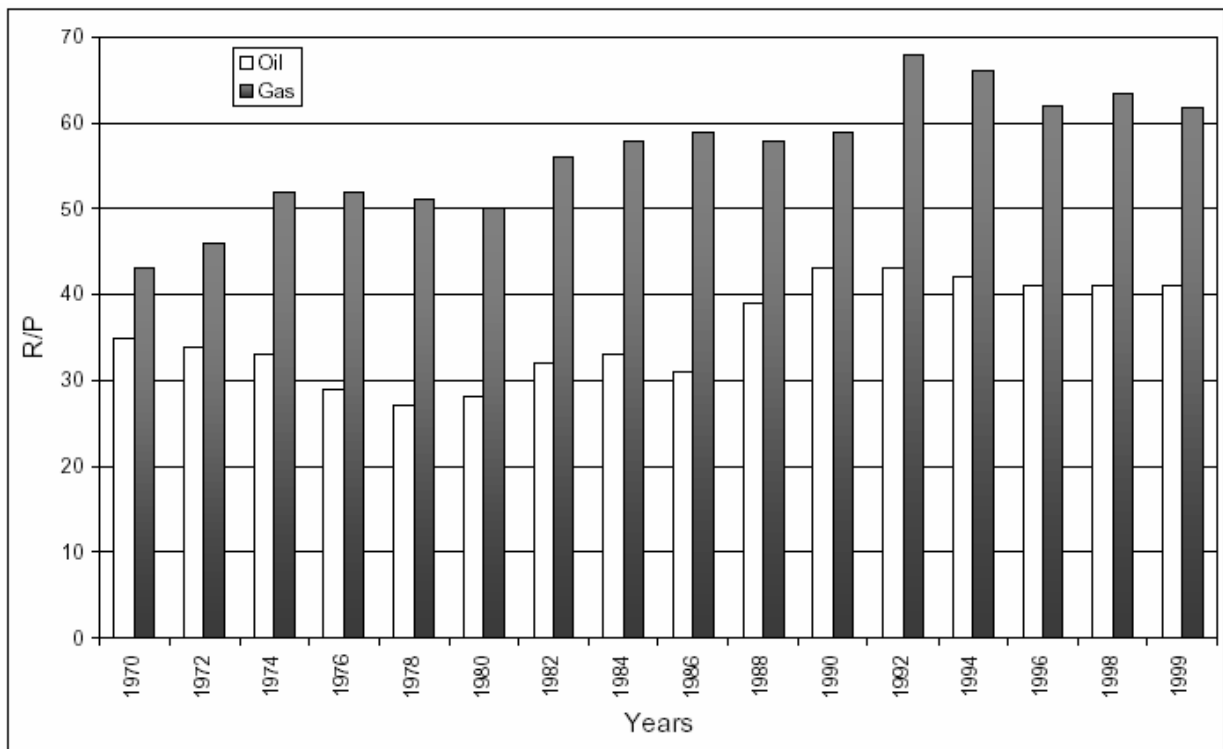
Figure 1.1: Gas and oil R/P ratios

Therefore, it is expected that in the decades to come natural gas will gain prominence among the world's energy resources. Moreover, it is expected that higher crude oil prices (Figures 1.2a and 1.2b) will stimulate exploration activities and permit exploitation of gas accumulations that are currently not commercially viable [4].
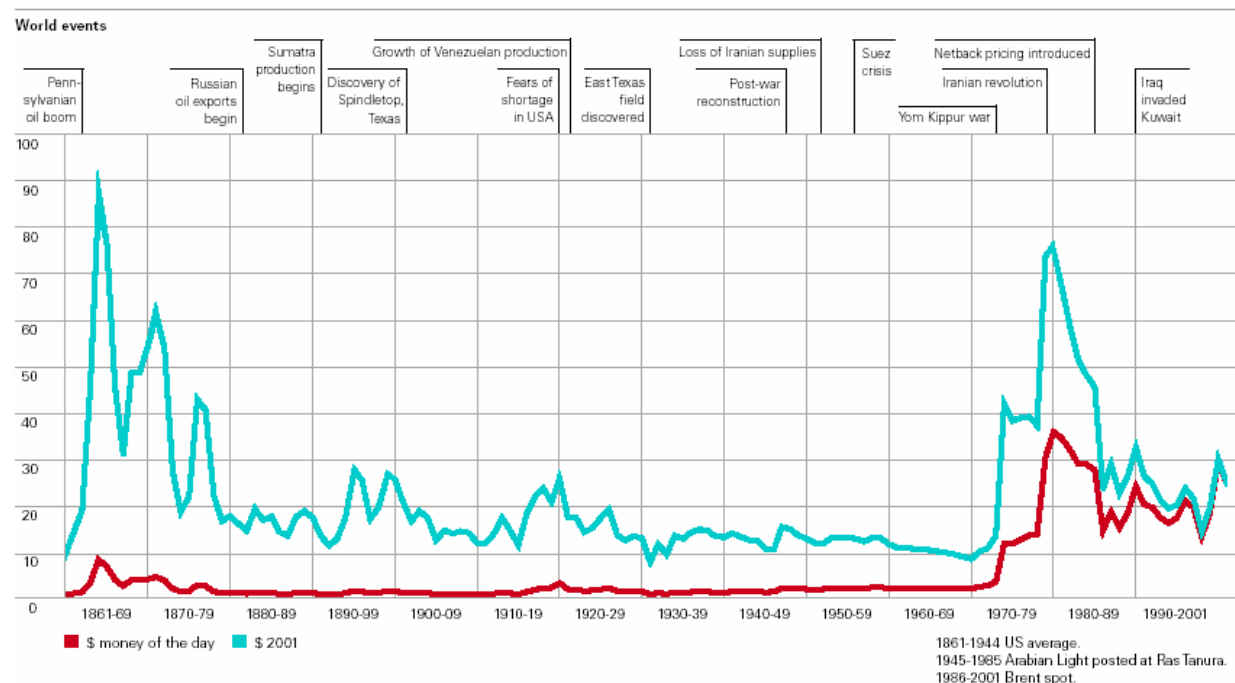
Figure 1.2a: Crude oil prices since 1861, US dollars per Barrel
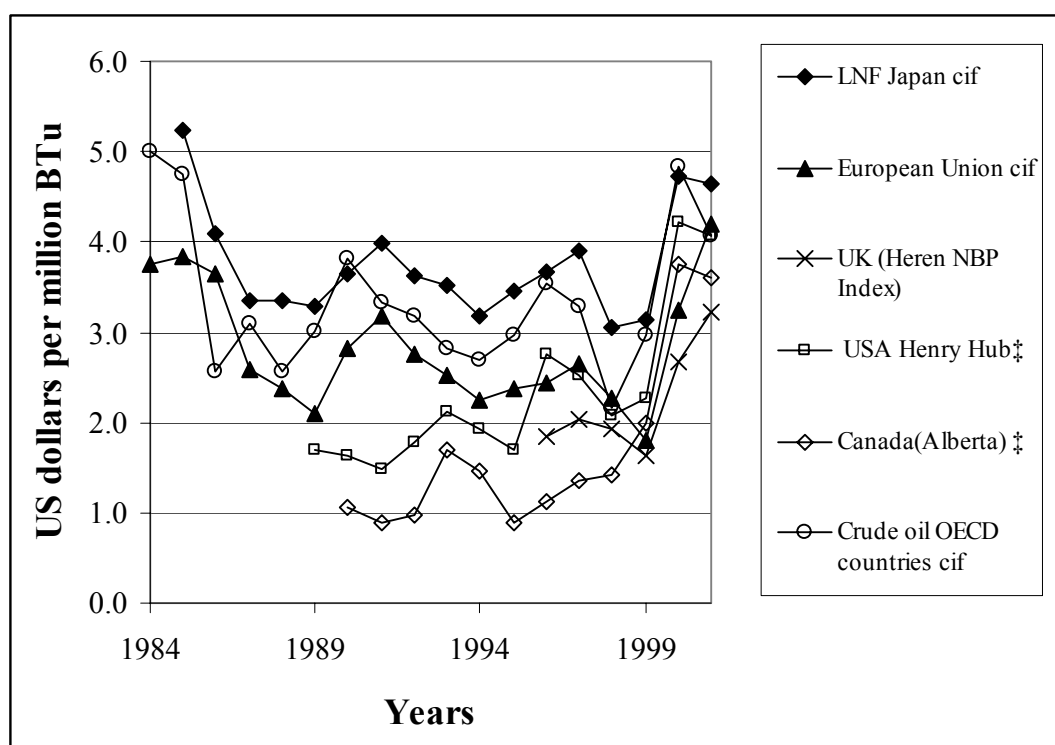
Figure 1.2b: Energy prices of oil and natural gases

Natural gas is rapidly growing in global importance both as a primary energy source and as a feedstock for downstream industry. Traditionally, natural gas production has been treated secondary in comparison with oil or as a by-product of the oil business. Nevertheless, natural gas consumption has constantly continued to increase from 50 % of oil consumption in 1950 to 98 % in 1998. This growth is being driven by a number of economic, ecologic and technological factors together with an overall increasing energy demand:

1. It is an abundant resource with an increasing reserve base.
2. It is environmentally cleaner than oil and coal.
3. Technology improvements in gas production, processing and transport.

Natural gas occurs in subsurface rock formations in association with oil (associated gas) or on its own (non-associated gas). It is estimated that 60 percent of natural gas reserves are non-associated. The main constituent of natural gas is methane with the remainder being made up of varying amounts of the higher hydrocarbon gases (ethane, propane, butane, etc.) and non-hydrocarbon gases such as carbon dioxide, nitrogen, hydrogen sulphide, helium, and argon. A typical composition of natural gas is given in TABLE 1.1:

Hydrocarbons		Non Hydrocarbons	
Component	Mole %	Component	Mole %
Methane	70 - 98	Nitrogen	trace - 15
Ethane	1 - 10	Carbon dioxide[*]	trace - 20
Propane	trace - 5	Hydrogen sulphide[*]	trace - 20
Butane	trace - 2	Helium	up to 5 (none usually)
Pentane	trace - 1		
Hexane	trace – 1/2		
Heptane and +	Trace		

TABLE 1.1 – COMPONENTS OF TYPICAL NATURAL GASES

*Natural gases can be found which are predominately carbon dioxide or hydrogen sulphides.

Inside reservoir, oil and natural gas normally coexist with water. This water comes from the sub adjacent aquifer. The presence of water causes problems during production (e.g. water drive and water coning) that lead to decreasing reservoir pressures. The presence of water also causes crystallisation of salts and formation of hydrates. Natural gas hydrates, also referred to as clathrates, are crystalline structures of water that surround low molecular weight gases such as methane, ethane, propane or butane.

Moreover, when gas is produced offshore, the separation of liquid fractions and the removal of water are not always carried out before the production flow is sent into pipelines.

Consequently, the unprocessed well gas streams coming from a production field can contain water and light hydrocarbon molecules (methane, ethane, propane etc.). Given the correct temperature and pressure conditions (particularly large temperature gradients), this can lead to hydrate formation during the transport through pipelines. The formation of gas hydrates in gas and oil sub-sea pipelines often results in their blockage and shutdown. However, gas hydrate formation may be controlled by adding a thermodynamic inhibitor such as methanol or ethylene glycol into the pipeline. The addition of such compounds changes (shifts) the condition required for gas hydrate formation to lower temperatures and (or) higher pressures. These problems can become more severe and more difficult to resolve in deeper wells.

Accurate knowledge of the thermodynamic properties of the water/hydrocarbon and water-inhibitor/hydrocarbon equilibrium near hydrate forming conditions, at sub-sea pipeline conditions and during transport is therefore crucial for the petroleum industry. These properties are essential throughout the natural gas production and transport process (Figure 1.3) to avoid hydrate formation and blockage, to optimise the process and the use of inhibitors.
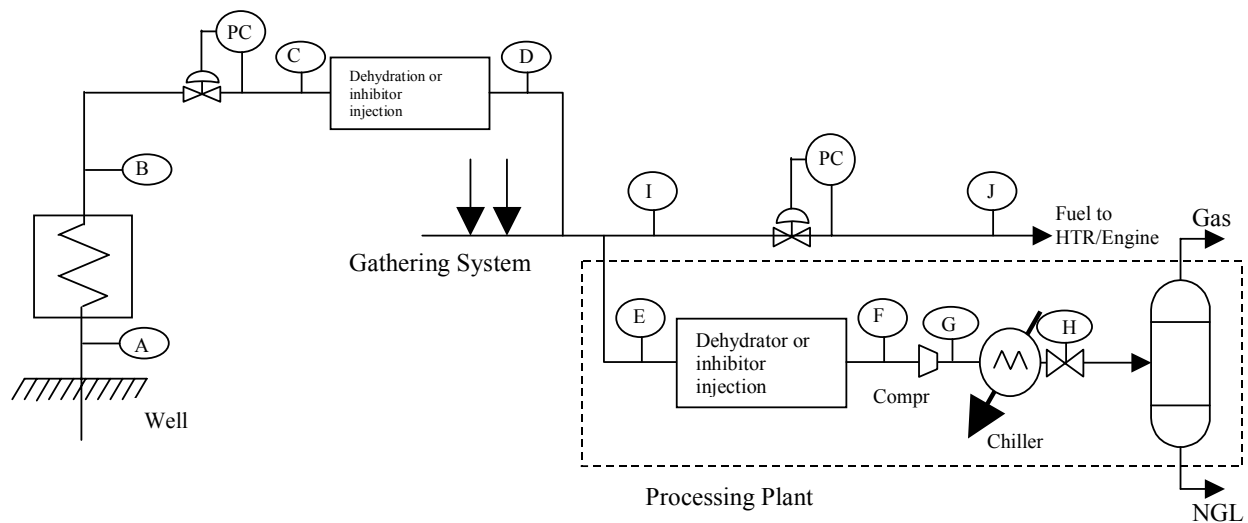
Figure 1.3: Typical gas production, gathering and processing plant (from *Sloan*, 1990 [5])

(The gas comes from the well at point A and may be heated before B. The pressure is regulated before C and depending on the conditions inhibitor may be injected before D and before the gas enters the gathering system. Gases from several wells may be gathered for economic reasons. Then the gas enters the processing plant and again there may be an injection of inhibitor depending on the temperature and pressure conditions (F). The gas is then compressed (G), cooled in a chiller (H) and used).

Unfortunately high-pressure data of water-hydrocarbon(s) systems at these conditions are scarce and rather dispersed. At low temperatures the water content of natural gas is very low and therefore difficult to measure accurately with trace analysis. Accurate water content

measurements require special attention. As natural gas is normally in contact with water in reservoirs. During production and transportation, dissolved water in the gas phase may form condensate, ice and / or gas hydrate. Forming a condensed water phase may lead to corrosion and / or to two-phase flow problems. Ice and / or gas hydrate formation may cause blockages during production and transportation. To give a qualified estimate of the amount of water in the gas phase, thermodynamic models are required. Therefore, accurate gas solubility data, especially near the hydrate-stability conditions, are necessary to develop and validate thermodynamic models.

Gas solubility in water is also an important issue from an environmental aspect due to new legislation on the restriction of hydrocarbon content in disposed water. Unfortunately, gas solubility data for most light hydrocarbons at low temperature conditions (in particular near the hydrate stability) are also scarce and dispersed. The main objective of this work is to provide the much needed solubility data at the above-mentioned conditions.

The aim of this work is to study the phase equilibrium in water – light hydrocarbons - acid gases – inhibitor systems by generating new experimental data at low temperatures and high pressures as well as extending a thermodynamic model. In this dissertation, a bibliographic review has been done on the phase behaviour of water-hydrocarbons systems and is reported in the second chapter. The water content and gas solubilities of similar systems have been gathered from the literature. In order to generate the outlined thermodynamic data, the commonly used methods for measuring water content / water dew point and gas solubility are reviewed in the third part.

An apparatus based on a static–analytic method combined with a dilutor apparatus to calibrate the gas chromatograph (*GC*) detectors with water was used to measure the water content of binary systems (i.e.: water –methane and ethane- water) as well of a synthetic hydrocarbon gas mixture (i.e.: 94% methane, 4% ethane and 2% *n*-butane). This same apparatus was also used to generate data of methane, ethane, propane, n-butane, carbon dioxide and nitrogen solubility data in water and also the solubilities of a synthetic mixture in water.

Additionally, a series of new data on the solubility of carbon dioxide in water has been generated over a wide temperature range. A technique based on measuring the bubble point pressure of known CO_2-water binary mixture at isothermal conditions, using through a

variable volume PVT cell, was used in this work. Solubility measurements of methane in three different aqueous solutions containing ethylene glycol (20, 40 and 60 wt.%) were also performed at low and ambient temperatures. The different corresponding isotherms presented herein were obtained using an apparatus based on a static-analytic method coupled with a gas meter.

Then, a thermodynamic model based on two different equations of state: the Peng-Robinson equation of state (*PR- EoS*) and the Valderrama modification of the Patel and Teja equation of state (*VPT - EoS*) associated with the classical mixing rules and the non density dependent (*NDD*) mixing rules, respectively was extended in order to predict phase behaviour of these systems.

In order to improve the calculation capabilities of the Peng - Robinson equation of state, the temperature dependency of the attractive parameter was assessed. Generalized alpha functions are preferably used because of their predictive ability and the reduction of the number of parameters. Three different alpha functions have been compared: a new proposed form, a generalized Trebble-Bishnoi (*TB*) and a generalized Mathias-Copeman (*MC*) alpha function for particular cases involving natural gas compounds, i.e.: light hydrocarbons (methane, ethane, propane, butane, pentane), water, carbon dioxide, nitrogen and hydrogen sulphide. The vapor pressures of 22 pure compounds were used to develop and generalize a new alpha function for the Peng-Robinson equation of state (*PR-EoS*).

Thermodynamic modelling of water content of different vapour phases: methane, ethane and the synthetic gas mixture in equilibrium with liquid water as well as gas hydrates has been investigated as well as gas solubilities in water at low temperature conditions. Finally, the prospect of using this model to predict phase equilibrium of acid gases – water systems has also been investigated.

Finally, the data generated along with existing data were used for development and validation of an empirical correlation for water-hydrocarbon phase behaviour in industrial applications. This correlation takes into account the gravity of the gas, the presence or not of acid gases and the salinity of the aqueous solution to predict the water content of the vapour in equilibrium with water in liquid or solid water.

Literature Survey

Dans ce chapitre, un résumé des propriétés remarquables de l'eau est exposé. De ces propriétés découlent le fait que l'eau permette la formation des hydrates de gaz.

Après avoir expliqué les propriétés et caractéristiques des hydrates de gaz, une revue des données disponibles dans la littérature concernant les propriétés d'équilibres entre phases des systèmes hydrocarbures – eau est présentée à savoir: les solubilités de gaz dans l'eau, les teneurs en eau des phases "vapeur" et les pressions de dissociation d'hydrates.

2. State of the Art, Bibliography Review

2.1. Properties and Characteristics of Water

It has been largely observed that water is not a regular solvent. Indeed the thermodynamic properties deviate from those of a regular solution and the water molecule has unusual properties. Many of these properties can be explained by the structure of the water molecule and the consequences coming from this structure. The structure of the water molecule leads to the possibility of hydrate formation.

Water is an unusual liquid [6-10]. At low enough temperatures and pressures, it expands when cooled, becomes less viscous when compressed and more compressible when cooled, and its already large isobaric heat capacity increases brusquely upon cooling. Some of the main unusual properties of water can be cited as below:

- High boiling point, melting point and critical point
- Low density of liquid phase
- Higher density of its liquid phase than of its solid phase
- High heat of fusion and heat of vaporization
- High specific heat
- High dielectric constant….

The first example of unusual properties of the water molecule is its density. The water density has a maximum value at 277.13 K (3.98°C) in the liquid state. Water is unusual in that it expands, and thus decreases in density, as it is cooled below 277.13 K (its temperature of maximum density). Another unusual property of water is that it expands upon freezing. When water freezes at 273.15 K, at atmospheric pressure, its volume increases by about 9%. This means that ice floats on water, i.e. the density of liquid water ($1000kg/m^3$) is greater than the density of ice ($917kg/m^3$) at the freezing point [10].
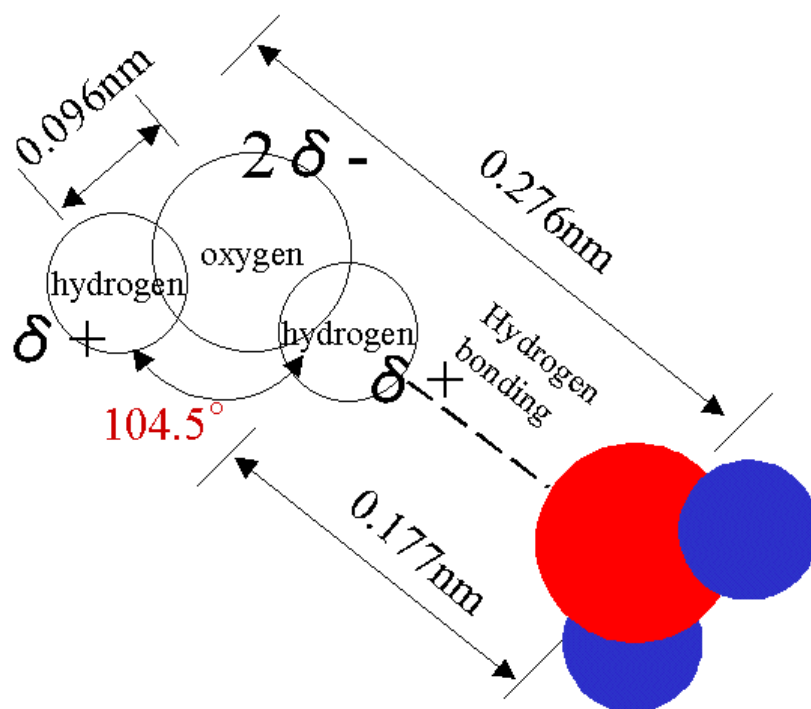
Figure 2.1: Shape of the water molecule (from http://www.lsbu.ac.uk/water)

Other examples of the unusual properties of water are its melting point, boiling point and critical point. Elements in the columns of the periodic table of elements have similar properties or at least properties that vary in a periodic, predictable manner. The 6A column in the table consists of oxygen, sulphur, selenium, and tellurium. It is expected that these elements and their compounds have similar properties, or at least to behave in a predictable pattern. The hydrogen compounds of the column 6A elements are water (hydrogen oxide), hydrogen sulphide, hydrogen selenide, and hydrogen telluride. All have the chemical formula H_2X, where X represents the group 6A element. If we look at their normal boiling points, it could be possible to predict the boiling point of water.

The melting point of water is over 100 K higher than expected by extrapolation of the melting points of other Group 6A hydrides, H_2S, H_2Se, and H_2Te, are shown compared with Group 4A hydrides in Figure 2.2.
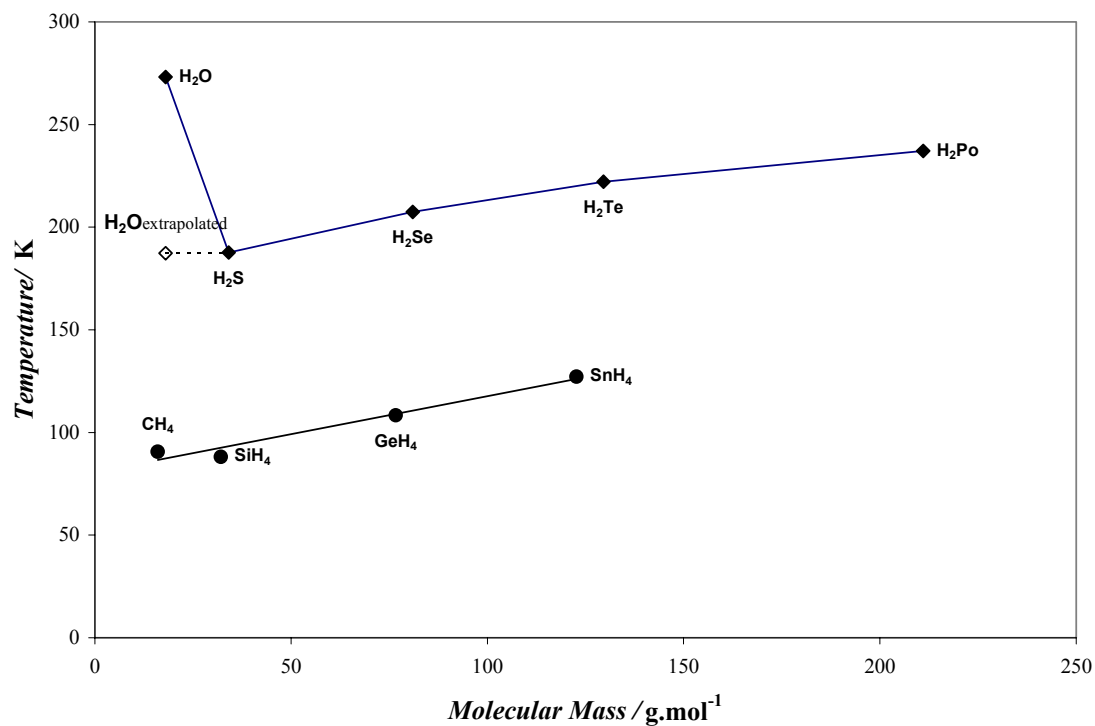
Figure 2.2: Melting points of the 6A and 4A hydrides

The boiling point of water is also unusually high (Figure 2.3). Although it is not exactly linear, the same linear approximation could be used to estimate the boiling point of water. This extrapolation yields an estimated boiling point of 195.15 K compared to 373.15 K.
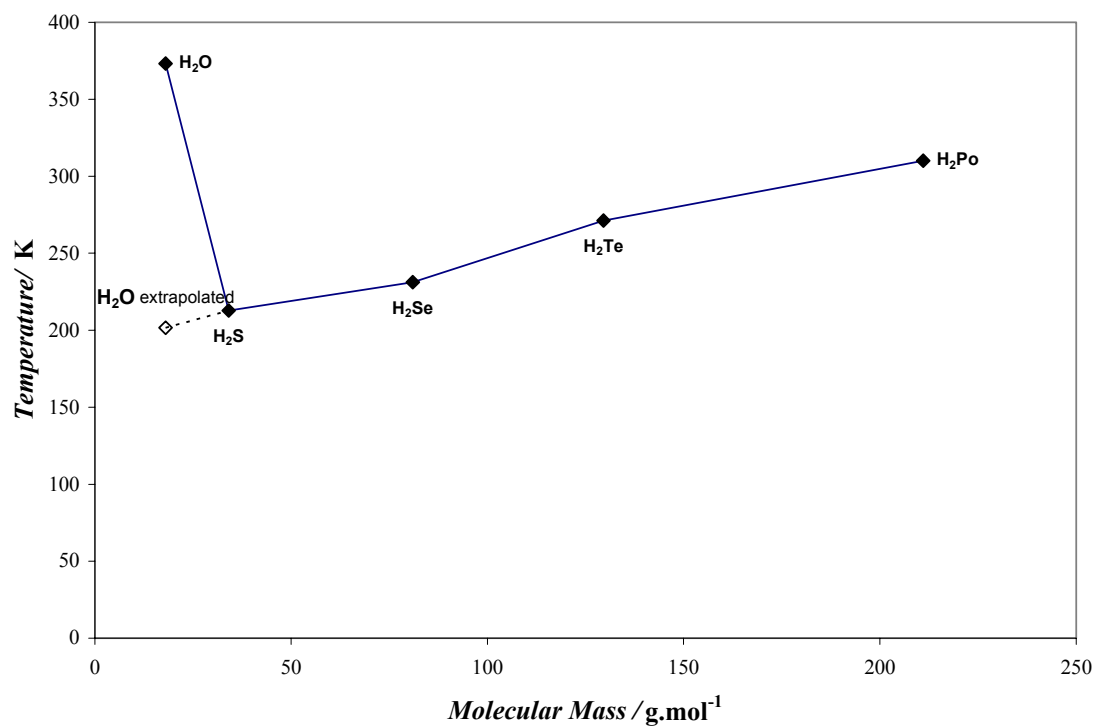
Figure 2.3: Boiling points of the 6A hydrides

Following the same assumptions, the critical point of water is over 250 K higher than expected by extrapolation of the critical points of other Group 6A hydrides (see Figure 2.4).
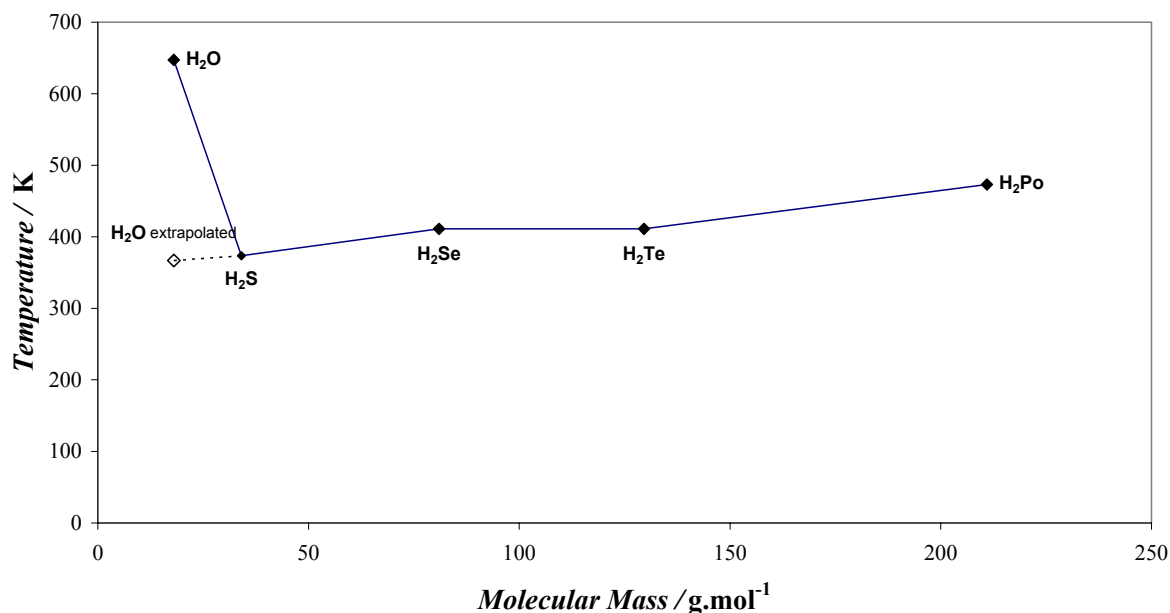
Figure 2.4: Critical points of the 6A hydrides

In TABLE 2.1, the enthalpies of vaporization are listed for several components at their boiling point. From this table including both polar and non-polar compounds, it can be noticed that water has a larger enthalpy of vaporization, even in comparison to other polar substances within the exception of ethylene glycol.

Compound	Nature	Enthalpy of Vaporization (kJ/mol)
Water	Polar	40.8
Methanol	Polar	35.3
Ethanol	Polar	38.6
Acetone	Polar	29.6
Ethylene Glycol	Polar	52.7
Hydrogen Sulphide	Polar	18.7
Methane	Non- polar	8.2
Ethane	Non- polar	14.7

TABLE 2.1 – ENTHALPIES OF VAPORIZATION OF VARIOUS COMPOUNDS AT THEIR BOILING POINT

To finish with the unusual properties of water, one of a more particular interest in the lighting of this dissertation, which can be outlined is that the solubilities of non-polar gases in water decrease with temperature to a minimum and then rise.

All of the unusual properties of water noted earlier can be explained by the shape of the water molecule and the interactions resulting from its shape. Water seems to be a very simple molecule, consisting of just two hydrogen atoms attached to an oxygen atom (Figure 2.1). In the water molecule, the bond between the oxygen and hydrogen atoms is a covalent bond. The two hydrogen atoms bound to one oxygen atom to form a 'V' shape with the hydrogen atoms at an angle around 104.5°. When the hydrogen atoms combine with oxygen, they each give away their single electron and form a covalent bond. And because electrons are more attracted to the positively charged oxygen atom, the two hydrogen atoms become slightly positively charged and the oxygen atom becomes negatively charged. This separation between negative and positive charges produces a polar molecule, and the hydrogen lobes now having a positive charge. The oxygen atom on the opposite side having two negative charges produces the 'V' shape of the molecule (because of the interaction between the covalent bond and the attracting/repulsion between the positive and negative charges). The electrostatic attraction between the positively charged hydrogen and the negatively charged lone pair electrons of oxygen lead to the possibility of hydrogen bonding and thus the water molecules will tend to align, with a hydrogen molecule lining up with an oxygen molecule. Because of the V shape, when the water molecules line up, they form a hexagonal pattern.

In ice, all water molecules participate in four hydrogen bonds (two as donor and two as acceptor). In liquid water, some hydrogen bonds must be broken to allow the molecules to move around. The large energy required for breaking these bonds must be supplied during the melting process and only a relatively minor amount of energy is reclaimed from the change in volume. The free energy change ($\Delta G = \Delta H - T\Delta S$) must be zero at the melting point. As temperature is increased, the amount of hydrogen bonding in liquid water decreases and its entropy increases. Melting will only occur when there is sufficient entropy change to provide the energy required for the bond breaking. As the entropy may be described as the degree of disorder in a system, the greater degree of disorder is associated with the greater entropy. In pure liquid water, the molecules are free to move about, but they are somewhat hindered (through ordering) by the intermolecular interactions, especially hydrogen bonding. The low entropy of liquid water (lower than in a regular liquid) causes this melting point to be high

(higher than the other 6A hydrides where the entropy change is greater and thus leading to lower melting point to allow the free energy to be zero).

In comparison with the other 6A hydrides there is considerable hydrogen bonding in liquid water, which prevents water molecules from being easily released from the water's surface. This reduces the vapour pressure. Boiling only occur when the vapour pressure equals the external pressure, therefore this occurs at a consequentially higher temperature than predicted by the extrapolation. The high heat of vaporization of water is also explained by the hydrogen bonding. Even at 373.15 K there is still strong hydrogen bonding in liquid water and thus requires a greater deal of energy to break it. For similar reason, the higher critical point can be explained: the critical point can only be reached when the interactions between the water molecules fall below a certain threshold level. Due to the strength of the hydrogen bonding, much energy is needed to cause this reduction in molecular interaction and this requires therefore higher temperatures.

Gases are poorly soluble in water with the exception of some gases: carbon dioxide, hydrogen sulphide. The solubilization of gases may be considered as the sum of two processes: the endothermic opening of a clathrate pocket in the water, and the exothermic placement of a molecule in that pocket, due to the van der Waals interactions. In water at low temperatures, the energy required by the opening process is very small as such pockets may be easily formed within the water clustering. The solubilization process is therefore exothermic. As an exothermic process is favoured by low temperature (Le Chatelier's principle), the gas solubility (energy source in this case) decreases with temperature rise. At high temperatures the natural clustering is much reduced, therefore more energy is required for opening of the pocket in the water. In that case the solubilization process is an endothermic process and as predicted by the Le Chatelier's principle, the gas solubility increases with temperature rise. Between these two cases the solubilization process is athermic, i.e. the opening and the molecule placements processes give as much energy to the system and thus the gas solubility goes through a minimum.

It is also a result of the hydrogen bond that water can form gas hydrates. Because of hydrogen bonding, the water molecules will tend to align, with a hydrogen molecule lining up with an oxygen molecule. Because of the V shape, when the water molecules line up, they

form a regular pattern, the presence of certain guest compounds tends the water molecule to stabilize, precipitating a solid mixture of water and of this (these) guest(s).

2.2. Gas Hydrates

Gas hydrates are solid crystalline compounds formed from mixtures of water and guest molecules of suitable sizes. Based on hydrogen bonding, water molecules form unstable lattice structures with several interstitial cavities. The gas molecules can occupy the cavities and, when a minimum number of cavities are occupied, the crystalline structure becomes stable and solid gas hydrates are formed, even at temperatures well above the ice point. Gas hydrates are solid crystalline compounds formed from mixtures of water and guest molecules of suitable sizes. The water molecules are referred to as the *host molecules*, and the other compounds, which stabilize the crystal, are called the *guest molecules*. The hydrate crystals have complex, three-dimensional structures in which the water molecules form a cage and the guest molecules are entrapped in the cages.

Structure I hydrate consists of two types of cavities, a small pentagonal dodecahedral cavity consisting of 12 pentagonal rings of water, referenced as 5^{12}, and a large tetrakaidecahedral cavity consisting of 12 pentagonal and two hexagonal rings of water (Figures 2.5 and 2.6). Typical gases are: Methane, Ethane, Ethylene, Acetylene, H_2S, CO_2, SO_2, Cl_2.

Structure II hydrate consists also of two types of cavities, the small pentagonal dodecahedral cavity consisting of 12 pentagonal rings of water, referenced as 5^{12}, and a larger hexakaidecahedral cavity consisting of 12 pentagonal and four hexagonal rings of water, referenced as $5^{12}6^{4.}$ Typical gases are: Propane, iso-Butane, Propylene, iso-Butylene.

Structure I hydrate is formed from 46 water molecules and structure II from 136 water molecules. Another structure has been discovered, called the H structure, formed from 34 water molecules and consisting in three types of cavities:

1. The small pentagonal dodecahedral cavity consisting of 12 pentagonal rings of water, referenced as 5^{12}.

2. A larger hexakaidecahedral cavity consisting of 12 pentagonal and 8 hexagonal rings of water, referenced as $5^{12}6^8$.

3. An intermediate cavity consisting of 3 squares, 6 pentagonal and 3 hexagonal rings of water, referenced as $4^3\ 5^6\ 6^3$. Typical gases are: Methylbutane, 2.3 or 3.3-Di methyl 1-2-butene.
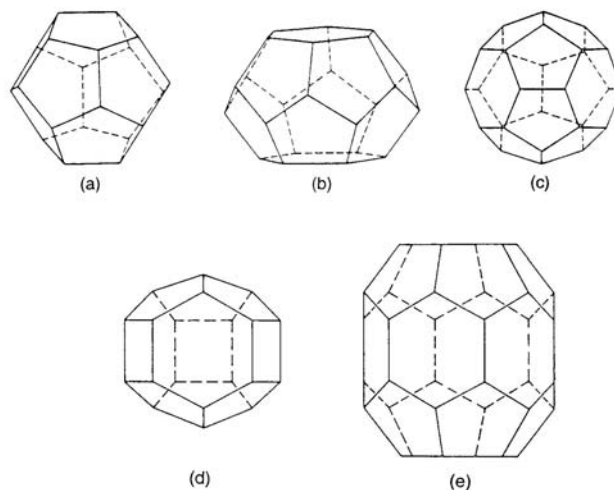
Figure 2.5: Cavity Geometry 5^{12}(a), $5^{12}6^2$(b), $5^{12}6^4$(c), $4^35^66^3$(d) and $5^{12}6^8$(e)
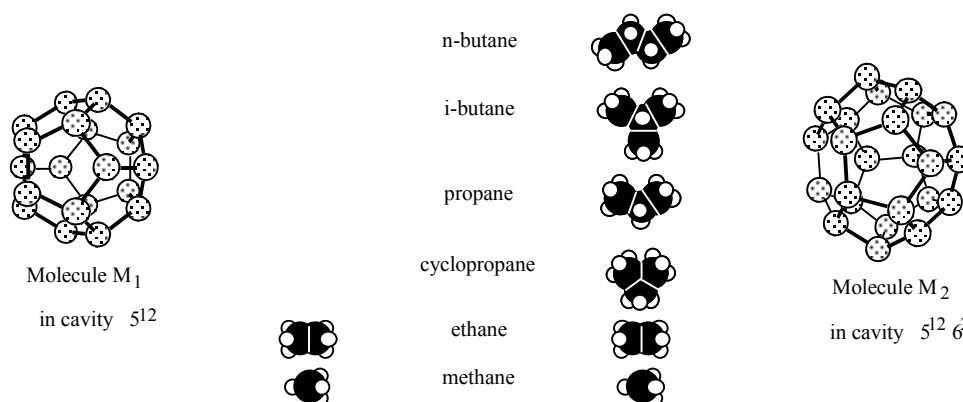
Figure 2.6: Cavities 5^{12} and $5^{12}6^2$ with their guest molecules

Another interesting thing about gas hydrates is that guest molecules to fill the cavities without bonding they are held in place by van der Waals forces. The guest molecules are free to rotate inside the cages built up from the host molecules. To sum up the formation of a gas hydrate requires the following three conditions [10]:

1. *The right combination of temperature and pressure*. Hydrate formation is favoured by low temperatures and high pressures.

2. *A hydrate former*. Hydrate formers include methane, ethane, and carbon dioxide.

3. *A sufficient amount of water.*

2.3. Experimental Data

The knowledge of phase equilibrium data on water - hydrocarbons systems are fundamental in the environmental sciences, in petroleum and chemical engineering industries for many reasons:

- to set dehydration specifications for processed hydrocarbons
- to avoid the occurrence of hydrates during the transport or the processing, for the recovery of hydrocarbons dissolved in the water basins and because of the change in phase diagram occurring due to the presence of water (Figure 2.7).
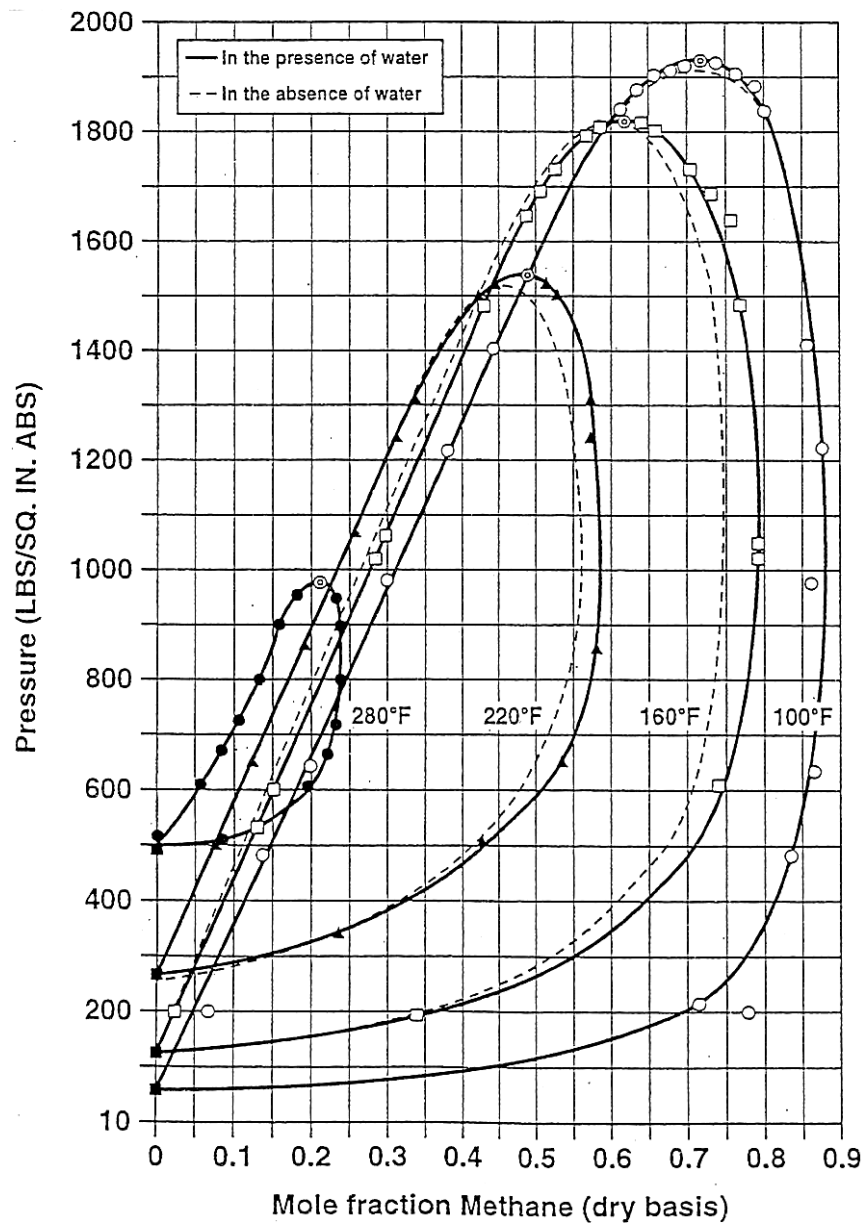
Figure 2.7: Water effect on the methane-n-butane system from
McKetta and Katz, 1948 [11]

33

It is also necessary to have the more accurate data to provide a means for developing or improving the accuracy of predictive equilibria models. *Pendergraft et al.* [12] even reported that limited data for water-hydrocarbon systems have been reported and quality ranged from average to poor.

The studies of water in vapour gas phases and the solubilities of hydrocarbons in water have been separated in two particular cases.

2.3.1. Water Content in the Gas Phase

2.3.1.1. Water Content in the Gas Phase of Binary Systems

The water content of a natural gas in saturation condition is mainly dependent on pressure and temperature conditions. The water content in a hydrocarbon gas phase decreases with the pressure and the temperature (Figure 2.8). Various authors have conducted studies of the water content of various water - hydrocarbon(s) and water - gas systems. It should be noticed that essentially binary systems have been investigated.

The TABLE 2.2 shows all the water content data reported for all natural gas main components. As can be seen, most of these data have been reported for methane – water and carbon dioxide water systems and at high temperatures. These systems have been investigated for their majority at temperatures higher than 298 K. Only few authors have studied that kind of systems at lower temperatures, near hydrate forming conditions, because of the very low water content and the difficulties associated with the analysis of water traces.

The presence of salts in the aqueous phase decreases the water vapour pressure and thus the water content in the gas phase. A correction could be applied to take into account the salinity of the liquid phase (Figure 2.8).

Figure 2.8: Water contents of natural gases (from GPA handbook [13])

Component	Reference	T_{min} /K	T_{max} /K	P_{min} /MPa	P_{max} /MPa
Methane	Dhima *et al.* (2000) [14]	298.15	298.15	1	35
	Althaus (1999) [15]	253.15	293.15	0.5	10
	Ugrozov (1996) [16]	310.95	377.55	2.53	70.93
	Yokoama *et al.* (1988) [17]	298.15	323.15	3	8
	Yarym-Agaev *et al.* (1985) [18]	298.15	338.15	2.5	12.5
	Gillepsie and Wilson (1982) [19]	323.15	588.70	1.4	13.8
	Kosyakov *et al.* (1979) [20]	273.16	283.16	1	10.1
	Aoyagi *et al.* (1980) [21]	240	270	3.45	10.34
	Kosyakov *et al.* (1982) [22]	233.15	273.15	1	10.1
	Rigby and Prausnitz (1968) [23]	298.15	373.15	2.3	9.3
	Culberson and Mc Ketta (1951) [24]	310.93	310.93	5.2	35.7
	Olds *et al.* (1942) [25]	310.93	510.93	2.672	68.856
Ethane	Althaus (1999) [15]	253.15	293.15	0.5	3
	Song and Kobayashi (1994) [26]	240	329.15	0.34	3.45
	Coan and King (1971) [27]	298.15	373.15	2.3	3.6
	Anthony and McKetta (1967) a [28]	308.15	408.15	2.6	10.8
	Anthony and McKetta (1967) b [29]	311.15	377.15	3.5	34.7
	Culberson and McKetta (1951) [24]	310.93	310.93	4.2	12
	Reamer *et al.* (1943) [30]	310.93	510.93	2.2	68.2
Propane	Song and Kobayashi (1994) [26]	235.6	300.15	0.6	1.1
	Klausutis (1968) [31]	310.93	310.93	0.545	1.31
	Kobayashi and Katz (1953) [32]	310.93	422.04	0.703	19.33
Butane	Anthony and McKetta (1967) [28]	344.15	344.15	0.86	0.87
	Wehe and McKetta (1961) [33]	311.15	378.15	0.36	1.8
	Reamer *et al.* (1952) [34]	310.93	510.93	0.14	68.95
	Brooks *et al.* (1951) [35]	310.93	377.59	7.27	68.36
	Reamer *et al.* (1944) [36]	311.15	423.15	0.36	4.4
Carbon dioxide	Dohrn *et al.* (1993) [37]	323.15	323.15	10	30.1
	D'Souza *et al.* (1988) [38]	323.15	348.15	10	15.2
	Briones *et al.* (1987) [39]	373.15	413.15	0.3	3.2
	Nakayama *et al.* (1987) [40]	298.15	348.15	0.1	70.9
	Song and Kobayashi (1986) [41]	251.8	302.7	0.69	13.79
	Mueller *et al.* (1983) [42]	323.15	348.15	2.5	30.4
	Gillepsie and Wilson (1982) [19]	289.15	394.15	0.7	20.3
	Coan and King (1971) [27]	298.15	373.15	1.7	5.2
	Takenouchi and Kennedy (1964) [43]	383.15	423.15	10	150
	Sidorov *et al.* (1953) [44]	298.2	298.2	3.6	6.4
	Wiebe and Gaddy (1941) [45]	323.15	323.15	6.8	17.7
Nitrogen	Althaus (1999) [15]	248.15	293.15	0.5	10
	Ugrozov *et al.* (1996) [19]	310.15	310.15	1.4	13.8
	Namiot and Bondareva (1959) [46]	310.95	366.45	0.34	13.79
	Kosyakov *et al.* (1979) [19]	233.15	273.15	1	10.1
	Maslennikova *et al.* (1971) [47]	298.15	623.15	5.1	50.7
	Rigby and Prausnitz (1968) [23]	298.15	373.15	2.1	10.2
	Sidorov *et al.* (1953) [44]	373.15	373.15	5.1	40.5
Hydrogen sulphide	Burgess and Germann (1969) [48]	323.15	443.15	1.7	2.3
	Selleck et al. (1952) [49]	310.93	444.26	0.7	20.7
	Gillepsie and Wilson (1982) [19]	310.93	588.71	4.13	20.68

TABLE 2.2 – SOURCE OF VAPOUR-LIQUID EQUILIBRIUM DATA FOR WATER – GAS BINARY SYSTEMS

2.3.1.2. Water Content in Natural Gas Systems

The majority of the available data on water content are for binary systems; nevertheless some authors have reported water content of synthetic gas mixture as well as natural gases. Historically *McKetta and Katz* [11] were the first to report water content data of a mixture of methane and n-butane. *Althaus* [15] has reported the water content of seven different synthetic mixtures up to 10 MPa. Excepted for the last mixture, the systems investigated are only concerning lean and sweet gases.

Gas Gravity Component	0.565 (NG₁)	0.598 (NG₂)	0.628 (NG₃)	0.633 (NG₄)	0.667 (NG₅)	0.6395 (NG₆)	0.8107 (NG₇)
Helium	0.015	0.028	-	0.152	0.004	0.043	0.038
Nitrogen	0.84	1.938	0.912	4.863	0.8	10.351	1.499
Carbon Dioxide	0.109	0.851	-	0.167	1.732	1.291	25.124
Methane	98.197	93.216	88.205	86.345	84.339	83.847	70.144
Ethane	0.564	2.915	8.36	6.193	8.724	3.46	2.52
Propane	0.189	0.715	1.763	1.55	3.286	0.657	0.394
i-Butane	0.029	0.093	0.293	0.214	0.311	0.093	0.067
n-Butane	0.038	0.135	0.441	0.314	0.584	0.126	0.074
C₅	0.014	0.058	0.027	0.13	0.163	0.067	0.054
C₆₊	0.007	0.049	-	0.064	0.049	0.069	0.118

TABLE 2.3 – COMPOSITION (MOL. %) OF DIFFERENT NATURAL GASES FROM ALTHAUS [15]

The author has also investigated the water content of a mixture of methane and ethane at identical conditions, i.e. from 258.15 to 288.15 K and pressures up to 10 MPa. More investigators have generated data on systems containing carbon dioxide and hydrogen sulphide. Systems containing carbon dioxide and hydrogen sulphide contain more water at saturation than sweet natural gases, this is even more pronounced if the pressure is above 5 MPa.

McKetta and Katz [11] were the first to measure the water content of mixtures containing methane and n-butane. *Lukacs and Robinson* [50] measured the water content of mixtures containing methane and hydrogen sulphide at 344.26 K up to 9.6 MPa. These mixtures are composed in majority of methane (from 71 up to 84 mol %). In 1985 *Huang et al* [51] generated data on the water content of synthetic gas mixtures containing methane (10 to 30 mol %), carbon dioxide (10 to 60 mol %) and hydrogen sulphide (10 to 80 mol %). These systems were studied at 310.95, 380.35 and 449.85 K up to 18 MPa. *Song and Kobayashi* [52] reported numerous water content data of a mixture composed in majority of carbon dioxide

(94.69 mol %) and methane (5.31 mol %) in 1989. They worked between 288.7 and 323.15 K up to 13.8 MPa. More recently *Ng et al.* [53] reported water content data for different sour gases from 322 and 366.5 K up to 69 MPa.

2.3.2. Hydrocarbon Solubility in Water

Natural gases are not very soluble in water even at high pressures. The solubility of natural gases is indeed function of pressure and temperature. Figure 2.9 shows the methane solubility in water at different pressures and temperatures. For pressures higher than 5 MPa a minimum is observed on the isobaric curves. These curves are limited at low temperatures by the hydrate-forming curve.
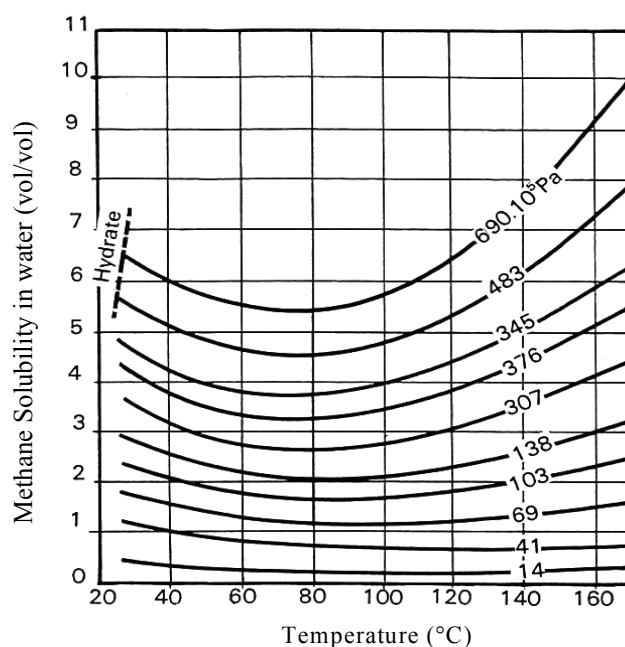
Figure 2.9: Methane solubility in water from *Culberson and McKetta*, 1951 [54]

At a given temperature and pressure, it is observed that the solubilities of different hydrocarbons decrease strongly with the number of carbon atoms (Figure 2.10). It can be also noticed that the pressure effect is only important for light hydrocarbons, the solubilities of hydrocarbons with more than four carbon atoms are practically constant and then only slightly dependent of the pressure.
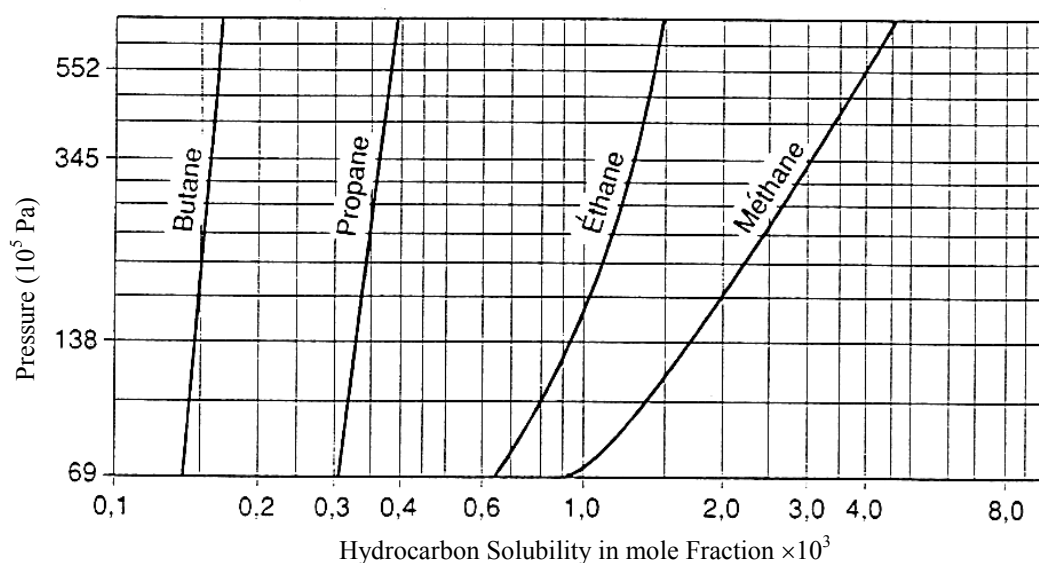
Figure 2.10: Solubilities of various hydrocarbons at 377.59 K (from *Brooks et al.*, 1951 [35])

- Methane in water

Bunsen conducted the first study of the solubility of methane in water in 1855 [55]. The solubilities of several gases including methane were measured at atmospheric pressures. Then *Winkler* in 1901 [56] conducted the same experiments and found deviations from the data of *Bunsen*. Following the results of these two researchers, there have been many further studies on methane-water system at atmospheric pressure, all authors yield solubility values lying between the results of the two first studies (*Claussen and Polglase* in 1952 [57], *Morisson and Billet* in 1952 [58], *Wetlaufer et al.* in 1964 [59], *Wen and Hung* in 1970 [60], *Ben–Naim et al.* in 1973 [61] *Ben–Naim and Yaacobi* in 1974 [62], *Yamamoto and Alcauskas* in 1976 [63], *Muccitelli and Wen* in 1980 [64] and *Rettich et al.* in 1981 [65]). The latest is supposed to have obtained results of the highest accuracy [66] and they are close to those obtained by *Bunsen*. The first study reporting intermediate and high-pressure solubility data for methane in water was the study of *Frohlich et al.* in 1931 [67]. Since then many studies have been performed: *Michels et al.* in 1936 [68], *Culberson et al.* in 1950 [69], *Culberson and Mc Ketta* in 1951 [54], *Davis and Mc Ketta* in 1960 [70], *Duffy et al.* in 1961 [71], *O'Sullivan and Smith* in 1970 [72], *Sultanov et al.* in 1971 [73], *Amirijafari and Campbell* in 1972 [74], *Sanchez and De Meer* in 1978 [75], *Price* in 1979 [76], *Stoessel and Byrne* in 1982 [77] and *Abdulgatov et al.* in 1993 [78]. All these researchers have measured solubility of methane at intermediate and high pressures but only at high temperatures. The number of researcher reporting data of methane in water at low temperatures (T≤ 298.15 K) is far more limited and more recent: *Cramer* in 1984 [79], *Yarym-Agaev et al.* in 1985 [18], *Yokoyama et*

al. in 1988 [80], *Toplak* in 1989 [81], *Wang et al.* in 1995 [82], *Lekvam and Bishnoi* in 1997 [66], *Song et al* in 1997 [83], *Yang et al.* in 2001 [84] *Servio and Englezos* in 2002 [85], *Wang et al.* in 2003 [86] and *Kim et al.* in 2003 [87].

Reference	T /K	P /MPa
T ≥ 298.15 K		
Frohlich *et al.* (1931) [67]	298.15	3 – 12
Michels *et al.* (1936) [68]	298.15 – 423.15	4.063 – 46.913
Culberson *et al.* (1950) [69]	298.15	3.620 – 66.741
Culberson and Mc Ketta (1951) [54]	298.15 – 444.26	2.227 – 68.91
Davis and McKetta (1960) [70]	310.93 – 394.26	0.352 – 3.840
Duffy *et al.* (1961) [71]	298.15 – 303.15	0.317 – 5.171
O'Sullivan and Smith (1970) [72]	324.65 – 398.15	10.132 – 61.606
Sultanov *et al.* (1971) [73]	423.15 – 633.15	4.903 – 107.873
Amirijafari and Campbell (1972) [74]	310.93 – 344.26	4.136 – 34.464
Sanchez and De Meer (1978) [75]	423.15 – 573.15	10 – 250
Price (1979) [76]	427.15 – 627.15	3.543 – 197.205
Stoessel and Byrne (1982) [77]	298.15	2.412 – 5.170
Yarym-Agaev *et al.* (1985) [18]	313.15 – 338.15	2.5 – 12.5
Yokoyama *et al.* (1988) [80]	298.15 – 323.15	3 – 8
Toplak (1989) [81]		
Abdulgatov *et al.* (1993) [78]	523.15 – 653.15	2 – 64
Yang *et al.* (2001) [84]	298.1 – 298.2	2.33 – 12.68
Kim *et al.* (2003) [87]	298.15	2.3 – 16.6
T < 298.15 K		
Cramer (1984) [79]	277.15 – 573.15	3 – 13.2
Wang *et al.* (1995) [82]	283.15 – 298.15	1.15 – 5.182
Reichl (1996) [93]	283.1 6 – 343.16	0.178 – 0.259
Lekvam and Bishnoi (1997) [66]	274.19 – 285.68	0.567 – 9.082
Song *et al.* (1997) [83]	273.15 – 288.15	3.45
Servio and Englezos (2002) [85]	278.65 – 284.35	3.5 – 6.5
Wang *et al.* (2003) [86]	283.2 – 303.2	2 – 40.03 0

TABLE 2.4 – EXPERIMENTAL SOLUBILITY DATA OF METHANE IN WATER [B5]

- Other light hydrocarbons in water

Ethane in water: this system has not been so widely examined; only a few researchers have conducted solubility experiments on this system: *Culberson et al.* [87], *Culberson and McKetta* in 1950 [90], *Anthony and Mc Ketta* in 1967 [88-89], *Danneil et al.* also in 1967 [91], *Sparks and Sloan* in 1983 [92], *Reichl* in 1996 [93], *Wang et al.* in 2003 [86] and *Kim et al.* in 2003 [87].

The solubilities of propane, n-butane and n-pentane have been reported by some authors: The propane – water system by *Kobayashi and Katz* in 1953 [32], *Umano and Nakano* in 1958 [94], *Azarnoosh and McKetta* in 1958 [95], *Wehe and McKetta* in 1961 [96], *Klausutis* in 1968 [31], *Sanchez and Coll* in 1978 [97], *De Loos et al.* in 1980 [98]. The n-butane – water system by *Brooks et al.* in 1951 [35], *Reamer et al.* in 1952 [34], *Le Breton*

and McKetta in 1964 [99]. The n-pentane- water system by *Gillepsie and Wilson* in 1982 [19], and in VLLE by *Jou and Mather* in 2000 [100].

Reference	T /K	P /MPa
Ethane		
Culberson and Mc Ketta (1950) [88]	310.93 – 444.26	0.407 – 68.499
Culberson *et al.* (1950) [87]	310.93 – 444.26	0.407 – 8.377
Anthony and Mc Ketta (1967) [89-90]	344.3 – 377.65	3.48 – 28.170
Danneil *et al.* (1967) [91]	473.15 – 673.15	20 – 370
Sparks and Sloan (1983) [92]	259.1– 270.45	3.477
Reichl (1996) [93]	283.17 – 343.16	0.063 – 0.267
Kim *et al.* (2003) [87]	298.15	1.4 – 3.9
Wang *et al.* (2003) [86]	283.2 – 303.2	0.5 – 4
Propane		
Wehe and McKetta (1961) [96]	344.26	0.514 – 1.247
Klausutis (1968) [31]	310.93 – 327.59	0.537 – 1.936
Sanchez and Coll (1978) [97]	473.15 – 663.15	20 – 330
Kobayashi and Katz (1953) [32]	285.37 – 422.04	0.496 – 19.216
Azarnoosh and McKetta (1958) [95]	288.71 – 410.93	0.101 – 3.528
Sparks and Sloan (1983) [92]	246.66 – 276.43	0.772
n- Butane		
Brooks *et al.* (1951) [35]	310.93 – 377.59	7.274 – 69.396
Reamer *et al.* (1952) [34]	310.93 – 510.93	0.007 – 68.948
Le Breton and McKetta (1964) [99]	310.93 – 410.93	0.136 – 3.383
n- Pentane		
Gillespie and Wilson (1982) [19]	310.93 – 588.71	0.827 – 20.684

TABLE 2.5 – EXPERIMENTAL SOLUBILITY DATA OF ETHANE, PROPANE, *n*-BUTANE AND *n*-PENTANE IN WATER

- Carbon dioxide, nitrogen and hydrogen sulphide in water

The carbon dioxide − water system has been largely investigated by many authors. Recently, two good reviews on the solubility of carbon dioxide in water have been published [101-102]. The authors have gathered a large number of available experimental data. At low temperatures (273.15< T< 277.15 K) and in vapour-liquid conditions the system has been investigated firstly by *Zel'vinskii* in 1937 [103] and more recently by *Anderson* in 2002 [104]. At more intermediate temperatures the number of researchers reporting data of carbon dioxide solubilities in water is far more consequent: *Kritschewsky et al.* in 1935 [105], *Zel'vinskii* in 1937 [103], *Wiebe and Gaddy* in 1939 and 1940 [106-107], *Bartholomé and Friz* in 1956 [108], *Matous et al.* in 1969 [109], *Malinin and Savelyeva* in 1972 [110], *Malinin and Kurovskaya* in 1975 [111], *Gillespie and Wilson* in 1982 [19], *Oleinik* in 1986 [112], *Yang et al.* in 2000 [113] and finally *Anderson* in 2002 [104]. At higher temperatures, many authors have also investigated the system: *Zel'vinskii* in 1937 [103], *Wiebe and Gaddy* in 1939 and 1940 [106-107], *Matous* in 1969 [109], again *Malinin and Savelyeva* in 1972 [110], *Malinin and Kurovskaya* in 1975 [111], *Zawisza and Malesinska* in 1981 [114], *Shagiakhmetov and*

Tarzimanov also in 1981 [115], *Gillespie and Wilson* in 1982 [19], *Oleinik* in 1986 [112], *Mueller et al*. in 1988 [116] and more recently *Bamberger et al*. in 2000 [117].

Reference	T / K	P / MPa
$273.15 < T \leq 277.13$		
Anderson (2002) [104]	274.15 – 276.15	0.07 – 1.42
Zel'vinskii (1937) [103]	151.7 – 192.5	1.082
$277.13 < T \leq T_c$		
Anderson (2002) [104]	278.15 – 288.15	0.83 – 2.179
Yang et al. (2000) [113]	298.31 – 298.57	2.7 – 5.33
Oleinik (1986) [112]	283.15 – 298.15	1 – 5
Gillespie and Wilson (1982) [19]	298.15 – 302.55	5.07 – 5.52
Malinin and Kurovskaya (1975) [111]	298.15	4.955
Malinin and Savelyeva (1972) [110]	298.15	4.955
Matous et al. (1969) [109]	303.15	0.99 – 3.891
Bartholomé and Friz (1956) [108]	283.15 – 303.15	0.101 – 2.027
Wiebe and Gaddy (1939 & 40) [106-107]	291.15 – 304.19	2.53 – 5.06
Zel'vinskii (1937) [103]	298.15	1.11 – 5.689
Kritschewsky et al. (1935) [106]	293.15 – 303.15	0.486 – 2.986
$T_c < T \leq 373.15$		
Bamberger et al. (2000) [117]	323.15 – 353.15	4 – 13.1
Mueller et al. (1988) [116]	373.15	0.3 – 1.8
Gillespie and Wilson (1982) [19]	304.25 – 366.45	0.69 – 20.27
Oleinik (1986) [112]	323.15 – 343.15	1 – 16
Shagiakhmetov and Tarzimanov (1981) [115]	323.15 – 373.15	10 – 60
Zawisza and Malesinska (1981) [114]	323.15 – 373.15	0.488 – 4.56
Malinin and Kurovskaya (1975) [111]	373.15	4.955
Malinin and Savelyeva (1972) [110]	323.15 – 348.15	4.955
Matous (1969) [109]	323.15 – 353.15	0.993 – 3.88
Wiebe and Gaddy (1939, 1940) [106-107]	308.15 – 373.15	2.53 – 70.9
Zel'vinskii (1937) [103]	323.15 – 373.15	1.94 – 9.12

TABLE 2.6 – EXPERIMENTAL SOLUBILITY DATA OF CARBON DIOXIDE IN WATER UP TO 373.15 K [B6]

A few researchers have investigated the nitrogen – water system: *Goodman and Krase* in 1931 [118] were the first to investigate the solubility of nitrogen in water at pressures higher than the atmospheric pressure, followed by *Wiebe et al*. in 1932 [119], *Wiebe et al*. again in 1933 [120], *Saddington and Krase* in 1934 [121], *Pray et al*. in 1952 [122], *Smith et al*. in 1962 [123], *O'Sullivan et al*. in 1966 [124], *Maslennikova et al*. 1971 [47] and more recently *Japas and Franck* in 1985 [125] (TABLE 2.7).

Studies of hydrogen sulphide solubilities in water have been reported by: *Selleck et al*. (1952) [49], *Kozintseva* in 1964 [126], *Burgess and Germann* (1969) [48], *Gillespie and Wilson* in 1982 [19] and by *Carroll and Mather* in 1989 [127] (TABLE 2.7).

Reference	T /K	P /MPa
Nitrogen		
Wiebe et al. (1932) [119]	298.15	2.533 – 101.325
Wiebe et al. (1933) [120]	298.15 – 373.15	2.533 – 101.325
Saddington and Krase (1934) [121]	323.15 – 513.15	10.132 – 30.397
Pray et al. (1952) [122]	533.15 – 588.71	1.034 – 2.758
Smith et al. (1962)[123]	303.15	1.103 – 5.895
O'Sullivan et al. (1966)[124]	324.65	10.132 – 60.795
Maslennikova et al. (1971)[47]	473.15 – 623.15	10.538 – 50.156
Japas and Franck (1985)[125]	523 – 636	20.5 – 200
Goodman and Krase (1931)[118]	273.15 – 442.15	10.132 – 30.397
Hydrogen Sulphide		
Selleck et al. (1952)[49]	310.93 – 444.26	0.689 – 20.685
Kozintseva (1965)[126]	502.15 – 603.15	2.834 – 128.581
Burgess and Germann (1969)[48]	303.15 – 443.15	1.724– 2.344
Gillespie and Wilson (1982)[19]	310.93 – 588.71	4.137– 20.684
Carroll and Mather (1989)[127]	313.15 – 378.15	28 – 92.4

TABLE 2.7 – EXPERIMENTAL SOLUBILITY DATA OF NITROGEN AND HYDROGEN SULPHIDE IN WATER

The solubility data of light hydrocarbons (C1-C5), carbon dioxide, nitrogen and hydrogen sulphide for pressure up to 70 MPa and temperature higher than 298.15 K can be considered to be complete. Nevertheless, only a few data have been reported in the open literature for gas solubility in water at low temperature and in vapour-liquid condition. This is especially true for hydrocarbons and gas other than methane and carbon dioxide, because of the difficulties associated with such measurements.

In the case of gas mixtures, the number of studies reporting hydrocarbons and gas solubilities is far more limited and in any case limited at temperature higher than 311 K.

Components	Reference	Tmin (Kelvin)	Tmax (Kelvin)	Pmin (MPa)	Pmax (MPa)
C1+C2	Amirijafari (1969) [128]	311	311	4.8	55
C1+C2	Wang et al. [86]	275.2	283.2	1	4
C1+C3	Amirijafari (1969) [128]	378	378	4.8	55
C1+C4	McKetta and Katz (1948) [11]	311	311	1.3	21
C1+C5	Gillespie and Wilson (1982) [19]	311	589	3.1	21
C2+C3	Amirijafari (1969) [128]	378	378	4.8	55
C1+C2+C3	Amirijafari (1969) [128]	344	344	4.8	55

TABLE 2.8 – SOLUBILITY OF HYDROCARBON MULTI COMPONENTS IN WATER

In their paper, *Amirijafari and Campbell* [74] concluded that the total solubility of binary or ternary hydrocarbon systems in water is more important than the solubility of each hydrocarbon taken alone at same pressure and temperatures. Oppositely *Wang et al.* in 2003 [39] found in the C1 (90% mol) + C2 (10% mol) that the solubility of methane in water are of the same order as in the methane-water at pressure higher than 2 MPa and that the solubility

of ethane is not influenced by the pressure. However, for the smaller pressure the same phenomenon is observed, a higher total solubility.

- Influence of the addition of an inhibitor

For system containing hydrate inhibitor, limited data have been produced. For the methane-methanol-water system, experimental data have been reported by: *Battino* [129] in 1980, *Fauser* in 1951 [130], *Hong et al.* in 1987 [131], *Schneider* in 1978 [132] and *Wang et al.* in 2003 [39].

The ethane-methanol-water has also been investigated by *Schneider* [132], *Hayduck* in 1982 [133], *Yaacobi and Ben-Naim* in 1974 [62], *Mc Daniel* in 1911 [134], *Ma and Kohn* in 1964 [135], *Ohagakiet al.* in 1976 [136], *Weber* in 1981 [137] *Ishihara et al.* in 1998 [138] and *Wang et al.* in 2003 [39].

For system containing ethylene glycol, similar solubility data are scarce, once again the *Wang et al*. [39] paper can be cited: the solubilities of pure methane and pure ethane in an aqueous solution of ethylene glycol have been studied as well as the solubilities of methane and ethane for a synthetic gas mixture (90% C and 10% C2) in a aqueous solution of ethylene glycol.

From all these studies, it can be concluded that at a given temperatures and pressures, the gas solubility increases smoothly with increasing inhibitor up to 80 wt.% and sharply when the inhibitor concentration exceeds 80 wt. % . It can be also noticed that at same temperature and pressure conditions, gas solubility is higher in aqueous methanol solution than in aqueous ethylene glycol solution.
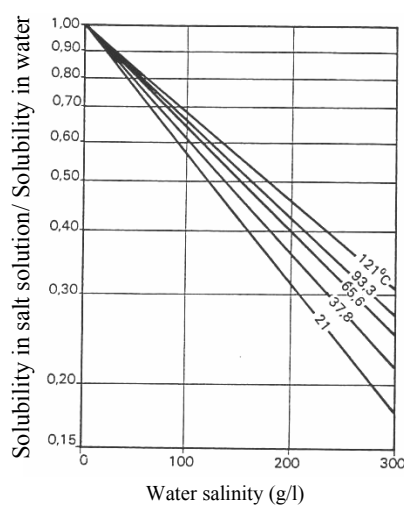
- Presence of salt in water

The solubility of gases is highly influenced by the salinity of the liquid phase. In aqueous salt solutions, the hydrocarbons are less soluble than in pure water solution.

Figure 2.11: Salt effect on the quantity of gas dissolved in water (*McKetta and Wehe*, 1962 [139])

2.3.3. Hydrate Forming Conditions

Since *Hammerschmidt* in 1934 [140] pointed out that gas hydrate were the cause of blockage during transportation of natural gases in pipelines, the study on gas hydrate raised substantial attention in the oil and gas industry.

Gas hydrates are crystalline solid inclusion compounds (Figure 2.12) consisting of host water lattice composed of cavities, which « enclathrate » gas molecules. This lattice contains cavities, which are stabilized by small apolar molecules such as methane, ethane, etc. At usual sub-sea pipeline conditions, gas hydrate might form. The two most common gas hydrates, which appear naturally, are structure I and structure II hydrates.

Figure 2.12: Ethane gas hydrate in the PVT sapphire cell

Most of the experimental works have been focused on hydrate formation pressures or temperatures in pure water system. Experimental hydrate forming conditions for pure gases have been widely reported in the literature (TABLE 2.9).

Component	Structure	Reference	ΔTmin (Kelvin)	Number of exp. pts
Argon	I	[141]	90-149	6
	I	[142]	274-291	8
Krypton	I	[141]	149-203	6
	I	[143]	273,283	2
	I	[144]	275-278	4
Xenon	I	[141]	211-268	6
	I	[145]	273	1
Oxygen	I	[146, 147]	268-284	45
	I	[148]	273-284	4
Nitrogen	I	[149]	273-288	19
	I	[146, 147]	269-288	38
	I	[149]	273-281	8
	I	[148]	274-283	3
Carbon dioxide	I	[150]	175-232	13
	I	[151]	277-282	5
	I	[152]	274-283	6
	I	[153]	272-283	7
	I	[154]	274-283	9
Hydrogen Sulphide	I	[49]	250-303	23
Methane	I	[144]	275-281	6
	I	[149]	273-294	8
	I	[154]	273-286	11
	I	[155]	262-271	5
	I	[156]	285-296	6
	I	[157]	273-286	9
	I	[158]	275-284	6
Ethane	I	[151]	200-243	10
	I	[156]	263-273	4
	I	[159]	280-287	4
	I	[160-161]	277-287	13
Propane	II	[156]	261-277	11
	II	[162]	248-262	7
	II	[144]	274-278	5
	II	[153]	274-279	5
	II	[163]	273-278	9
Isobutane	II	[162]	241-270	9
	II	[164]	273-275	5
	II	[165]	273-275	5

TABLE 2.9 – EXPERIMENTAL DATA OF HYDRATE FORMING CONDITIONS WITH A SINGLE GAS

In most of the studies the accuracy on hydrate dissociation pressure is mentioned to be not greater than 1-4%, even for the old data the accuracy of the results is surprising good [5]. For multicomponent systems the available data are listed in TABLE 2.10:

Components	Structure	Reference	$\Delta Tmin$ (Kelvin)	N. of exp. pts
Ar + N$_2$	I	[166]	275-289	7
Ar + C$_1$	I	[166]	276-299	21
Ar + C$_1$	I	[143]	273, 283	2
Kr+C$_1$	I	[143]	273,283	2
Kr+C$_3$	II	[144]	276	17
N$_2$+C$_1$	I	[148]	277-295	31
N$_2$+C$_3$	II	[167]	274-289	28
CO$_2$+C$_1$	I	[151]	275-286	17
CO$_2$+C$_1$	I	[168]	274-288	42
CO$_2$+C$_2$	I	[154]	274-288	40
CO$_2$+C$_3$	I, II	[154]	274-282	55
CO$_2$+C$_3$	II	[152]	274-286	13
CO$_2$+iso-C$_4$	I, II	[154]	274-281	53
CO$_2$+n-C$_4$	I, II	[154]	274-278	21
H$_2$S+C$_1$	I	[169]	276-304	16
C$_1$+C$_2$	I	[156]	284-304	16
C$_1$+C$_2$	I	[160]	279-287	15
C$_1$+C$_3$	II	[155]	275-278	32
C$_1$+C$_3$	II	[156]	291-304	12
C$_1$+C$_3$	II	[158]	275-300	11
C$_1$+iso-C$_4$	II	[144]	274	19
C$_1$+iso-C$_4$	II	[156]	289-305	11
C$_1$+iso-C$_4$	II	[170]	274-294	47
C$_1$+n-C$_4$	II	[171]	276-286	13
C$_1$+n-C$_4$	II	[172]	251-273	20
C$_2$+C$_3$	I, II	[161]	274-278	44
C$_1$+CO$_2$+H$_2$S	I	[173]	279-284	17
C$_1$+CO$_2$+H$_2$S	I	[174]	278-298	49
C$_1$+C$_2$+C$_3$	I, II	[161]	276-285	13
C$_1$+C$_3$+H$_2$S	II	[175]	276-301	13
C$_1$+C$_2$+C$_3$+n-C$_4$+C$_5$	II	[176]	227-297	12
C$_1$+C$_2$+C$_3$+iso-C$_4$+n-C$_4$+C$_5$+N$_2$	II	[176]	279-298	9
C$_1$+C$_2$+C$_3$+CO$_2$+N$_2$	II	[176]	278-297	15
C$_1$+C$_2$+C$_3$+iso-C$_4$	II	[155]	274-282	6
C$_1$+C$_2$+C$_3$+C$_4$+CO$_2$+H$_2$S	II	[177]	285-297	7
C$_1$+C$_2$+C$_3$+iso-C$_4$	II	[156]	294-303	7
C$_1$+C$_2$+C$_3$+iso-C$_4$	II	[178]	284-291	4
C$_1$+C$_2$+CO$_2$+N$_2$+Ar	I	[179]	283-286	7
C$_1$+C$_2$+C$_3$+iso-C$_4$+n-C$_4$+CO$_2$+N$_2$	II	[179]	273-293	21
C$_1$+C$_2$+C$_3$+iso&nC$_4$+C$_5$+H$_2$S+N$_2$	II	[180]	268-292	15
C$_1$+C$_2$+C$_3$+iso-C$_4$+C$_5$+CO$_2$+N$_2$	II	[181]	258-291	13
C$_1$+C$_2$+C$_3$+iso-C$_4$+C$_5$+CO$_2$+N$_2$	II	[182]	279-293	5
C$_1$+C$_2$+C$_3$+iso-C$_4$+ n-C$_4$	II	[154]	274-282	4
C$_1$+C$_2$+C$_3$+iso-C$_4$+ n-C$_4$+CO$_2$	I, II	[154]	274-282	16

TABLE 2.10 – EXPERIMENTAL DATA OF GAS HYDRATE FORMING CONDITIONS WITH GAS MIXTURES

To control the risk of gas hydrate formation, it is possible to add a thermodynamic inhibitor such as methanol or ethylene glycol into the pipeline. The addition of such compounds moves the conditions required for the gas hydrate formation to lower

temperatures and (or) higher pressures. The presence of salts has the same effect. Experimental studies on hydrate dissociation pressure for system containing inhibitor have been less investigated, only a few authors have presented experimental results for hydrate inhibition, among them we can cite *Kobayashi et al.* (1951) [183], and the work of *Ng and Robinson* reported in a series of articles (TABLE 2.11).

Component	Inhibitors or salt (wt %)	Structure	Reference	ΔTmin (Kelvin)	N. of exp. pts
Methane	10 & 20 % Methanol	I	[184]	263-286	2×6
Methane	35 & 50 % Methanol	I	[185]	233-270	7+5
Methane	50 & 65 % Methanol	I	[186]	214-259	5+6
Methane	74 & 85 % Methanol	I	[186]	195-230	2×3
Methane	10, 30 &50 % EG	I	[185]	263-287	4+4+3
Methane	15 % Ethanol	I	[183]	273-284	5
Methane	10 % Sodium Chloride*	I	[183]	270-284	8
Methane	20 % Sodium Chloride*	I	[183]	266-276	7
Methane	Sodium Chloride*	I	[187]	264-275	23
Ethane	10 & 20 % Methanol	I	[184]	263-284	16+11
Ethane	35 & 50 % Methanol	I	[188]	237-268	9+9
Propane	20 & 50 % Methanol	II	[187]	229-251	6+4
Propane	5 & 10 % Methanol	II	[184]	269-275	8+9
Propane	10 % Sodium Chloride*	II	[183]	268-273	8
Propane	2, 5 & 10 % Sodium Chloride*	II	[189]	270-275	3×4
iso-Butane	1.1 & 10 % Sodium Chloride*	II	[190]	268-274	6+3
iso-Butane	Sodium Chloride*	II	[191]	266-272	56
Carbon dioxide	10 & 20 % Methanol	I	[184]	264-284	10+14
Carbon dioxide	Hydrogen Chloride	I	[192]	274-283	12
Carbon dioxide	Sodium Hydroxide*	I	[192]	273-283	14
Carbon dioxide	Sodium Chloride*	I	[192]	274-280	4
Hydrogen sulphide	16.5 % Methanol	I	[193]	273.-290	3
Hydrogen sulphide	10 & 20 % Methanol	I	[184]	266-300	12+8
Hydrogen sulphide	35 & 50 % Methanol	I	[188]	256-286	8+11
Hydrogen sulphide	10 & 26 % Sodium Chloride*	I	[193]	275-295	3+5
Hydrogen sulphide	Calcium Chloride*	I	[193]	265-295	9
Hydrogen sulphide	16.5 % Ethanol	I	[193]	280-292	3
Hydrogen sulphide	Dextrose & Sucrose	I	[193]	285-296	3+4
C_1+C_2	10 & 20 % Methanol	I	[194]	263-289	8+7
C_1+C_3	10 & 20 % Methanol	I	[194]	265-291	6+5
C_1+C_3	35 & 50 % Methanol	I, II	[195]	249-276	6+7
$C_1 + CO_2$	10 & 20 % Methanol	I, II	[194]	263-287	14+13
$C_1 + CO_2$	35 & 50 % Methanol	I	[185]	240-267	4+5
$C_1 + H_2S$	20 % Methanol	I	[188]	264-290	5
$C_2 + CO_2$	20, 35 & 50 % Methanol	I	[188]	237-280	7+11+12
$C_3+ n$-C4	3 & 15 % Sodium Chloride*	I	[196]	273-275	2×15
$C_1 + CO_2 + H_2S$	10 & 20 % Methanol	II	[188]	265-291	6+8
Synthetic Gas Mix[o]	10 & 20 % Methanol	II	[194]	265-289	7+6
Synthetic Gas Mix[+]	10 & 20 % Methanol	II	[194]	264-288	2×9
Synthetic Gas Mix[++]	35 & 50 % Methanol	II	[184]	234-273	2×7

* Aquous solution of sodium chloride

[o] (7 % N_2 + 84 % C_1 + 4.7 % C_2 + 2.3 % C_3 + 0.9 % n-C_4+ 0.9 % n-C_5)

[+] (6 % N_2 + 71.6 % C_1 + 4.7 % C_2 +2 % C_3 + 0.8 % n-C_4+0.8 % n-C_5+14 % CO_2)

[++] (5 % N_2 + 71.9 % C_1 + 4 % C_2 +2 % C_3 + 0.8 % n-C_4+0.8 % n-C_5+13 % CO_2)

TABLE 2.11 – EXPERIMENTAL DATA OF GAS HYDRATE FORMING CONDITIONS FOR SYSTEMS CONTAINING HYDRATE INHIBITOR

To approximate the hydrate depression temperature for different kinds of inhibitors in a 5 - 25 wt % range we can use experimental values of hydrate dissociation pressures of systems without inhibitor using the expression developed by Hammerschmidt in 1939 for methanol inhibition [197]:

$$\Delta T = \frac{2.335\,W}{100M - M \times W} \tag{2.1}$$

where:

   ΔT is the hydrate temperature depression, °F.

   M is the molecular weight of the alcohol or glycol.

   W is the weight per cent of the inhibitor in the liquid.

This correlation gives acceptable results for methane and ethane but less acceptable for other gases [184]. It can be only applied to methanol concentrations lower than 0.2 (in mol fraction of the liquid phase) [198] and without modification to about 0.4 ethylene glycol concentration [5]. However, to use this equation, the hydrate formation temperature in the gas without the inhibitor being present must be known.

Some improvements have been made over the year to improve the accuracy of this equation [10], the original 2.335 constant can be replaced by other values depending on which kind of inhibitor is used. Some of these preferred values are listed in TABLE 2.12:

	Original [197]	*GPSA* [13]	*Arnold and Steward* [199]	*Pedersen et al.* [200]
Methanol	1.297	1.297	1.297	1.297
Ethanol	1.297	-	1.297	1.297
Ethylene glycol	1.297	2.222	1.222	1.5
Diethylene glycol	1.297	2.222	2.427	2.222
Triethylene glycol	1.297	2.222	2.472	3

TABLE 2.12 – COEFFICIENTS FOR THE HAMMERSCHMIDT EQUATION

However Carroll [10] recommends using the original values of 1.297 for ethylene glycol, because better predictions are obtained using this value.

An improved version has been proposed by Nielsen and Bucklin [198] applicable only for methanol solution, which is accurate for concentrations up to 0.8 mol fraction and temperatures down to 165 K:

$$\Delta T = -129.6 \ln(1 - x_{MeOH}) \tag{2.2}$$

with:

ΔT is the hydrate temperature depression, °F.

x_{MeOH} is the methanol mole fraction.

The Gas Processors and Suppliers Association (GPSA) Engineering Data Book [13] recommends the Hammerschmidt equation up to 25 wt% methanol concentrations and the Nielsen-Bucklin equation only for methanol concentrations ranging from 25-50 wt%.

To improve the prediction over a larger range, Carroll [10] proposed a modified version of the Nielsen-Bucklin equation to take into account the concentration of the inhibitor it includes the water activity coefficient:

$$\Delta T = -72 \ln(\gamma_w x_w) \tag{2.3}$$

with:

x_w is the water mole fraction.

γ_w is the activity coefficient of water.

The author use the two-suffix Magules equation to estimate the activity coefficient

$$\ln \gamma_w = \frac{a}{RT} x_I^2 \tag{2.4}$$

with: x_I is the inhibitor mole fraction.

Finally assuming that a/RT is temperature independent, the equation becomes:

$$\Delta T = -72 \, (Ax_I^2 + \ln[1 - x_I]) \tag{2.5}$$

The Margules coefficient, A, were fitted by the author using experimental data, the values obtained are listed in TABLE 2.13.

	Margules Coefficient	Concentration limit (wt%)
Methanol	0.21	85
Ethanol	0.21	35
Ethylene glycol	-1.25	50
Diethylene glycol	-8	35
Triethylene glycol	-15	50

TABLE 2.13 – MARGULES COEFFICIENTS AND INHIBITOR CONCENTRATION LIMITS

As measurements made for ethanol are relatively scarce, the author set the value of the Margules coefficient equal to that for methanol. For similar reason the value of the Margules coefficient for diethylene glycol is set to the average of the values of ethylene glycol and triethylene glycol.

Modelling of Thermodynamic Equilibria

Dans ce chapitre, une revue bibliographique de la modélisation des équilibres thermodynamiques est proposée. Dans un premier temps, nous verrons la modélisation des corps purs avec les différentes approches. On s'intéressera plus particulièrement aux principales équations d'état cubiques ainsi qu'aux différentes fonctions « alpha » introduites pour l'amélioration de la représentation des tensions de vapeur.

Les principaux modèles utilisés pour la représentation des données expérimentales sont ensuite exposés. Dans un premier temps, la modélisation des équilibres sera décrite. Il existe deux grandes approches pour le calcul des équilibres liquide – vapeur : une approche symétrique où une même équation est choisie pour décrire la phase vapeur et la phase liquide, et une approche dissymétrique où la phase vapeur est décrite par une équation d'état alors que la phase liquide est décrite par un modèle de solution. Finalement, différents modèles de calcul de pression de dissociation d'hydrates sont présentés.

3. Thermodynamic Models for Fluid Phase Equilibrium Calculation

The knowledge of phase diagram and fluid properties is fundamental in petroleum and chemical engineering. It is necessary to have the more accurate tool to predict these properties. Different approaches and models can be taken into account, including activity models and equations of state. The latest have become essential in modelling of vapour-liquid equilibrium. Many developments have been performed to improve these models, and it is not easy to select the appropriate model for a particular case.

3.1. Approaches for VLE Modelling

There are mainly two different approaches to model phase equilibrium [201]. The two approaches are based on the fact that at thermodynamic equilibrium, fugacity values are equal in both vapour and liquid phases, at isothermal conditions.

$$f_m^L(P,T) = f_m^V(P,T) \tag{3.1}$$

The first approach is based on activity model for the liquid phase and an equation of state for the vapour phase, the $\gamma - \Phi$ approach. The equilibrium equation (eq. 3.1) can be written:

$$\Phi_i^V y_i P = \gamma_i x_i f_i^{0L} \tag{3.2}$$

because

$$f_i^L(P,T) = \gamma_i x_i f_i^{0L} \tag{3.3}$$

and the vapour fugacity is calculated as follows:

$$f_i^V(P,T) = \Phi_i^V y_i P \tag{3.4}$$

The fugacity coefficient in the vapour phase is calculated using an equation of state. The fugacity of the pure compound, i, in the liquid phase can be written using the vapour pressure as:

$$f_i^{0L} = P_i^{Sat} \Phi_i^0\left(T, P_i^{Sat}\right) \exp\left(\frac{v_i^L\left(P - P_i^{Sat}\right)}{RT}\right) \tag{3.5}$$

The exponential factor is known as the Poynting factor and v_i^L is the molar volume, at saturation, of the compound i.

In case of gas solubility, the previous approach can be use for the solvent and for the solute using the following assumptions. A Henry's law approach is used for each component. As the solute(s) is (are) at infinite dilution, the asymmetric convention ($\gamma_{(i)} \rightarrow 1$ when $x_{(i)} \rightarrow 0$) is used to express the Henry's law (eq. 3.6) while the symmetric convention ($\gamma_{(1)} \rightarrow 1$ when $x_{(1)} \rightarrow 1$) is used for the solvent (eq. 3.7)

$$f_i^L(P,T) = H_i^L(T) \ x_i(T) \ \exp((\frac{v_i^\infty(T)}{RT})(P - P_i^{Sat})) \tag{3.6}$$

$$f_i^L(P,T) = \gamma_i^L \Phi_i^{sat} P_i^{sat} x_i(T) \times \exp((\frac{v_i^{sat}(T)}{RT})(P - P_i^{sat})) \tag{3.7}$$

Oppositely the second approach, the $\Phi - \Phi$ approach, uses an equation of state for each phase of the system. Thus the thermodynamic equilibrium can be written:

$$x_i \Phi_i^L(T,P,x_i) = y_i \Phi_i^V(T,P,y_i) \tag{3.8}$$

For each approach, the use of an equation of state is necessary. Equations of state can be classified in several categories: empirical equations, cubic equations, and equations based on statistical mechanics.

3.1.1. Virial Equations

These equations are used to accurately represent experimental properties of pure compounds. That is why these equations are dependent on numerous adjustable parameters, which require for their determination a large experimental database. However the large number of empirical parameters is a restriction to any kind of extrapolation, pressure or temperature independently of how accurate this kind of equation is. Moreover the extension from pure compounds to fluid mixtures is problematic, as in theory a mixing rule is needed for each parameter.

The virial equation of state is one of the most known of the large number of equations, which have been proposed. This equation is a development of the compressibility factor in series expanded in powers of the molar density with density-independent coefficients, B, C, and D:

$$Z = 1 + B(T)/v + C(T)/v^2 + D(T)/v^3 + \dots \tag{3.9}$$

where: $Z = \dfrac{Pv}{RT}$ (3.10)

The density-independent coefficients are known as virial coefficients. (B called the second virial coefficient, C the third and so on). In practice this equation is truncated after the third or the fourth coefficient. Some authors have found a rigorous theoretical basis for the virial equations in statistical thermodynamics, exact relations have been provided between the virial coefficients and the interactions between molecules [202]. Thus, the second virial coefficient depends on the interaction between two molecules, the third between three molecules, etc…

Following the same approach, different authors have proposed empirical equations. It can be cited for example one of the most known derivative equation of the virial equation, the *BWR* equation (eq. 3.11) developed by *Benedict, Webb and Rubin* [203] with 8 adjustable parameters. Many modifications have been proposed for this equation

$$Z = 1 + \left(\frac{B_0 RT - A_0 - C_0}{RTv} \right) + \left(\frac{bRT - a}{RTv^2} \right) + \frac{\alpha a}{RTv^5} + \left(\frac{c}{RT^3 v^2} \right) \left(1 + \frac{\gamma}{v^2} \right) \exp\left(\frac{-\gamma}{v^2} \right) \tag{3.11}$$

3.1.2. Cubic Equations of State

Since *van der Waals* has proposed the first cubic equation of state, a large number of equations have been proposed to predict thermodynamic properties of pure compounds or mixtures. Cubic equations of state are extension of the classical semi theoretical *van der Waals* equation of state; they were the first to predict successfully vapour phase properties. Many improvements and correction of this type of equation have been proposed. Among the large number of equations of state the *Redlich and Kwong* (*RK*), *Redlich Kwong and Soave* (*RKS*) and the *Peng-Robinson* (*PR*) are the most widely used in engineering applications.

3.1.2.1. van der Waals Equation of State

The first equation, which was capable of representing both gas and liquid phases, was proposed by *van der Waals* [204]. He tried to take into account the interaction between molecules. Considering the attractive and repulsive forces, he proposed to modify the kinetic pressure by a negative molecular pressure, $-a/v^2$, where attractive interaction between molecules are taken into account. The expression of the molecular pressure is directly linked to the potential expression of interaction between molecules. Moreover, he observed that considering the ideal gas law the volume should tend to zero when the pressure increases. That is why repulsive interaction by means of the molar co-volume b was added. This gives the van der Waals equation:

$$\left(P+\frac{a}{v^2}\right)(v-b)=RT \tag{3.12}$$

where a is the interaction parameter (or the energetic parameter) and b the molar co volume. The two van der Waals parameters a and b can be determined by applying the critical point conditions:

$$\left(\frac{\partial P}{\partial v}\right)_T=\left(\frac{\partial^2 P}{\partial v^2}\right)_T=0 \tag{3.13}$$

The values of the parameters at the critical point can be expressed as a function of the critical temperature and pressure:

$$a=\frac{27}{64}\frac{R^2T_C^2}{P_C} \tag{3.14}$$

$$b=\frac{1}{8}\frac{RT_C}{P_C} \tag{3.15}$$

$$Z_C=\frac{P_Cv_C}{RT_C}=0.375 \tag{3.16}$$

The *VdW-EoS* was the first able to describe the liquid - vapour transition and the existence of a critical point. It can be also noticed that this equation provides a better representation of the vapour phase than the liquid phase and that the liquid compressibility factor at critical point, 0.35, is overestimated in comparison with experimental factor, in

general lower than 0.3. Thus a large number of modifications have been proposed to improve the quality of predictions.

3.1.2.2. RK and RKS Equation of State

These equations are only modifications of the *VdW-EoS* through modification of molar pressure expression (term involving the attractive parameter *a*). In 1949, *Redlich and Kwong* [205] modified the attractive parameter in which the v^2 term was replaced by $v(v+b)$ and dependent on the temperature in order to improve vapour pressure calculations. *Soave* in 1972 [206] kept the *RK-EoS* volume function and introduced a temperature dependent function to modify the attractive parameter (α-function). He developed his function by forcing the *EoS* to represent accurately the vapour pressure at a reduced temperature equals to 0.7 in introducing a new parameter, the acentric factor of *Pitzer* [207], *ω*. Therefore *RKS-EoS* predicts accurately vapour pressures around a reduced temperature of 0.7:

$$\left(P + \frac{a(T)}{(v+b)v}\right)(v - b) = RT \tag{3. 17}$$

$$a(T) = a_c \, \alpha(T_r) \tag{3. 18}$$

with

$$\alpha(T_r) = \frac{1}{\sqrt{T}} \quad \text{for } RK\text{-}EoS \tag{3. 19}$$

$$\alpha(T_R) = \left[1 + m\left(1 - T_R^{1/2}\right)\right]^2 \quad \text{for } RKS\text{-}EoS \text{ with } m = 0.480 + 1.574\omega - 0.175\omega^2 \tag{3. 20) and (3. 21}$$

In analogy with the *VdW-EoS*, *a* and *b* were calculated from critical point conditions:

$$a = \Omega_a \frac{R^2 T_C^2}{P_C} \tag{3. 22}$$

$$b = \Omega_b \frac{RT_C}{P_C} \tag{3. 23}$$

$$\Omega_a = 0{,}42748 \tag{3. 24}$$

$$\Omega_b = 0{,}086640 \tag{3. 25}$$

$$Z_C = \frac{1}{3} \qquad\qquad (3.\,26)$$

However, it can be observed that even if the critical compressibility factor is smaller than the *VdW* critical compressibility factor, it is still overestimated. *RKS-EoS* is relatively predictive for non-polar compound (or compounds with acentric factor non-exceeding 0.6)

3.1.2.3. Peng-Robinson Equation of State

In 1976, *Peng and Robinson* [208] proposed a modified *Redlich and Kwong* equation of state through a modification of the attractive parameter. This equation gives better liquid density and critical compressibility factor, 0.307, than the *RKS-EoS*. This equation is used for polar compounds and light hydrocarbons (and heavy hydrocarbons through a modification of the α-function).

$$\left(P + \frac{a(T)}{(v^2 + 2bv - b^2)} \right)(v - b) = RT \qquad\qquad (3.\,27)$$

For the parameter:

$$a = \Omega_a \frac{R^2 T_C^2}{P_C} \qquad\qquad (3.\,28)$$

$$b = \Omega_b \frac{RT_C}{P_C} \qquad\qquad (3.\,29)$$

$$\Omega_a = 0,457240 \qquad\qquad (3.\,30)$$

$$\Omega_b = 0,07780 \qquad\qquad (3.\,31)$$

$$Z_C = 0,3074 \qquad\qquad (3.\,32)$$

Paragraph 5.1 will focus on temperature dependency of the attractive parameter through alpha function.

3.1.2.4. Three-Parameter Equation of State

A third parameter can be introduced into a cubic *EoS*. By introducing this additional factor, the critical compressibility factor becomes substance dependent and can be forced to predict the correct critical compressibility factor. Many cubic three-parameter equation of state have been proposed. *Schmidt and Wenzel* [209] proposed a general mathematical form to describe 4-parameter *EoS*:

$$P = \frac{RT}{v-b} - \frac{a\alpha(T_r)}{v^2 + ubv + wb^2}$$

(3. 33)

From the choice of the *u* and *w* comes the type of cubic *EoS*. If *u* and *w* are assigned to constant values a two parameters *EoS* is obtained and if one of the parameter either *u* or *w* are assigned to a constant values or some mathematical relationships between *u* and *w* are chosen, a three-parameters equation of state is obtained (TABLE 3.1).

Values of u and w	*Type of EoS*
$u = 0$ and $w = 0$	van der Waals [204]
$u = 1$ and $w = 0$	Redlich / Kwong [205], Soave / Redlich / Kwong [206]
$u = 2$ and $w = -1$	Peng/Robinson [208]
$w = 0$	Fuller [210], Usdin and Mc Auliffe[211]
$w = u^2 / 4$	Clausius [212]
$u + w = 1$	Heyen, Schmidt and Wenzel, Harmens and Knapp, Patel and Teja [213, 209, 214, 215]
$u - w = 3$	Yu *et al* [216]., Yu and Lu[217]
$u - w = 4$	Twu *et al.* [218]
$w = 2 (u + 2)^2 / 9 - u - 1$	VT-SRK [219]
$w = (u - 2)^2 / 8 - 1$	VT-PR [220]

TABLE 3.1 – RELATIONSHIP BETWEEN *u* AND *w*

The parameters can also be determined by applying the critical point conditions:

$$\left(\frac{\partial P}{\partial v}\right)_T = \left(\frac{\partial^2 P}{\partial v^2}\right)_T = 0$$

(3. 34)

In contrary to the classical *SRK* and *PR* cubic equation, the *Patel and Teja* [215] and the *Harmens and Knapp* [214] equations use the experimental compressibility factor. The calculation procedure is the following:

$$(v - v_C)^3 = v^3 - 3v_C v^2 + 3v_C^2 v - v_C^3 = 0 \qquad (3.35)$$

From equation (3.33) developed as a function of the volume and written at the critical condition, it comes:

$$v^3 - \left[\frac{RT_C}{P_C} - (u-1)b \right]v^2 - \left[\frac{RT_C}{P_C}ub - (w-u)b^2 - \frac{a}{P_C} \right]v - \left[\frac{RT_C}{P_C}wb^2 + wb^3 + \frac{ab}{P_C} \right] = 0 \quad (3.36)$$

Where

$$a = \Omega_a \frac{R^2 T_C^2}{P_C} \qquad (3.37)$$

$$b = \Omega_b \frac{RT_C}{P_C} \qquad (3.38)$$

$$c = \Omega_c \frac{RT_C}{P_C} \qquad (3.39)$$

From equations (3.35) and (3.36), the following system of equations (3.40) to (3.42) must be solved:

$$u\Omega_b = 1 + \Omega_b - 3Z_C \qquad (3.40)$$

$$\Omega_b^3 + \left[(1 - 3Z_C) + (u + w) \right]\Omega_b^2 + 3Z_C^2 \Omega_b - Z_C^3 = 0 \qquad (3.41)$$

$$\Omega_a = 1 - 3Z_C(1 - Z_C) + 3(1 - 2Z_C)\Omega_b + \left[2 - (u + w) \right]\Omega_b^2 \qquad (3.42)$$

Therefore, the values of a, b and c parameters can be found. Many cubic equations have been developed and virtually all of them can be generalised in using an attractive and a repulsive compressibility factor to decompose the compressibility factor:

$$Z = Z^{rep} - Z^{att} \qquad (3.43)$$

Where for *van der Waals EoS*, these two parameters are:

$$Z^{rep} = \frac{v}{v - b} \qquad (3.44)$$

$$Z^{att} = \frac{a}{RTv} \tag{3. 45}$$

TABLE 3.2 lists the different equations of state where the attractive parameter has been modified. In this table only the part concerning the attractive compressibility factor of the equation (3.43) is reported. *a(T)* means that the authors have chosen a temperature dependent *a* parameter.

Authors	*Attractive Term (Z^{att})*
Redlich and Kwong (RK) (1949) [205]	$\dfrac{a(T_C)}{RT^{1.5}(v+b)}$
Soave (SRK) 1972 [206]	$\dfrac{a(T)}{RT(v+b)}$
Peng and Robinson (PR)(1976) [208]	$\dfrac{a(T)v}{RT[(v+b)v+(v-b)b]}$
Fuller (1976) [210]	$\dfrac{a(T)}{RT(v+cb)}$
Heyen (1980) [213]	$\dfrac{a(T)v}{RT[v^2+(b(T)+c)v-b(T)c]}$
Schmidt and Wenzel (1980) [209]	$\dfrac{a(T)v}{RT(v^2+ubv+wb^2)}$
Harmens and Knapp (1980) [214]	$\dfrac{a(T)v}{RT(v^2+cbv-(c-1)b^2)}$
Kubic (1982) [221]	$\dfrac{a(T)v}{RT(v+c)^2}$
Patel and Teja (PT) (1982) [215]	$\dfrac{a(T)v}{RT[v(v+b)+c(v-b)]}$
Adachi *et al.* (1983) [222]	$\dfrac{a(T)v}{RT[(v-b^2)(v+b^3)]}$
Trebble and Bishnoi (TB) (1987) [223]	$\dfrac{a(T)v}{RT[v^2+(b+c)v-(bc+d^2)]}$

TABLE 3.2 – EXAMPLES OF CUBIC EQUATIONS OF STATE

Many studies have been done to compare the abilities of equations of state. The study of *Trebble and Bishnoi* [223] compared the vapour pressures of the 60 most used compounds in chemical process (hydrocarbons and light compounds) calculated with different equations of state.

TABLE 3.3 presents comparisons on pure compound vapour pressures, liquid and vapour volume in average absolute deviation. ($\Delta Y = \left| \dfrac{Y_{\exp} - Y_{cal}}{Y_{\exp}} \right|$).

It can be concluded that virtually all the equations give a fairly good representation of the pure compound vapour pressures, thanks to the development of alpha functions. The *SRK EoS* has some difficulties to correctly represent liquid densities.

Authors	$\Delta\left(P^{sat}\right)$ %	$\Delta\left(v_{liq}\right)$ %	$\Delta\left(v_{vap}\right)$ %
Soave (SRK) (1972) [206]	1.5	17.2	3.1
Peng and Robinson (PR) (1976) [208]	1.3	8.2	2.7
Fuller (1976) [210]	1.3	2.0	2.8
Heyen (1980) [213]	5.0	1.9	7.2
Schmidt and Wenzel (1980) [209]	1.0	7.9	2.6
Harmens and Knapp (1980) [214]	1.5	6.6	3.0
Kubic (1982) [221]	3.5	7.4	15.9
Patel and Teja (PT) (1982) [215]	1.3	7.5	2.6
Adachi *et al.* (1983) [222]	1.1	7.4	2.5
Trebble and Bishnoi (TB) (1987) [223]	2.0	3.0	3.1

TABLE 3.3 – DEVIATION ON THE PREDICTIONS OF VAPOUR PRESSURE, LIQUID AND VAPOUR MOLAR VOLUMES

A similar kind of study for gas-oil reservoir systems was also performed by *Danesh et al.* [225]. It can be concluded again that the *SRK-EoS* cannot correctly represent liquid densities (17.2% deviation in [224] and 25 % maximum deviation in [225]) while the *Peng Robinson EoS* with 2 parameters also give reliable results.

Danesh et al. [225] compared 10 equations of state with classical mixing rules for predicting the phase behaviour and volumetric properties of hydrocarbon fluids. They concluded that the *Valderrama* modification of the *Patel and Teja* cubic equation of state was superior to the other tested equations of state, particularly when the *EoSs* were compared without any use of binary interaction parameters. The *Valderrama-Patel-Teja* (*VPT*) [226] equation of state (*EoS*) is defined by:

$$P = \frac{RT}{v-b} - \frac{a\alpha(T_r)}{v(v+b)+c(v-b)} \tag{3.46}$$

with:

$$a = \frac{\Omega_a R^2 T_c^2}{P_c} \tag{3.47}$$

$$b = \frac{\Omega_b R T_c}{P_c} \qquad (3.48)$$

$$c = \frac{\Omega_c R T_c}{P_c} \qquad (3.49)$$

$$\alpha(T_r) = \left[1 + F\left(1 - T_r^{\Psi}\right)\right]^2 \qquad (3.50)$$

where P is the pressure, T is the temperature, v is the molar volume, R is the universal gas constant, and $\Psi = 1/2$. The subscripts c and r denote critical and reduced properties, respectively. The coefficients Ω_a, Ω_b, Ω_c, and F are given by:

$$\Omega_a = 0.66121 - 0.76105 Z_c \qquad (3.51)$$

$$\Omega_b = 0.02207 + 0.20868 Z_c \qquad (3.52)$$

$$\Omega_c = 0.57765 - 1.87080 Z_c \qquad (3.53)$$

$$F = 0.46286 + 3.58230(\omega Z_c) + 8.19417(\omega Z_c)^2 \qquad (3.54)$$

where Z_c is the critical compressibility factor, and ω is the acentric factor.

3.1.2.5. Temperature Dependence of Parameters

To have an accurate representation of vapour pressures of pure compounds a temperature dependence of the attractive term through the alpha function is imposed. Many alpha functions have been proposed to improve the precision of cubic equation of state via a more accurate prediction of pure compound vapour pressures. Some selected alpha functions are shown in TABLE 3.4.

Generally the mathematical expressions of alpha functions are either polynomials of various order in reduced temperature or exponential functions or switching functions. It is well established that alpha functions do not always represent accurately supercritical behaviour and they could have limited correct temperature utilization range. To improve their potential different approaches have been developed: use of alpha functions with specific compound parameter or switching alpha functions, even if mathematical constraints are associated with the latest, particularly in the continuity of the function and its derivatives. The alpha functions must verify some requirements:

- They must be finite and positive at all temperatures.

- They must be equal to 1 at the critical point.

- They must tend to zero when T tends to infinity.

- They must belong to the C2 function group, i.e. function and its derivatives (first and second) must be continuous, (for $T>0$) to assure continuity in thermodynamic properties.

Functions	Generalization	References
$\alpha(T_R) = \left[1 + m\left(1 - T_R^{1/2}\right)\right]^2$	For SRK Eos $m = 0.480 + 1.574\omega - 0.175\omega^2$	Soave [206]
	For SRK EoS $m = 0.47830 + 1.6337\omega - 0.3170\omega^2 + 0.760\omega^3$	Soave [227]
	For PR EoS $m = 0.374640 + 1.542260\omega - 0.26992\omega^2$	Peng and Robinson [208]
	$m = c_0 + c_1\left(1 + T_R^{0.5}\right)\left(0.7 - T_R\right)$ with $c_0 = 0.378893 + 1.4897153\omega - 0.17131848\omega^2 + 0.0196554\omega^3$ and c_1 is an adjustable parameter.	Stryjek and Vera [228]
$\alpha(T_R) = \left[1 + c_1\left(1 - T_R^{1/2}\right) + c_2\left(1 - T_R^{1/2}\right)^2 + c_3\left(1 - T_R^{1/2}\right)^3\right]^2$ if $T>T_C$ $\alpha(T_R) = \left[1 + c_1\left(1 - T_R^{1/2}\right)\right]^2$		Mathias and Copeman [229]
$\alpha(T_R) = \exp[m \times (1 - T_r)]$	$m = 0.418 + 1.58\omega - 0.580\omega^2$ when $\omega < 0.4$ $m = 0.212 + 2.2\omega - 0.831\omega^2$ when $\omega \geq 0.4$	Daridon et al. [230]

$\alpha(T_R) = \alpha^{(0)}(T_R) + \omega\left(\alpha^{(1)}(T_R) - \alpha^{(0)}(T_R)\right)$
with
$\alpha^{(i)}(T_R) = T_R^{N(M-1)}\left[\exp(L\left(1 - T_R^{NM}\right))\right]$

For SRK EoS

Parameters	$T_R \leq 1$		$T_R > 1$		Twu et al. [231-232]
	$\alpha^{(0)}(T)$	$\alpha^{(1)}(T)$	$\alpha^{(0)}(T)$	$\alpha^{(1)}(T)$	
L	0.141599	0.500315	0.441411	0.032580	
M	0.919422	0.799457	6.500018	1.289098	
N	2.496441	3.291790	-0.200000	-8.000000	

For PR EoS

Parameters	$T_R \leq 1$		$T_R > 1$	
	$\alpha^{(0)}(T)$	$\alpha^{(1)}(T)$	$\alpha^{(0)}(T)$	$\alpha^{(1)}(T)$
L	0.125283	0.511614	0.401219	0.024955
M	0.911807	0.784054	4.963075	1.248088
N	1.948153	2.812522	-0.20000	-8.00000

TABLE 3.4 – PRINCIPAL ALPHA FUNCTIONS [B3]

Different mathematical expressions satisfy these requirements. Historically *Redlich and Kwong* [205] were the first to propose a temperature dependence of the attractive parameter through an alpha function:

$$\alpha(T) = \frac{1}{\sqrt{T}}$$ (3. 55)

Classically, the alpha function expressions are:

- Exponential expression,

The *Trebble-Bishn*oi (*TB*) [224] alpha function is one of this kind of examples selected in this study

$$\alpha(T) = \exp\left[m \times \left(1 - \frac{T}{T_c} \right) \right]$$ (3. 56)

- Quadratic expression,

Different quadratic forms have been proposed:

- The *Soave* alpha function with one adjustable parameter [206].

$$\alpha(T) = \left[1 + m \left(1 - \sqrt{\frac{T}{T_c}} \right) \right]^2$$ (3. 57)

- The *Mathias-Copeman* (*MC*) alpha function with three adjustable parameters [229].

$$\alpha(T) = \left[1 + c_1 \left(1 - \sqrt{\frac{T}{T_C}} \right) + c_2 \left(1 - \sqrt{\frac{T}{T_C}} \right)^2 + c_3 \left(1 - \sqrt{\frac{T}{T_C}} \right)^3 \right]^2 \quad \text{if } T < T_c$$ (3. 58)

otherwise,

$$\alpha(T) = \left[1 + c_1 \left(1 - \sqrt{\frac{T}{T_C}} \right) \right]^2$$ (3. 59)

c_1, c_2 and c_3 are the three adjustable parameters

The repulsive parameter contrary to the attractive parameter is usually kept independent of the temperature.

3.1.2.6. EoS Extension for Mixture Application

Representation of mixtures phase equilibrium needs the knowledge of the parameters of the equation of state. With the two parameters (a, b) equations of state, the aim is to extend the calculation of the two parameters in taking into account the influence of each components. Various mixing rules exist to extend the equation discussed previously to mixtures.

The first mixing rules are the *van der Waals* mixing rules (known as the classical quadratic mixing rules) [204]. These mixing rules can be deduced from the composition dependence of the virial coefficients. Indeed, in developing the *vdW-EoS* in power series around zero density and in identifying the virial coefficients, different conditions can be obtained:

$$a = \sum_i \sum_j x_i x_j a_{ij} \tag{3. 60}$$

where

$$a_{ij} = \sqrt{a_i a_j} \left(1 - k_{ij}\right) \tag{3. 61}$$

And

$$b = \sum_i x_i b_i \tag{3. 62}$$

k_{ij} is called the binary interaction parameter. This parameter takes into account the attractive interaction between components and the fact that these interactions are different between each others.

The classical mixing rules can be applied for a 3-parameter cubic equation of state. Binary interactions in fluid mixtures are described by applying classical mixing rules as follows:

$$a = \sum_i \sum_j x_i x_j a_{ij} \tag{3. 63}$$

$$b = \sum_i x_i b_i \tag{3. 64}$$

$$c = \sum_i x_i c_i \tag{3. 65}$$

$$a_{ij} = \left(1 - k_{ij}\right) \sqrt{a_i a_j} \tag{3. 66}$$

where k_{ij} is the standard binary interaction parameter.

For polar-nonpolar interaction, however, the classical mixing rules are not satisfactory and more complicated mixing rules are necessary [233]. The non-density dependent (*NDD*) mixing rules developed by *Avlonitis et al.* [233] can be applied to describe mixing in the *a*-parameter:

$$a = a^C + a^A \tag{3.67}$$

where a^C is given by the classical quadratic mixing rules (eqs. 3.60 and 3.61). The term a^A corrects for asymmetric interaction which cannot be efficiently accounted for by classical mixing:

$$a^A = \sum_p x_p^2 \sum_i x_i a_{pi} l_{pi} \tag{3.68}$$

$$a_{pi} = \sqrt{a_p a_i} \tag{3.69}$$

$$l_{pi} = l_{pi}^0 - l_{pi}^1 (T - T_0) \tag{3.70}$$

where *p* is the index of polar components.

Many researchers have developed other mixing rules, derived from the classical mixing rules or based on excess Gibbs energy models, it can be cited for example the *Huron and Vidal* mixing rules [234], *Wong and Sandler* [235], the Modified *Huron and Vidal* mixing rules 1 and 2 [236-237]

Using an *EoS* and the associated mixing rules the fugacity of each component in all fluid phases is calculated from:

$$f_i = x_i \phi_i P \tag{3.71}$$

where *P* is the pressure, and x_i and ϕ_i are respectively the mole fraction and the fugacity coefficient of component *i*. The calculation of the fugacity coefficients using the *NDD* mixing rules, for a general *EoS* as well as the *VPT-EoS*, is given in Appendix B.

3.1.3. The γ – Φ approach

For each approach to solve the equilibrium (eq. 3.1) the use of an equation of state was necessary, to determine the fugacity of both vapour and liquid phase in the *Φ – Φ* approach, to express the fugacity in the vapour phase in the *γ – Φ* approach. The knowledge of different properties is necessary for the use of the *γ – Φ* approach. In case of gas solubility a Henry's

law approach is used for each component and the fugacities of the solute(s) i (eq. 3.6) in the solvent and of the solvent (eq. 3.7) can be expressed by:

$$f_i^L(P,T) = H_i^L(T) \; x_i(T) \; \exp\left(\left(\frac{v_i^\infty(T)}{RT}\right)(P - P_i^{Sat})\right) \tag{3.72}$$

$$f_i^L(P,T) = \gamma_i^L \Phi_i^{sat} P_i^{sat} x_i(T) \; \times \exp\left(\left(\frac{v_i^{sat}(T)}{RT}\right)(P - P_i^{sat})\right) \tag{3.73}$$

The Henry's constant, the molar volume at infinite dilution must be determined to express the fugacity of the solute, the activity coefficient and the molar volume at saturation for the solvent. The different models to determine the activity coefficient will be treated in the next paragraph (§3.1.5).

The Henry's constant can be calculated from various literature correlations. Some are given in TABLE 3.5. It can be noticed that mainly all Henry's constant for light hydrocarbons (from C1 to C8), acid gases (CO_2 and H_2S) and air gases, which are the main components of the natural gas are available in the literature.

Expression of the Henry's constant	Number of Solutes	Reference
$H_{i,w}(T) = 10^{A + B/T + C \times \log_{10}(T) + D \times T}$ (3.74)	>30	Yaws et al [238] (1999)
$H_{i,w}(T) = \exp\left(A + \dfrac{B}{T} + \dfrac{C}{T^2} + \dfrac{D}{T^3}\right)$ (3.75)	2	Prini and Crovetto [239] (1989)
$H_{i,w}(T) = \exp\left(A + B \cdot T + \dfrac{C}{T^2} + D \cdot \ln(T)\right)$ (3.76)	3	Tsonopoulos and Wilson [240](1983)
$H_{i,w}(T) = \exp\left(A + B \cdot T + \dfrac{C}{T^2} + D \cdot \ln(T)\right)$ (3.77)	3	Heidman et al. [241] (1985)
$H_{i,w}(T) = \exp\left(f_w^{sat} + A + \dfrac{B}{T} + \dfrac{C}{T^2}\right)$ (3.78)	7	Li and Nghiem [242] (1986)

TABLE 3.5 – EXPRESSION OF HENRY'S CONSTANTS OF SOME SOLUTES IN WATER

In TABLE 3.5, f_w^{sat} is the water fugacity at saturation. All A, B, C, D coefficients are given in the respective references; in table 3.6 their values are given for correlation (3.74). It should be noticed that the Henry's constant correlations are obtained from experimental data, solubility data in water or measurement via a dilutor technique.

Solute	A	B (10^3)	C	D	Tmin	Tmax
Argon	65.3235	-3.2469	-20.1398	0	273.15	348.15
Carbon Tetrafluoride	1507.2737	-41;9725	-599.35	0.409087	273.15	323.15
Methane	146.8858	-5.76834	-51.9144	0.0184936	273.15	360.95
Carbon Monoxide	74.5962	-3.6033	-23.3376	0	273.15	353.15
Carbonyl Sulphide	96.0707	-5.2224	-30.3658	0	273.15	303.15
Carbon Dioxide	69.4237	-3.796460	-21.6694	0.000478857	273.15	353.15
Acetylene	67.9714	-3.54393	-21.403	0	274.15	343.15
Vinyl Chloride	61.1868	-3.43853	-19.0984	0.00251906	273.15	323.15
Ethylene	107.7298	-6.3399	-31.7169	-0.0132533	283.15	360.95
Ethane	108.9263	-5.51363	-34.7413	0	275.15	323.15
Cycloproprane	-141.973	-5.87466	50.9015	0	298.15	361.15
Propylene	-2570.0227	68.674	1033.84	-0.719694	283.15	360.95
Propane	2874.113	-85.6732	-1128.09	0.70158	283.15	360.95
1-Butene	12.9593	-2.78226	0	0	311.15	378.15
Isobutene	103.9814	-5.54785	-32.8909	0	273.15	343.15
N-Butane	121.8305	-6.34244	-38.7599	0	273.15	349.15
Isobutane	161.2644	-7.9495	-52.4651	0	278.15	318.15
Chlorine Dioxide	-24.6413	-0.06.2181	10.7454	0	283.15	333.15
Chlorine	232.4396	-8.2198	-86.9997	0.0442155	283.15	353.15
Hydrogen	54.6946	-2.40098	-16.8893	0	273.15	345.15
Hydrogen Sulphide	10.8191	-1.51009	-39.93	-0.00681842	273.15	353.15
Helium	46.0252	-1.84993	-14.0094	0	273.15	348.15
Krypton	77.5359	-3.9528	-24.2207	0	273.15	353.15
Nitric Oxide	30.2512	-2.42215	-5.7049	-0.0119149	273.15	353.15
Nitrogen	78.8622	-3.744980	-24.7981	0	273.15	350.15
Nitrous Oxide	68.8882	-3.857750	-21.253	0	273.15	313.15
Neon	60.7869	-2.65134	-18.9157	0	273.15	348.15
Oxygen	77.8881	-3.79901	-24.4526	0	273.15	348.15
Phosphine	67.5831	-3.57648	-20.9165	0	298.15	323.15
Radon	109.3341	-5.64696	-35.0047	0	273.15	323.15
Sulfur Hexafluoride	191.8514	-9.19008	-62.9116	0	276.15	323.15
Sulfur Dioxide	22.3423	-1.98711	-5.6857	0	283.15	323.15
Xenon	87.3918	-4.56921	-27.4664	0	273.15	348.15

TABLE 3.6 – COEFFICIENT VALUES FOR (EQ. 3.74) AND RANGE OF UTILIZATION

Many correlations exist to estimate the partial molar volume of water at saturation: for example those developed by *Saul and Wagner* (1987) [243] or by *Rackett* [244].

$$\frac{\rho}{\rho_c} = 1 + 1.99206 \cdot \tau^{1/3} + 1.10123 \cdot \tau^{2/3} - 0.512506 \cdot \tau^{5/3} - 1.75263 \cdot \tau^{16/3} - 45.4485 \cdot \tau^{43/3} - 675615 \cdot \tau^{110/3}$$

with $\dfrac{1}{\rho} = v_w^{sat}$ and $\tau = 1 - \dfrac{T}{T_c}$ $\qquad$ (3. 79)

or $v_w^{sat} = \dfrac{RT_c}{P_C} \cdot (0.2905 - 0.08775 \cdot \omega)^{(1+(1-T_r)^{2/7})}$ $\qquad$ (3. 80)

In these expressions, T_c is the water critical temperature, P_c is the water critical pressure, ω is the water acentric factor and T_r is the water reduced temperature.

Values of the partial molar volume of the gas at infinite dilution in water can be found in the literature for some compounds, but also with a correlation, which is based on the work of *Lyckman et al.* [245] and reported by *Heidmann and Prausnitz* [246] in the following form:

$$\left(\frac{P_{c,i} \cdot v_i^\infty}{R \cdot T_{c,i}} \right) = 0.095 + 2.35 \cdot \frac{T \cdot P_{c,i}}{c \cdot T_{c,i}} \qquad (3. 81)$$

with P_{ci} and T_{ci}, solute critical pressure and temperature and c the cohesive energy density of water:

$$c = \frac{\Delta U_w}{v_w^{sat}} \text{ with } \Delta U_w = \Delta H_w - R \cdot T \tag{3. 82}$$

with ΔUw, energy of water vaporization (at zero pressure). For better high temperature dependence the following correction is used:

$$v_i^\infty(T) = \left[v_i^\infty(T)\right]_{Lyckman} + \left(\frac{dv_w}{dT}\right)^{sat} \times (T - 298.15) \tag{3. 83}$$

3.1.4. Activity Coefficient

The knowledge of activity coefficient values is necessary for the use of the $\gamma - \Phi$ approach. Activity coefficient, γ, is a useful tool to describe the non-ideality of a condensed phase. By definition, activity coefficient is mean to quantify the difference between the ideality and the real mixture:

$$f_i = \gamma_i f_i^{id} \tag{3. 84}$$

thus activity coefficient is defined by the equation:

$$\gamma_i = \frac{f_i}{f_i^{id}} = \frac{f_i}{x_i f_i^0} \tag{3. 85}$$

Activity a of a compound i is:

$$a_i = \gamma_i x_i \tag{3. 86}$$

As fugacity coefficients are related to the residual Gibbs energy, similar expressions for the activity coefficient can be expressed:

$$G^M = \sum_i N_i RT \ln a_i = G^E + \sum_i N_i RT \ln x_i \tag{3. 87}$$

And then the activity coefficient can be related at the excess free enthalpy by the following relation:

$$G^E(T, P, x) = \sum N_i RTLn(\gamma_i) \tag{3. 88}$$

or

$$\left(\frac{\partial G^E}{\partial N_i}\right)_{T,P,N_j} = RT \ln \gamma_i \tag{3. 89}$$

All excess properties can be deduced from the excess free enthalpy:

$$\left(\frac{\partial G^E/T}{\partial T}\right)_{P,N_i,N_j} = -\frac{H^E}{T^2} \tag{3.90}$$

$$\left(\frac{\partial G^E}{\partial T}\right)_{P,N_i,N_j} = -S^E \tag{3.91}$$

$$\left(\frac{\partial G^E}{\partial P}\right)_{T,N_i,N_j} = V^E \tag{3.92}$$

Non-ideality of mixtures is easily quantified using the excess Gibbs energy or the activity coefficient. For these purposes, different excess Gibbs models (G^E models) have been developed:

- NRTL model (Non Random Two Liquids)
- UNIQUAC.model (Universal Quasi Chemical)
- UNIFAC and Modified UNIFAC models, which are predictive models contrarily to the two previous models.

3.1.4.1.NRTL Model

The NRTL equation was proposed by *Renon and Prausnitz* [247] in 1968 and is based on expression of internal energy of mixing in terms of local compositions. The activity coefficient can be expressed as:

$$Ln(\gamma_i) = \frac{\sum_j \tau_{j,i} G_{j,i} x_j}{\sum_j G_{j,i} x_j} + \sum_j \frac{G_{i,j} x_j}{\sum_k G_{k,j} x_k}\left(\tau_{i,j} - \frac{\sum_k G_{k,j}\tau_{k,j} x_k}{\sum_k G_{k,j} x_k}\right) \tag{3.93}$$

with:

$$\tau_{j,i} = \frac{C_{i,j}}{RT} \tag{3.94}$$

$$G_{i,j} = Exp\left(-\alpha_{j,i}\frac{C_{j,i}}{RT}\right) \tag{3.95}$$

$$C_{i,i} = 0 \tag{3.96}$$

And the excess free enthalpy can be written as:

$$g^E = \sum_i x_i \sum_j \frac{x_j Exp\left(-\alpha_{j,i}\dfrac{C_{j,i}}{RT}\right)}{\sum_k x_k Exp\left(-\alpha_{k,i}\dfrac{C_{k,i}}{RT}\right)} C_{j,i} \tag{3.97}$$

It can be noticed that for a binary system the NRTL equation has 3 parameters ($\alpha_{i,j}$, $C_{i,j}$ and $C_{j,i}$) that can be adjusted on experimental data. Generally α_{ij} ($=\alpha_{ji}$) parameters are taken constant (for example : 0.2 or 0.3).

3.1.4.2.UNIQUAC Model

The UNIQUAC model was developed by *Abrams and Prausnitz* [248] (1975), and then by *Maurer and Prausnitz* (1978) [249]. This model is also based on the local composition concept. It expresses the mixing energy balance in function of the molecule external surfaces. Their authors have assumed that each compound can be divided in segments (volume parameter r_i) and that the interactions are dependent of the external surface of the compound (surface parameter q_i). Deriving the mixing internal energy, they have thus expressed the excess free enthalpy (or the activity coefficient) as a combination of two excess free enthalpies, which take into account the interactions between components (the residual excess free enthalpy (or a residual activity coefficient)) and the size parameters (r_i and q_i) of each component (the combinative excess free enthalpy (or a combinative activity coefficient)). The activity coefficient can be expressed in the following form:

$$Ln(\gamma_i) = Ln(\gamma_i)^{Com} + Ln(\gamma_i)^{Res} \tag{3. 98}$$

with

$$Ln(\gamma_i)^{Com} = Ln\left(\frac{\Phi_i}{x_i}\right) + \frac{z}{2} q_i Ln\left(\frac{\Theta_i}{\Phi_i}\right) + l_i - \frac{\Phi_i}{x_i} \sum_j x_j l_j \qquad \text{with} \quad z = 10 \tag{3. 99}$$

$$l_i = (r_i - q_i)\frac{z}{2} - (r_i - 1) \tag{3. 100}$$

$$\Theta_i = \frac{x_i q_i}{\sum_j x_j q_j} \tag{3. 101}$$

$$\Phi_i = \frac{x_i r_i}{\sum_j x_j r_j} \tag{3. 102}$$

and

$$Ln(\gamma_i)^{Res} = q_i \left[1 - Ln\left(\sum_j \Theta_j \tau_{ji}\right) - \sum_j \frac{\Theta_j \tau_{ij}}{\sum_k \Theta_k \tau_{kj}} \right] \tag{3. 103}$$

And the resulting excess Gibbs energy is:

$$g^E = g^{E,com} + g^{E,res} \tag{3. 104}$$

$$g^{E,com} = RT\left[\sum_i x_i Ln\left(\frac{\Phi_i}{x_i}\right) + \frac{z}{2}\sum_i x_i q_i Ln\left(\frac{\Theta_i}{\Phi_i}\right)\right] \tag{3. 105}$$

$$g^{E,res} = -RT\left(\sum_i q_i x_i Ln\left(\sum_j \Theta_j \tau_{ji}\right)\right) \tag{3. 106}$$

Therefore two kinds of parameters are needed for the UNIQUAC model, the geometric parameters (a volume parameter and a surface parameter) that are characteristic of each component and the binary parameters, which are determined from binary mixture experimental data. The geometric parameters have been determined from the molecule surface and volume proposed by *Bondi* (1964, 1968)

The UNIQUAC model such as the NRTL model is not a "full" predictive model, as they need experimental data for parameter adjustment. That is why predictive models based on the group contribution theory have been developed.

3.1.4.3. UNIFAC and Modified UNIFAC

The UNIFAC method was poposed by *Fredenslund et al.* in 1975 [252] and is based on the similar assumption as UNIQUAC: the excess free enthalpy (or the activity coefficient) is expressed as a combination of the residual excess free enthalpy and the combining excess free enthalpy. However, the authors have assumed that group interactions take place instead of molecule interactions provided the concerned compound is composed of these groups. The main difficulties associated with this model are therefore in the group decomposition of the compounds and that interactions between groups must be taken into account instead of component interactions. Parameters for group interactions can be found in the literature. The expression of the activity coefficient takes the form:

$$Ln\left(\gamma_i^{res}\right) = \sum_k \upsilon_k^{(i)}\left[Ln(\Gamma_k) - Ln\left(\Gamma_k^{(i)}\right)\right] \tag{3. 107}$$

with:

$$Ln(\Gamma_k) = Q_k\left[1 - Ln\left(\sum_m \Theta_m \Psi_{mk}\right) - \sum_m \frac{\Theta_m \Psi_{km}}{\sum_n \Theta_n \Psi_{nm}}\right] \tag{3. 108}$$

where:

$$\Theta_m = \frac{X_m Q_m}{\sum_n X_n Q_n} \qquad (3.\,109)$$

and X_m is the molar group fraction in the mixture and υ_k is the number of groups k in the mixture

$$\Psi_{mn} = Exp\left(-\frac{a_{mn}}{T}\right) \qquad (3.\,110)$$

where a_{mn} is the interaction parameter between the different groups. The combinatory parameter r_i and q_i are calculated with the following rules:

$$r_i = \sum_m \upsilon_{m,i} R_m \qquad (3.\,111)$$

$$q_i = \sum_m \upsilon_{m,i} Q_m \qquad (3.\,112)$$

with R_m and Q_m being respectively the volume and surface parameters of each group, m.

A modified version of the UNIFAC model has been developed (Modified UNIFAC). The expressions of the combining activity coefficients were modified to take into account the van der Waals volume and surface (r_i and q_i):

$$Ln(\gamma_i)^{Combinatoire} = 1 - V'_i + Ln(V'_i) - 5q_i\left(1 - \frac{V_i}{F_i} + Ln\left(\frac{V_i}{F_i}\right)\right) \qquad (3.\,113)$$

where:

$$V'_i = \frac{r_i^{3/4}}{\sum_j x_j r_j^{3/4}} \qquad (3.\,114)$$

$$V_i = \frac{r_i}{\sum_j x_j r_j} \qquad (3.\,115)$$

$$F_i = \frac{q_i}{\sum_j x_j q_j} \qquad (3.\,116)$$

3.2. Hydrate Phase Equilibria

Since many years, several studies have been performed on the prediction of hydrate forming conditions for various gas mixtures and inhibitors. Various correlations and models can be used.

3.2.1. Empirical Determination

Various correlations have been presented in the literature for predicting gas hydrate forming conditions. The first kind of method to determine hydrate-forming conditions is the *K*-values or the distribution coefficient method, which utilizes the vapour-solid equilibrium constant for predicting hydrate-forming conditions [253]. In assuming that hydrates are solid solutions, this *VSE* variable is empirically estimated from *K*-charts.

$$K_{vs,i} = \frac{y_i}{x_i} \tag{3.117}$$

where y_i is the mole fraction of the ith hydrocarbon in the gas phase and x_i is the mole fraction of the same component in the solid phase on water free basis. The hydrate forming conditions must verify the following equation:

$$\sum_{i=1}^{n} \frac{y_i}{K_{vs,i}} = 1 \tag{3.118}$$

K-charts can cover a wide range of temperatures and pressures. Many charts have been developed, by *Carson and Katz* [253], by *Mann et al.* [254]. However, the presence of non-hydrocarbon components leads to inaccurate prediction. The charts have been updated for the use of non-hydrocarbon gases: carbon dioxide, hydrogen sulphide, and nitrogen [254].

Another graphic determination is the use of gas-gravity method developed by *Katz* [255]. The gas gravity is defined as the apparent molecular weight of gas divided by that of air. The hydrate forming conditions, either pressure or temperature is read directly to a *P-T* graph, where hydrate-forming lines at constant gas gravity are plotted. These graphs are based on a limited amount of experimental data.

An alternative use to graph determination is the use of empirical correlations. The first, which can be cited, is the correlation developed by *Holder et al.* [256] for some selected pure gases:

$$P_H = \exp(a + \frac{b}{T}) \tag{3.119}$$

with *a* and *b* empirical coefficients, which are characteristic of the temperature range and the selected compound.

For natural gases, another method is the correlation developed by *Markogon* [257] taking into account the gas gravity:

$$\ln(P_H) = 2.3026\beta + 0.1144\,(T + kT^2)$$ (3. 120)

where

$$\beta = 2.681 - 3.811\,\gamma_g + 1.679\,\gamma_g^{\,2} \text{ and } k = -0.006 + 0.011\,\gamma_g + 0.011\,\gamma_g^{\,2} \text{ ((3.121) and (3.122))}$$

γ_g is the gas gravity.

A correlation was also proposed by *Kobayashi et al.* [258] based on the fit of gas-gravity plot.

$$T_H = 1/[A_1 + A_2\,\ln(\gamma_g) + A_3\,\ln(P) + A_4\,\ln(\gamma_g)^2 + A_5\,\ln(P)\ln(\gamma_g) + A_6\,\ln(P)^2 + A_7\,\ln(\gamma_g)^3 + A_8\,\ln(P)\ln(\gamma_g)^2$$
$$+ A_9\,\ln(P)^2\ln(\gamma_g) + A_{10}\,\ln(P)^3 + A_{11}\,\ln(\gamma_g)^4 + A_{12}\,\ln(P)\ln(\gamma_g)^3 + A_{13}\,\ln(P)^2\ln(\gamma_g)^2$$
$$+ A_{14}\,\ln(P)^3\ln(\gamma_g) + A_{15}\,\ln(P)^4]$$

(3. 123)

The coefficients are listed in TABLE 3.7.

Coefficients	Values
A_1	2.7707715×10^{-3}
A_2	-2.782238×10^{-3}
A_3	-5.649288×10^{-4}
A_4	-1.298593×10^{-3}
A_5	1.407119×10^{-3}
A_6	1.7885744×10^{-3}
A_7	1.130284×10^{-4}
A_8	5.972835×10^{-4}
A_9	$-2.3279181 \times 10^{-4}$
A_{10}	$-2.6840758 \times 10^{-5}$
A_{11}	4.6610555×10^{-3}
A_{12}	5.5542412×10^{-4}
A_{13}	$-1.4727765 \times 10^{-5}$
A_{14}	1.3938082×10^{-5}
A_{15}	$1.48850510 \times 10^{-5}$

TABLE 3.7 – COEFFICENTS OF THE EQUATION 3.123

All these empirical determinations have some restrictions and are not strongly accurate, even the latest with its 15 coefficients.

3.2.2. van der Waals-Platteeuw Model (Parrish and Prausnitz Development)

In case of *V(L)H* equilibrium, where *H* stands for the hydrate phase (structure I or II or h), the equilibrium conditions are:

$$f_g^L(P,T) = f_g^V(P,T) = f_g^H(P,T) \tag{3.124}$$

$$\mu_w^L(P,T) = \mu_w^V(P,T) = \mu_w^H(P,T) \tag{3.125}$$

Van der Waals and Platteeuw [259] were the first to propose a model for gas hydrate modelling. They have assumed some hypotheses:

- Each cavity contains at most one gas molecule
- No interaction between encaged molecules.
- The ideal gas partition is applicable to the guest molecules

They derived the statistical thermodynamic equations for the particular case of gas hydrate in assuming that the solid phase can be described by a model similar to that of *Langmuir* for gas adsorption.

The chemical potential of water in the filled hydrate lattice is expressed by the following equation:

$$\mu_w^H(P,T) = \mu_w^\beta + RT \sum_i^{NCAV} \lambda_i \ln\left(1 - \frac{\sum_k f_k C_{ki}}{1 + \sum_{ki} f_k C_{ki}}\right) \tag{3.126}$$

where:

- μ_w^β is the potential of water in empty lattice.
- λ_i is the number of cavities of type *i* per water molecule in the lattice.
- f_k is the fugacity of the component *i* in the gas phase.

The fugacity of the gaseous compound i in the vapour phase is calculated with an equation of state. (*EoS*).

$$f_i^V(P,T,y) = \varphi_m^V(P,T,y,EoS) \times P \times y_i \tag{3.127}$$

- C_{ki} is the Langmuir constant

Using the *Lennard-Jones-Devonshire* cell theory, they showed that the *Langmuir* constant can be expressed as:

$$C(T) = \frac{4\pi}{kT} \int_0^\infty \exp\left[\frac{-w(r)}{kt}\right] r^2 dr \tag{3.128}$$

where *w(r)* is the spherically symmetric cell potential and *k* is the Boltzmann's constant.

Here the first modification can be cited, this approach has been extended by *Parrish and Prausnitz* [260] to account for multiple guests in the hydrate structures. They described guest-host interaction in using a *Kihara* potential with a spherical core, therefore the cell potential becomes:

$$w(r) = 2z\varepsilon \left[\frac{\sigma^{12}}{R^{11}r} \left(\delta^{10} + \frac{a}{R} \delta^{11} \right) - \frac{\sigma^6}{R^5 r} \left(\delta^4 + \frac{a}{R} \delta^5 \right) \right] \tag{3. 129}$$

with

$$\delta^N = \left[\left(1 - \frac{r}{R} - \frac{a}{R} \right)^{-N} - \left(1 + \frac{r}{R} - \frac{a}{R} \right)^{-N} \right] / N \tag{3. 130}$$

R is the cell radius of the cavity, *z* is the coordination number, *a* is the core radius, *ε* is the characteristic energy and *σ+2a* is the collision diameter.

The chemical potential of water in a *β* phase (liquid or ice) is:

$$\mu_w^\alpha(P,T) = \mu_w^0(P,T) + RT \ln(a_w) \tag{3. 131}$$

where μ^0 is the chemical potential of pure water as ice or liquid and a_w is the activity of pure water as ice or liquid. It can be defined from equations 3.124 and 3.125 :

$$\Delta\mu_w^\alpha(P,T) = \Delta\mu_w^H(P,T) \tag{3. 132}$$

with:

$$\Delta\mu_w^\alpha(P,T) = \mu_w^\alpha(P,T) - \mu_w^\beta(P,T) \tag{3. 133}$$

and

$$\Delta\mu_w^H(P,T) = \mu_w^H(P,T) - \mu_w^\beta(P,T) \tag{3. 134}$$

The equation 3.132 can be written by use of 3.131 and classical thermodynamic as:

$$\frac{\Delta\mu_w^\alpha}{RT} = \frac{\Delta\mu^\alpha{}_0}{RT_0} - \int_{T_0}^{T} \frac{\Delta H_w^\alpha}{RT^2} dT + \int_{P_0}^{P} \frac{\Delta V}{RT} dP - \ln(a_w) \tag{3. 135}$$

where $\Delta\mu_0$ is the difference in the chemical potential of water in the empty lattice and in ice or liquid water at T_0=293.15 K, ΔH_w and ΔV are respectively the molar difference in enthalpy and volume between the empty lattice and ice or liquid water. The difference of enthalpy can be written as:

$$\Delta H_w^H = \Delta H_0 + \Delta C_p(T - T_0) \tag{3. 136}$$

ΔH_0 and ΔV are both considered to be pressure independent because pressure effects on condensed phases are small.

Therefore, to find the hydrate forming pressure at a given temperature or the hydrate forming temperature at a given pressure, the following equation must be solved:

$$\frac{\Delta\mu_0^\alpha}{RT_0} - \int_{T_0}^{T}\frac{\Delta H_0 + \Delta C_p(T-T_0)}{RT^2}dT + \frac{\Delta V}{R\overline{T}}(P-P_0) = \ln(a_w) - \sum_{i}^{NCAV}\lambda_i \ln\left(1 - \frac{\sum_k f_k C_{ki}}{1 + \sum_{ki} f_k C_{ki}}\right) \quad (3.137)$$

with

$$\overline{T} = (T - 273.15)/2 \quad (3.138)$$

The activity of water is calculated using one of the activity models described in the paragraph §3.1.5 and the other properties can be obtained from TABLE 3.8 [261]

Properties	Unit	Structure I	Structure II
$\Delta\mu_o$ (liq)	J/mol	1264	883
ΔH_o (liq)	J/mol	-4858	-5201
ΔH_o (ice)	J/mol	1151	808
ΔV_o (liq)	m³/mol	4.6e-6	5e-6
ΔV_o (ice)	m³/mol	3.0e-6	3.4e-6
ΔC_p (liq)	J/mol/K	39.16	39.16
ΔC_p (ice)	J/mol/K	0	0

TABLE 3.8– THERMODYNAMIC REFERENCE PROPERTIES FOR GAS HYDRATES

To simplify the calculations it can be noticed that the *Langmuir* coefficients have been already evaluated by various authors, as *Munck et al.* (eq 3.139 and TABLE 3.9) [261]:

$$C_i(T) = \frac{A}{T}\exp\left(\frac{B}{T}\right) \quad (3.139)$$

	Structure I				Structure II			
	Small cavity		Big cavity		Small cavity		Big cavity	
Components	A ($\times10^3$)	B	A ($\times10^3$)	B	A ($\times10^3$)	B	A ($\times10^3$)	B
Methane	0.7228	3187	23.35	2653	0.2207	3453	100	1916
Ethane	0	0	3.039	3861	0	0	240	2967
Propane	ND	ND	ND	ND	0	0	5.455	4638
i-butane	ND	ND	ND	ND	0	0	189.3	3800
n-butane	ND	ND	ND	ND	0	0	30.51	3699
Nitrogen	1.617	2905	6.078	2431	0.1742	3082	18	1728
Carbon dioxide	0.2474	3410	42.46	2813	0.0845	3615	851	2025
Hydrogen sulphide	0.025	4568	16.34	3737	0.0298	4878	87.2	2633

TABLE 3.9 – *A* AND *B* PARAMETERS FOR LANGMUIR COEFFICIENT EVALUATION

3.2.3. Modifications of the vdW-P Model

Various authors have extended the *vdW-P* model to improve the accuracy of the prediction. Instead of using the equality of the chemical potentials (3.125) they have chosen to solve the equality of the water fugacity (3.140).

$$f_w^\alpha(P,T) = f_w^V(P,T) = f_w^H(P,T) \qquad (3.140)$$

where α stands for the ice or liquid phase and the fugacity of the hydrate phase can be written in the following form:

$$f_w^H(P,T) = f_w^\beta(P,T) \exp\left(\frac{\Delta\mu_w^H(T,P)}{RT} \right) \qquad (3.141)$$

with f_w^β the fugacity of the hypothetical empty hydrate lattice

3.2.3.1. Classical Modifications

Sloan et al. (1976) [262] were the first to relate the fugacity of water in the hydrate phase to the chemical potential difference of water in the filled and empty hydrate. The empty hydrate fugacity of water can be expressed using the common phase equilibria equation with:

$$f_w^\beta(P,T) = \Phi_w^\beta P_w^\beta \ \exp\int_{P_w^\beta}^{P} (\frac{v_w^\beta}{RT}) dP \qquad (3.142)$$

The values of the fugacity of the empty hydrate or of the vapour pressure of the empty hydrate have been fitted to experimental data. The equation for the two empty hydrate structures vapour pressures proposed by *Sloan et al.* (1987) [263] are:

$$P_w^\beta (in\ atm) = 17.440 - \frac{6003.9}{T} \ \text{for structure I} \qquad (3.143)$$

$$P_w^\beta (in\ atm) = 17.332 - \frac{6017.6}{T} \ \text{for structure II} \qquad (3.144)$$

These correlations have been obtained by data fitting at a number of temperatures for different compounds.

Ng and Robinson [264] have reported the fugacity of the empty hydrate as a function of the temperature by fitting experimental data:

$$\ln(f_w^\beta) = \ln(f_w^{\beta 0}) + \left(\frac{d}{dP} \ln(f_w^\beta) \right)_T P \qquad (3.145)$$

where

$$\ln(f_w^{\beta 0}) = A^{I\,or\,II} - \frac{B^{I\,or\,II}}{T} \tag{3.146}$$

and

$$\left(\frac{d}{dP}\ln(f_w^{\beta})\right)_T = C^{I\,or\,II}T - D^{I\,or\,II} \tag{3.147}$$

Excellent results are obtained with this equation, but this model is not considered as a predictive one, it is used to represent experimental data. Moreover the thermodynamic consistency of this approach has been discussed and proved not to be acceptable [265], because the equation 3.147 is not in agreement with the classical thermodynamic:

$$\left(\frac{d}{dP}\ln(f_w^{\beta})\right)_T = \frac{v_w^{\beta}}{RT} \tag{3.148}$$

Moreover, it predicts a negative molar volume of the empty lattice for temperature below 287.8 K.

Klauda and Sandler [266] have also developed a modification of the *vdW-P* model. Their approach is similar to the *Sloan et al.* approach, previously described. They proposed a new approach to calculate the cell potential and they have developed different correlations to estimate the values of the molar volume and the vapour pressure of the empty lattice.

3.2.3.2. Chen and Guo Approach

They [267-268] have chosen to solve the following equilibrium equation:

$$f_i^{\alpha}(P,T) = f_i^{V}(P,T) = f_i^{H}(P,T) \tag{3.149}$$

The fugacity of the *i* hydrate former in the vapour phase is calculated with an equation of state:

$$f_i^{V}(P,T,y) = \varphi_m^{V}(P,T,y,EoS) \times P \times y_i \tag{3.150}$$

To model the hydrate phase they have proposed a two-step hydrate formation mechanism. The fugacity is expressed as the product of the hydrate former fugacity in the case of the gas phase is in equilibrium with an empty lattices hydrate phase and a second term based on the Langmuir theory.

For the first step of the mechanism, they assume the gas molecules dissolved in the aqueous phase will form clusters with a number of water molecules surrounding each guest molecule. These clusters and the dissolved gas molecules will form the first base of the hydrate also called « *basic hydrate* » by associating with each other. All the cavities (big

cavities) of the basic hydrate will be filled contrary to the cavities (small cavities) created by the clusters associations, which stay empty. This process is described by the following equation:

$$\mu_B(P,T) = \mu_w(P,T) + \lambda_2 \mu_g(P,T)$$ (3. 151)

where μ_B is the chemical potential of this basic hydrate. μ_w and μ_g are respectively the chemical potential of water and of the gas species, and λ_2 is the number of gas molecules per water in the basic hydrate.

In a second time the gas molecules dissolved into water are adsorbed by the linked cavity created by the association of the basic hydrate. Only small gas molecules (Ar, N_2, O_2, CH_4) can filled the linked cavities. The *Langmuir* adsorption theory is applied to describe the filling of the linked cavities by the small gas molecules. It can be noticed that this mechanism does not occur for larger molecule (ethane, propane…). The equation describing this mechanism is:

$$\mu_B(P,T) = \mu_B^0(P,T) + \lambda_1 RT \ln(1 - \sum_i \theta_i)$$ (3. 152)

$$\text{with } \sum_i \theta_i = \frac{\sum_i f_i C_i}{1 + \sum_i f_i C_i}$$ (3. 153)

and λ_1 is the number of linked cavities per water molecule in the basic hydrate.

With the classical thermodynamic equation 3.125 and in combining the previous equation, the equilibrium relation becomes:

$$\mu_g(P,T) = \mu_g^0(P,T) + RT \ln(f_i)$$ (3. 154)

$$f_i = x_i f_i^0 \left(1 - \sum_j \theta_j\right)^\alpha$$ (3. 155)

where

$$f^0_i = \exp\left[\frac{\mu_B^0(P,T) - \mu_W(P,T) - \lambda_2 \mu_g^0(P,T)}{\lambda_2 RT}\right]$$ (3. 156)

and

$$\alpha = \lambda_1 / \lambda_2$$ (3. 157)

As in the exponential term of equation 3.156, the term μ_w and μ_g are only dependent on the temperature, pressure and the water activity, the authors have assumed that this equation can be rewritten as the product of three functions representing the contributions of the temperature, the pressure and the water activity:

$$f_i^0(P,T) = f_i^0(P) \times f_i^0(T) \times f_i^0(a_w)$$ (3. 158)

with

$$f_i^0(a_w) = a_w^{-1/\lambda_2}$$ (3. 159)

$$f_i^0(P) = \exp\left(\frac{\beta P}{T}\right)$$ (3. 160)

where β equals to 0.4242 K/bar for structure I, and 1.0224 K/bar for structure II, respectively.

$$f_i^0(T) = A' \exp\left(\frac{B'}{T - C'}\right)$$ (3. 161)

The A', B' and C' coefficients are listed in TABLE 3.10:

Components	Structure I			Structure II		
	A' $(\times 10^{10})$	B'	C'	A' $(\times 10^{-23})$	B'	C'
Methane	158.44	-6591.43	27.04	0.52602	-12570	6.79
Ethane	4.75	-5465.6	57.93	0.00399	-11491	30.4
Propane	0.09496	-3732.47	113.6	0.23854	-13106	30.2
i-Butane	0.1	0	0	0.45138	-12850	37
n-Butane	0.1	0	0	0.35907	-12312	39
Argon	5.8705	-5393.68	28.81	0.73677	-12889	-2.61
Carbon dioxide	0.96372	-6444.5	36.67	0.34474	-12570	6.79
Hydrogen sulphide	443.42	-7540.62	31.88	0.32794	-13523	6.7
Krypton	3.8719	-5682.08	34.7	0.31982	-12893	4.11
Nitrogen	9.7939	-5286.59	31.65	0.68165	-127770	-1.1
Oxygen	6.2498	-5353.95	25.93	0.43195	-12505	-0.35

TABLE 3.10 – A', B' AND C' PARAMETERS FOR FUGACITY EVALUATION

The *Langmuir* constants have been correlated using the following expression:

$$C_i(T) = X \exp\left(\frac{Y}{T - Z}\right)$$ (3. 162)

The coefficients *X, Y* and *Z* are given in TABLE 3.11:

Compounds	$X\,(10^x)$	Y	Z
Ar	5.6026	2657.94	-3.42
Kr	4.5684	3016.7	6.24
N$_2$	4.3151	2472.37	0.64
O$_2$	9.4987	2452.29	1.03
CO$_2$	1.6464	2799.66	15.9
H$_2$S	4.0596	3156.52	27.12
CH$_4$	2.3048	2752.29	23.01

TABLE 3.11 – *X, Y* AND *Z* PARAMETERS FOR THE LANGMUIR CONSTANT EVALUATION

In case of equilibrium with ice the following equation is used to take into account of the temperature dependence:

$$f_i^0(T) = A'\exp\left(\frac{B'}{T-C'}\right) \times \exp\left(\frac{D(T-273.15)}{T}\right) \tag{3.163}$$

with $D = 22.5$ for structure I and $D = 49.5$ for structure II.

Experimental Study

Dans ce chapitre, diverses techniques expérimentales seront présentées. Dans un premier temps les techniques de mesures classiques des équilibres liquide-vapeur seront résumées, celles-ci pouvant être séparées en deux catégories : les techniques en circuit ouvert et les techniques en circuit fermé. Chacune de ces catégories pouvant elle aussi être subdivisées en deux sous catégories selon que la méthode est synthétique ou analytique.

Après avoir décrit ces différentes techniques, une revue plus spécifique aux méthodes de mesures de teneur d'eau est faite. La technique statique analytique avec échantillonnage des phases sera finalement la méthode employée pour la mesure des teneurs en eau des phases vapeur. Cette méthode sera également celle choisie pour la mesure de solubilité des différents gaz dans l'eau. Néanmoins une technique basée sur une cellule à volume variable sera utilisée pour la mesure de solubilité du dioxyde de carbone dans l'eau.

L'appareil, basé sur une technique statique analytique, utilisé au Centre for Gas Hydrate (Ecosse) sera finalement présenté.

4   Experimental Study

4.1   Literature Survey of Experimental Techniques and Apparatus

The study of phase equilibria is essential in petroleum, pharmaceutical and chemical industries. The deviations to ideality in phase equilibria are rarely negligible and these phenomena are particularly emphasized when the experimental condition are extreme (high pressure, low or high temperatures) or when the components are not alike (polar and non-polar compounds). The knowledge of phase equilibrium data is the basis for the design optimisation of many chemical processes, like separation process (distillation) or reservoir simulation during drilling or production or transport of petroleum fluids. The data are usually fitted thanks to the help of a model with adjustable parameters in order to interpolate and extrapolate the measured properties. There are many ways to obtain informations about the phase behaviour of fluid mixtures. The direct measurement of phase equilibrium data remains an important source of information; even predictive model needs a number of experimental points to adjust the interaction parameters and then obtain sufficiently accurate results. Unfortunately, for many systems particularly in extreme conditions, data are rare and prediction methods are inadequate.

Many instruments have been described in literature. The choice of the experimental technique depends on the temperature and pressure conditions. At low pressure (< 1 atm) the technique used is the ebulliometry. For high and intermediate -pressure phase equilibria the experimental methods can be divided into classes depending of:

- How the composition is determined:
    - by direct sampling methods (analytical methods)
    - or by indirect methods (synthetic methods)
- How the equilibrium is achieved:
    - by static method (the equilibrium is achieved by stirring of the phases)
    - or dynamic method, at least one of the phases circulates

4.1.1 Synthetic Methods

The principle of this method is to prepare a mixture of known composition [269] and then observe the phase behaviour in an equilibrium cell. The main difficulty of synthetic method is thus in the preparation of such a mixture. The pressure (or the temperature) is modified until the formation or the disappearance of a phase. This modification is detected either by visual observation of the resulting phenomenon (turbidity or meniscus) in a view cell or by recording a physical property presenting a discontinuity at the phase transition (break point in a graph). Each experiment yields one point of the *PTx* (or *PTy*) phase envelope. Different alternatives of these methods exist:

- "Synthetic-Dynamic" method, vibrating tube densimeters.

Various authors [270-271] have used a vibrating tube to measure the pressure, liquid and vapour densities at given temperatures. This technique allows a complete description of the compressed phases up to saturation points. The general principle of the vibrating tube densimeter has been reported by various authors, and is schematized in Figure 4.1.
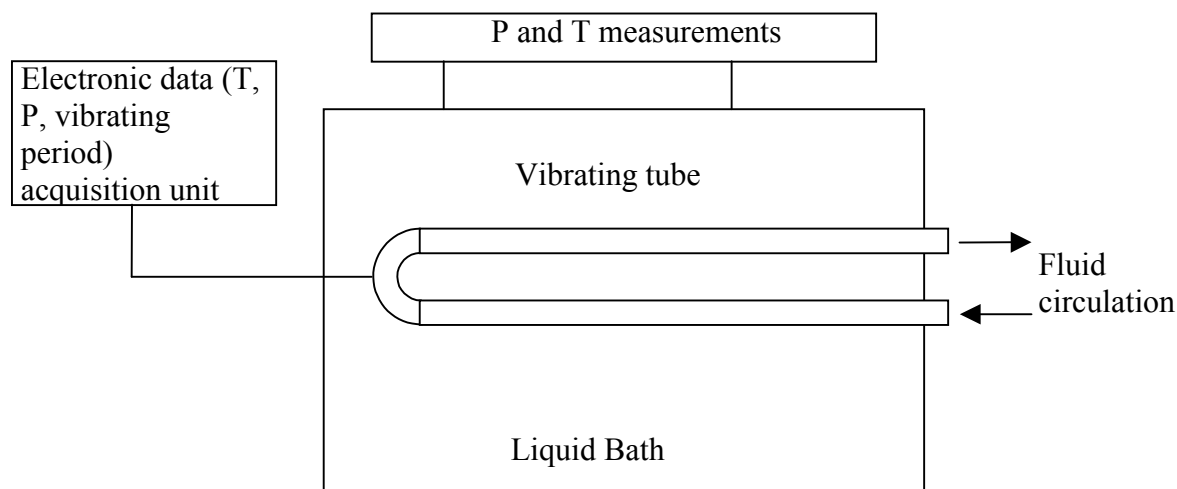
Figure 4.1: Principle of the vibrating tube densimeter

- Synthetic method with variable-volume cell

The variable-volume cell method (*Lesavre et al.* [272], *Fontalba et al.* [273]) allows the determination of bubble points. By changing the total volume of a cell, the appearance of a new phase can be obtained from the abrupt change in slope on the volume-pressure plot. For example a piston can allow liquid expansion until the apparition of the bubble point. The principle of the technique is described in the following figure:
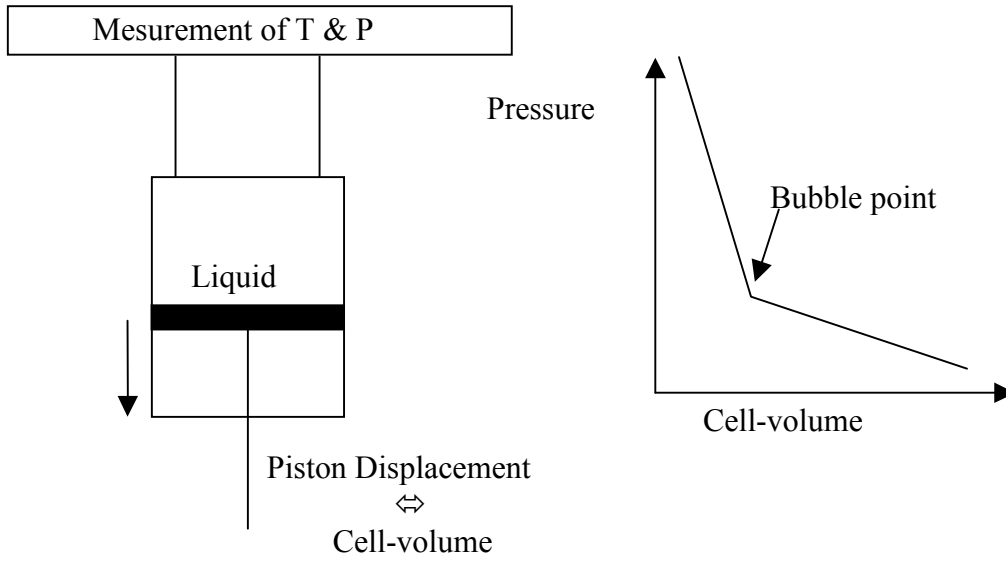
Figure 4.2: Principle of the variable volume cell method

Some difficulties are associated with this method especially when the operating conditions are close to the critical conditions of the mixture under study because the discontinuity in the slope becomes less and less distinct the more the conditions are close to the critical point.

- Synthetic methods with a fixed volume cell

The total pressure method using a fixed volume cell allows the determination of the vapour and liquid compositions from mass balance and thermodynamic equilibrium equations. The principle of this method has been described by *Legret et al.* [274]. The equilibrium at a given pressure and temperature is achieved in a cell of known volume. The vapour and liquid properties of the system can be calculated by solving the following equations (for a binary system):

$$n^L + n^V = n_1 + n_2 \tag{4.1}$$

$$n^L x_1 + n^V y_1 = n_1 \tag{4.2}$$

$$n^L v^L + n^V v^V = V_T \tag{4.3}$$

and at thermodynamic equilibrium: $y_i = K_i x_i$ \hfill (4.4)

This set of equations is solved in using an iterative method where at each step of the iteration the liquid and vapour molar volumes are calculated by means of a thermodynamic

model. For systems containing three components or more, solving of sets of equations become inaccurate.

4.1.2 Analytical Methods

Analytical techniques allow direct determination of the composition in both vapour and liquid phases in analysing each phase [275]. The principle of this technique is based on taking samples of the considered phase and then analysing them outside the equilibrium cell. Withdrawing a large sample from the cell would cause a non-negligible pressure drop, which would disturb the cell equilibrium. Therefore, the main difficulty is to find the more accurate tool to withdraw samples without disturbing the equilibrium. Avoiding any pressure drop can be achieved by using a variable – volume cell or a large equilibrium cell. The analysis of samples is generally carried out by gas or liquid chromatography. Different analytical methods exist:

- The recirculation method: one or more phases of the equilibrium can be re-circulated. In case of vapour-liquid equilibrium, the vapour (and the liquid) phase is (are) withdrawn continually and passed back in the equilibrium cell through the liquid (and vapour) phase by the action of a pump. Samples can be withdrawn by means of a sampling valve, generally a six-port valve with an external loop, placed in the recirculation loop. As the loop is filled continually with the flow of the recirculation, no pressure drop problem is encountered during the filling of the loop and the sampling, if the volume of the loop is negligible by comparison with the total volume of the set-up.
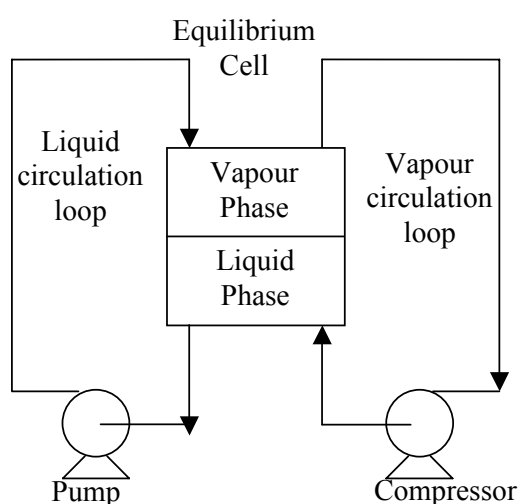
Figure 4.3: Principle of the recirculation technique

The temperature and the pressure in the loop and in the cell must be particularly well regulated to avoid any temperature or pressure variation, which could lead to complete incorrect results.

- The static-analytic technique: at a given temperature an equilibrium cell is charged with the desired system and after adjusting the pressure, an efficient stirring is started to achieve equilibrium. The pressure inside the cell generally decreases within a given period of time before reaching a plateau. At equilibrium samples are directly withdrawn from the desired phase and then swept for analysis. A flow diagram of this method is shown in Figure 4.4.
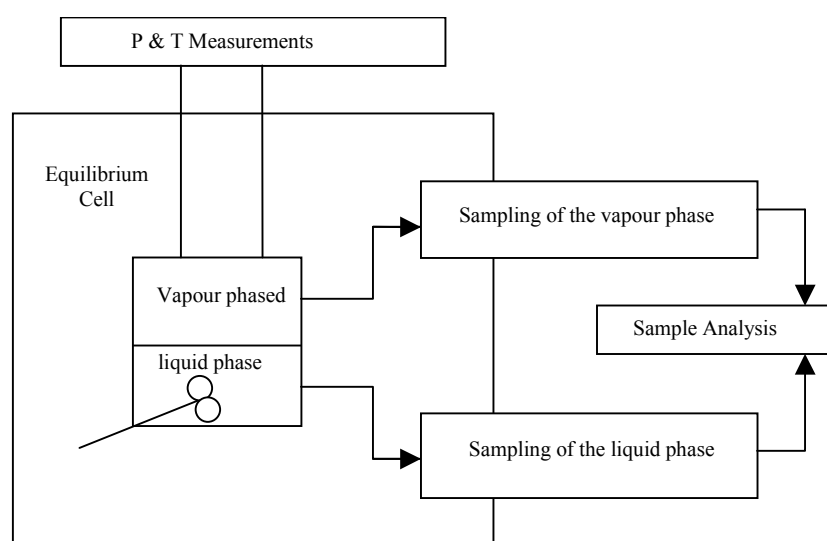
Figure 4.4: Flow diagram of static analytic apparatus

One of the apparatus used in this work is based on a static-analytic method with vapour and liquid phase sampling, which is carried out using a capillary sampler injector, ARMINES patent [276] Rolsi ™.

4.1.3 Stripping Methods, Measurement of Activity Coefficient and Henry's Constant at Infinite Dilution

Equilibrium is obtained dynamically inside the cell. This method is based on the variation of vapour phase composition when the highly diluted components of the liquid mixture are stripped from the solution by a constant flow of inert gas (helium or nitrogen) [277]. The variation with time of the concentration of the solute in the gas phase measured by gas chromatography provides a measure of infinite dilution activity coefficient.
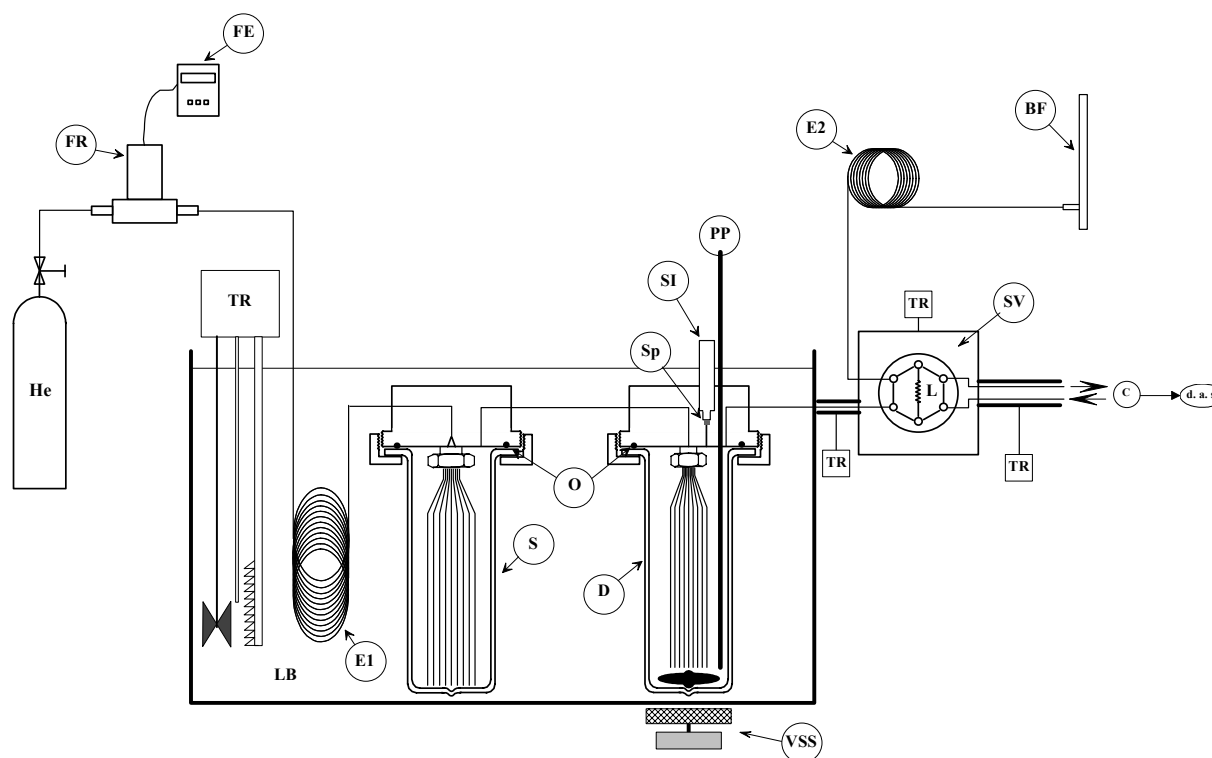
Figure 4.5: Flow diagram of the dilutor

BF : Bubble flow meter ; C : Chromatograph ; D : Dilutor ; d. a. s. : data acquisition system ; E1, E2 : Thermal exchangers ; FE : Flow Electronic ; FR : Flow Regulator ; L : Loop ; LB : Liquid Bath; O : O-ring ; PP : Platinum resistance thermometer Probe; S : Saturator ; SI : Solute Injector ; Sp : Septum ; SV : Sampling Valve ; TR : Temperature Regulator; VSS : Variable Speed Stirrer.

The principles and equipment have been fully described previously by *Legret et al.* [277]. A simplified flow diagram of the apparatus appears in Figure 4.5. On this figure, two 60 cm^3 cells are displayed, one upstream (saturator), permits to saturate the gas with the solvent while the second (dilutor) contains the highly diluted solute stripped from the solvent by the solvent saturated stripping gas.

Pure solvent is introduced in the "saturator cell" and in the "dilutor cell", while a small amount of the solute is introduced in the "dilutor cell". A constant stripping gas "helium" flow adjusted to a given value by means of a mass flow regulator bubbles through the stirred liquid phase and strips the volatile solute into the vapour phase. The composition of the gas leaving the dilutor cell is periodically sampled and analysed by gas chromatography using a gas-sampling valve. Equilibrium must be reached between the gas leaving the cell and the liquid phase in the cell. This can be checked by verifying the measured activity coefficient value does not depend on the selected eluting gas flow-rate. The peak area, S_i, of solute i decreases exponentially with time if the analysis is made in the linearity range of the detector. In these conditions, the activity coefficient, γ^∞, of solute i can be calculated with the equation

(4.5) where D is the carrier gas flow rate, N is the total number of moles of solvent in the cell, V_G is the volume of vapour phase in the dilutor cell, S_i the chromatograph peak area, t the time, T the temperature in the cell and R the ideal gas constant.

$$\gamma_i^{\infty} = -\frac{1}{t}\ln(\frac{S_i}{(S_i)_{t=0}}) \times \frac{R.T.N}{D + \frac{V_G}{t}\ln(\frac{S_i}{(S_i)_{t=0}})} \tag{4.5}$$

4.1.4 Review of the Experimental Set-Ups for Determination of the Water Contents

Many techniques have been developed for the analysis of water content /water dew point in gases. This investigation of the principles of water content /water dew point measurement will cover a brief description of the commonly used methods. Some parts of the material in this report are based on those reported by *van Rossum* [278] and by reference [B7].

The methods of gas water content / water dew point measurements can be divided following in to the different categories:

- Direct Methods
- Indirect Methods

4.1.4.1 Direct Methods

The direct methods (absolute methods) measure the dew point as temperature (or the water content as mass of water). These methods utilize a direct relationship between the measured quantity and the water content. In the ideal case, no calibration is necessary. Therefore, these techniques also are called absolute techniques. The following measuring methods belong to the direct methods:

1) The dew point mirror (Chilled mirror)
2) Karl-Fischer titration
3) The gravimetric hygrometer. The measuring principles are given in the TABLE 4.1.

Method	Measuring principle
Dew point mirror (Chilled mirror)	Temperature at which water or ice appears on a cooled surface
Karl-Fischer titration	Titration of absorbed water vapour with iodine
Gravimetric hygrometer	Increase in weight by absorption of water

TABLE 4.1– MEASUREMENT PRINCIPLES OF DIRECT METHODS [278]

Dew Point Mirror. The observation of dew point via a chilled surface, using either visual observation or instrumental detection of dew formation is a popular technique. For determination of the dew point with a dew point mirror, the gas flows over a chilled metal mirror- a small high polished plate of gold, rhodium, platinum or nickel- in a pressure tight chamber. Historically, the cooling of the surface is accomplished with acetone and dry ice, liquid gases, mechanical refrigeration and, more recently, by thermoelectric heat pumps. During cool down of the mirror, condensate forms on the mirror at the dew point temperature. Condensate is detected by suitable means. The mirror temperature can be measured with a resistance thermometer directly attached to the backside of the mirror. The mirror method is subject to contamination from heavy hydrocarbons and other components present in the gas. Depending on the kind of set-up, this method can measure dew point temperatures from 200 K to 370 K and accuracy of better than 0.3 K is possible.

Karl-Fischer Titration. This method involves a chemical reaction between water and "*Karl Fischer Reagent*", which is typically a mixture of sulphur dioxide, iodine, pyridine, and methanol. For many years, this method was limited to laboratory use because of the equipment and chemicals required to carry out the determination. Recently, the newer Karl Fischer methods are faster and more convenient than conventional methods for measuring water in hydrocarbons. The Karl Fischer titration can be divided into two basic analytic groups with respect to dosing or production of iodine, respectively:

a) The volumetric titration,

b) The coulometric titration.

During volumetric Karl Fischer titration, the water-containing sample is solved in a suitable alcoholic solvent and is titrated with a Karl Fischer solution. The volumetric titration is applied for estimation of larger amounts of water typically in the range of 1 to 100 mg. Compared to that, the coulometric Karl Fischer is a micro method. Iodine is not dosed in form of a solution but is directly used in an iodine containing solution via anodic oxidation. Due to its high analytic accuracy, it is suited for estimation of extremely low amounts of water (10 μg to 50 mg). Therefore, for measuring the water content of gases the coulometric Karl Fischer titration is the preferred choice, compared to the volumetric Karl Fischer titration.

Gravimetric Hygrometer. Gravimetric hygrometer gives absolute water content; since the weight of water absorbed and the precise measurement of gas volume associated with the water determine the absolute water content of incoming gas. Gravimetric methods are of two types: *freeze out* and *adsorption*. The freeze out technique can be used for gases containing light components (e.g. methane and ethane), because the condensation temperatures for these hydrocarbons are lower than that of water vapour. For the analysis of systems containing intermediate or heavy hydrocarbons (e.g. propane), the freeze out technique is very difficult because the intermediate or heavy hydrocarbons tend to condense along with water; as a consequence the separation of condensed phases is required before the amount of water can be determined. The small amounts of water and the loss that would occur on separation of the condensed hydrocarbons from the water rendered such a method of insufficient accuracy.

In the adsorption method, a test gas is pumped from a humidity generator through a drying train and a precision gas volume measuring system contained within a temperature-controlled bath. The precise measurements of the weight of water absorbed from the test gas and the associated volume of gas as measured at closely controlled temperature and pressure, accurately defines the absolute water content of the test gas in units of weight per unit volume. This system has been chosen as the primary standard because the required measurements of weight, temperature, pressure and volume can be made with extreme precision. The gravimetric hygrometer is a rather unwieldy instrument to use, and in the low water content ranges may require up to 30 hours per calibration point. For this reason, the gravimetric hygrometer is not used for normal measurement purposes and would not be useful for industrial measurement or control.

4.1.4.2   Indirect Methods

With the indirect methods as physical property depending on the water content is measured from which, the dew point or the water content has to be calculated. The indirect methods, being relative methods, always require calibration. When calibrating the relation between the properties measured (e.g. conductivity, frequency etc.) and the water content / water dew point is fixed empirically by comparing with a reference method. In other word, these methods can be made useful if the relationship between the water content / water dew point and the measured quantity can be determined empirically by comparison with a reference method. Such a reference method must be an absolute standard or a derivative of such a standard.

The indirect methods can be divided into three sub group: 1) Spectroscopic: a) Microwave b) Infrared c) Laser 2) Chromatographic: a) Detection of water b) Conversion to Acetylene   c) Conversion to Hydrogen   3) Hygroscopic methods: a) Electrolytic   b)

Capacitance   c) Change in mass (Quartz Crystal) d) Conductivity. The measuring principles of the most applicable indirect methods are given in TABLE 4.2.

Method	*Measuring principle*
Spectroscopic	The water content is measured by detecting the energy absorption due to the presence of water vapour.
Gas Chromatography	Size of the peak is proportional to the amount of the analysed sample.
Electrolytic*	The current due to electrolysis of the absorbed water at known constant gas flow rate is directly proportional to water vapour concentration
Capacitance*	The dielectric constant of aluminium oxide is a function of water vapour concentration
Change in mass (Quartz Crystal)*	Hygroscopic coating adsorbs water; crystal resonant frequency is a function of mass and thus related to water vapour concentration
Conductivity*	Salt / Glycerol solution absorbs water vapour; conductivity is a function of water vapour concentration

TABLE 4.2 – MEASUREMENT PRINCIPLES OF INDIRECT METHODS

* from [278]

Spectroscopic. The spectroscopic methods belong to optical instruments that measure the water content of gases by detecting the energy absorbed to vaporize water. The basic unit consists of an energy source, a detector, an optical system for isolating specific wavelengths, and a measurement system for determining the attenuation of radiant energy caused by the water vapour in the optical path.

These techniques for water content detection generally use radiations ranging from microwave (*MW*) frequencies to near infrared (*NIR*). In general, the higher the frequency, the less the depth to which waves penetrates. Therefore, *MW* tends to be used more for bulk measurements, while *NIR* would be used for small samples. Because of the large differences in wavelengths, even though all the instruments are measuring the same thing (water content), the mechanics of wave generation and detection differ. *MW* and *NIR* spectroscopic water content detectors cover a wide range of water content detectability, typically from 0.01% to over 99 % mol. For many applications, the technologies overlap, and the choice of detector will depend on the size of the sample, process flow, degree of precision, and cost. In contrast with the *MW* and *N*IR techniques that are used, Tunable Diode Laser Absorption Spectroscopy (*TDLAS*) is an extremely sensitive technique used for measuring very low levels—as small as typically 100 parts per trillion (*ppt*) of water content, or other species, in gases. In a *TDLAS* water content analyzer, an infrared laser beam traverses the gas of interest

and changes in the intensity due to water absorption are measured. Path lengths are increased by a mirrored cell to bounce the laser light back and forth, thus improving the sensitivity. The gas of interest can be flowing through the chamber, giving real-time monitoring capability. However, these analyzers are expensive and require continual maintenance to care for the optical system. Absorption by gases can also cause severe interference to this method.

Chromatographic. *GC* is extensively used in various forms for water content determination. Methods vary in complexity from simple injection and separation by *GC* where the sensitivity is low, to reaction with a reactant in *GC* where the water is converted into another compound, which exhibits a greater chromatographic response. The chromatographic technique allows analyzing water content on the thermal conductivity detector (*TCD*), which is a quasi-universal detector. The most difficult part associated with this technique is the calibration of the response of the detector as a function of the number of moles in the sample.

The sample can be treated with calcium carbide to produce acetylene (acetylene can be detected on a high sensitivity detector i.e.; a flame ionization detector (*FID*)) followed by determination of the gaseous product by *GC*. The determination of water using calcium carbide conversion has been the subject of several studies [279-286] and this technique has been proved to be accurate because the calcium carbide conversion could avoid absorption phenomena and allows a greater chromatographic response. The reaction of water vapour with calcium carbide is as follows:

$CaC_2 + 2 H_2O \rightarrow Ca(OH)_2 + C_2H_2$
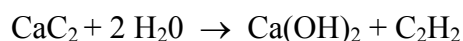
However it is known that when calcium carbide is present in excess, a further slow reaction takes place between calcium carbide and calcium hydroxide yielding another molecule of acetylene as expressed by the following equation:

$CaC_2 + Ca(OH)_2 \rightarrow CaO + C_2H_2$
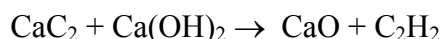
Nevertheless this method will not be accurate for the study of methanol containing samples as methanol reacts slowly with calcium carbide to form calcium methoxide and acetylene.

$2 CH_3OH + CaC_2 \rightarrow Ca(CH_3O)_2 + C_2H_2$
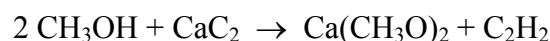
An alternative to calcium carbide is to find another product, which suits the following conditions: reactivity with water, complete decomposition of water in another compound, and no reactivity with C_1-C_4 hydrocarbons. Hydrides are compounds, which suit all the conditions. Hydrides generate hydrogen according to the following reaction:

$MH_x + x H_2O \rightarrow M(OH)_x + xH_2$
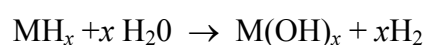
Where M is a metal of valence x. The most suitable hydride to conduct some tests is lithium aluminum hydride [287-288], because it has been proven that it can decompose completely water to hydrogen, as expressed by the following equation:

$LiAlH_4 + 4 H_2O \rightarrow Al(OH)_3 + LiOH + 4 H_2$
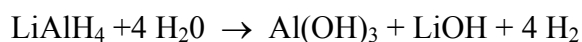
Hygroscopic methods. The hygroscopic methods make use of sensors that respond to the water vapour pressure in the gas. The surface properties of the sensors are important. They will be sensitive to temperature variations, contaminants in the gas, co-adsorption of other gaseous constituents, and past history of exposure.

Electrolytic. The electrolytic method is sometimes considered as being a direct method. This is only true if all of the water vapour flowing through the sensor is completely absorbed. For constant gas flow the amount of charge (current $\times$ time) is, by Faraday's law, a direct measure of the water content. In practice, however, instruments based on this method require to be calibrated because of the non-zero background current and because of the difficulty of ensuring that all of the water vapour is absorbed from the gas.

These sensors use a winding coated with a thin film of P_2O_5. As the desiccant absorbs incoming water vapour, an electrical potential is applied to the windings that electrolyses the water to hydrogen and oxygen. The current consumed by the electrolysis determines the mass of water vapour entering the sensor. The flow rate, and pressure of the incoming sample must be controlled precisely to maintain a standard sample mass flow rate into the sensor. Because the mechanism within the cell is complex, several additional phenomena may affect its operation.

Capacitance The sensor is fabricated from a thin strip of pure aluminium. The aluminium strip is anodized in sulphuric acid, resulting in a layer of porous aluminium oxide on its surface. A layer of gold or noble metal is evaporated over the aluminium oxide. This sandwich of compounds is essentially a capacitor, with the aluminium oxide layer the dielectric. Water vapour is rapidly transported through the noble metal layer and adsorbs onto the oxide as a function of partial pressure of water surrounding the sensor. The water molecules adsorbed on the oxide will cause a change in the dielectric constant of the sensor. A measure of the sensor impedance is a measure of the sample water partial pressure.

Depending on the water present in the stream, the impedance of the sensor can vary typically from 2 MΩ to 50 kΩ. Thus, the sensor receives a signal from the hygrometer electronics, and returns a signal to the electronics that is proportional to the water content in the measured stream.

These sensors can detect water content levels from as low as 1 part per billion (*ppb*) to as high as approximately 200,000 parts per million (*ppm*). It is not, however, designed to

measure water vapour at or near saturation conditions. Slugs of liquid condensate, glycol, methanol or water do not destroy it. It is designed for in-process mounting whenever possible, so as to eliminate the additional expense and complexity of sample conditioning.

The biggest limitation of the Aluminium Oxide sensor is periodic calibrations against standards are required to determine if its response has changed due to contact with corrosive substances such as strong acids or bases.

Change in mass (Quartz Crystal). This instrument compares the changes in frequency of two hydroscopically coated quartz oscillators. As the mass of the crystal changes due to adsorption of water vapour, its frequency changes correspondingly. The detector crystal is first exposed to the wet sample gas for a fixed period of time and then dried by a known dry reference gas. The difference in frequency between the wet and dry readings is proportional to the amount of water in the sample. In following this wet- dry cycle, the water partial pressure difference between the sample and detector is kept as great as possible. Thus, the quartz crystal type water content analyzer can inherently respond very rapidly to small changes in water content.

The quartz crystal method is one of the best methods for clean and single component gas; however it can suffer from co-adsorption of other gas constituents by the hygroscopic coating, and degradation of this coating.

This type of instrument is relatively expensive in commercial versions. In addition its flow sensitivity and calibration dependence, make it a difficult instrument to apply in general industrial applications.

Conductivity. The principle of measurement is based on the variation of the electrical conductivity of an unsaturated salt solution at varying gas water content. The saturation vapour pressure over an unsaturated salt solution is lower than over pure water. In this manner, the salt solution can absorb as much water from the surrounding medium until the vapour pressure of salt solution and that of the measuring medium are in equilibrium. The absorption of water in the salt solution causes it to become increasingly more conductive. The process is reversible, that is, with descending gas water content out of the salt solution and this decreases the conductivity. The vapour pressure equilibrium is more quickly achieved; the smaller the supply of salt solution there is and the faster the measuring mediums is transported to the salt solution. At the same time, the temperature of the sensor influences the response speed. In order to make the response speed of the sensor as fast as possible, one would have to construct very small sensors, so that the mass of the salt solution remains small. Because natural gases contain impurities, just a very small impurity would suffice with very little measuring electrolyte to destroy the sensor. The long-term stability of the sensor would not be very large. Conversely, the use of a very large amount of electrolyte in the

sensor would make the long-term stability very good, but the response speed would be unreasonably small. A solution to these opposing demands has been found in the construction of sensors today.

A typical sensor consists of two high grade steel plates, which are electrically isolated from each other by a ceramic layer. Small holes are drilled in the layer package, whose inside walls are coated with a very thin film of a salt / glycerol electrolyte.

In this manner a more or less conductive connection between the two steel plates occurs. Several parallel wired single electrodes are created in this way. Because of the parallel wiring of the electrodes, the danger of becoming soiled is much smaller than with just one electrode, while the response speed is the same as for one tiny single electrode.

In normally polluted natural gas the life time of the sensor is typically one year. The measuring accuracy after this time period is still sufficient, but the residue causes the sensors to be slower. For this reason, the sensors are replaced every three months. Afterwards, the sensors can be cleansed and newly coated with electrolyte. It is important in this context that the sensor calibrates itself and this by replacement no adjustment in the analyzing electronics are necessary. The most severe problem in this method is that the salt solution can be washed off in the event of exposure to liquid water.

4.1.5 Review of the Experimental Set-ups for Determination of Gas Solubilities

Solubility measurements at pressure higher than the atmospheric pressure are generally generated using static analytic apparati. The main difference between apparati is due to the sampling devices and the analytical way to quantify this solubility.

4.2 Description of the Apparati for Measurement of the Water Content and Gas Solubilities

A description of the different set-ups used for measurements of water content in the vapour phases of binary and multicomponents system as well of apparati for determination of gas solubilities in water will be given. A static analytic apparatus will be used for determination of the water content in the following system:

- Methane – water
- Ethane – water
- Methane – ethane – *n*-butane – water
- Methane – ethane – *n*-butane – water – methanol
- Methane – ethane – *n*-butane – water – ethylene glycol

Set ups based on the static analytic method will be used for determination of the gas solubilities in the following system:

- Methane – water
- Ethane – water
- Propane – water
- Nitrogen – water
- Carbon dioxide – water
- Hydrogen sulphide – water
- Methane – ethane – *n*-butane – water
- Methane – water – ethylene glycol

An apparatus based on the synthetic method with variable-volume cell will also be used for the determination of the carbon dioxide solubilities in water.

4.2.1 The Experimental Set-ups for Determination of the Water Content and Gas Solubilities

To determine the composition in the vapour phase of vapour –liquid and vapour-hydrate equilibria and the determination of the liquid composition of vapour liquid equilibria a static-analytic apparatus was used.

The group of measurements concerning the following systems is called GROUP 1:

- Methane – water, water content measurements
- Ethane – water, water content measurements
- Methane – ethane – *n*-butane – water, water content measurements
- Methane – ethane – *n*-butane – water – methanol, water and methanol content measurements
- Methane – ethane – *n*-butane – water – ethylene glycol, water content measurements
- Methane – water, gas solubility measurements
- Methane – ethane – *n*-butane – water, gas solubility measurements

The solubility measurements concerning the propane – water are called GROUP 2. The solubility measurements concerning the ethane –water, nitrogen –water, carbon dioxide – water and hydrogen sulphide – water system are called GROUP 3.

The phase equilibria for GROUP 1 were achieved in a cylindrical cell made of Hastelloy C276, the cell volume is about 34 cm^3 (*ID* = 25 mm, *H* = 69.76 mm) and it can be operated under pressures up to 40 MPa and from 223.15 to 473.15 K. The phase equilibria for GROUP 2 and GROUP 3 have been achieved in a cylindrical cell made partly with a sapphire tube; the cell volume is about 28 cm^3 (*ID* = 25 mm) and it can be operated at pressures of up to 8 MPa and from 223.15 to 473.15 K.

The different cells are immersed into an ULTRA-KRYOMAT LAUDA constant–temperature liquid bath that controls and maintains the desired temperature within 0.01 K. In order to perform accurate temperature measurements in the equilibrium cell and to check for thermal gradients, temperature is measured in two locations corresponding to the vapour and liquid phase by two Pt100 Platinum Resistance Thermometer Devices connected to an HP data acquisition unit (HP34970A). Pressures are measured by means of two Druck pressure transducers for all groups (type PTX 610 range 0-30 MPa and type PTX611, range: 0 - 1.5 MPa for GROUP1, 0 to 0.6 MPa and 0 to 6 MPa for GROUP2, 0 to 2 MPa and 0 to 6 MPa for GROUP3) connected to the same HP data acquisition unit (HP34970A) like the two Pt100; the pressure transducers are maintained at constant temperature (temperature higher than the highest temperature of the study) by means of home-made air-thermostat, which is controlled by a PID regulator (WEST instrument, model 6100).
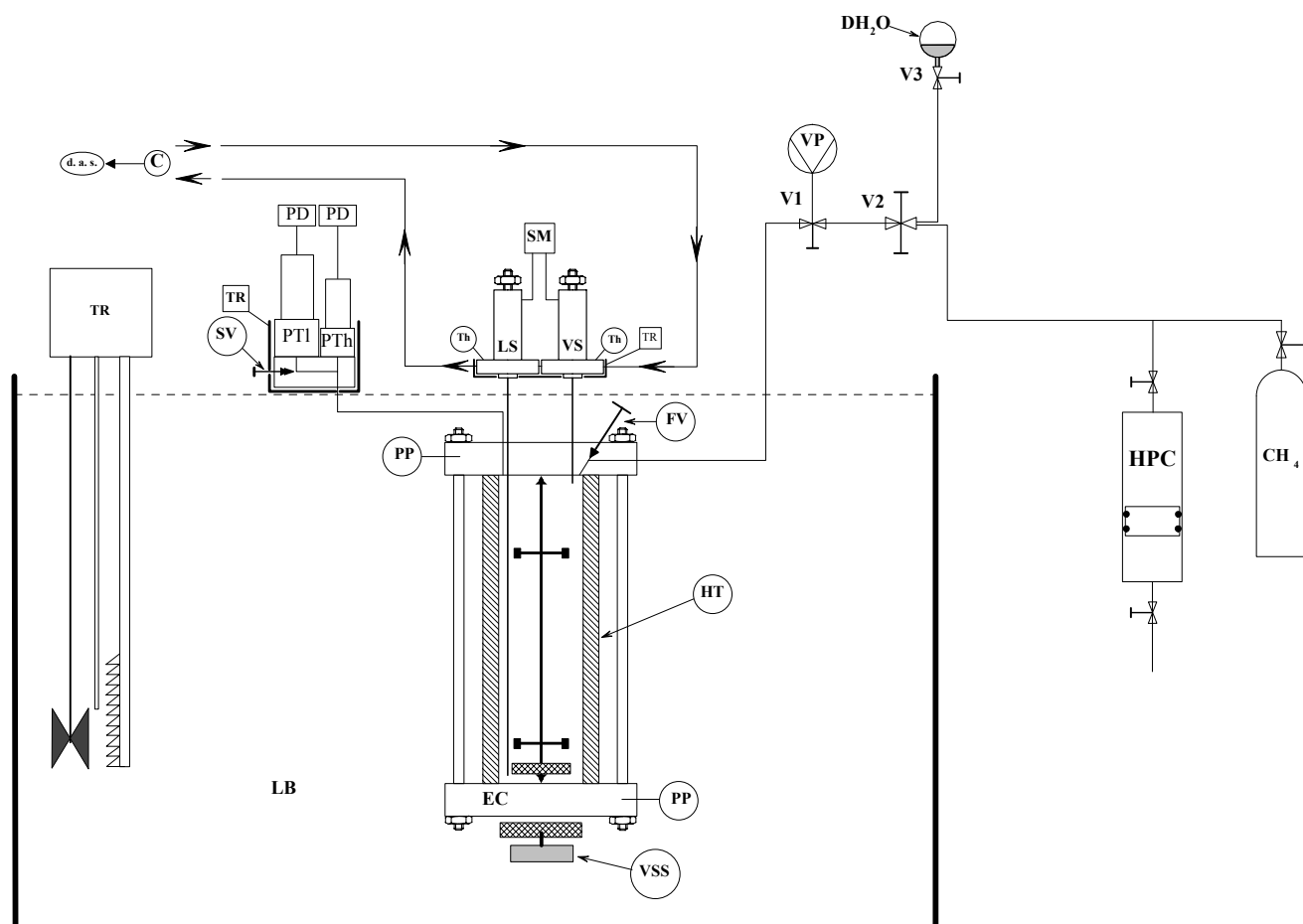
Figure 4.6: Flow diagram of the equipment

C : Carrier Gas; d.a.s: data acquisition system; DH$_2$O: Degassed Water; EC : Equilibrium Cell; FV : Feeding Valve; HPC: High Pressure Compressor; HT : Hastelloy Tube LB : Liquid Bath; LS : Liquid Sampler; PP : Platinum resistance thermometer Probe; PT : Pressure Transducer; SM : Sampler Monitoring; SV: Special Valve; Th : Thermocouple; TR : Temperature Regulator; Vi: Valve number i, VS : Vapour Sampler; VSS : Variable Speed Stirrer; VP : Vacuum Pump.

The HP on-line data acquisition system is connected to a personal computer through a RS-232 interface. This complete system allows real time readings and records of temperatures and pressures all along the different isothermal runs.

To achieve a fast thermodynamic equilibrium and to provide a good mixing of the fluids, a magnetic Teflon-coated stirrer, which is driven by an adjustable speed external magnetic system, is placed inside the cell.

The sampling is carried out using a capillary sampler injector, ARMINES patent, for each phase (Figures 4.7 and 4.8) [276]. Two capillary sampler-injectors, for each phase, are connected to the cell through two 0.1mm internal diameter capillary tube. The withdrawn samples are swept to a Varian 3800 gas chromatograph for analysis.
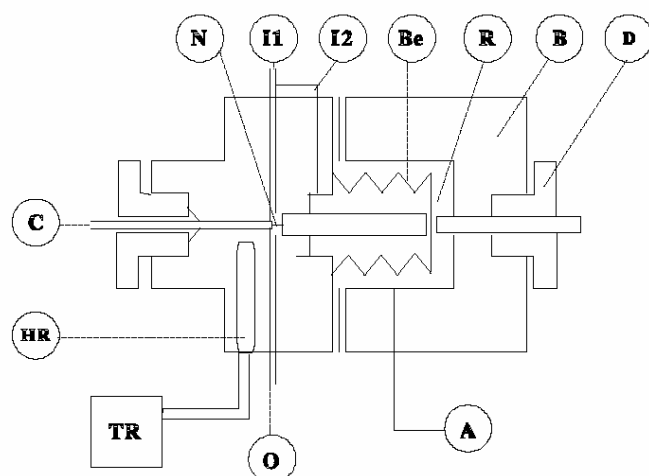
Figure 4.7: Flow diagram of the sampler-injector

A : Air inlet ; B : body ; Be : Bellow ; C : capillary tube ; D : differential screw; N :Micro needle; HR: Heating resistance; R: Expansion room; TR: Thermal regulator; I1, I2: Carrier gas inlet; O: Carrier gas outlet

Figure 4.8: Picture of a ROLSI [TM]

The capillaries of the two samplers are in contact with each phase and the carrier gas through the expansion room. This room is crossed by the gas, which sweeps the sample to be analyzed. They allow direct sampling at the working pressure without disturbing the cell equilibrium. The size of the sample can be varied continuously from 0.01 to several mg. The two samplers are heated independently from the equilibrium cell to allow the samples to be a vapour.

4.2.1.1 Chromatograph

Based on the laboratory experience and on the existing laboratory equipment the gas chromatography method was selected to perform the analyses. The Gas Chromatograph used is the Varian 3800 GC model. The chromatographic technique allows separating and quantifying the products of a sample.
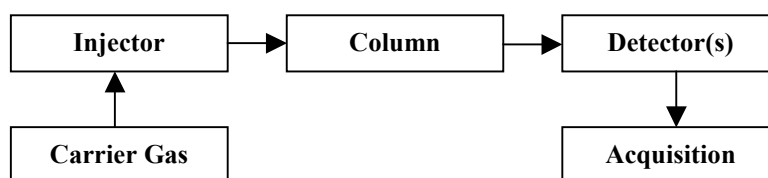
Figure 4.9: GC principle

The separation and the quality of the analysis is a function of the following parameters:

- Choice of the column
- Temperature of the oven column
- Choice of the carrier gas
- Flow rate of the carrier gas
- Parameters of the detectors

The chosen carrier gas, which has been used for most of the study, is helium (except for a set of test, where the carrier gas was nitrogen). To obtain a maximum sensitivity of the detector (thin peaks) the carrier gas flow rate is adjusted. Helium from Air Liquide is pure grade with 3 ppm water trace and 0.5 ppm hydrocarbon traces. To purify the carrier gas, the gas is cleaned by a molecular sieve, positioned at the outlet of the helium bottle.

Two detectors are used to perform the analyses: a Thermal Conductivity Detector and a Flame Ionization Detector, connected in series.

The TCD measures continuously the variation of the thermal conductivity of the carrier gas. The TCD is a non-destructive detector. To achieve a good analysis of the samples, the thermal conductivity of each compound must be as different as possible of that of the carrier gas (TABLE 4.3).

Compound	Thermal Conductivity at 373 K and 1 atm $(W.m^{-1}.K^{-1})$
Helium (Carrier Gas)	0.178
Methane	0.045
Ethane	0.032
n-Butane	0.024
Water	0.0244

TABLE 4.3 – THERMAL CONDUCTIVITY OF VARIOUS GASES

The FID is a detector, which measures the compound capabilities to form ions when it goes through the flame. The FID is a destructive detector, thus it is connected in series, at the outlet of the TCD.

4.2.1.2 Calibration of Measurement Devices and GC Detectors

The compositions of the vapour phase and of the liquid phase in a gas – water system are completely different, the vapour phase is mainly composed of the gaseous component and the liquid phase is mainly composed of water. Therefore to estimate the compositions of these two phases, different procedures and calibrations are needed.

4.2.1.2.1 Calibration of Pressure Measurement Sensors

All pressure transducers were calibrated against a dead weights balance (Desgranges and Huot, Model 520). Figure 4.10 shows the calibration curve of the PTX 611 0 – 30 MPa pressure transducer and Figure 4.11 illustrates the experimental calibration accuracy, which agrees with manufacturer specifications.). The uncertainties in the pressure measurements are estimated to be within ±0.5 kPa for the 0-1.6 MPa pressure transducer in a range up to 2.5 MPa and ±5 kPa for the 0-30 MPa pressure transducer from 2.5 to 38 MPa. Two polynomial expressions (of the second order) are used to estimate the pressure of both transducers.
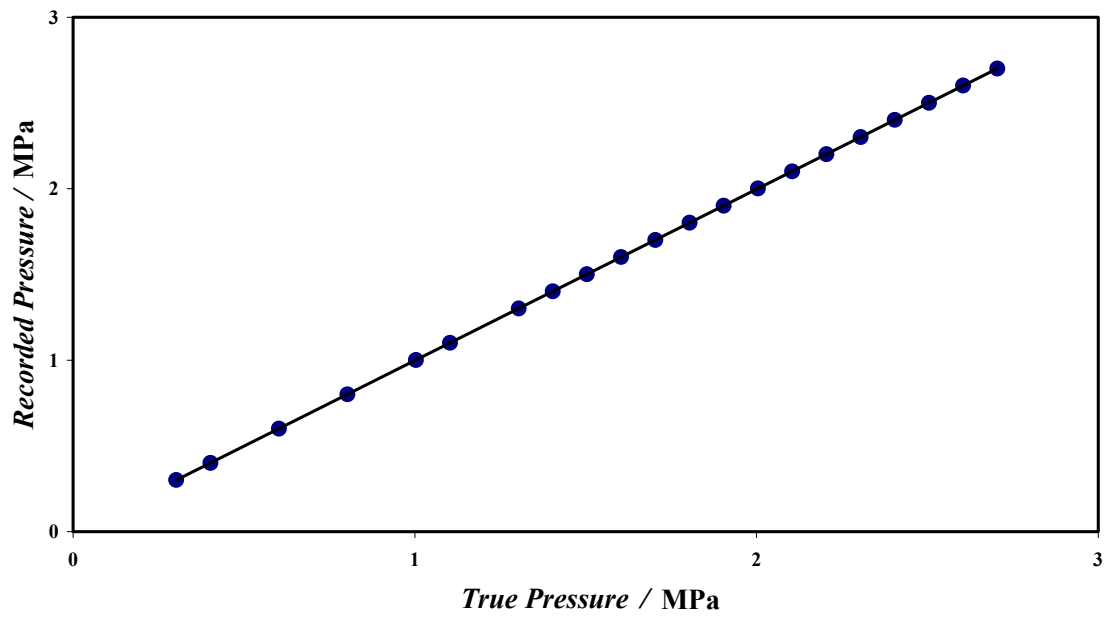
Figure 4.10: Pressure transducer calibration curve 0-1.6 MPa
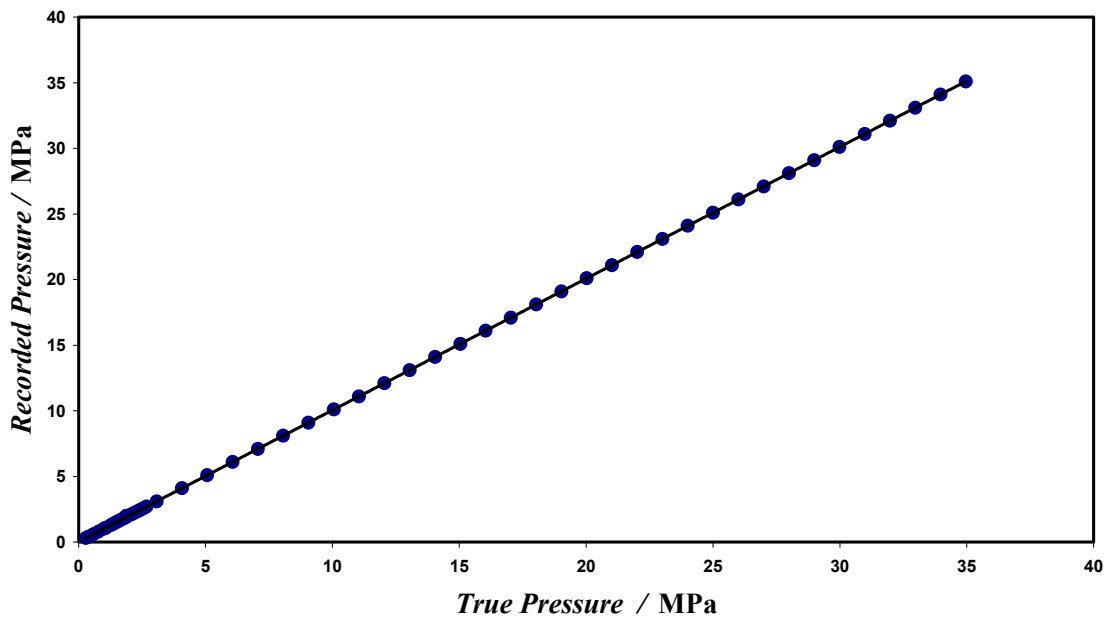
Figure 4.11: Pressure Transducer Calibration Curve 0-30 MPa
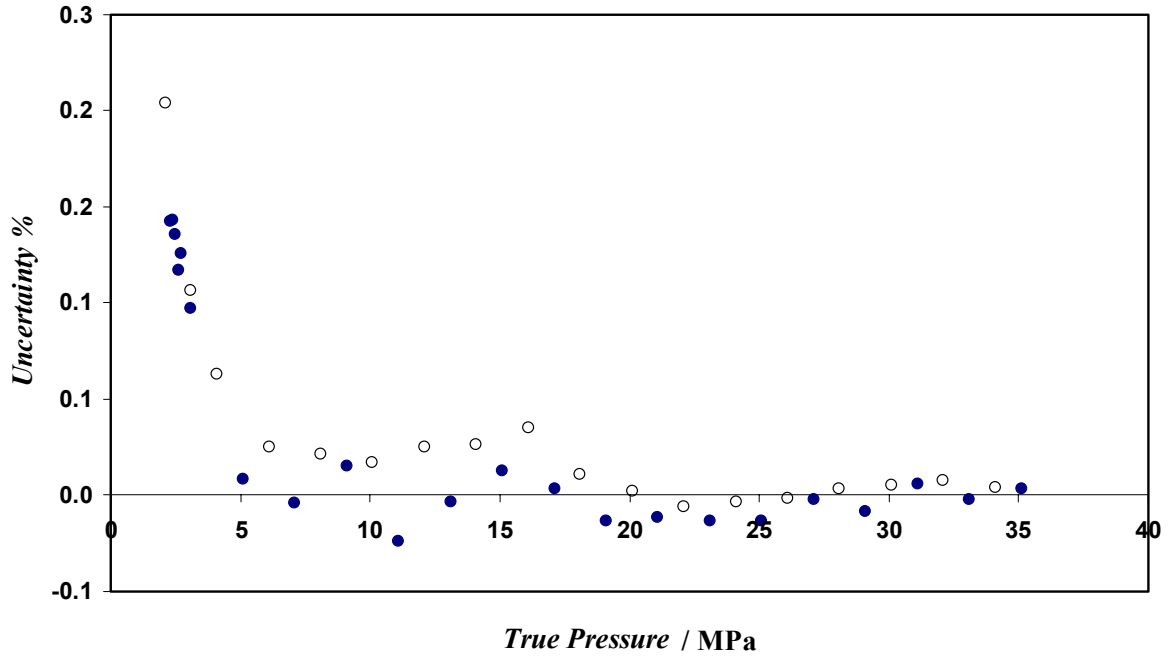
Figure 4.12: Pressure Transducer Calibration Relative Uncertainty 0-30 MPa

●, increasing pressure; ○, decreasing pressure; the uncertainty is the deviation between measured and calculated pressure

4.2.1.2.2 Calibration of Temperature Measurement Devices

The four Pt100 Ω are carefully and periodically calibrated against a reference four-wire Pt25 Ω Platinum Resistance Thermometer probe (TINSLEY type 5187 SA Precision Instruments). The resulting uncertainty is not higher than 0.02 K. The 25 Ω reference platinum resistance thermometer was calibrated by the Laboratoire National d'Essais (Paris) based on the 1990 International Temperature Scale (ITS 90).

The probes are finally calibrated from 253.15 to 313.15 K. The estimated uncertainty resulting from this calibration is +/- 0.02 K. Four polynomial expressions (of the first order) are used to calculate true temperatures through the four probes.
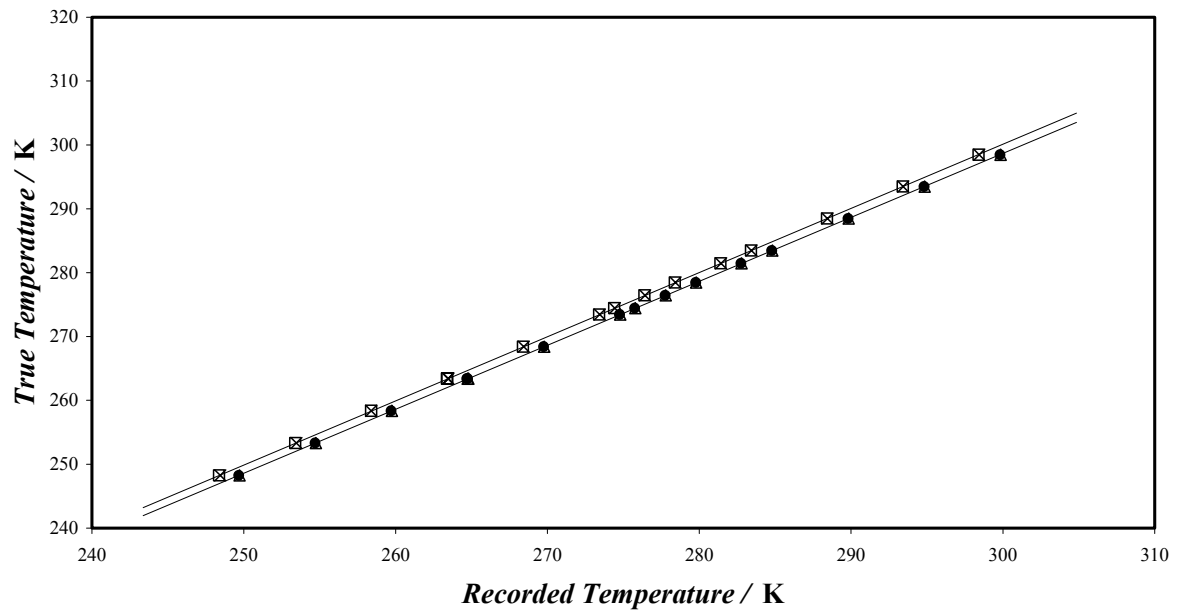
Figure 4.13: Pt 100 Platinum resistance thermometer probe calibrations

□, RTD1; ▲, RTD2; ●, RTD3; ✕, RTD4.
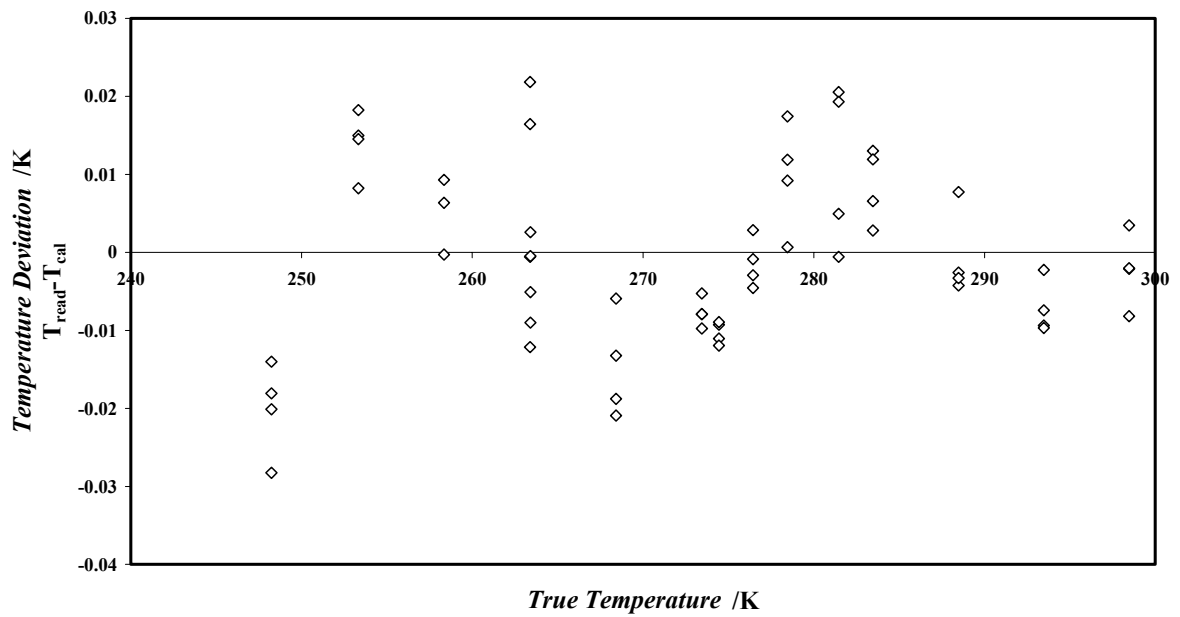
Figure 4.14: Temperature Probe Uncertainty (RTD1)

4.2.1.3 Determination of the Composition in the Vapour Phase

4.2.1.3.1 Calibration of the FID with Hydrocarbons (Vapour Phase)
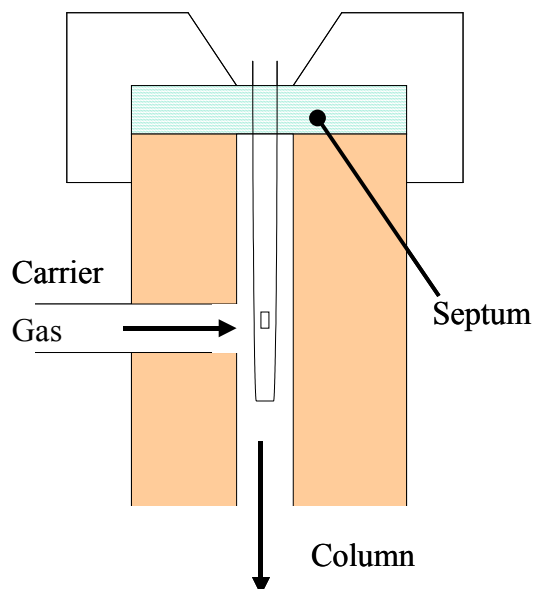
Only the FID was utilized to detect the hydrocarbons. The gases are simply injected in the chromatograph via the injector with gas syringes of given volumes: 1000-µl syringe for methane calibration and a 100-µl syringe for ethane and n-butane (Figure 4.15).

Figure 4.15: Simplified flow diagram of the injector

Calibration curves for the different hydrocarbons are obtained, that is a relationship between the response of the detector and the injected quantity. (Figures 4.16-4.18 for methane, ethane and n-butane respectively).
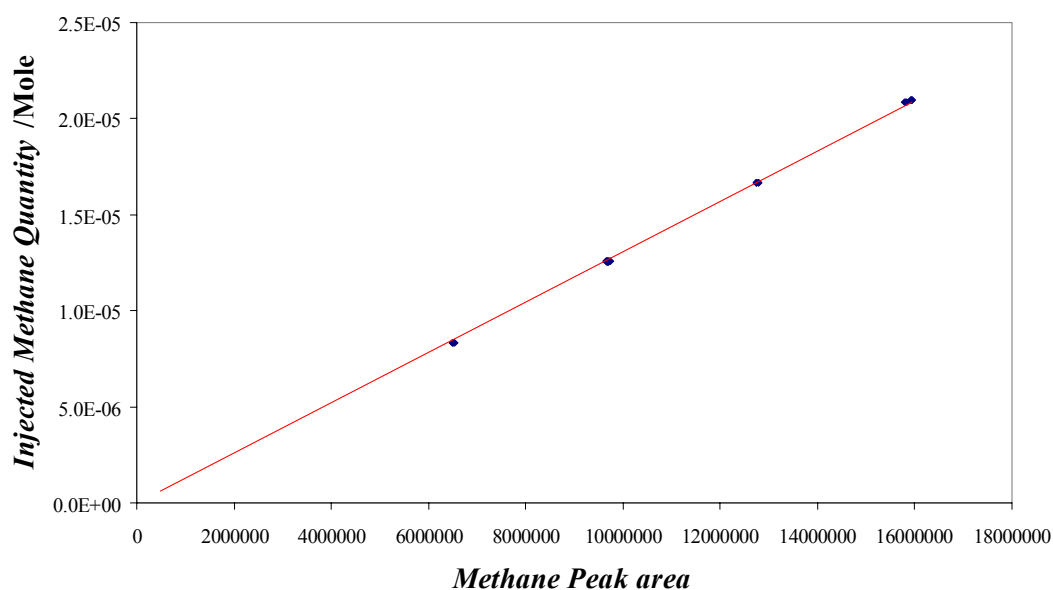
Figure 4.16: FID / methane calibration curve
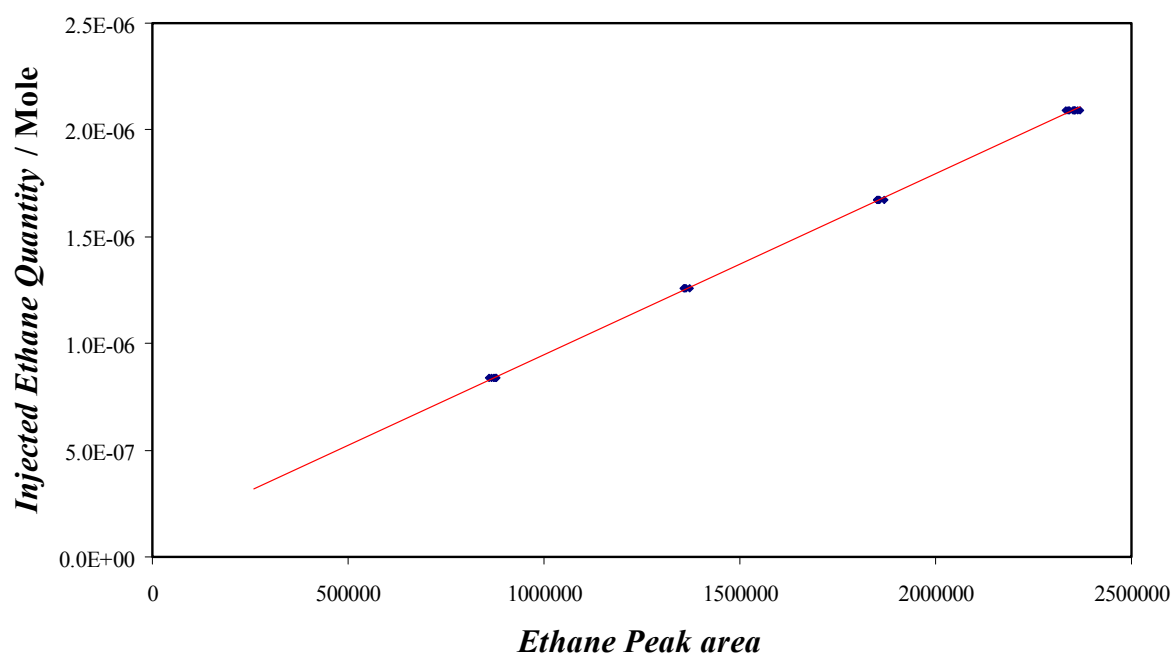
Figure 4.17: FID / ethane calibration curve
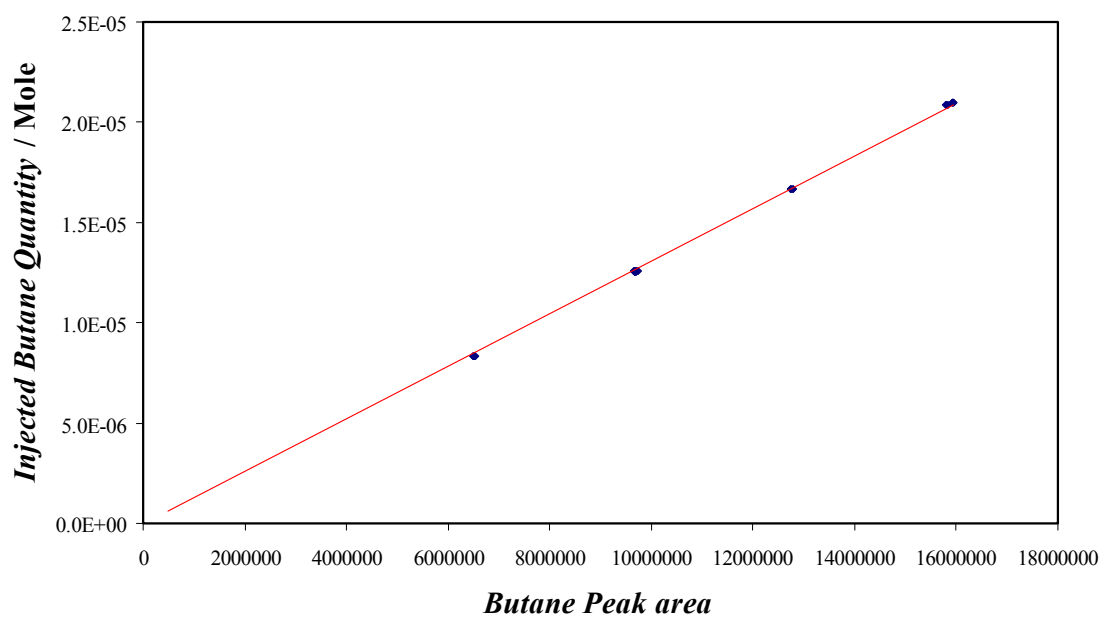
Figure 4.18: FID / n-butane calibration curve

Comparison between injected quantities and calculated quantities (after adjustment of the parameters of polynomial expressions) allows to estimate the calibration uncertainty, which is in a range of +/- 1% for methane (second order polynomial adjustment), of +/- 3%

for ethane (first order polynomial adjustment), (Figure 4.19) and of +/- 3% for n-butane (first order polynomial adjustment).
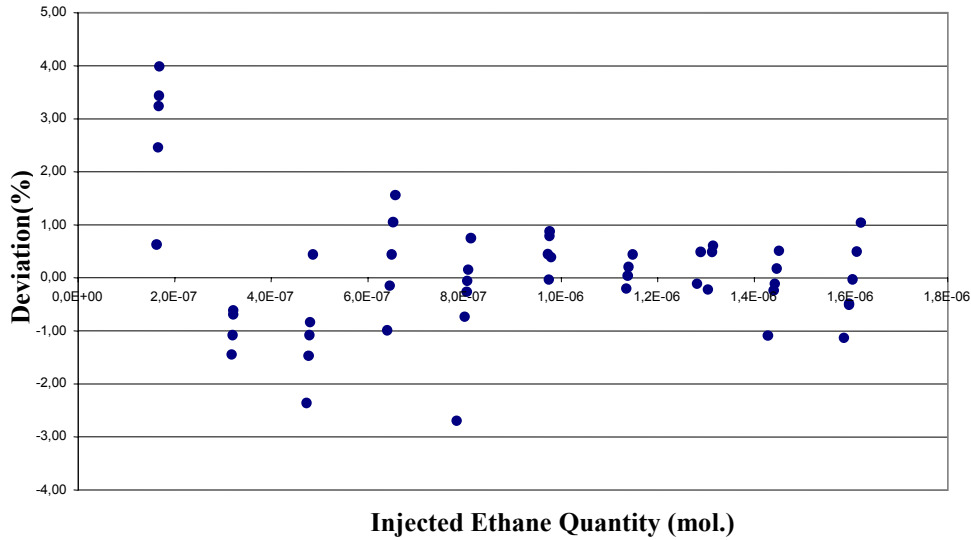
Figure 4.19: FID / ethane calibration uncertainty

4.2.1.3.2   Calibration of the TCD with Water (Vapour Phase)

The amount of water in the vapour phase is expected to be very low. Moreover it is known that the determination of traces of water in gases is one of the most difficult problems of trace analyses.

4.2.1.3.2.1 Estimation of the Water Content

For the estimation of the water content in the vapour phase of a dry and sweet gas, the water content of the water - methane systems has been investigated (Figure 4.20).

The water content in the vapour phase cannot be smaller than the water content in an ideal system at same pressure and temperature conditions. Thus the minimum water content, y_w^{min}, which can be present in the vapour phase is determined using the Raoult's law:

$$y_w^{min} = \frac{P_w^{sat}}{P_T}$$

(4. 6)

111

For example, if there is no hydrate at 268.15 K and 35 MPa, the minimum water content would be 1×10^{-5} mol fraction.
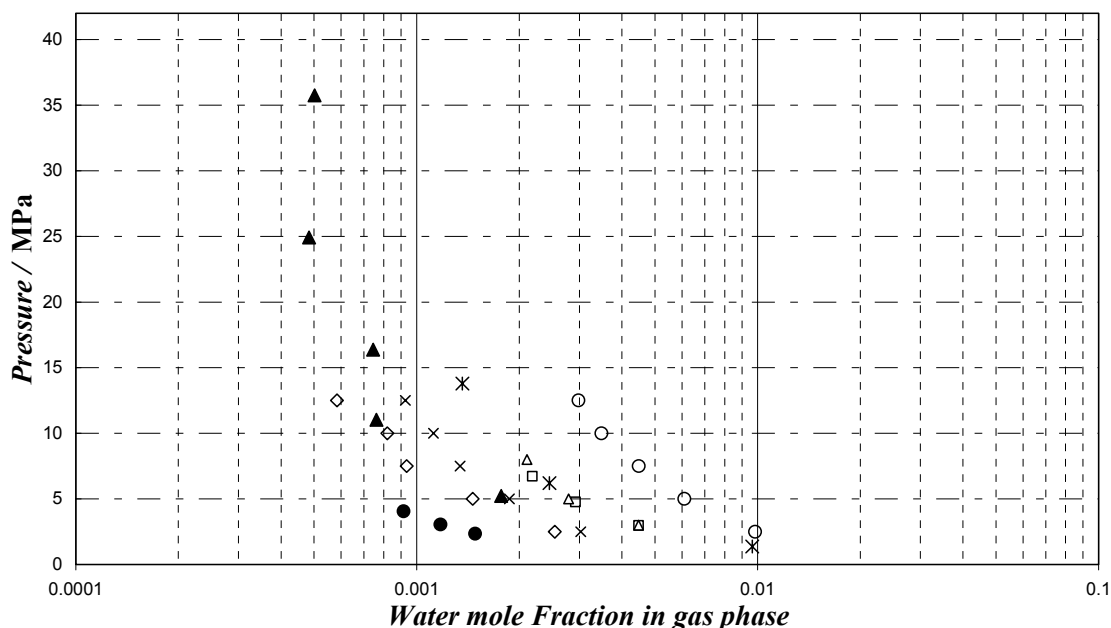
Figure 4.20: *Py*-diagram comparing selected experimental data at *T* > 298 K (semi logarithm scale): ●: data at 298.15 K from *Rigby and Prausnitz* (1968) [23], □: data at 298.15 K from *Rigby and Prausnitz* (1968) [23], ◇: data at 298.15 K from *Yarym-Agaev et al.* (1985) [18], ▲: data at 310.93 K from *Culberson and Mc Ketta* (1951) [24], ○: data at 338.15 K from *Yarym-Agaev et al.* (1985) [18], ×: data at 313.15 K from *Yarym-Agaev et al.* (1985) [18], *: data at 323.15 K from *Gillepsie and Wilson* (1982) [19], △: data at 323.15 K data from *Yokoyama et al.* (1988) [17].

These different examples show that at low temperatures and under high pressures the solubility of water in hydrocarbon gas phase can be lower than 50 ppm. Furthermore it is expected that addition of alcohol to the water –hydrocarbons system will increase the solubility of hydrocarbons in water and decrease the solubility of water in the gas. Thus the water calibration should be done in a range of 10^{-10} to 10^{-8} mole of water.

4.2.1.3.2.2 Calibration Method

The water concentration is expected to be very low, so calibrating the detectors under these conditions is very difficult. It is indeed impossible to correctly inject such a small quantity in the chromatograph using syringes. In fact the water quantity, which must be detected and quantified, is of the same order as the water quantity adsorbed on the syringe

needle walls (due to the ambient humidity). For calibration purposes, the cell of a dilutor apparatus [277] is used with a specific calibration circuit (Figure 4.21).

The cell of the dilutor is immersed in a thermo-regulated liquid (ethanol) bath. Helium is bubbled through the dilutor cell filled with water to be water saturated, and then swept directly into the chromatograph through a 5µl internal loop injection valve (V1). Figure 4.22 shows the flow diagram of the valve used.
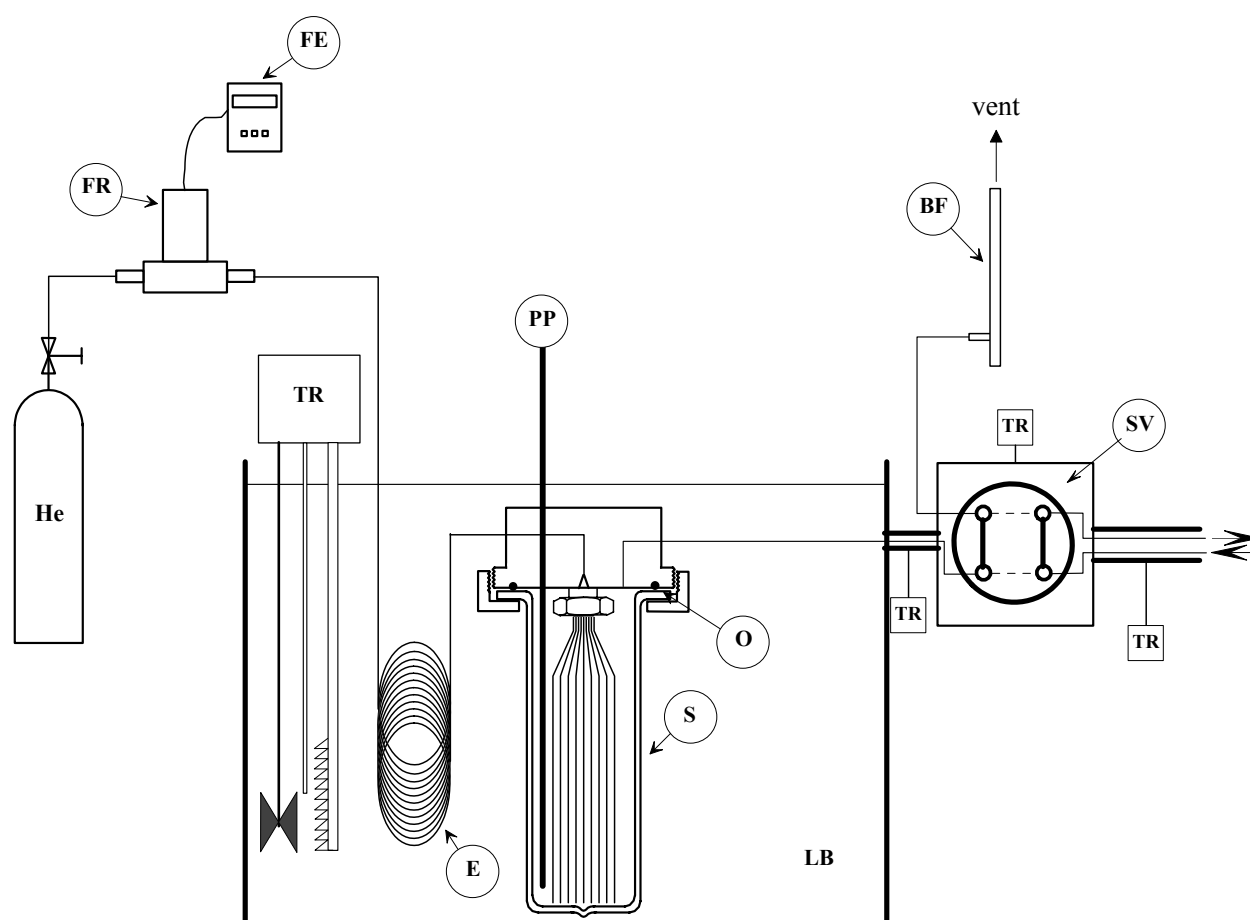
Figure 4.21: Flow diagram of the calibration circuit

BF: Bubble Flowmeter; C : Carrier Gas; d.a.s: data acquisition system; E: Thermal Exchanger; FE : Flow rate Electronic; FR : Flow rate Regulator; LB : Liquid Bath; PP : Platinum resistance thermometer Probe; S: Saturator; SV: Internal Loop Sampling Valve; Th : Thermocouple; TR : Temperature Regulator; VP : Vacuum Pump
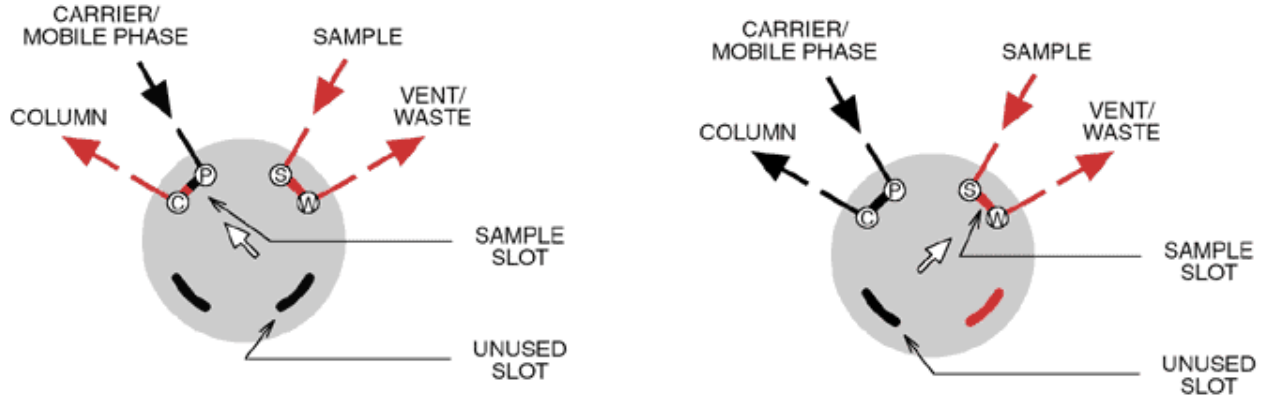
Figure 4.22: Flow diagram of the internal injection loop.

In using the dilutor, a well-defined amount of water can be injected into the Chromatograph. The calculation of the amount of water is carried out using equilibrium and mass balance relations. At thermodynamic equilibrium the fugacity of water is the same in both vapour and liquid phases and the water mole fraction remains constant when the saturated gas is heated in the internal valve:

$$f_w^L = f_w^V \tag{4.7}$$

with

$$f_w^L = f_w^{L\,ref} \times \gamma_w^L \times x_w \tag{4.8}$$

for a pressurized liquid:

$$f_w^{Lref} = f_w^{Sat} \exp\left(\int_{P^{Sat}}^{P} \left(\frac{\upsilon^L}{RT}\right)dP\right) \tag{4.9}$$

assuming the Poynting correction:

$$f_w^{Lref} = f_w^{Sat} \exp\left(\left(\frac{\upsilon^L}{RT}\right)(P - P^{Sat})\right) \tag{4.10}$$

Eq. 4.8 becomes:

$$f_w^V = \gamma_w^L\, x_w f_w^{Sat} \exp\left(\left(\frac{\upsilon^L}{RT}\right)(P - P^{Sat})\right) \tag{4.11}$$

$$f_w^V = \gamma_w^L\, x_w P_w^{Sat}\, \phi_w^{Sat} \exp\left(\left(\frac{\upsilon^L}{RT}\right)(P - P^{Sat})\right) \tag{4.12}$$

because:

$$P_w^{Sat}\, \phi_w^{Sat} = f_w^{Sat} \tag{4.13}$$

on the other hand:

$$f_w^V = \phi_w^V P_{dilutor}\, y_w \tag{4.14}$$

thus:

$$y_w = \gamma_w^L \; x_w \; \frac{P_w^{Sat}}{P_{dilutor}} \; \frac{\phi_w^{Sat}}{\phi_w^V} \exp((\frac{\upsilon^L}{RT})(P - P^{Sat})) \qquad (4.15)$$

with:

$$y_w = \frac{n_w}{n_T} \qquad (4.16)$$

An exact relationship is obtained:

$$n_w = \gamma_w^L \; x_w \; \frac{P_w^{Sat}}{P_{dilutor}} \; \frac{\phi_w^{Sat}}{\phi_w^V} \left(\frac{P.Vol}{ZRT} \right)^{loop} \exp((\frac{\upsilon^L}{RT})(P - P^{Sat})) \qquad (4.17)$$

In the above relations, *f, γ, x, v, R, T, P, ϕ, y, n, Z,* and *Vol* are fugacity, activity coefficient, mole fraction in the liquid phase, molar volume, universal gas constant, temperature, pressure, fugacity coefficient, mole fraction in the vapour phase, number of moles, compressibility factor and volume of the loop, respectively. The superscripts and subscripts *L, V, ref, Sat, loop, w, T* and *dilutor* correspond to the liquid phase, vapour phase, reference state, saturation state, loop, water, total and dilutor, respectively.

The above equation can be simplified ($P^{dilutor} \cong P^{loop} \cong P^{atm}$, the Poynting factor is close to unity):

$$n_w^v = P_w^S \left[\frac{V}{RT} \right]^{loop} \qquad (4.18)$$

4.2.1.3.3 Optimization of the Calibration Conditions

To avoid adsorption of water and to obtain a maximum of sensitivity, we have tried to optimize the calibration conditions.

4.2.1.3.3.1 Optimization of the Chromatographic Conditions

It is known that bigger the difference of temperature between the wire and the TCD oven is, bigger sensitivity of the detector is. So the following picture (Figure 4.23) is obtained by injecting a constant amount of water (4×10^{-9} mol).

However there are some factors, which limit the increase of the wire temperature and the decrease of the TCD oven temperature:

❖ The oven TCD temperature must be higher than the oven column temperature in order to avoid the compounds to condense again.

❖ A good separation of the compounds is necessary.

- ❖ Wire deterioration must be avoided.
- ❖ Water adsorption has to be minimized.
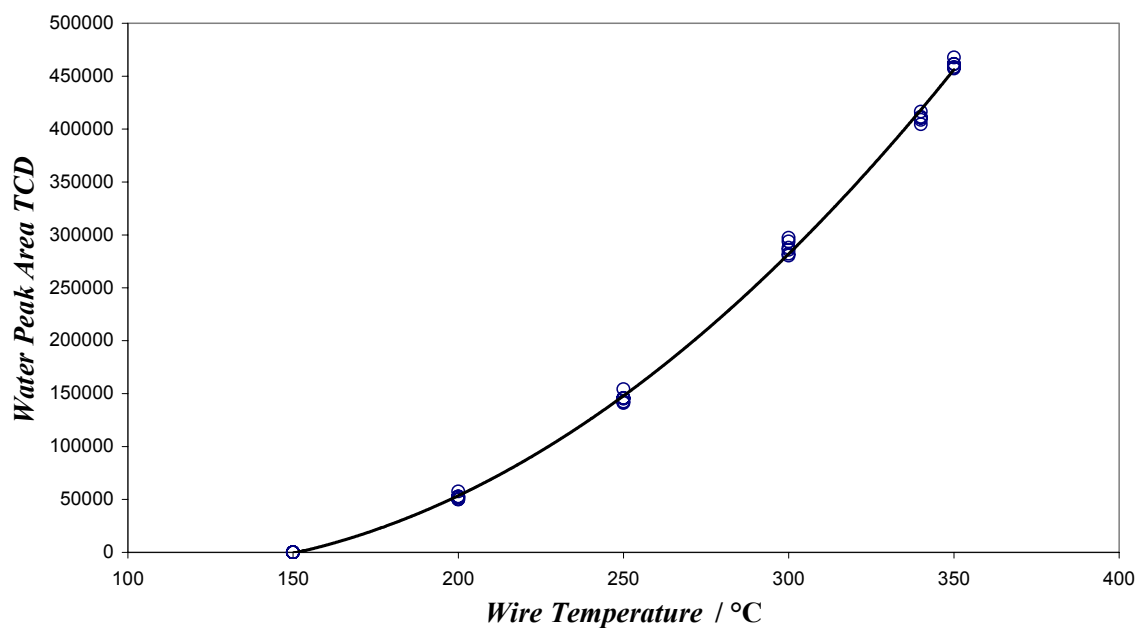
Figure 4.23: Wire temperature Optimization (TCD oven at 423.15 K)

The wire temperature is limited by the resistance of the wire material. In this case the wire is made of tungsten. The maximum wire intensity is a function of the TCD oven temperature. (Figure 4.24) and of carrier gas nature.
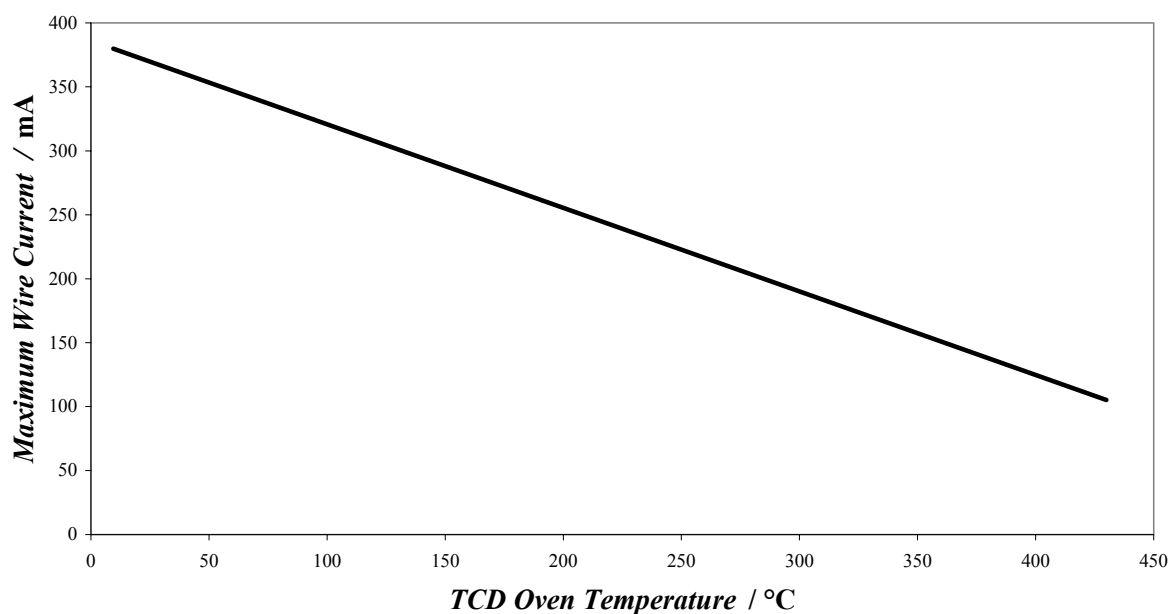
Figure 4.24: Maximum Wire Current

Finally the optimized chromatographic conditions are the following:

- Oven column temperature: 373.15 K
- Carrier gas flow rate (helium): 20 ml.m^{-1}
- Column type: Hayesep C 2m x 1/8"
- TCD oven temperature: 383.15 K
- Wire temperature : 580.15 K ($\Leftrightarrow$320mA)
- FID temperature : 573.15 K
- Hydrogen flow rate: 30 ml.m^{-1}
- Air flow rate: 300 ml.m^{-1}

In order to check that the adsorption of water inside the internal injection loop is limited, a series of tests were performed. The number of water molecules adsorbed inside the loop is a function of both the loop valve temperature and the contact time with the helium saturated in water.

To minimize the adsorption phenomenon, the internal injection valve should be maintained at high temperature, at 540 K. The loop sweeping time varies from 5 to 30 seconds and the water peak area does not vary with the loop sweeping time (Figure 4.25).
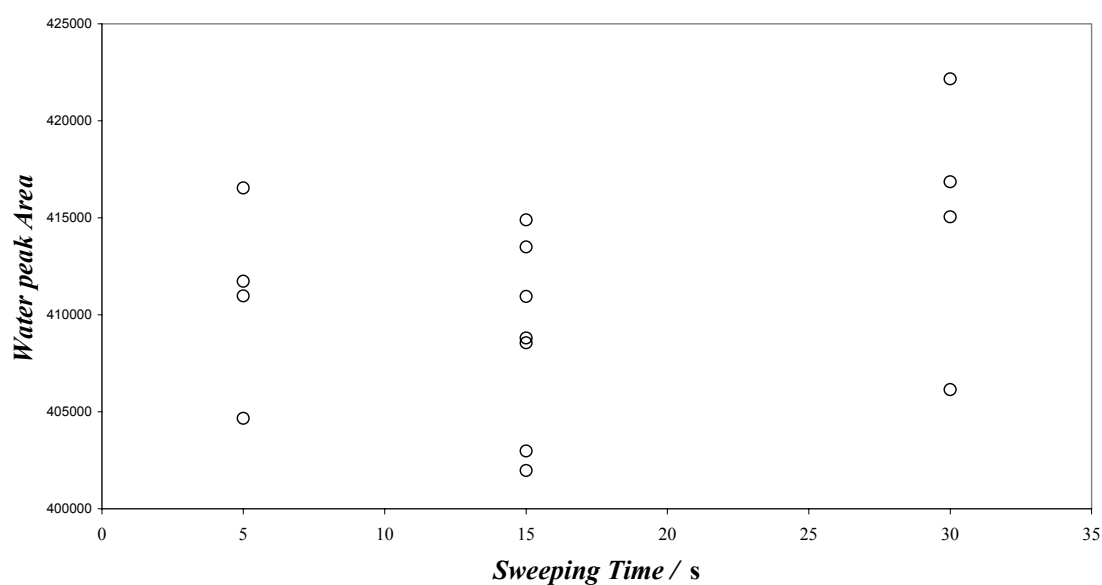
Figure 4.25: Loop Sweeping Time Effect

4.2.1.3.3.2 Calibration Results

It is of essential interest to know precisely the volume and the dead-volume of the sampling valve (volume + dead volume= V^{loop}). First of all, the volume of the loop is roughly calculated (around 5 µL) and then a calibration with methane as a reference gas using a $0-25$ µL gas syringe is done around the value of the rough estimation. After this careful methane calibration, methane is passed through the sampling valve and injected into the GC. Knowing the number of mol of methane swept into the GC through the previous calibration, the volume and the dead volume of the loop can be estimated to at 5.06 µl (+/-0.25%) at 523.15 K. Thus knowing the volume of the loop, the water calibration is obtained (see Figure 4.26). A second order polynomial expression is used to calculate the number of water molecules flowing through the TCD.
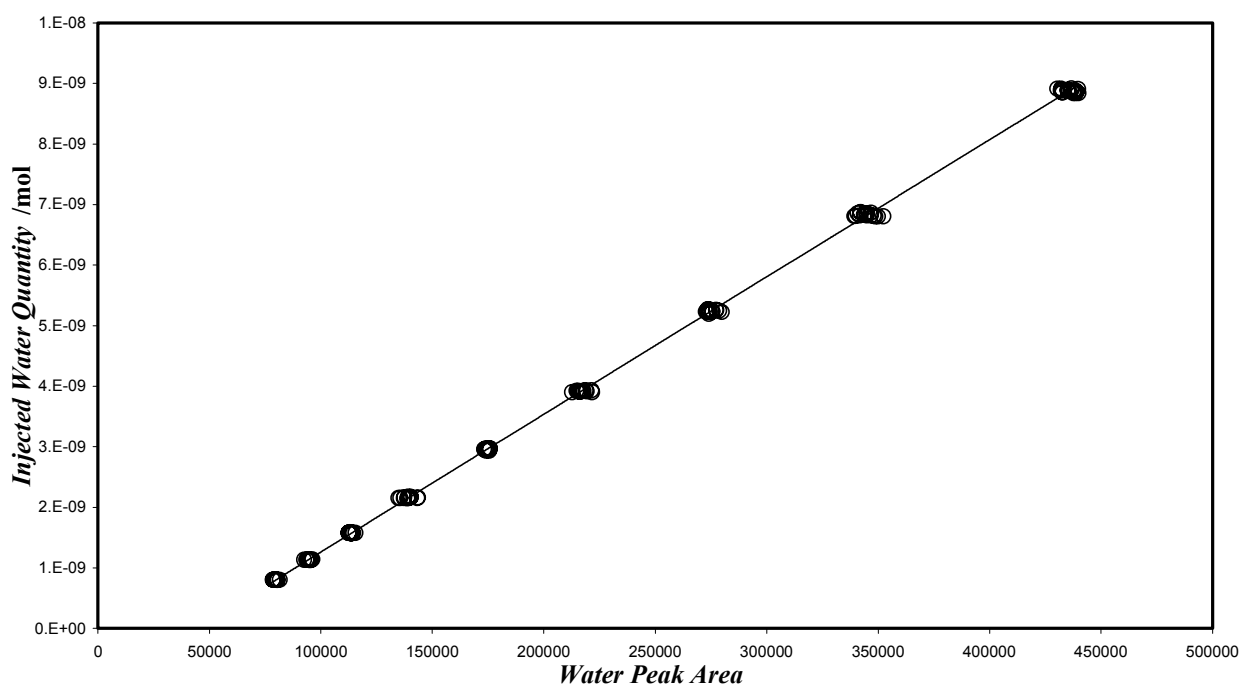
Figure 4.26: TCD/Water calibration (peak area are in µV^2)

The experimental accuracy of the TCD calibration for water is estimated in the worst case at +/-6% (see Figure 4.27).
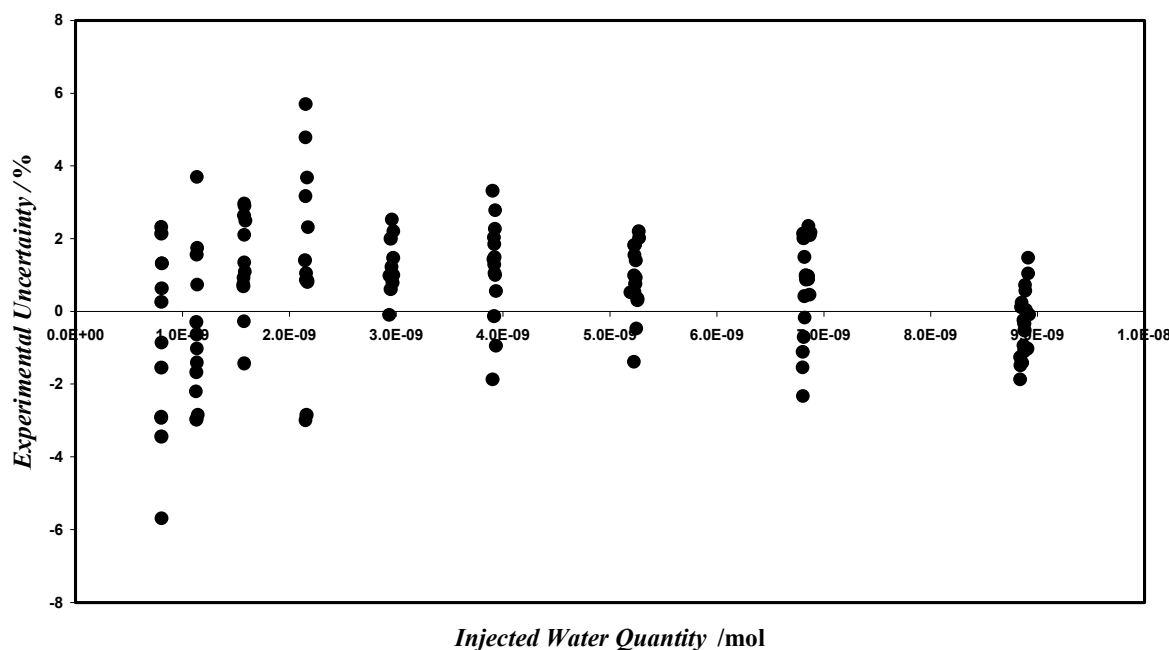
Figure 4.27: TCD/water calibration deviation

4.2.1.3.4 Experimental Procedure for determination of the vapour phase composition

The equilibrium cell and its loading lines are evacuated down to 0.1 Pa and the necessary quantity of the preliminary degassed water (approximately 10 cm^3) is introduced using an auxiliary cell. Then, the desired amount of gas is introduced into the cell directly from the commercial cylinder or via a gas compressor.

For each equilibrium condition, at least 10 samples are withdrawn using the pneumatic samplers ROLSI ^{TM} and analyzed in order to check for measurement repeatability. As the volume of the withdrawn samples is very small compared to the volume of the vapour phase present in the equilibrium cell, it is possible to withdraw many samples without disturbing the phase equilibrium.

4.2.1.4 Determination of the Composition in the Aqueous Phase

4.2.1.4.1 Calibration of the TCD with Water

The procedure to calibrate the TCD with water is quite similar to the procedure of calibration of the FID for the hydrocarbons. Different volumes of water are simply injected in

the chromatograph via the injector with a 5 µl liquid syringe. (a second order polynomial expression is also used to calculate the number of injected water molecules)
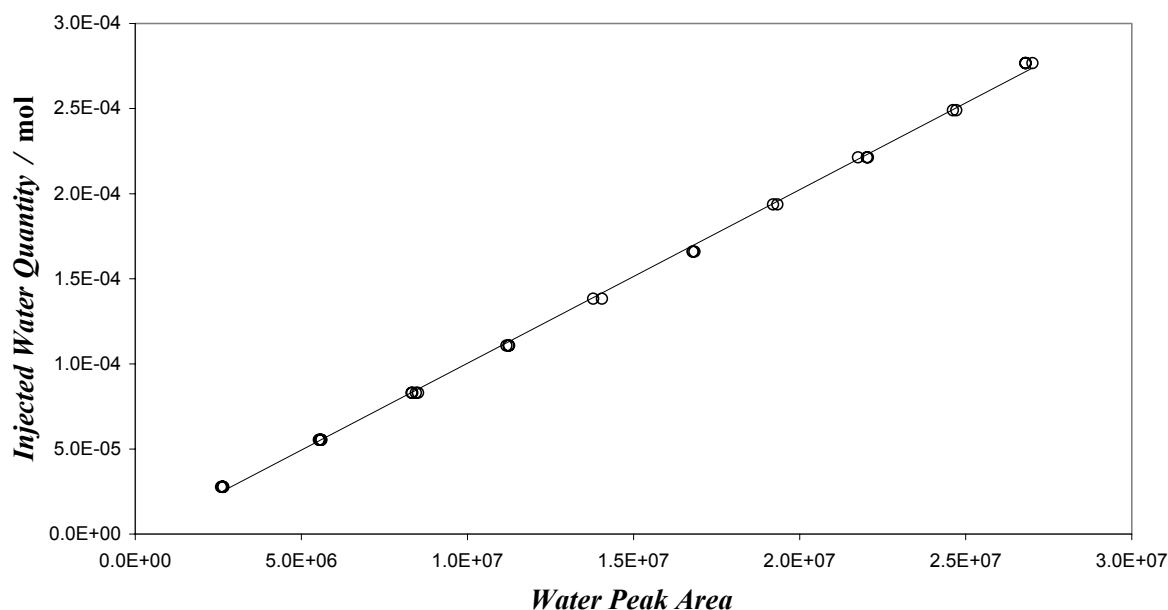
Figure 4.28: TCD/Water calibration. (peak area are in μV^2)
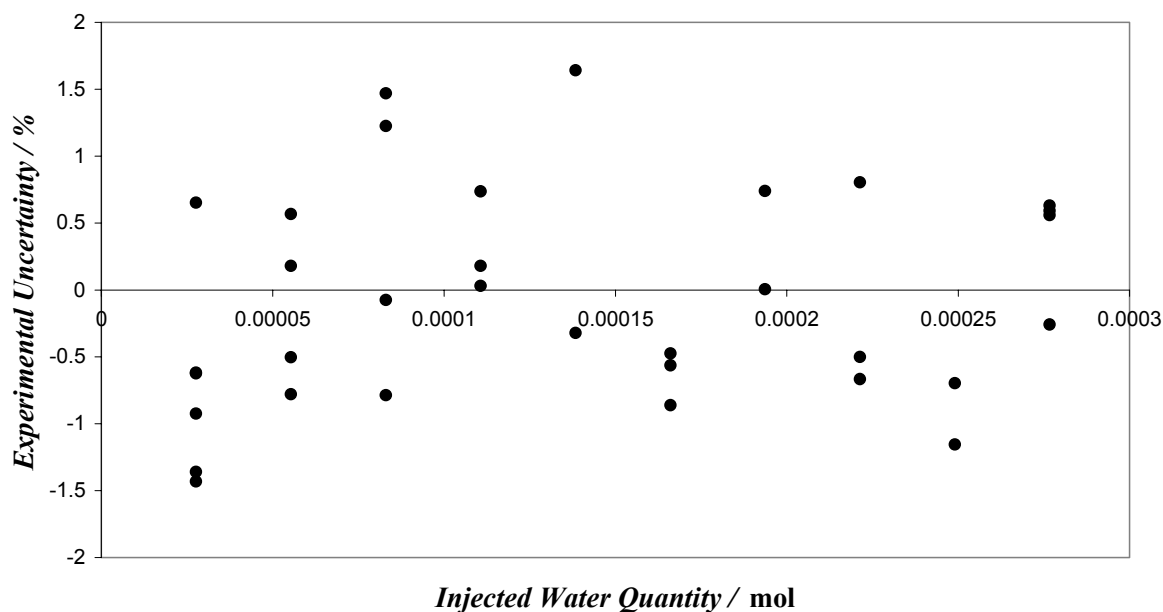
Figure 4.29: TCD/water calibration uncertainty.

The TCD was used to detect the water; it was repeatedly calibrated by injecting known amount of water through "liquid type" syringes. The uncertainties on the calculated mole numbers of water are estimated to be within ± 1.5 % in the 2.5×10^{-5} to 3×10^{-4} range of water mole number.

4.2.1.4.2 Calibration of the TCD and FID with the gases

The FID or TCD are calibrated by introducing known moles of ethane or nitrogen, respectively through a "gas type" syringe (ethane when the gas solubilized in water is nitrogen, nitrogen for all the other gases). The mole numbers of gas (ethane or nitrogen) is thus known within ± 1%. After this careful ethane or nitrogen calibration, different ethane or nitrogen + gas (to be studied) mixtures of known low gas (to be studied) composition were prepared inside the equilibrium cell. Then, samples of different (a priori) unknown sizes are withdrawn directly from the cell through the ROLSI sampler for GC analyses.
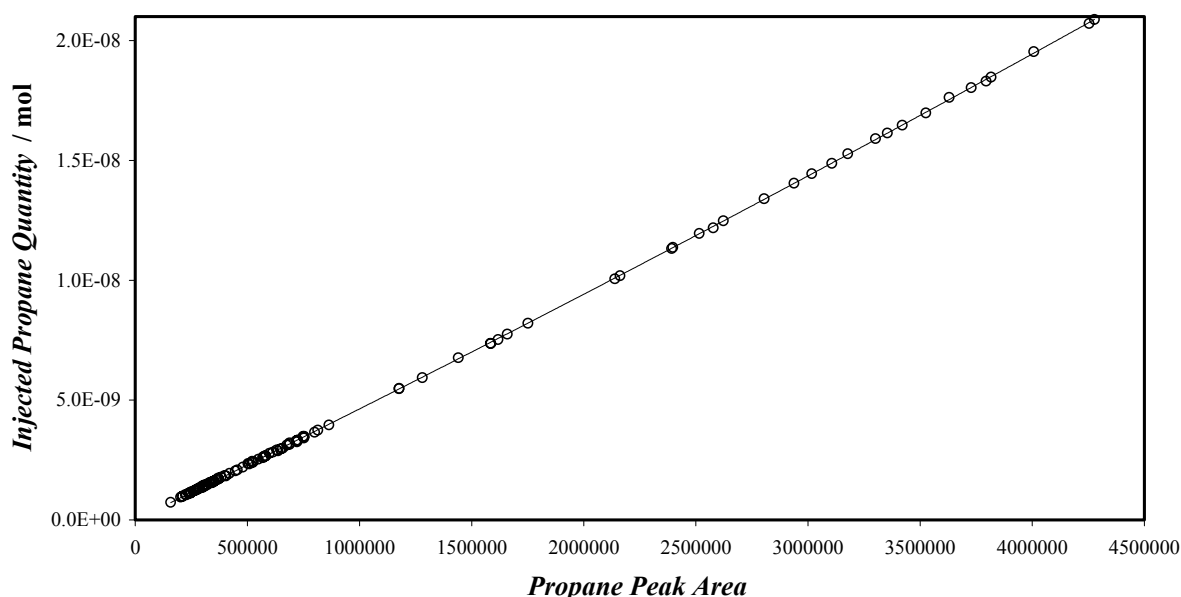
Figure 4.30: FID/Propane Calibration Curve. (peak area are in μV^2)

Knowing the composition of the mixture and the number of sampled moles of ethane or nitrogen (through the response of the FID or TCD) it is possible to estimate the amount of gas (to be studied) and hence calibrate the FID/TCD for this compound. As an example, the calibration curve corresponding to the FID with propane is plotted in Figure 4.30. The resulting relative uncertainty is about ± 3% in mole number of propane (Figure 4.31).
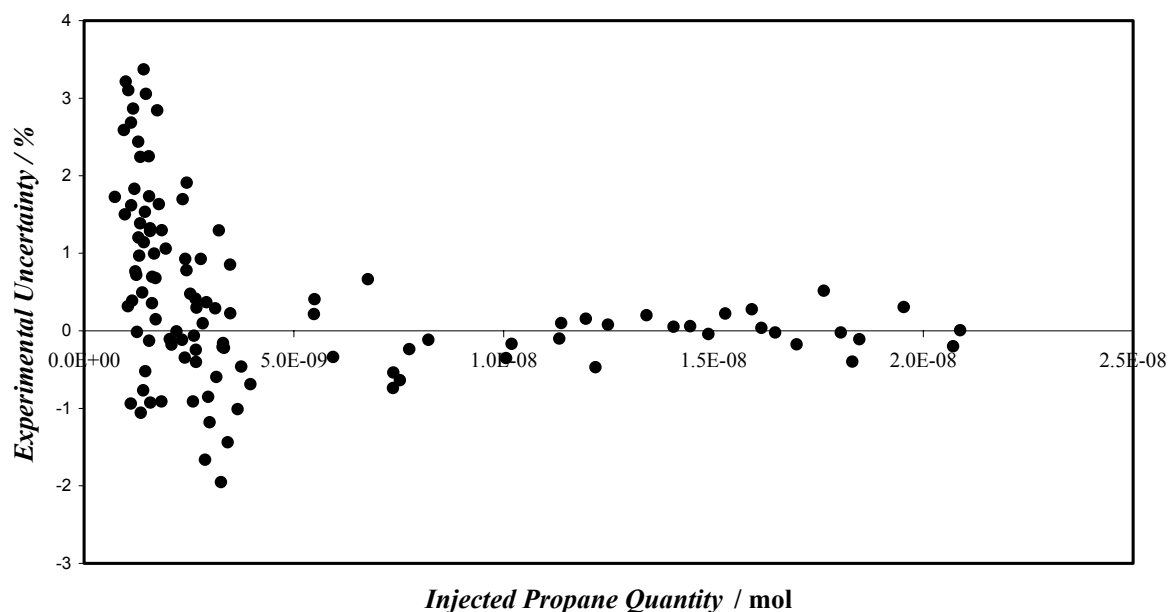
Figure 4.31: Propane calibration deviation.

4.2.1.4.3 Experimental procedure for determination of the aqueous phase composition

The equilibrium cell and its loading lines are evacuated down to 0.1 Pa and the necessary quantity of the preliminary degassed water (approximately 5 cm^3) is introduced using an auxiliary cell. Then, the desired amount of gas is introduced into the cell directly from the commercial cylinder.

For each equilibrium condition, at least 10 samples of liquid phase are withdrawn using the pneumatic samplers ROLSI ^{TM} and analyzed in order to check for measurement repeatability. As the volume of the withdrawn samples is very small compared to the volume of the liquid phase present in the equilibrium cell (around 5 cm^3), it is possible to withdraw many samples without disturbing the phase equilibrium.

4.2.2 The Experimental Set-ups for Determination of Gas Solubilities

4.2.2.1 Apparatus based on the PVT techniques

4.2.2.1.1 Principle

The apparatus used in this work is based on measuring the bubble point pressure of various known gas - water binaries at isothermal conditions, using graphical technique. The experimental set-up consists of a variable volume PVT cell as described by *Fontalba et al.* [273]. This technique has only been used to measure the solubility of carbon dioxide in water.
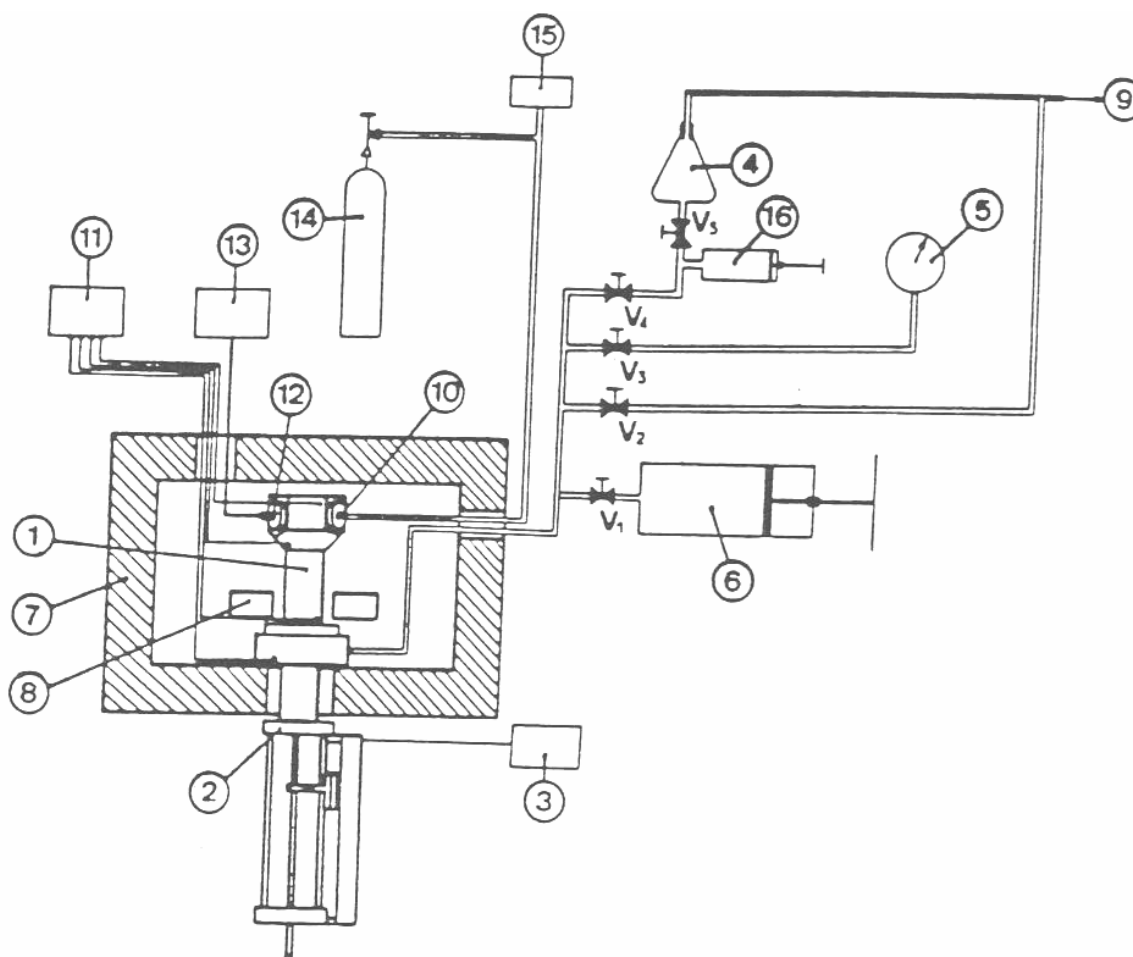
Figure 4.32: Flow diagram of the PVT apparatus

(1) : Equilibrium cell ; (2) : Assembly for piston level measurements; (3) :Electronic for piston level measurements; (4) : Pressurizing liquid reservoir; (5) : Manometer ; (6) : Hydraulic press; (7) : Air thermostat ; (8) : Solenoids to create a rotating magnetic field ; (9) : Vacuum circuit; (10) : Loading valve ; (11) : Temperature measurement device; (12) : Pressure transducer ; (13) : Pressure measurement device; (14) : Gas cylinder (in our case CO_2) ; (15) : Digital manometer; (16) : low pressure hydraulic press.

The cell body is made of a titanium alloy; it is cylindrical in shape (see Figure 4.33) and contains a piston, which can be displaced by introducing a pressurizing liquid (octane) by means of a high-pressure pump. The temperature is controlled by an air thermostat within 0.1 K. The top of the cell is fitted with a feeding valve and a membrane pressure transducer (SEDEME 250 bar) to measure the pressure inside the cell. An O'ring allows the sealing between the mixture to be studied and the pressurizing liquid and a magnetic rod provides good mixing of the fluids. At the bottom of the piston a rigid rod of metal is screwed and allows measurement of the piston level by means of a displacement transducer.
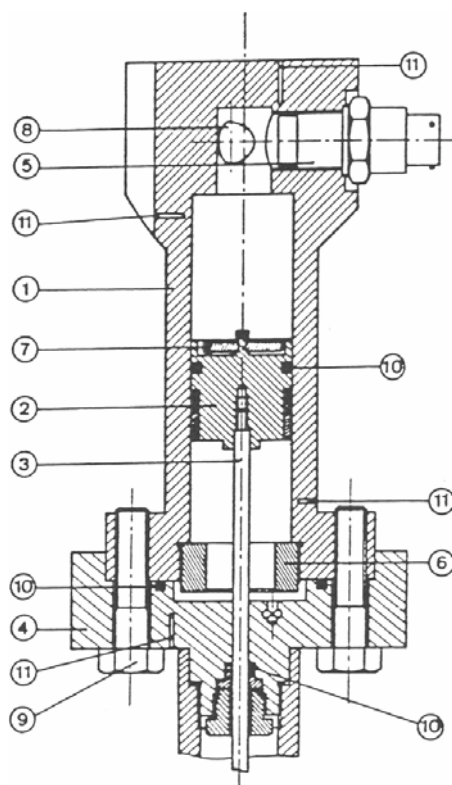
Figure 4.33: Equilibrium Cell

(1) : Cell body ; (2) : piston ; (3) : probe for piston level measurements ; (4) : pressurizing assembly ; (5) : membrane pressure transducer ; (6) : Stop screw ; (7) : Magnetic rod; (8) : Seat of the feeding valve; (9) : Bolts ; (10) : O ring; (11) : Thermocouple wells.

4.1.2.2.2 Experimental Procedures

The composition of the system is determined by measuring the exact amounts of water and CO_2 loaded into the cell using an analytical balance with a reported accuracy of 2 mg (up to 2 kg). Then the system pressure is increased step by step (by reducing the cell volume) and mixed thoroughly to ensure equilibrium. The stabilized system pressure is plotted versus cell volume, where a change in slope indicates the system bubble point for the given temperature.

The uncertainties in the measured pressure and temperature conditions are within ± 0.002 MPa and ± 0.1 K, respectively.

4.2.2.2   Apparatus based on the static method (HW University)

4.2.2.2.1 Principle

The apparatus used in this work (Figure 4.34) is based on a static-analytic method with liquid phase sampling. The phase equilibrium is achieved in a cylindrical cell made of stainless steel, the cell volume is about 540 cm^3 and it can be operated up to 69 MPa between 253 and 323 K.
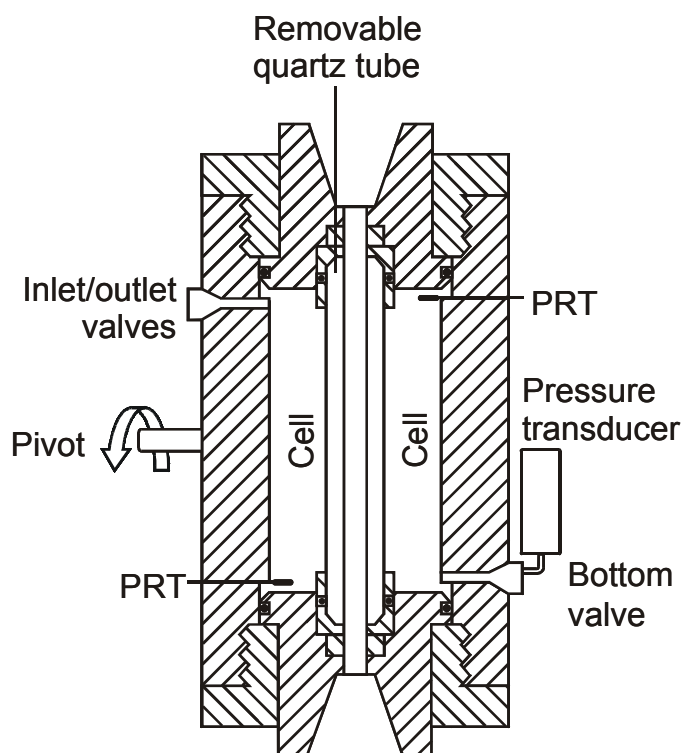
Figure 4.34: Flow Diagram of the Equipment**.**

The equilibrium cell is held in a metallic jacket heated or cooled by a constant–temperature liquid bath (an optically clear quartz glass tube can be housed inside the cell for visual observation). The temperature of the cell is controlled by circulating coolant from a cryostat within the jacket surrounding the cell. The cryostat is capable of maintaining the cell temperature to within 0.05 K. To achieve good temperature stability, the jacket is insulated with polystyrene board and the pipes, which connect it to the cryostat, are covered with plastic

foam. Four platinum resistance probes monitor the temperature: two in the equilibrium cell, and two in the heating jacket (not seen in the flow diagram), connected directly to a computer for direct acquisition. The four platinum resistance probes are calibrated at intervals using a calibrated probe connected to a precision thermometer. The calibrated probe has a reported accuracy of ± 0.025 K. Whilst running a test, all four probes and the cryostat bath temperature are logged so any discrepancy can be detected.

The pressure is measured by means of a CRL 951 strain gauge pressure transducer mounted directly on the cell and connected to the same data acquisition unit. This system allows real time readings and storage of temperatures and pressures throughout the different isothermal runs. Pressure measurement uncertainties are estimated to be within ± 0.007 MPa in the operating range.

To achieve a faster thermodynamic equilibrium and to provide a good mixing of the fluids, the cell is mounted on a pivot frame, which allows a rocking motion around a horizontal axis. Rocking of the cell, and the subsequent movement of the liquid phase within it, ensures adequate mixing of the system.

When the equilibrium in the cell is reached (constant pressure and temperature), the rocking of the cell is stopped and the bottom valve is fitted to a separator vessel, which is fitted itself to a gas meter (*VINCI Technologies*), see Figure 4.35. The gas-meter is equipped with pressure, temperature and volume detectors.

4.2.2.2.2 Experimental Procedures

The equilibrium cell and its loading lines are primarily evacuated by drawing a vacuum, and the necessary quantity of the aqueous solution is then introduced into the cell. Then, the desired amount of methane is introduced into the equilibrium cell directly from the commercial cylinder to reach the desired pressure. The sampling of the liquid phase is performed through the bottom-sampling valve while the top valve connected to a gas reserve remains permanently open to maintain a constant pressure inside the equilibrium cell during the withdrawal of the sample. The aqueous liquid phase is trapped in a separator vessel and after the sampling, immersed in a liquid-glycol bath (253.15 K). The gas obtained by the sampling is accumulated in a gas-meter.
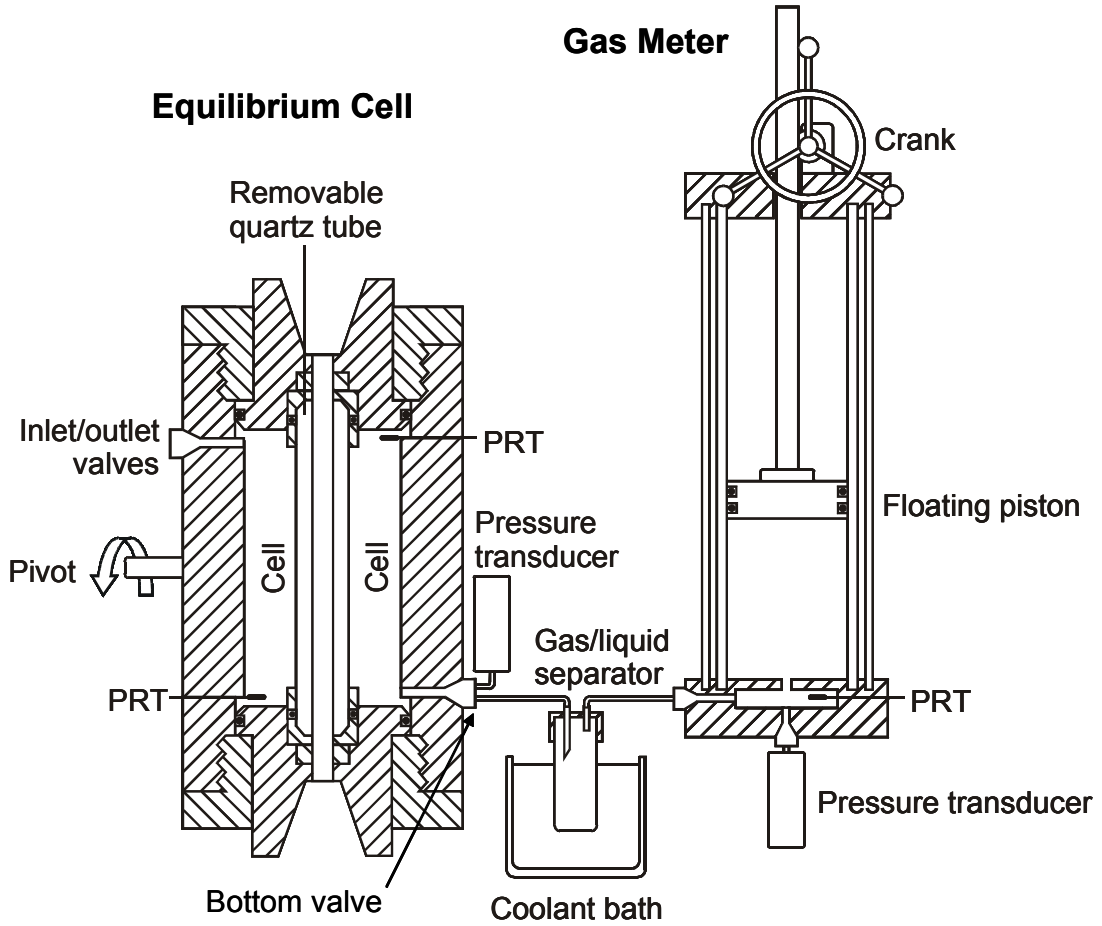
Figure 4.35: Flow Diagram of the Equipment in Sampling Position.

The amount of the aqueous solution obtained from the sampling is known by weighing the water trap before and after the sampling. The total amount of gas collected during the sampling is calculated from the volume variation of the gas-meter at ambient pressure P^{GM} and room temperature, T^{GM}, corrected for the volume of the aqueous solution recovered V_{aq}:

$$\Delta V = \left(V_1^{GM} - V_2^{GM} \right) - V_{aq} \text{ with } V_{aq} = \sum_i x_i m_T v_i \left(P_{trap}, T_{trap} \right) \tag{4. 19}$$

The solubility of methane is then calculated by:

$$x_{C_1} = \frac{\dfrac{P^{GM} s}{RT^{GM}} \cdot M_T}{1 + \dfrac{P^{GM} s}{RT^{GM}} \cdot M_T} \tag{4. 20}$$

where s is:

$$s = \frac{\Delta V}{m_T}$$ (4. 21)

It should be noted that eq. 4.20 assumes that all the methane dissolved in water is released in the gas phase and that no water and ethylene glycol is present in the gas. The former assumption is justified as ice, at the condition of the liquid glycol bath, has a very low vapour pressure and ethylene glycol has even a lower vapour pressure. The amount of methane trapped in the aqueous solution under one atmosphere and at around 253 K is assumed to be negligible with respect to the amount of methane accumulated in the gas phase of the gas meter.

Water – Hydrocarbons Modelling

Dans un premier temps, un travail a été réalisé pour améliorer la prédiction des tensions de vapeur des principaux composés du gaz naturel : méthane, éthane, propane, n-butane, dioxyde de carbone, eau….Une nouvelle fonction alpha qui permet d'améliorer la dépendance en température du paramètre attractif de l'équation d'état de Peng-Robinson est proposée.

Dans ce chapitre les deux différentes approches pour modéliser les résultats expérimentaux seront présentées. Une approche ϕ-ϕ en premier lieu est exposée, elle utilise l'équation d'état de Patel-Téja modifiée par Valderrama. La seconde approche est basée sur une méthode dissymétrique, une approche ϕ-γ. L'équation d'état de Peng-Robinson sera utilisée pour traiter la phase vapeur et la loi d'Henry pour la phase liquide.

5   Modelling and Results

5.1   Pure Compound Vapour Pressure

The representation of thermodynamic properties and phase equilibria of mixtures depends strongly on pure compound calculations. The accuracy of the calculation is clearly not only dependent on the choice of an equation of state or the mixing rules but also on a sufficiently accurate representation of pure compound vapour pressures. The capacity to correlate the phase equilibria is then directly related to the adequate choice of an alpha function.

Many alpha functions have been proposed to improve the precision of cubic equations of state via a more accurate prediction of pure compound vapour pressures. Generally the mathematical expressions of alpha functions are high order polynomials in either acentric factor or reduced temperature, exponential functions, or truncated functions (see §3.1.2.5). The main difficulties associated with most of alpha functions are their incapacity to represent accurately supercritical behaviour or their limited temperature utilization range. To avoid these difficulties, different approaches have been developed: use of alpha functions with specific compound parameter or switching alpha functions, even if mathematical constraints are associated with the latest, particularly in the continuity of the function and its derivatives.

Generalized alpha functions are preferably used because of their predictive ability and the reduction of the number of parameters. In this work, the capacities of three different alpha functions have been compared: a new proposed form, a generalized *Trebble-Bishnoi* (*TB*) [230] and a generalized *Mathias-Copeman* (*MC*) alpha function for particular cases involving natural gas compounds, i.e.: light hydrocarbons (methane, ethane, propane, butane, pentane), water, carbon dioxide, nitrogen, hydrogen sulphide.

The vapour pressures of 22 pure compounds were used to develop and generalize a new alpha function for the *Peng-Robinson* equation of state (*PR-EoS*).

5.1.2 Temperature Dependence of the Attractive Parameter

To have an accurate representation of vapour pressures of pure compounds a temperature dependence of the attractive term through the alpha function is proposed. The alpha functions must verify some requirements:

- They must be finite and positive at all temperatures
- They must be equal to 1 at the critical point
- They must tend to zero when T tends to infinity
- They must belong to the C2 function group, i.e. function and its derivatives (first and second) must be continuous, (for $T>0$) to assure continuity in thermodynamic properties

The *Trebble-Bishnoi* (*TB*) [224] alpha function is one of the examples selected in this study

$$\alpha(T) = \exp\left[m \times \left(1 - \frac{T}{T_c}\right)\right] \tag{5. 1}$$

The form of the *Mathias-Copeman* (*MC*) alpha function with three adjustable parameters [229] is given by eq 5.2 if $T \leq T_c$.

$$\alpha(T) = \left[1 + c_1\left(1 - \sqrt{\frac{T}{T_C}}\right) + c_2\left(1 - \sqrt{\frac{T}{T_C}}\right)^2 + c_3\left(1 - \sqrt{\frac{T}{T_C}}\right)^3\right]^2 \tag{5. 2}$$

And by eq. 5.3 if $T>T_C$,

$$\alpha(T) = \left[1 + c_1\left(1 - \sqrt{\frac{T}{T_C}}\right)\right]^2 \tag{5. 3}$$

c_1, c_2 and c_3 are three adjustable parameters

In addition, a new alpha function (eq 5.4 valid for if $T \leq T_c$) is proposed, which is a combination of both of mathematical forms from 5.1 and 5.2. This alpha function verifies every just described requirements. c_1, c_2 and c_3 are three adjustable parameters.

$$\alpha(T) = \exp\left[c_1 \times \left(1 - \frac{T}{T_c}\right)\right] \times \left[1 + c_2\left(1 - \sqrt{\frac{T}{T_C}}\right)^2 + c_3\left(1 - \sqrt{\frac{T}{T_C}}\right)^3\right]^2 \tag{5. 4}$$

If $T>T_C$, an exponential form is chosen similar to the *Trebble Bishnoi* expression (eq. 5.6) and the single parameter m of this expression should verify eq. 5.5:

$$m = -\left(\frac{\partial \alpha}{\partial T_R}\right)_{T_R=1} = c_1 \qquad (5.5)$$

$$\alpha(T) = \exp\left[c_1 \times \left(1 - \frac{T}{T_c}\right)\right] \qquad (5.6)$$

5.1.3   Comparison of the α-function abilities

The alpha function ability to represent properties is usually tested by comparing pure compound vapour pressures. 22 compounds were selected to perform the comparison and the generalization of the alpha functions. All the critical coordinates and vapour pressure correlations are taken from "The properties of gases and liquids" [289] (TABLE 5.1).

Component	Pc (Pa) [289]	Tc(K) [289]	ω [289]	C_1 (SRK)	C_2 (SRK)	C_3 (SRK)	C_1 (PR)	C_2 (PR)	C_3(PR)
Hydrogen	1296960	33.19	-0.2160	0.161	-0.225	-0.232	0.095	-0.275	-0.029
Methane	4600155	190.56	0.0110	0.549	-0.409	0.603	0.416	-0.173	0.348
Oxygen	50804356	154.58	0.0222	0.545	-0.235	0.292	0.413	-0.017	0.092
Nitrogen	3394388	126.20	0.0377	0.584	-0.396	0.736	0.448	-0.157	0.469
Ethylene	5041628	282.35	0.0865	0.652	-0.315	0.563	0.512	-0.087	0.349
Hydrogen sulphide	8936865	373.53	0.0942	0.641	-0.183	0.513	0.507	0.008	0.342
Ethane	4883865	305.32	0.0995	0.711	-0.573	0.894	0.531	-0.062	0.214
Propane	4245518	369.95	0.1523	0.775	-0.476	0.815	0.600	-0.006	0.174
Isobutane	3639594	408.80	0.1808	0.807	-0.432	0.910	0.652	-0.149	0.599
n-Butane	3799688	425.15	0.2002	0.823	-0.267	0.402	0.677	-0.081	0.299
Cyclohexane	4073002	553.58	0.2096	0.860	-0.566	1.375	0.684	-0.089	0.549
Benzene	4895001	562.05	0.2103	0.840	-0.389	0.917	0.701	-0.252	0.976
Carbon dioxide	7377000	304.21	0.2236	0.867	-0.674	2.471	0.705	-0.315	1.890
Isopentane	3381003	460.43	0.2275	0.876	-0.386	0.660	0.724	-0.166	0.515
Pentane	3369056	469.70	0.2515	0.901	-0.305	0.542	0.763	-0.224	0.669
Ammonia	11287600	405.65	0.2526	0.916	-0.369	0.417	0.748	-0.025	0.001
Toluene	4107999	591.75	0.2640	0.923	-0.301	0.494	0.762	-0.042	0.271
Hexane	3014419	507.40	0.3013	1.005	-0.591	1.203	0.870	-0.588	1.504
Acetone	4701004	508.20	0.3065	0.993	-0.322	0.265	0.821	0.006	-0.090
Water	22055007	647.13	0.3449	1.095	-0.678	0.700	0.919	-0.332	0.317
Heptane	2740000	540.20	0.3495	1.036	-0.258	0.488	0.878	-0.031	0.302
Octane	2490001	568.70	0.3996	1.150	-0.587	1.096	0.958	-0.134	0.487

TABLE 5.1 – ADJUSTED MATHIAS-COPEMAN ALPHA FUNCTION PARAMETERS (eq. 5.2) FOR THE SRK-EoS AND PR-EoS FROM DIPPR® CORRELATIONS

5.1.3.1 Mathias – Copeman alpha function

c_1, c_2 and c_3, the three adjustable parameters of the *MC* alpha function were evaluated from a reduced temperature of 0.4 up to 1 ($0.4 \leq T_r \leq 1$) using a modified Simplex algorithm [290] for the 22 selected compounds. The objective function is:

$$F = \frac{100}{N} \sum_{1}^{N} \left(\frac{P_{\exp} - P_{cal}}{P_{\exp}} \right)^2 \tag{5. 7}$$

where N is the number of data points, P_{exp} is the measured pressure, and P_{cal} is the calculated pressure.

The adjusted parameter values for each compound are reported in TABLE 5.1 for both the *SRK-EoS* and the *PR-EoS*. For each equation of state, it appears that the three *MC* adjusted parameters of the 22 pure compounds can be quadratically or linearly correlated as a function of the acentric factor (eqs. 5.8-5.13):

For *SRK-EoS*,

$$c_1 = -0.1094\omega^2 + 1.6054\omega + 0.5178 \tag{5. 8}$$

$$c_2 = -0.4291\omega + 0.3279 \tag{5. 9}$$

$$c_3 = 1.3506\omega + 0.4866 \tag{5. 10}$$

For *PR-EoS*,

$$c_1 = 0.1316\omega^2 + 1.4031\omega + 0.3906 \tag{5. 11}$$

$$c_2 = -1.3127\omega^2 + 0.3015\omega - 0.1213 \tag{5. 12}$$

$$c_3 = 0.7661\omega + 0.3041 \tag{5. 13}$$

The generalized alpha function predicts pure compound vapour pressures with an overall *AAD* of 1.4 % (0.4% bias) compared to 3.4 % *AAD* (2.7% bias) with the classical *Soave* alpha function [206] (TABLE 5.2).

The generalization of the *MC* for the *SRK-EoS* improves pure compound vapour pressure calculations. Deviations with the *MC* alpha function are generally smaller than those obtained with the classical *Soave* alpha function.

	Generalized MC Alpha Function[1]		Generalized Soave Alpha Function [206]	
Component	Bias %	AAD %	Bias %	AAD %
Hydrogen	5.3	5.3	1.1	4.1
Methane	-0.2	0.3	-0.1	1.5
Oxygen	-1.5	1.5	1.1	2.1
Nitrogen	-0.1	0.3	0.8	1.4
Ethylene	-1.7	1.7	0.6	1.3
Hydrogen sulphide	-0.8	1.5	1.8	1.8
Ethane	-0.6	0.7	1.5	2.5
Propane	-0.6	0.8	2.1	2.5
Isobutane	-0.1	1.7	1.4	1.5
n-Butane	-0.3	0.5	0.5	1.8
Cyclohexane	-0.4	0.8	2.4	2.4
Benzene	-1.2	1.3	1.4	1.9
Carbon dioxide	0.6	0.6	0.7	0.8
Isopentane	-0.1	0.3	3.0	3.6
Pentane	-0.02	0.3	3.4	3.9
Ammonia	1.9	1.9	3.2	3.6
Toluene	-0.2	0.4	1.5	2.3
Hexane	-0.2	1.0	2.6	3.7
Acetone	2.3	2.4	7.3	7.35
Water	4.3	5.2	9.2	9.8
Heptane	1.0	1.1	6.9	7.0
Octane	1.3	1.6	6.7	7.0
Overall	**0.4**	**1.4**	**2.7**	**3.4**

TABLE 5.2 – COMPARISON OF PURE COMPONENT VAPOUR PRESSURES USING THE SRK-EoS

With the *PR-EoS*, the generalized alpha function predicts pure compound vapour pressures with an overall *AAD* of 1.2 % (0.5% bias) compared to 2.1 % *AAD* (–1.2% bias) with the classical Soave alpha function [206] (TABLE 5.3). However, this generalization leads to poor results especially with water because for this compound the adjusted and calculated c_1 parameters using the generalization differ strongly (Figure 5.1).
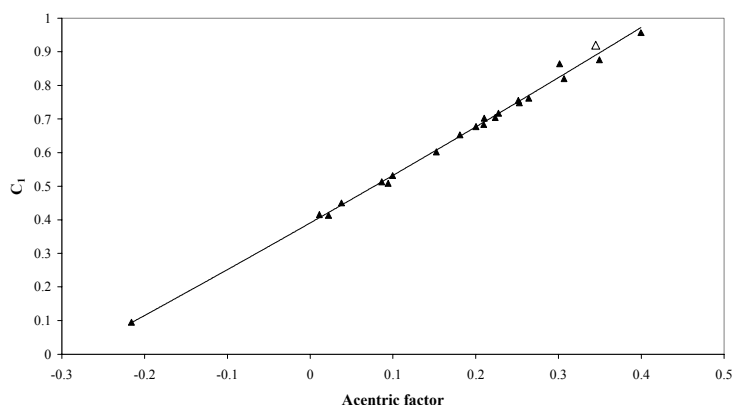
Figure 5.1: Mathias-Copeman c_1 parameter as a function of the acentric factor for the PR-EoS; △: c_1 parameter for water.

---

[1] This work, Eqs. (5.8-5.10).

	Generalized PR Alpha Function [208]		Generalized MC Alpha Function[2]		Generalized New Alpha Function[3]	
Component	Bias %	AAD %	Bias %	AAD %	Bias %	AAD %
Hydrogen	0.8	3.7	3.0	3.0	1.2	1.2
Methane	-0.7	0.7	0.2	0.5	0.0	0.4
Oxygen	-1.8	1.8	0.1	0.5	-0.2	0.3
Nitrogen	-0.9	0.9	-0.3	0.3	-0.3	0.3
Ethylene	-2.3	2.3	-0.6	0.6	-0.5	0.5
Hydrogen sulphide	-1.1	1.5	-0.8	1.2	-0.7	1.0
Ethane	-1.4	1.4	0.3	0.7	0.4	0.7
Propane	-2.1	2.3	-0.2	0.5	-0.1	0.5
Isobutane	-3.8	4.0	-1.5	1.5	-1.4	1.4
n-Butane	-1.7	1.8	0.5	1.0	0.5	1.0
Cyclohexane	-1.5	1.7	-1.1	1.1	-1.0	1.1
Benzene	-0.7	1.2	-0.4	0.7	-0.3	0.6
Carbon dioxide	0.7	0.7	0.6	0.6	0.5	0.5
Isopentane	-1.8	1.9	0.5	0.8	0.4	0.8
Pentane	-2.4	2.5	0.3	0.6	-0.1	0.3
Ammonia	0.7	0.7	1.3	1.4	1.2	1.3
Toluene	-1.9	2.1	0.3	0.5	-0.2	0.3
Hexane	-3.7	3.9	-0.8	1.4	-1.8	2.1
Acetone	1.2	1.2	3.2	3.2	2.4	2.4
Water	*3.3*	*4.3*	*5.3*	*6.0*	*4.1*	*5.0*
Heptane	-3.2	3.3	0.1	0.5	-1.9	2.1
Octane	-2.4	2.4	0.4	0.6	-2.2	2.4
Overall	**-1.2**	**2.1**	**0.5**	**1.2**	**0.1**	**1.2**

TABLE 5.3 –COMPARISON OF PURE COMPONENT VAPOUR PRESSURES USING THE PR-EoS

To obtain more accurate pure compound vapour pressures, the three parameters were correlated to the acentric factor ω only for light hydrocarbons (up to pentane), water, carbon dioxide, hydrogen sulphide and nitrogen. The relationships obtained for the *PR-EoS* are the following:

$$c_1 = 1.0113\omega^2 + 1.1538\omega + 0.4021 \tag{5. 14}$$

$$c_2 = -7.7867\omega^2 + 2.2590\omega - 0.2011 \tag{5. 15}$$

$$c_3 = 2.8127\omega^2 - 1.0040\omega + 0.3964 \tag{5. 16}$$

---

[2] This work, Eqs. (5.11 - 5.13).

[3] This work, Eqs. (5.17 - 5.19).

This more specific generalized alpha function predicts water vapour pressure with an *AAD* of 0.4 % (0.3 % bias) compared to 6 % *AAD* (5.3 % bias) with the first generalization (eqs. 5.14 - 5.16).

5.1.3.2 The new proposed alpha function

It is proposed to improve the ability of the *PR-EoS* to predict pure compound vapour pressures. c_1, c_2 and c_3, the three adjustable parameters for this new form (eq. 5.4) were evaluated following the procedure described in *§ 5.1.3.1*

Component	c_1	c_2	c_3	F $(\times 10^4)$ (eq 5.7)
Hydrogen	0.09406	-0.22429	-0.02458	0.2
Methane	0.41667	-0.05156	0.38954	2.1
Oxygen	0.41325	0.10376	0.10971	3.0
Nitrogen	0.44950	-0.03278	0.49308	1.6
Ethylene	0.51014	0.06247	0.32052	1.8
Hydrogen sulphide	0.50694	0.14188	0.31438	0.9
Ethane	0.52539	0.11674	0.13968	7.6
Propane	0.59311	0.17042	0.10182	14.6
Isobutane	0.64121	0.07005	0.42647	11.6
n-Butane	0.67084	0.09474	0.23091	13.1
Cyclohexane	0.68259	0.04522	0.53089	2.0
Benzene	0.69709	-0.07749	0.86396	8.0
Carbon dioxide	0.68583	0.17408	0.18239	2.0
Isopentane	0.71103	0.06958	0.29784	8.2
Pentane	0.74373	0.05868	0.35254	10.6
Ammonia	0.74852	0.07849	0.10073	0.5
Toluene	0.75554	0.11290	0.22419	10.2
Hexane	0.83968	-0.19125	0.93864	42.2
Acetone	0.82577	0.04252	0.15901	3.3
Water	0.91402	-0.23571	0.54115	3.2
Heptane	0.87206	0.08945	0.28459	9.7
Octane	0.94934	-0.00379	0.43788	15.8

TABLE 5.4 – ADJUSTED NEW ALPHA FUNCTION PARAMETERS FOR THE PR-EoS FROM DIPPR® CORRELATIONS

The three parameters (TABLE 5.4) are also correlated as a function of the acentric factor for the all compounds:

$$c_1 = 0.1441\omega^2 + 1.3838\omega + 0.387 \tag{5.17}$$

$$c_2 = -2.5214\omega^2 + 0.6939\omega + 0.0325 \tag{5.18}$$

$$c_3 = 0.6225\omega + 0.2236 \tag{5.19}$$

This generalization leads to better results that the classical generalized *PR* alpha function [208] (TABLE 5.3). The new alpha function predicts pure compound vapour pressure with an overall *AAD* of 1.2 % (0.01 % Bias) compared to 2.1 % (-1.2 % Bias) with

the classical alpha function [206]. The deviations obtained by this new alpha function are in general smaller than those obtained with the classical alpha function. However, the predictions of water vapour pressures are degraded by this generalization as in the study of the previous paragraph.

To obtain more accurate vapour pressures, the three parameters were also correlated to the acentric factor ω for the same specific compounds, light hydrocarbons, water carbon dioxide, hydrogen sulphide and nitrogen. The relationships obtained for the *PR-EoS* are the following:

$$c_1 = 1.3569\omega^2 + 0.9957\omega + 0.4077 \tag{5.20}$$

$$c_2 = -11.2986\omega^2 + 3.5590\omega - 0.1146 \tag{5.21}$$

$$c_3 = 11.7802\omega^2 - 3.8901\omega + 0.5033 \tag{5.22}$$

This more specific generalized alpha function predicts water vapour pressure with an *AAD* of 0.4 % (0.02 % bias) compared to 6 % *AAD* (5.3 % bias) with the first generalization (eqs 5.17-5.19).

5.1.3.3   Comparison

The comparison of results with the 22 compounds leads to the conclusion that the three different generalized alpha functions represent accurately the vapour pressure except for the polar compounds, water and ammonia. That is why the *MC* and the new alpha functions were generalized using only the parameters obtained for light hydrocarbons, water, carbon dioxide, hydrogen sulphide and nitrogen.

Component	TB Generalized Alpha Function [230]		Generalized MC Alpha Function		Generalized New Alpha Function	
	Bias %	AAD %	Bias %	AAD %	Bias %	AAD %
Nitrogen	1.2	1.7	-0.1	0.2	-0.1	0.2
Methane	1.3	1.5	0.1	0.3	0.1	0.2
Hydrogen sulphide	0.8	2.7	-0.2	0.7	-0.3	0.6
Ethane	-1.1	3.7	1.2	1.6	1.2	1.6
Propane	-2.6	5.0	0.6	0.9	0.6	1.1
Carbon dioxide	2.2	2.2	0.7	0.7	0.4	0.4
Water	*0.7*	*1.2*	*0.3*	*0.4*	*0.0*	*0.4*
Butane	-2.8	5.1	0.4	0.8	0.5	1.1
Pentane	-4.8	6.6	-1.7	1.7	-1.5	1.5
Overall	**-0.6**	**3.3**	**0.1**	**0.8**	**0.1**	**0.8**

TABLE 5.5 – COMPARISON OF PURE COMPONENT VAPOUR PRESSURES USING THE PR-EoS

The pure compound vapour pressures of these selected compounds (TABLE 5.5) were calculated using the both generalized alpha function as well as generalized Trebble-Bishnoi alpha function (eq.5.1). The *m* parameter of the *Trebble Bishnoi* alpha function was correlated to the acentric factor ω specifically for alkanes (up to C_{20}), water and carbon dioxide by *Daridon et al.* [230]. The relationships obtained for the *PR-EoS* are the following:

$$m = 0.418 + 1.58\omega - 0.580\omega^2 \quad \text{when } \omega < 0.4 \tag{5.23}$$

$$m = 0.212 + 2.2\omega - 0.831\omega^2 \quad \text{when } \omega \geq 0.4 \tag{5.24}$$

The new generalized alpha function predicts pure compound vapour pressure with an overall *AAD* of 0.8 % (0.1% bias) compared to 3.3% (-0.6 % bias) with the generalized *Trebble-Bishnoi* alpha function. The results obtained with the generalized *MC* alpha function are similar, 0.8 % *AAD* (0.1% bias).

In order to futher evaluate the capabilities of the studied alpha functions, different properties such as the vapour and liquid fugacities, the vapour and liquid residual enthalphies, the compressibility factor… were also calculated and compared. From these comparisons, it can be noted that all the above-mentioned alpha functions are successful in the calculation of the residual enthalpies and of the compressibility factor (example: for water the *AAD* in the calculation of the vapour residual enthalphie is 0.7 % and 3.1 % with the new generalized alpha function and the generalized *MC* alpha function, respectively).

5.2   Modelling by the ϕ - ϕ Approach

A general phase equilibrium model based on uniformity of the fugacity of each component throughout all the phases [291-292] was used to model the gas solubility. The *VPT-EoS* [226] with the *NDD* mixing rules [233] was employed in calculating fugacities in fluid phases. This combination has proved to be a strong tool in modelling systems with polar and non-polar components [233].
The *VPT - EoS* is given by:

$$P = \frac{RT}{v - b} - \frac{a}{v(v + b) + c(v - b)} \tag{5.25}$$

with:

$$a = \bar{a}\alpha(T_r)$$ (5. 26)

$$\bar{a} = \frac{\Omega_a R^2 T_c^2}{P_c}$$ (5. 27)

$$b = \frac{\Omega_b R T_c}{P_c}$$ (5. 28)

$$c = \frac{\Omega_{c^*} R T_c}{P_c}$$ (5. 29)

$$\alpha(T_r) = \left[1 + F\left(1 - T_r^\Psi\right)\right]^2$$ (5. 30)

where P is the pressure, T is the temperature, v is the molar volume, R is the universal gas constant, and $\Psi = 0.5$. The subscripts c and r refer to critical and reduced properties, respectively. The coefficients Ω_a, Ω_b, Ω_{c^*}, and F are given by:

$$\Omega_a = 0.66121 - 0.76105 Z_c$$ (5. 31)

$$\Omega_b = 0.02207 + 0.20868 Z_c$$ (5. 32)

$$\Omega_{c^*} = 0.57765 - 1.87080 Z_c$$ (5. 33)

$$F = 0.46283 + 3.58230(\omega Z_c) + 8.19417(\omega Z_c)^2$$ (5. 34)

where Z_c is the critical compressibility factor, and ω is the acentric factor. *Tohidi-Kalorazi* [293] relaxed the α function for water, α_w, using experimental water vapour pressure data in the range of 258.15 to 374.15 K, in order to improve the predicted water fugacity:

$$\alpha_w(T_r) = 2.4968 - 3.0661 T_r + 2.7048 T_r^2 - 1.2219 T_r^3$$ (5. 35)

The above relation is used in the present work.

In this work, the *NDD* mixing rules developed by *Avlonitis et al.* [233] are applied to describe mixing in the *a*-parameter:

$$a = a^C + a^A$$ (5. 36)

where a^C is given by the classical quadratic mixing rules as follows:

$$a^C = \sum_i \sum_j x_i x_j a_{ij}$$ (5. 37)

and b, c and a_{ij} parameters are expressed by:

$$b = \sum_i x_i b_i \tag{5.38}$$

$$c = \sum_i x_i c_i \tag{5.39}$$

$$a_{ij} = \left(1 - k_{ij}\right)\sqrt{a_i a_j} \tag{5.40}$$

where k_{ij} is the standard binary interaction parameter (*BIP*).

The term a^A corrects for asymmetric interactions, which cannot be efficiently accounted for by classical mixing rules:

$$a^A = \sum_p x_p^2 \sum_i x_i a_{pi} l_{pi} \tag{5.41}$$

$$a_{pi} = \sqrt{a_p a_i} \tag{5.42}$$

$$l_{pi} = l_{pi}^0 - l_{pi}^1 \left(T - T_0\right) \tag{5.43}$$

where p is the index for polar components.

Using the *VPT-EoS* and the *NDD* mixing rules, the fugacity of each component in all fluid phases is calculated from:

$$ln\,\phi_i = \frac{1}{RT} \int_V^\infty \left[\left(\frac{\partial P}{\partial n_i}\right)_{T,V,n_{j\neq i}} - RT/V\right] dV - ln\,Z \qquad \text{for } i = 1, 2, ..., M \tag{5.44}$$

$$f_i = x_i \phi_i P \tag{5.45}$$

where ϕ_i, V, M, n_i, Z and f_i are the fugacity coefficient of component i in the fluid phases, volume, number of components, number of moles of component i, compressibility factor of the system and fugacity of component i in the fluid phases, respectively.

5.3   Modelling by the γ - ϕ Approach

This approach is based on activity model for the condensed phase and an equation of state for the fluid phase. The *Peng-Robinson* [208] equation of state (*PR-EoS*) is selected because of its simplicity and its widespread utilization in chemical engineering. Its formulation is:

$$P = \frac{RT}{v-b} - \frac{a(T)}{v(v+b)+b(v-b)} \tag{5.46}$$

in which :

$$b = 0.07780 \frac{RT_c}{P_c} \tag{5.47}$$

and

$$a(T) = a_c \alpha(T_r) \tag{5.48}$$

where

$$a_c = 0.45724 \frac{(RT_c)^2}{P_c} \tag{5.49}$$

To have an accurate representation of vapour pressures of each component and because of the quality of results provided by this generalized alpha function, the new alpha function was selected (§5.1.3.2) along with the classical quadratic mixing rules:

$$a = \sum_i \sum_j x_i x_j a_{ij} \tag{5.50}$$

where $a_{ij} = \sqrt{a_i a_j}(1 - k_{ij})$ (5.51)

$$b = \sum_i x_i b_i \tag{5.52}$$

At thermodynamic equilibrium, fugacity values of each component are equal in vapour and liquid phases.

$$f_i^L(P,T) = f_i^V(P,T) \tag{5.53}$$

The vapour fugacity is calculated as follows:

$$f_i^V(P,T) = \varphi_i^V \times P \times y_i \tag{5.54}$$

For the aqueous phase, a Henry's law approach is used for gaseous components and water, as the gaseous components are at infinite dilution the asymmetric convention ($\gamma_g \rightarrow 1$ when $x_g \rightarrow 0$) is used to express the Henry's law for the gas (Eq. 5.55) and a symmetric convention ($\gamma_w \rightarrow 1$ when $x_w \rightarrow 1$) for water (Eq. 5.56).

$$f_g^L(P,T) = H_w^L(T) \times x_g(T) \times \exp((\frac{v_g^\infty(T)}{RT})(P - P_w^{sat})) \qquad \text{for the gas} \tag{5.55}$$

$$f_w^L(P,T) = \gamma_w^L \times \varphi_w^{sat} \times P_w^{sat} \times x_w(T) \times \exp((\frac{v_w^{sat}(T)}{RT})(P - P_w^{sat})) \quad \text{for water} \tag{5.56}$$

$$x_g(T) = \frac{P \times \varphi_g^v \times y_g(T)}{H_w^L(T) \times \exp((\frac{v_g^\infty(T)}{RT})(P - P_w^{s\infty t}))} \tag{5.57}$$

The fugacity coefficient in the vapour phase is calculated using the *Peng-Robinson EoS*. Values of the partial molar volume of the gas at infinite dilution in water can be found in the literature for some compounds, but also with a correlation based on the work of *Lyckman et al.* [245] and reported by *Heidmann and Prausnitz* [246] in the following form:

$$\left(\frac{P_{c,i} \cdot v_i^\infty}{R \cdot T_{c,i}}\right) = 0.095 + 2.35 \cdot \frac{T \cdot P_{c,i}}{c \cdot T_{c,i}} \tag{5.58}$$

with P_{ci} et T_{ci}, solute critical pressure and temperature and c the cohesive energy density of water:

$$c = \frac{\Delta U_w}{v_w^{sat}} \text{ with } \Delta U_w = \Delta H_w - R \cdot T \tag{5.59}$$

with ΔU_w, energy of water vaporization (at zero pressure)

For better high temperature dependence the following correction is used:

$$v_i^\infty(T) = [v_i^\infty(T)]_{Lyckman} + \left(\frac{dv_w}{dT}\right)^{sat} \times (T - 298.15) \tag{5.60}$$

The Henry's law constants for the gases can be adjusted directly from experimental results or can be taken from the literature [238]. In both cases the Henry's constants are expressed using the mathematical equation below:

$$\log_{10}(H_{gas-w}(T)) = A + B \times 10^3 / T - C \times \log_{10}(T) + D \times T \quad \textbf{(\textit{H} in atm)} \tag{5.61}$$

The NRTL model [247] is used to calculate the water activity (Eqs 3.93 – 3.97)

Results

Dans ce chapitre, nous allons présenter les résultats expérimentaux et leurs modélisations pour les systèmes suivants :

- *Mesures de teneur en eau des systèmes : méthane, éthane et un mélange synthétique de méthane, éthane et n-butane.*

- *Mesures de teneur en eau en présence d'inhibiteur pour le même mélange en présence de méthanol et d'éthylène glycol.*

- *Mesures de solubilités de gaz dans l'eau pour le méthane, l'éthane, le propane, le mélange synthétique, le dioxyde de carbone, le sulfure d'hydrogène et l'azote.*

Pour finir les résultats expérimentaux sur la solubilité du méthane dans des solutions d'éthylène glycol seront présentés.

6   Experimental and Modelling Results

Natural gases normally are in equilibrium with water inside reservoirs. Numerous operational problems in gas industry can be attributed to the water produced and condensed in the production systems. Therefore, experimental data are crucial for successfully developing and validating models capable of predicting the phase behaviour of water/hydrocarbons systems over a wide temperature range. As water content measurements in vapour gas phases and gas solubilities measurements are completely different experiments, they are treated separately.

6.1   Water Content in Vapour Phase

6.1.1 Methane-Water System

This project involves new water solubility measurements in vapour of the methane-water binary system near the hydrate forming conditions. Isothermal vapour-liquid and vapour-hydrate equilibrium data of the vapour phase for the methane-water binary system were measured at 283.1, 288.1, 293.1, 298.1, 303.1, 308.1, 313.1 and 318.1 K and pressures up to 35 MPa. The experimental and calculated (using model described in §5.3) *VLE* data are reported in TABLE 6.1 and plotted in Figures 6.2a and 6.2b. The *BIP*s, k_{ij}, are adjusted directly to *VLE* data through a modified Simplex algorithm using the objective function, displayed in eq. 6.1:

$$F_y = \frac{100}{N} \sum_{1}^{N} \left(\frac{y_{i,\exp} - y_{i,cal}}{y_{i,\exp}} \right)^2 \tag{6.1}$$

where N is the number of data points, y_{exp} is the measured pressure and y_{cal} the calculated pressure. Our isothermal P, y data sets are well represented by the selected

approach $\left(AAD = \dfrac{1}{N} \sum^{N} \left| \dfrac{x_{experimental} - x_{calculated}}{x_{experimental}} \right| = 3.3\ \% \right)$. Adjusted binary interaction

parameters: k_{ij} have been adjusted on all isothermal data in *VLE* condition. Adjustments performed on each isotherms independently revealed binary interaction parameters are temperature independent:

$$k_{ij} = 0.4935\ ,\ \tau_{12} = 2375\ \text{J.mol}^{-1},\ \tau_{21} = 2780\ \text{J.mol}^{-1}$$
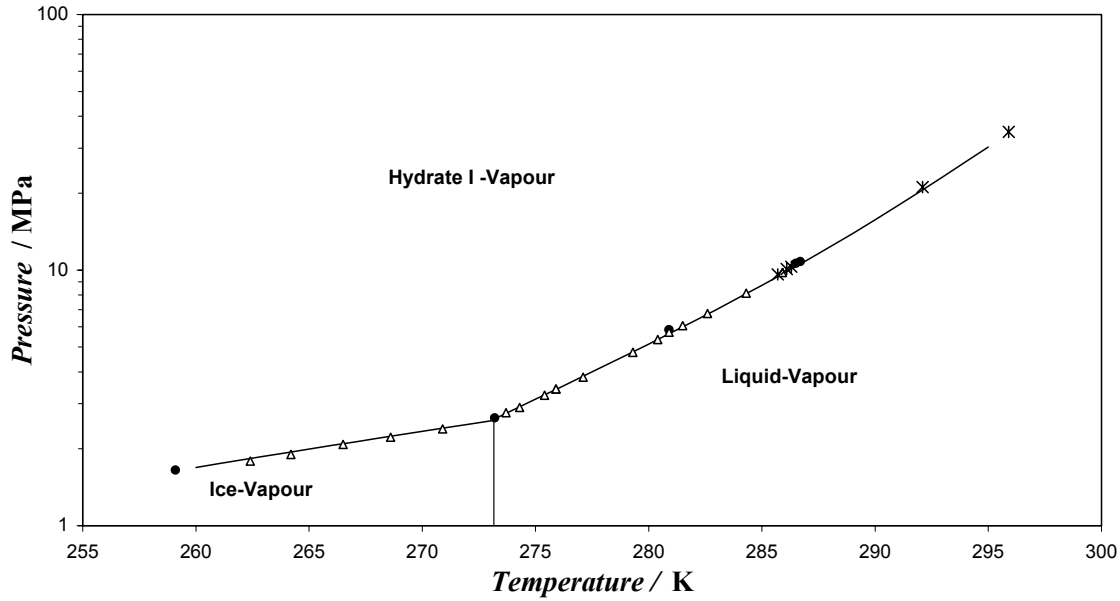
Figure 6.1: Pressure −Temperature diagram for methane and water

*: data from *Mc Leod and Campbell* (1961) [156], Δ : data from *Deaton and Frost Jr.* (1946) [155], ●: data from *Kobayashi and Katz* (1949) [32], Solid line is calculated using the approach proposed by *Chen and Guo* (1998) [267].

Above the hydrate forming conditions, the solubility of methane in the aqueous phase was calculated with the Henry's law approach using the correlation proposed for methane by *Yaws et al.* [238].

$$\log_{10}(H_{mw}(T)) = 146.89 - 5.768 \times 10^3 / T - 5.191 \times 10^1 \times \log_{10}(T) + 1.85 \times 10^{-2} \times T \qquad (6.1)$$

And the water activity is calculated through the NRTL model. The NRTL model parameters (τ_{12}, τ_{21}), except $\alpha_{ji} = 0.3$ have also been adjusted on all isothermal data in *VLE* condition. Adjustments performed on each isotherms independently revealed binary interaction parameters are temperature independent:

$$\tau_{12} = 2375 \text{ J.mol}^{-1}, \ \tau_{21} = 2780 \text{ J.mol}^{-1} \text{ (and } \alpha_{j,i} = 0.3).$$

The calculated data are reported in TABLE 6.1 and plotted in Figures 6.2a and 6.2b. As a validation of the use of the correlation (eq. 6.1), the Henry's constant for methane has been measured using the dilutor exponential technique [277] at different temperatures. The values of the Henry's constant are reported in TABLE 6.2.

Temperature (K)	Pressure (MPa)	Water Content, y_{exp} ($\times 10^3$)	Calculated Water Content, y_{cal} ($\times 10^3$)	$(y_{exp}-y_{cal})/\Delta y_{exp}$ %	Calculated Water Mole Fraction in Aqueous Phase, x_{cal}
283.08	1.006	1.240	1.261	-1.7	9.9967E-01
283.08	6.030	0.292	0.265	9.1	9.9834E-01
283.08	10.010*	0.213			
283.08	14.240*	0.150			
288.11	1.044	1.780	1.686	5.3	9.9969E-01
288.11	6.023	0.382	0.363	4.9	9.9851E-01
288.11	10.030	0.273	0.260	4.9	9.9783E-01
288.11	17.490*	0.167			
288.11	25.060*	0.126			
288.11	34.460*	0.092			
293.11	0.992	2.360	2.413	-2.2	9.9974E-01
293.11	5.770	0.483	0.507	-5.0	9.9869E-01
293.11	9.520	0.338	0.359	-6.3	9.9809E-01
293.11	17.680	0.267	0.264	1.0	9.9716E-01
293.11	24.950*	0.225	0.233	-3.4	
293.11	35.090*	0.168			
298.11	1.010	3.300	3.231	2.1	9.9976E-01
298.11	6.390	0.631	0.627	0.5	9.9870E-01
298.11	10.070	0.471	0.460	2.3	9.9816E-01
298.11	17.520	0.355	0.346	2.4	9.9737E-01
298.11	25.150	0.313	0.301	3.9	9.9679E-01
298.11	34.420	0.265	0.270	-2.0	9.9624E-01
303.11	1.100	4.440	4.027	9.3	9.9976E-01
303.11	6.060	0.889	0.864	2.9	9.9884E-01
303.11	9.840	0.625	0.613	1.9	9.9832E-01
303.11	17.500	0.456	0.449	1.4	9.9753E-01
303.11	25.060	0.371	0.388	-4.5	9.9697E-01
303.11	34.560	0.331	0.345	-4.3	9.9642E-01
308.11	1.100	5.820	5.345	8.2	9.9978E-01
308.11	5.990	1.114	1.142	-2.5	9.9893E-01
308.11	9.840	0.807	0.798	1.1	9.9842E-01
308.11	17.490	0.577	0.578	-0.2	9.9766E-01
308.11	25.090	0.495	0.494	0.2	9.9711E-01
308.11	34.580	0.447	0.437	2.2	9.9658E-01
313.12	1.100	7.460	6.745	9.6	9.9979E-01
313.12	6.056	1.516	1.470	3.1	9.9898E-01
313.12	9.980	1.045	1.021	2.3	9.9848E-01
313.12	17.470	0.715	0.738	-3.2	9.9777E-01
313.12	25.170	0.626	0.625	0.1	9.9722E-01
313.12	34.610	0.575	0.550	4.3	9.9670E-01
318.12	1.003	9.894	9.943	-0.5	9.9982E-01
318.12	6.0170	1.985	1.901	4.2	9.9904E-01
318.12	10.010	1.326	1.303	1.8	9.9855E-01
318.12	17.500	0.890	0.933	-4.9	9.9785E-01
318.12	25.120	0.763	0.787	-3.1	9.9732E-01
318.12	34.610	0.691	0.687	0.5	9.9679E-01

TABLE 6.1 – MEASURED AND CALCULATED WATER CONTENT IN MOLE FRACTION IN THE GAS PHASE AND CALCULATED WATER MOLE FRACTION IN THE AQUEOUS PHASE OF THE METHANE-WATER SYSTEM [B1]

* This measurement corresponds to hydrate-vapour equilibrium.

T/K	Calculated Henry's law constant /MPa	Measured Henry's law constant /MPa
273.15	396.1	405.4
278.15	429.1	442.5

TABLE 6.2 – CALCULATED HENRY'S LAW CONSTANTS WITH EQ. 6.2 AND MEASURED HENRY'S LAW CONSTANTS
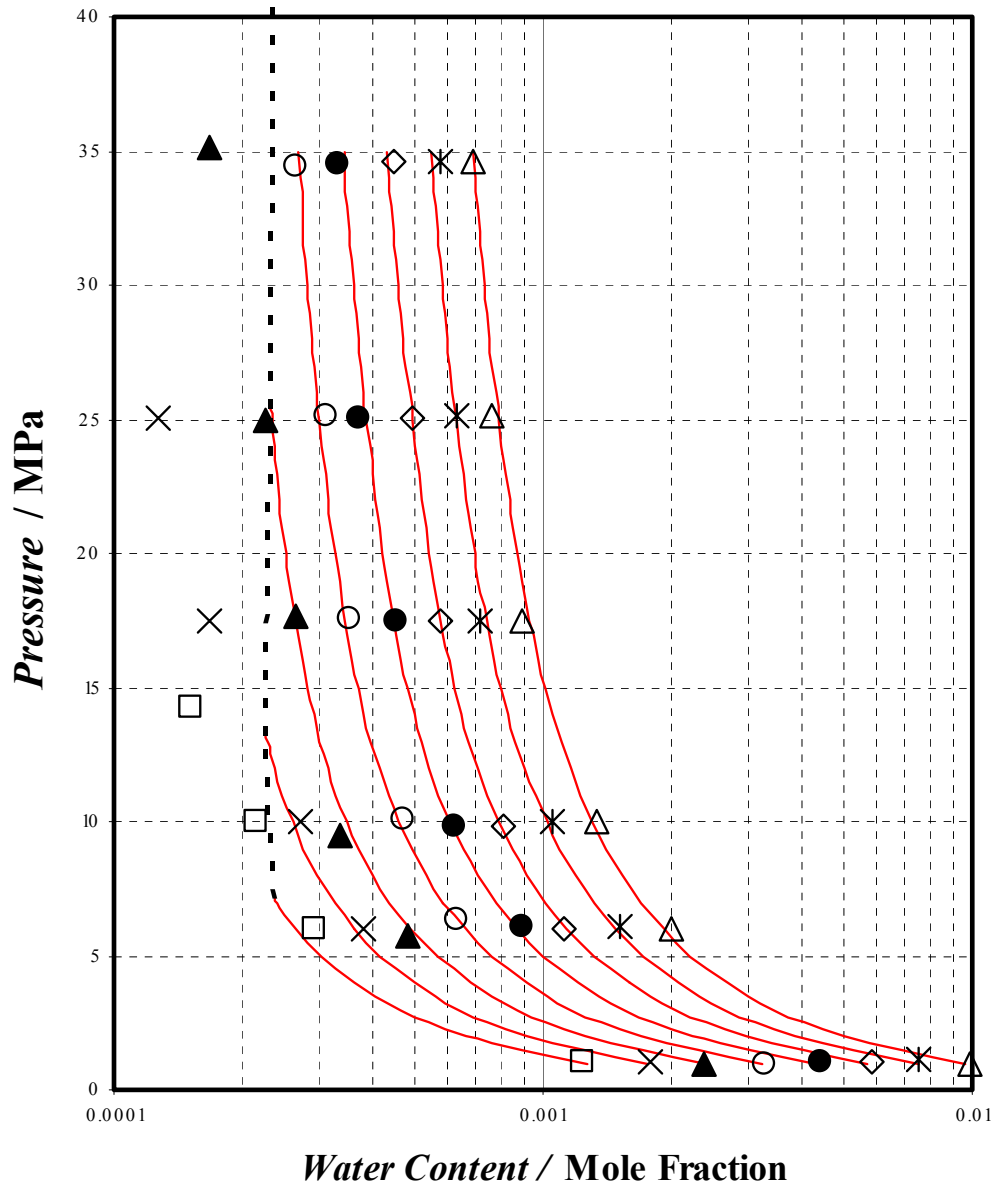
Figure 6.2a: Methane–Water system pressure as a function of water mole fraction at different temperatures. □ : 283.08 K, × : 288.11 K, ▲ :293.11 K, o: 298.11 K, ● : 303.11 K, ◊ : 308.11 K, ∗ : 313.12 K, Δ : 318.12 K.Solid lines : calculated with *PR-EoS* and the classical mixing rules. Dash line: Hydrate forming line calculated using the *van der Waals – Platteeuw* approach
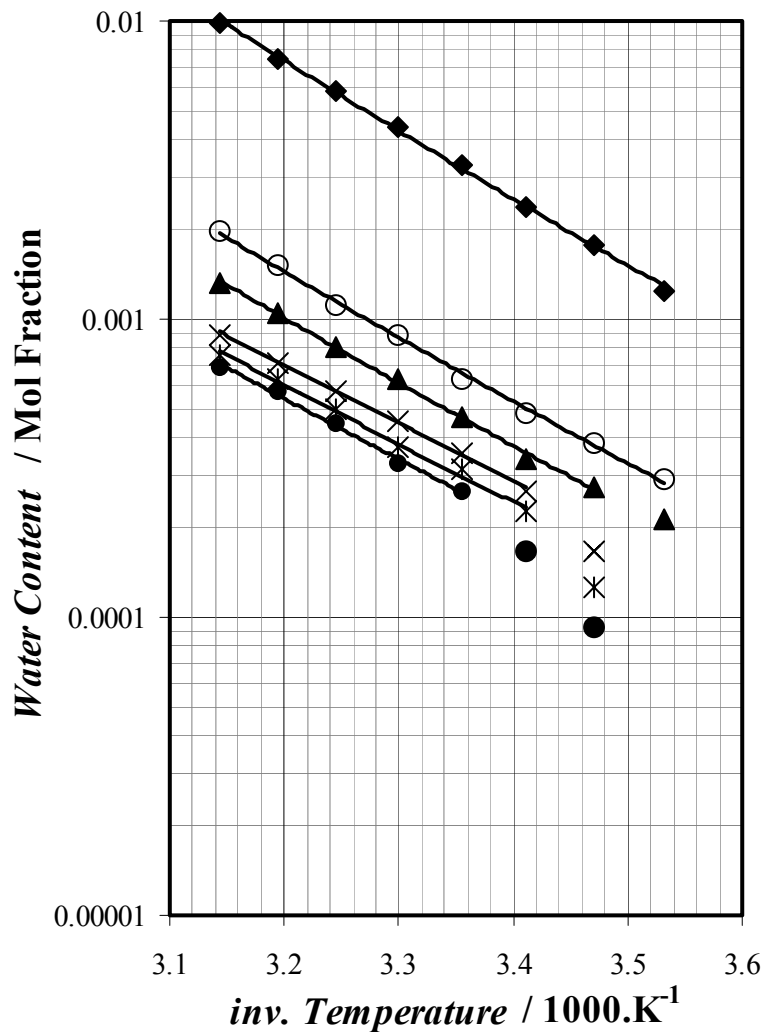
Figure 6.2b: Water content in the gas phase of the water – methane system
◆, 1 MPa; ○, 6 MPa; ▲, 10 MPa; ✕, 17.5 MPa; ✳,25 MPa; ●, 34.5 MPa

The solubility measurements of water in vapour of the methane-water binary system have been compared with available data in literature (Figure 6.3a and b). The results at temperature higher than 298 K are consistent with those of all the authors except *Yarym-Agaev et al.* at *T*=298.15 K [18]. As illustrated by the picture, the data of *Yarym-Agaev* and co-workers differ strongly at 298.15 K from those given by *Rigby and Prausnitz* [23]. The data reported by *Culberson and Mc Ketta* [24] are quite dispersed. In using the adjusted *BIPs*, it can be noticed that even at higher temperature (323.15 and 338.15 K) than in the adjusted temperature range, a good agreement is observed with the literature data.
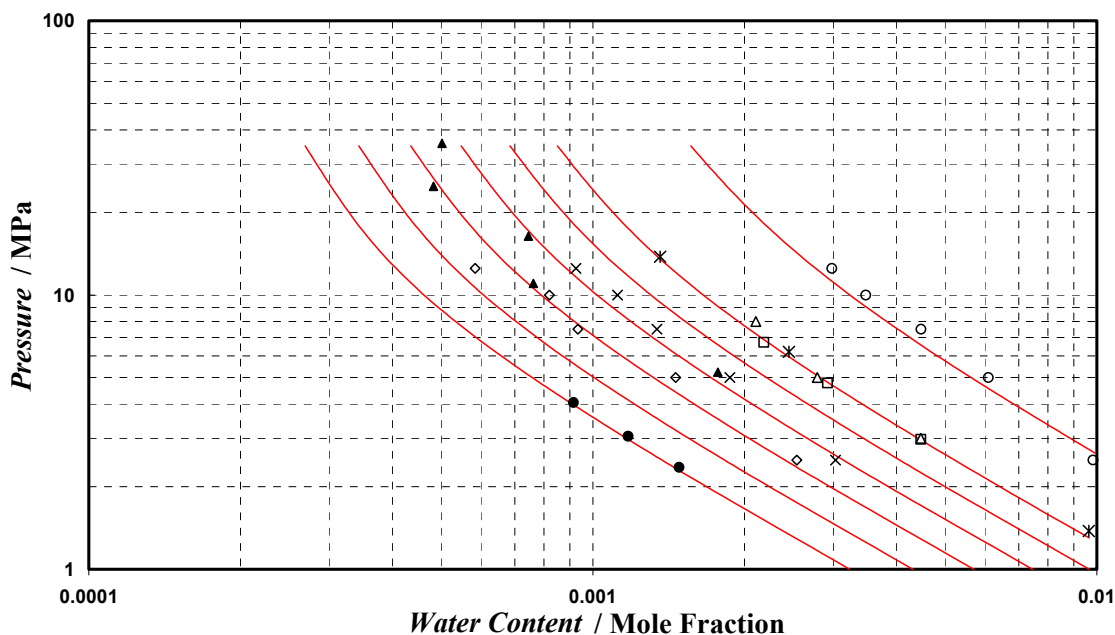
Figure 6.3a: Py-diagram comparing selected experimental data at $T > 298$ K
●, data at 298.15 K from *Rigby and Prausnitz* (1968) [23]; □, data at 323.15 K from *Rigby and Prausnitz* (1968) [23]; ◇, data at 298.15 K from *Yarym-Agaev et al.* (1985) [18]; ▲, data at 310.93 K from *Culberson and Mc Ketta* (1951) [24]; ○, data at 338.15 K from *Yarym-Agaev et al.* (1985) [18]; ✕, data at 313.15 K from *Yarym-Agaev et al.* (1985) [18]; ✱, data at 323.15 K from *Gillepsie and Wilson* (1982) [19]; △, data at 323.15 K data from *Yokoyama et al.* (1988) [17]; Solid lines represent y_w calculated values at 298.11-338.15 K.

At low temperatures ($T < 298$ K, i.e. 293.11, 288.11 and 283.08 K), and low pressures the water contents are in good agreement with the data of *Althaus* and *Kosyakov et al.* [15, 20] (at 1.04 MPa and 288.12 K, $y_w = 1.78 \times 10^{-3}$ and at 1 MPa and 283.08 K, $y_w = 1.24 \times 10^{-3}$ in this work, and the water mole fraction at 288.15 and 283.15 for 1 MPa correlated with the *PR-EoS* and the classical mixing rules for the work of *Althaus* is $y_w = 1.75 \times 10^{-3}$ and $y_w = 1.26 \times 10^{-3}$ respectively). In general in *VLE* condition, the new generated data along with both last cited data are in a satisfactory agreement.

However, slight deviations are observed in *VH* conditions (At 10 MPa, and 283.1 K, $y_w = 2.1 \times 10^{-4}$ and at 10 MPa and 283.15 K, $y_w = 1.8 \times 10^{-4}$ for the work of *Althaus*). That might be explained by different factors. For calibration and withdrawal of samples, adsorption of water is highly reduced by using Silcosteel™ tubing between the dilutor and the TCD, and between the sampler and the TCD.

152
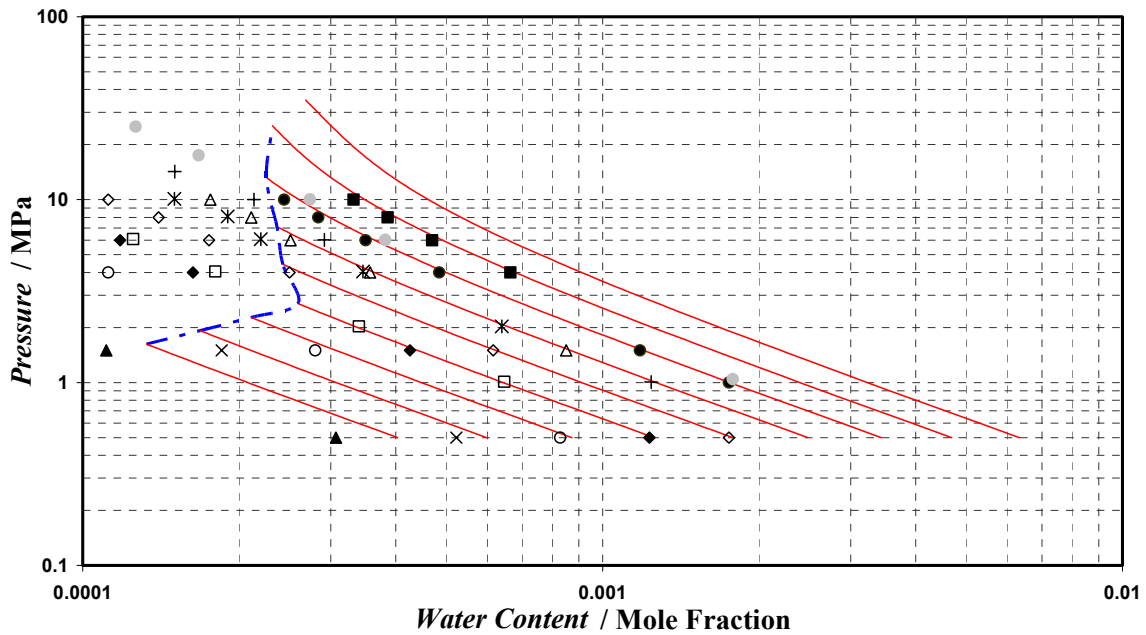
Figure 6.3b: Py-diagram comparing selected experimental data at $T < 298$ K
+, 283.1 K; ●, 288.1 K; ■, data at 293.15 K from *Althaus* (1999) [15]; ●, data at 288.15 K from *Althaus* (1999) [15]; △, data at 283.15 K from *Althaus* (1999) [15]; ◇, data at 278.15 K from *Althaus* (1999) [15]; ◆, data at 273.15 K from *Althaus* (1999) [15]; ○, data at 268.15 K from *Althaus* (1999) [15]; ×, data at 263.15 K from *Althaus* (1999) [15]; ▲, data at 258.15 K from *Althaus* (1999) [15]; ✳, data at 283.15 K from *Kosyakov* et al. (1982) [20]; □, data at 273.15 K from *Kosyakov* et al. (1982) [20].

Moreover, a series of tests was performed in order to check that the adsorption of water inside the internal injection loop was negligible. The number of water molecules adsorbed inside the loop is a function of both the valve loop temperature and the contact time with the water saturated helium. It was observed that absorption was really negligible for temperatures higher than 523 K. To completely avoid the adsorption phenomenon, the internal injection valve and tubing were maintained at 573 K. It was checked that varying the loop sweeping time from 5 to 60 seconds had no sensitive effect on the water peak area. Different sampling sizes have been selected during the experiments and the results repeatability is within 5%. The difference of composition might be also explained by the fact that phase transition (to a hydrate phase) had not enough time to take place (as hydrate formation is not instantaneous). But during the experiments, after introduction of the gas into the cell directly from the commercial cylinder or via a gas compressor, an efficient stirring is started and pressure is stabilized within about one minute, if no hydrate is formed. In case of hydrate formation the pressure in cell continue to decrease within a long period of time that can extend to 4 hours. In this case, solubility measurements were performed only when pressure was constant for about one hour (Furthermore pressure is verified to be constant all

along the sample analyses, 3 hours of measurements at least for one solubility). The technique used in [15] and generally to measure the water composition in a gas phase is a dynamic method i.e.: the gas is bubbled at ambient temperature into a saturator filled with water. The temperature of this saturated gas is reduced to the desired equilibrium temperature by a series of condensers. The main difficulty associated with that technique is about the possibility of reaching an equilibrated hydrate phase (in *PT* conditions of hydrate formation) due to small residence times.

The calculated Henry's law constant using the correlation is estimated to be within 3% in comparison with the measured Henry's law constant. The calculated water distributions in the aqueous phase of the system have been compared with data from *Yang et al.* [84] at 298.15 K, *Culberson and Mc Ketta* at 298.15 and 310.93 K [54] and *Lekvam and Bishnoi* [66] (Figure 6.4). A good agreement is found between all of these data within experimental uncertainties. The results of *Wang et al.* [86] at 283.2 K are higher than others from literature but lower at 293.2 and 303.2 K. However, the methane solubilities in water will be studied more in details further on. An equivalent of the *Mc Ketta* Chart has been produced using the adjusted parameters (Figure 6.5)
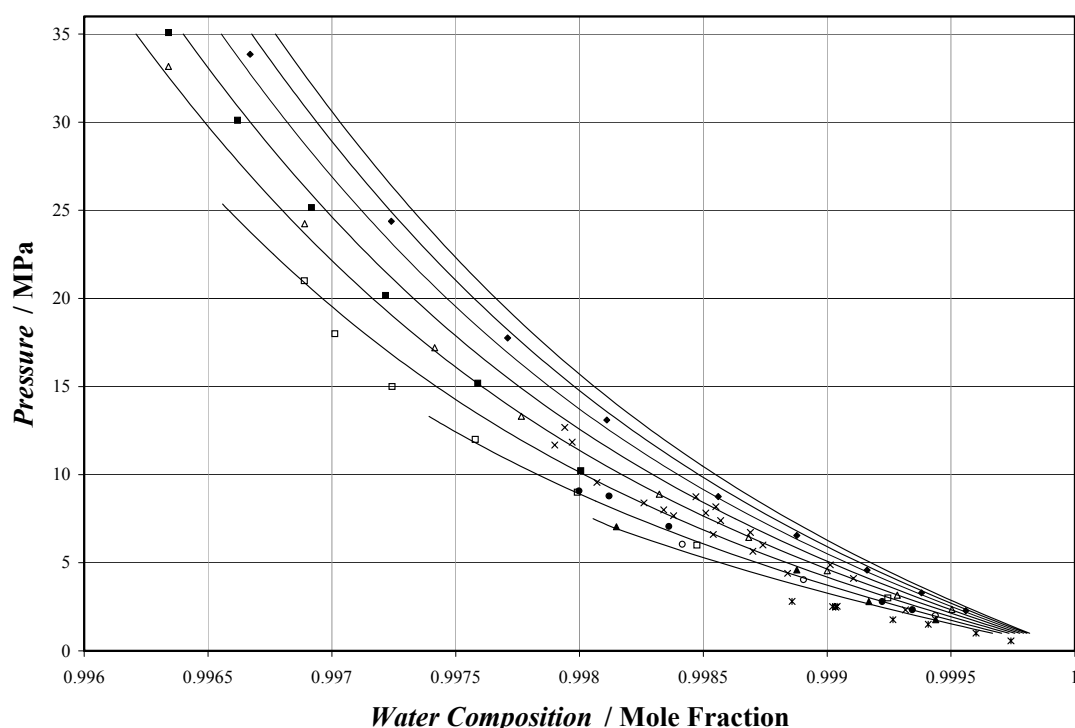
Figure 6.4: Calculated water mole fraction in the aqueous phase at different temperatures
Solid lines, calculated with the Henry's law approach for 283.08-318.12 K; ◇, *Culberson and Mc Ketta, Jr* (1951) at T=310.93 K [54]; △, *Culberson and Mc Ketta, Jr* (1951) at T= 298.15 K [54], ▲, *Lekvam and Bishnoi* (1997) at T=283.37 K [66]; ●, *Lekvam and Bishnoi* (1997) T=285.67 K [66], ✱, *Lekvam and Bishnoi* (1997) at T=274.35 K [66]; +, data of *Yang et al.* at 298.15 K [84], □ : *Wang et al.* (2003) at T=293.2 K [86]; ○, *Wang et al.* (2003) at T=283.2 K [86], ■: *Wang et al.* (2003) at T=303.2 K [86].
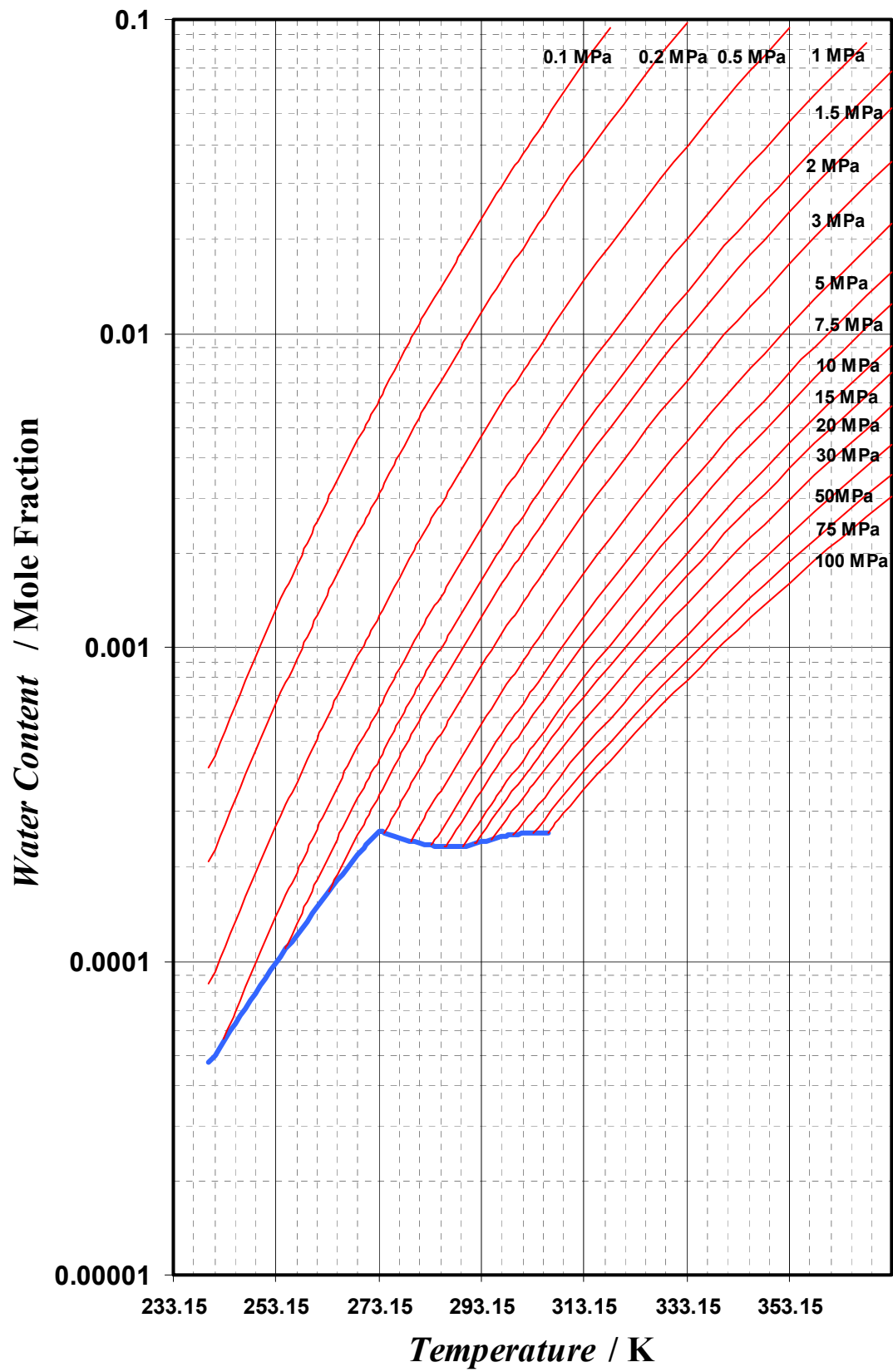
Figure 6.5: Water Content of Methane (Blue line: hydrate dissociation line)

6.1.2   Ethane-Water System

This system involves measurements of the vapour phase composition for the ethane - water binary system presenting phase equilibria near hydrate-forming conditions. The H_2O - C_2H_6 binary system isothermal vapour phase data, concerning both vapour-liquid and vapour-hydrate equilibria, were measured at (278.08, 283.11, 288.11, 293.11, 298.11 and 303.11) K and pressures up to the ethane vapour pressure.
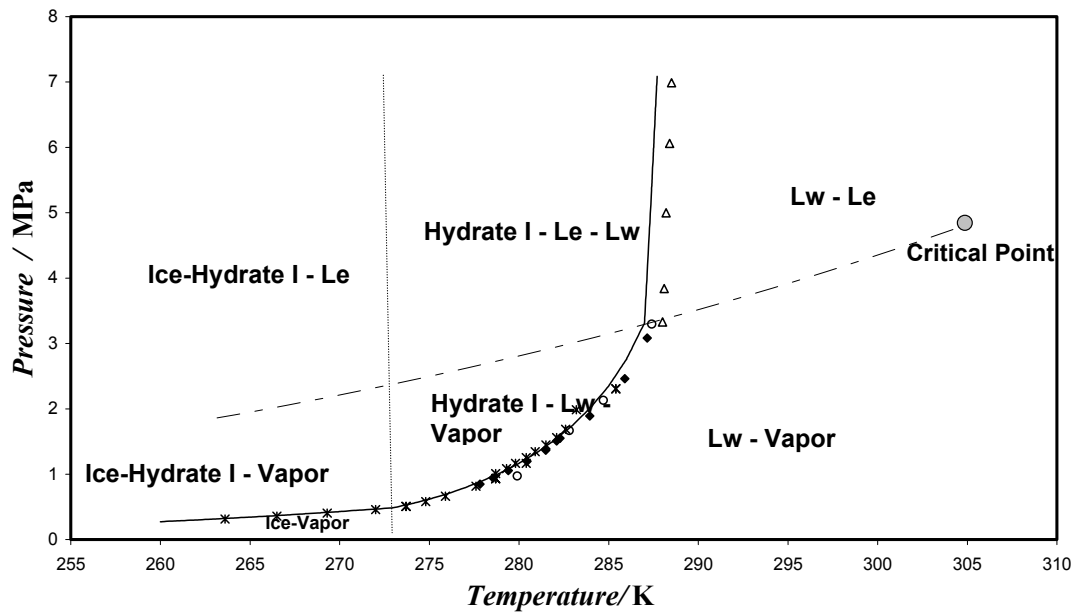
Figure 6.6: Pressure –Temperature diagram for ethane + water system
∗, data from *Deaton and Frost Jr.* [155] ; Δ, data from *Ng and Robinson* [184] ; ●, data from *Reamer et al.* [159] ; □, data from *Holder et al.* [160];……., Ice Vapour Pressure ;-------, Ethane Vapour Pressure ;Lw, Liquid Water ; Le, Liquid Ethane

As for methane, the *VLE* experimental and calculated (using model described in §5.3) data are reported in TABLE 6.3 and plotted in Figures 6.7. The *BIPs*, k_{ij}, are adjusted directly to *VLE* data through a modified Simplex algorithm using the objective function, displayed in eq 6.1. Adjusted binary interaction parameters: k_{ij} are found constant in the temperature range equals to 0.46.   And the water activity is calculated through the NRTL model for which adjusted parameters are: $\tau_{1,2}$=2795 J/mol and $\tau_{2,1}$=2977 J/mol and $\alpha_{j,i}$ = 0.3.

Temperature (K)	Pressure (MPa)	Water Content, y_{exp} ($\times 10^3$)	Water Content, Calculated, y_{cal} ($\times 10^3$)	$(y_{exp}-y_{cal})/\Delta y_{exp}$ %
278.08	0.455	2.050	2.11	-2.7
278.08	0.756	1.270	1.26	1.0
278.08	0.990	0.898		
278.08	1.23	0.673		
278.08	1.51	0.476		
278.08	1.58	0.453		
278.08	2.11	0.304		
278.08	2.71	0.215		
283.11	0.323	4.210	3.92	7.5
283.11	0.388	3.510	3.32	5.9
283.11	0.415	3.280	3.13	4.7
283.11	0.621	2.120	2.23	-5.1
283.11	0.774	1.710	1.78	-4.2
283.11	0.962	1.340		
283.11	1.05	1.170		
283.11	1.45	0.816		
283.11	1.82	0.575		
283.11	2.11	0.501		
283.11	2.35	0.436		
283.11	2.78	0.352		
283.11	2.99	0.304		
288.11	0.898	2.320	2.21	5.3
288.11	1.39	1.410	1.41	0.4
288.11	1.91	0.934	0.956	-2.3
288.11	2.49	0.644	0.663	-2.8
288.11	2.85	0.541	0.550	-1.6
288.11	3.19	0.461	0.461	0.0
288.11	3.36	0.427	0.422	1.2
293.11	0.401	6.790	7.01	-3.1
293.11	0.527	5.200	5.14	1.1
293.11	0.774	3.480	3.35	3.7
293.11	1.22	2.060	2.05	0.6
293.11	1.50	1.670	1.78	-6.5
293.11	2.56	0.895	0.883	1.4
293.11	3.24	0.660	0.660	-0.0
293.11	3.32	0.626	0.638	-1.9
293.11	3.48	0.595	0.595	0.0
293.11	3.75	0.525		
298.11	1.08	3.860	3.56	8.3
298.11	1.43	2.850	2.65	7.8
298.11	2.19	1.780	1.68	5.5
298.11	2.73	1.370	1.30	5.6
298.11	3.53	0.982	0.940	4.5
298.11	3.99	0.794	0.794	0.0
298.11	4.01	0.768	0.788	-2.5
298.11	4.12	0.749	0.755	-0.8
303.11	0.649	8.540	7.69	11.1
303.11	0.966	5.740	5.17	11.1
303.11	1.76	3.070	2.89	6.0
303.11	2.48	1.980	1.98	0.0
303.11	3.37	1.410	1.38	2.4
303.11	4.38	0.990	0.990	0.0
303.11	4.48	0.943	0.957	-1.4
303.11	4.63	0.911	0.901	1.0

TABLE 6.3 – MEASURED AND CALCULATED WATER CONTENT (MOLE FRACTION) IN THE VAPOUR PHASE OF THE ETHANE/WATER SYSTEM [B2]
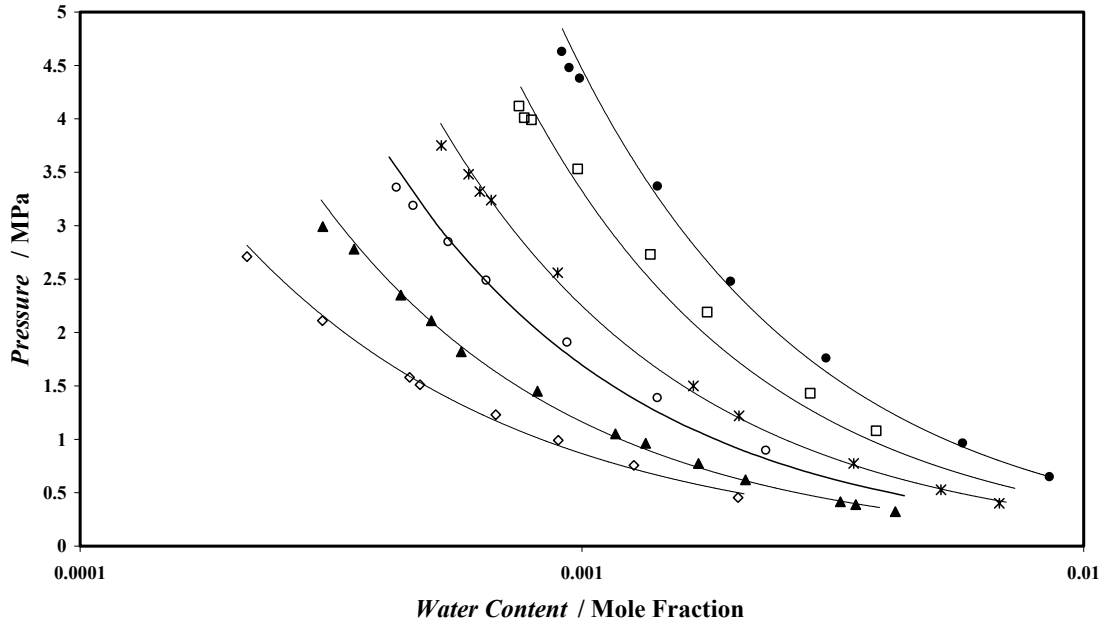
Figure 6.7: Water content in the vapour phase of the ethane - water system
◇, 278.08 K; ▲, 283.11 K; ○, 288.11 K; ✳, 293.11 K; □, 298.11 K; ●, 303.11 K.

Our isothermal P, y data sets are well represented with the *Peng-Robinson* equation of state using the new alpha function and the classical mixing rules (deviations generally less than ± 5 % and *AAD* = 3.4 %).

6.1.3 Water Content in the Water with -Propane, -*n*-Butane, -Nitrogen, -CO₂, -H₂S Systems

As no data have been generated in our laboratory for the propane – water and n-butane- water systems, literature data in *VLE* conditions are used to tune the parameters. Source of literature data for each system are reported in TABLE 2.2. As for methane and ethane, the *BIPs*, k_{ij}, are adjusted directly to *VLE* data through a modified Simplex algorithm using the objective function, displayed in eq 6.1. Adjusted k_{ij} binary interaction parameters are found constant in the concerned temperature range; their values are 0.3978 and 0.4591 for propane and n-butane, respectively. The water activity is calculated through the NRTL model and it is recommended to use $\tau_{1,2}$=2912 J/mol and $\tau_{2,1}$= 3059 J/mol for propane and $\tau_{1,2}$=3286 J/mol and $\tau_{2,1}$= 3321 J/mol for *n*-butane with $\alpha_{j,i}$ = 0.3. All adjusted parameters are finally listed in the table below. Unfortunately, no general pattern is observed for the k_{ij} parameter in function of the molecular weight of the gas or the acentric factor or the number of carbon atoms. However, the value of this parameter is close for all the systems.

Compounds	Molecular Weight	τ_{12} /J.mol^{-1}	τ_{21}/J.mol^{-1}	k_{ij}
Methane	*16.02*	2375	2778	0.49349
Ethane	*30.07*	2795	2977	0.45735
Propane	*44.10*	2912	3059	0.39780
n-Butane	*58.14*	3286	3321	0.45914
Carbon Dioxide	*44.01*	2869	2673	0.23241
Hydrogen Sulphide	*34.08*	659	3048	-0.05321
Nitrogen	*28.01*	2898	2900	0.52200

TABLE 6.4 – ADJUSTED PARAMETERS BETWEEN WATER, (1), AND LIGHT HYDROCARBONS OR OTHER GASES, (2), FOR THE PR-EoS.

The same adjustment work is carried out for carbon dioxide, nitrogen and hydrogen sulphide using available data from the literature and experimental data generated during this work. For carbon dioxide, a few measurements have been done, the experimental water content data are reported in Table 6.5 and plotted in Figure 6.8:

T / K	P / MPa	$y_{CO_2} \times 10^2$	$y_{H_2O} \times 10^2$
318.22	0.464	97.49	2.50
318.22	1.044	98.75	1.25
318.22	1.863	99.34	0.65
318.22	3.001	99.56	0.44
318.22	3.980	99.62	0.38
318.22	4.956	99.65	0.35
318.22	5.992	99.67	0.33
318.22	6.930	99.70	0.29
308.21	0.582	99.04	0.96
308.21	0.819	99.21	0.79
308.21	1.889	99.66	0.34
308.21	2.970	99.77	0.23
308.21	3.029	99.77	0.23
308.21	4.005	99.80	0.20
308.21	4.985	99.83	0.17
308.21	5.949	99.84	0.16
308.21	7.056	99.83	0.17
308.21	7.930	99.77	0.23
308.21	7.963	99.75	0.25
298.28	0.504	99.35	0.65
298.28	1.007	99.62	0.38
298.28	1.496	99.72	0.28
298.28	2.483	99.86	0.14
298.28	3.491	99.87	0.13
288.26	0.496	99.69	0.31
288.26	1.103	99.86	0.14
288.26	1.941	99.91	0.09
278.22	0.501	99.85	0.15
278.22	0.755	99.89	0.11
278.22	1.016	99.93	0.07

TABLE 6.5 – EXPERIMENTAL CARBON DIOXIDE AND WATER MOLE FRACTION IN THE VAPOUR PHASE OF THE CARBON DIOXIDE - WATER SYSTEM [B13]
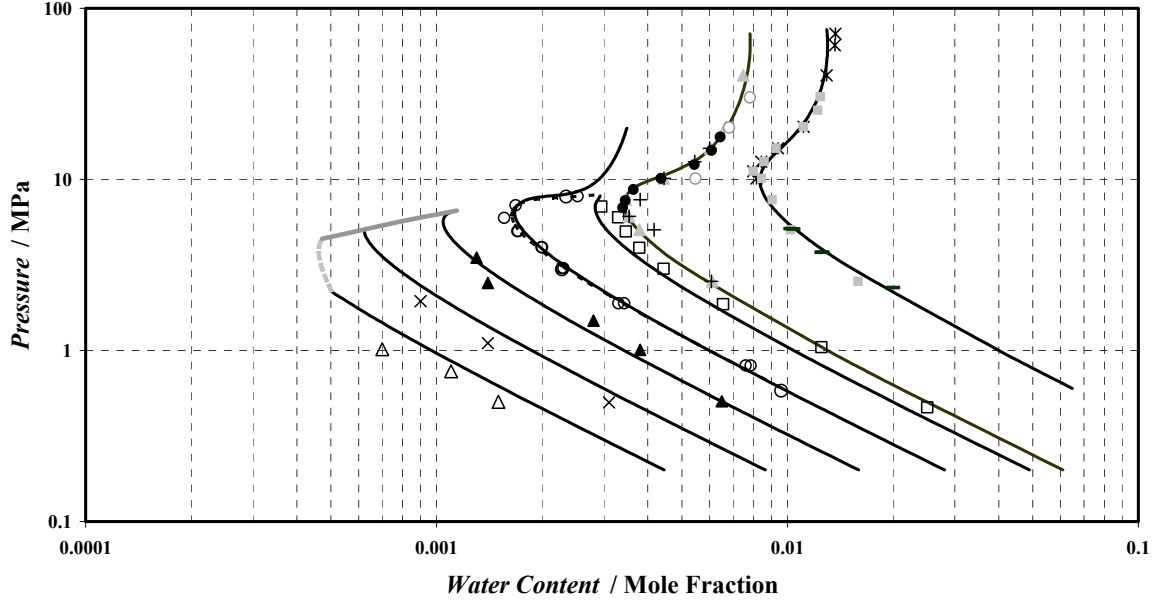
Figure 6.8: Water content in the vapour phase of the carbon dioxide - water system
□, 318.2 K; ○, 308.2 K; ▲, 298.2 K; ✕, 288.2 K; △, 278.2 K; Literature data: +, 323.15 K from [44]; ▲, 323.15 K from [45]; ●, 323.15 K from [39]; ○, 323.15 K from [37]; ■, 348.15 K from [44]; ✳, 348.15 K from [45]; ━, 348.15 K from [27]; Solid lines, calculated with the *PR-EoS* and Classical mixing rules with parameters from Table 6.4 at 278.22, 288.26, 298.28, 308.21, 318.22, 323.15 and 348.15 K. Grey solid line, water content calculated at CO_2 vapour pressure with model 1. Grey dashed line, water content calculated at CO_2 hydrate dissociation pressure

The k_{ij} are adjusted directly to *VLE* data (literature and from this work) through a modified Simplex algorithm using the objective function, displayed in eq 6.1. Adjusted binary interaction parameters are listed in Table 6.4. The isothermal *P*, *y* data sets are well represented with the *Peng-Robinson* equation of state using the new alpha function and the classical mixing rules with parameters adjusted on the data.

Water content measurements in vapour phase of nitrogen - water systems have been generated in the 282.86 to 363.08 K temperature range for pressures up to about 5 MPa. The new experimental water content data are reported in Table 6.6 and are plotted in Figure 6.9. Our isothermal *P*, *y* data sets are well represented with the first approach. The agreements between the experimental (*exp*) and predicted (*prd*) data are good, with typical *AD* (absolute

deviation $AD = \left| \dfrac{y_{2\exp} - y_{2\,prd}}{y_{2\exp}} \right|$) values between 0.1 and 8.1 %.

These data are also compared with the predictions of the second thermodynamic model. The agreements between the experimental and predicted data are good, with typical *AD* values between 0.1 and 8.7 %. The *AADs* (average absolute

deviation $AAD = \dfrac{1}{N} \sum\limits_{}^{N} \left| \dfrac{y_{2\exp} - y_{2prd}}{y_{2\exp}} \right|$) among all the experimental and predicted data is 2.4

% for the first model and 2.1 % for the second model, respectively. For further evaluation, a comparison is also made between the new data and some selected data from the literature. The results at all conditions are consistent with those of all the authors, as illustrated by Figure 6.10. The agreements between the new experimental data, predictions of both thermodynamic models and the selected literature data demonstrate the reliability of experimental data, technique and predictive methods used in this work.

T/K	P/MPa	Water Content, y_{exp} ($\times 10^4$)	γ - ϕ Approach		ϕ - ϕ Approach	
			$y_{cal} \times 10^4$	AD %	$y_{prd} \times 10^4$	AD %
282.86	0.607	20.40	20.20	1.0	20.30	0.5
282.99	1.799	7.14	7.23	1.3	7.24	1.4
282.99	3.036	4.46	4.51	1.1	4.50	0.9
283.03	4.408	3.17	3.29	3.8	3.27	3.2
293.10	0.558	42.50	42.00	1.2	42.60	0.2
293.19	1.828	13.60	13.60	0.0	13.70	0.7
293.10	2.991	8.44	8.61	2.0	8.66	2.6
293.10	4.810	5.58	5.72	2.5	5.73	2.7
304.02	0.578	79.30	77.10	2.8	78.70	0.8
304.36	1.257	37.00	37.00	0.0	37.70	1.9
304.51	2.539	18.80	19.30	2.7	19.60	4.3
304.61	4.638	11.20	11.40	1.8	11.50	2.7
313.30	0.498	153.00	148.00	3.3	152.00	0.7
313.15	1.246	60.90	60.20	1.1	61.60	1.1
313.26	2.836	27.80	28.00	0.7	28.50	2.5
313.16	4.781	17.50	17.50	0.0	17.80	1.7
322.88	0.499	240.00	241.00	0.4	248.00	3.3
323.10	1.420	87.20	88.20	1.1	90.40	3.7
322.93	3.397	39.60	38.70	2.3	39.50	0.3
322.93	4.841	29.20	28.30	3.1	28.80	1.4
332.52	0.461	427.00	414.00	3.0	426.00	0.2
332.45	1.448	134.00	135.00	0.7	139.00	3.7
332.52	2.454	85.50	82.10	4.0	84.30	1.4
332.52	4.358	48.80	48.60	0.4	49.80	2.0
342.31	0.425	719.00	696.00	3.2	718.00	0.1
342.31	0.462	658.00	641.00	2.6	661.00	0.5
342.39	1.466	219.00	208.00	5.0	214.00	2.3
342.42	2.899	103.00	109.00	5.8	112.00	8.7
342.31	4.962	66.60	66.70	0.2	68.40	2.7
351.87	0.540	849.00	822.00	3.2	848.00	0.1
352.12	1.480	335.00	310.00	7.5	320.00	4.5
351.92	2.957	162.00	159.00	1.9	164.00	1.2
351.95	4.797	111.00	102.00	8.1	105.00	5.4
363.00	0.555	1260.00	1240.00	1.6	1280.00	1.6
363.08	4.874	161.00	155.00	3.7	160.00	0.6

TABLE 6.6 – EXPERIMENTAL AND PREDICTED WATER CONTENTS IN THE NITROGEN - WATER SYSTEM.
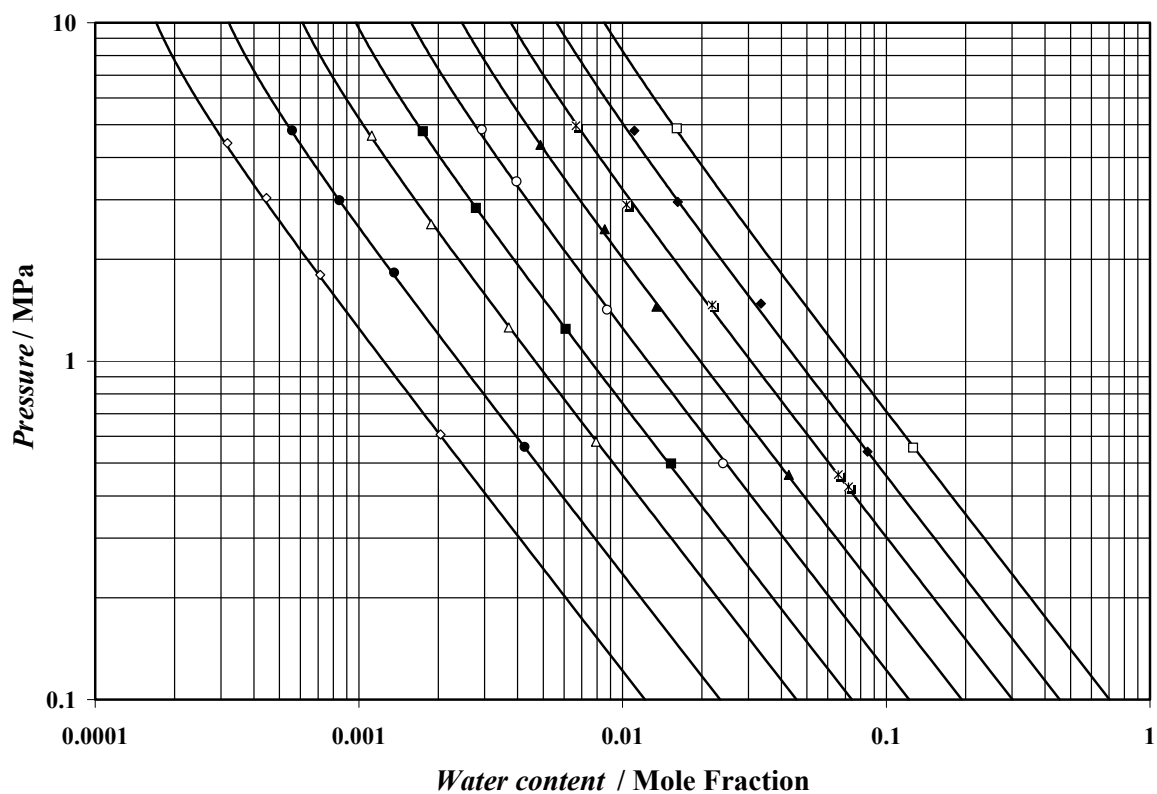
Figure 6.9: Water content in the vapour phase of the nitrogen - water system
$\diamond$, 283.0 K; $\bullet$, 293.1 K; $\triangle$, 304.4 K; $\blacksquare$, 313.2 K; $\bigcirc$, 323.0 K; $\blacktriangle$, 332.5 K; $\ast$, 342.3 K; $\blacklozenge$, 352.0 K; $\square$, 363.0 K. Solid lines, water content predicted at experimental temperatures with model 1.
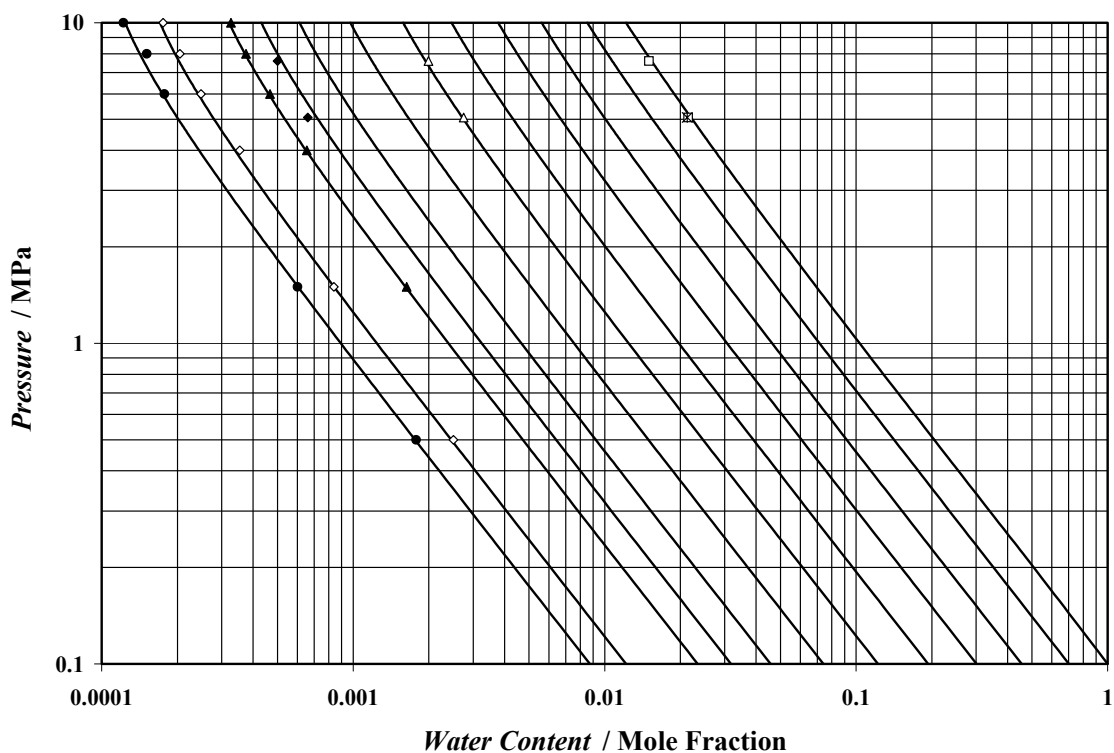
Figure 6.10: Water content in the vapour phase of the nitrogen - water system.
$\bullet$, 278.15 K from *Althaus* [15]; $\diamond$, 283.15 K from *Althaus* [15]; $\blacktriangle$, 293.15 K from *Althaus* [15]; 298.15 K from *Maslennikova et al.* [47]; $\triangle$, 323.15 K from *Maslennikova et al.* [47]; $\square$, 373.15 K from *Maslennikova et al.* [47]; $\ast$, 373.15 K from *Sidorov et al.* [44]. Solid lines, water content calculated at 278.15, 283.15, 293.15, 298.15, 303.15, 313.15, 323.15, 333.15, 343.15, 353.15, 363.15 and 373.15 K with model 1.

Water content measurements in vapour phase of hydrogen sulphide - water systems have been generated in the 298.2 to 338.3 K temperature range for pressures up to about 4 MPa. The new experimental water content data are reported in Table 6.7 and are plotted in Figure 6.10. Our isothermal P, y data sets are well represented with the first approach. The agreements between the experimental (*exp*) and predicted (*prd*) data are relatively good, with typical *AD* values between 0.0 and 12 %.

T /K	P /MPa	Water Content, y_{exp} ($\times 10^2$)	γ - ϕ approach		ϕ - ϕ approach	
			$y_{cal} \times 10^2$	AD %	$y_{prd} \times 10^2$	AD %
298.16	0.503	6.53	6.528	0.0	6.643	1.7
298.16	0.690	4.70	4.855	3.3	4.943	5.2
308.2	0.503	10.46	11.521	9.7	11.781	12.6
308.2	0.762	7.19	7.807	8.6	7.987	11.1
308.2	0.967	5.77	6.288	9.0	6.432	11.5
308.2	1.401	4.38	4.553	3.9	4.655	6.3
308.2	1.803	3.64	3.708	1.9	3.789	4.1
308.2	2.249	3.20	3.143	1.8	3.208	0.3
318.21	0.518	21.28	18.970	10.9	19.470	8.5
318.21	0.999	11.30	10.310	8.8	10.580	6.4
318.21	1.053	11.16	9.833	12.2	10.091	9.6
318.21	1.519	7.44	7.150	3.9	7.338	1.4
318.21	1.944	5.92	5.851	1.2	6.002	1.4
318.21	2.531	4.70	4.812	2.4	4.931	4.9
318.21	2.778	4.61	4.521	1.9	4.630	0.4

TABLE 6.7 – EXPERIMENTAL AND PREDICTED WATER CONTENTS IN THE HYDROGEN SULPHIDE - WATER SYSTEM.
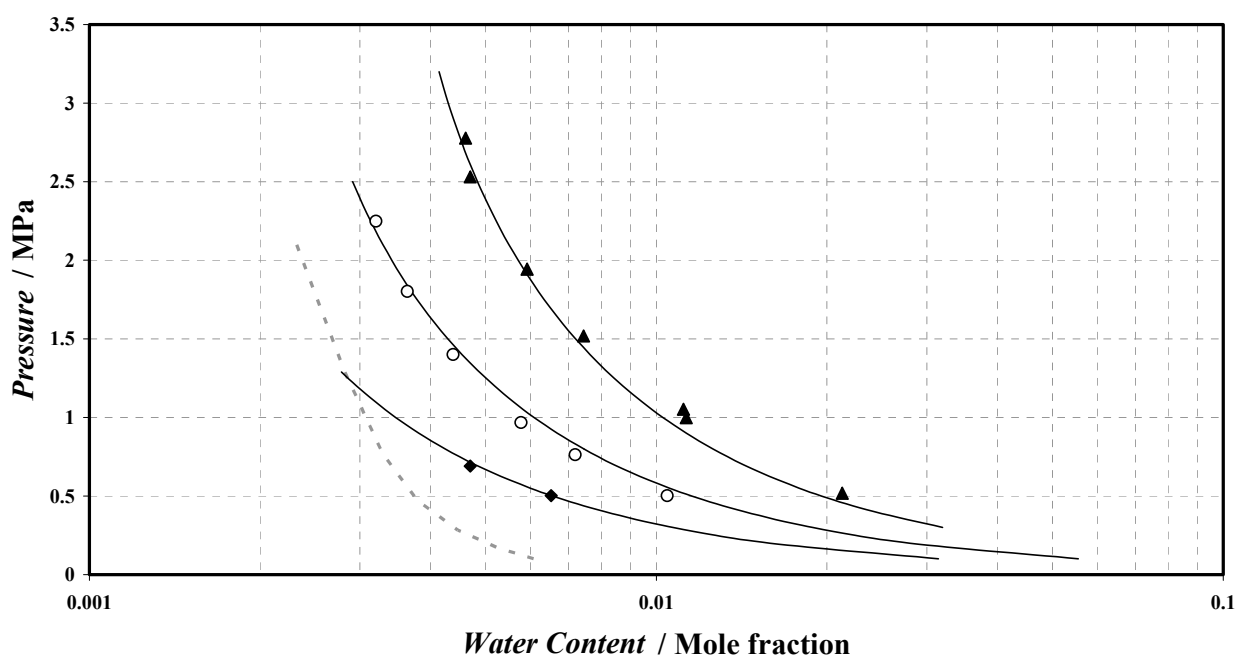
Figure 6.11: Water content in the vapour phase of the hydrogen sulphide - water system. ▲, 318.2 K; ○, 308.2 K; ◆, 298.2 K; Solid line, water content calculated with γ - ϕ model. Grey dashed line, water content calculated at H$_2$S hydrate dissociation pressure

6.1.4　Mix1- Water System

Water content data in the vapour phase of hydrocarbon gas mixture/water systems presenting phase equilibria near hydrate forming conditions have been generated from 268.15 to 313.11 K and up to 34.5 MPa.
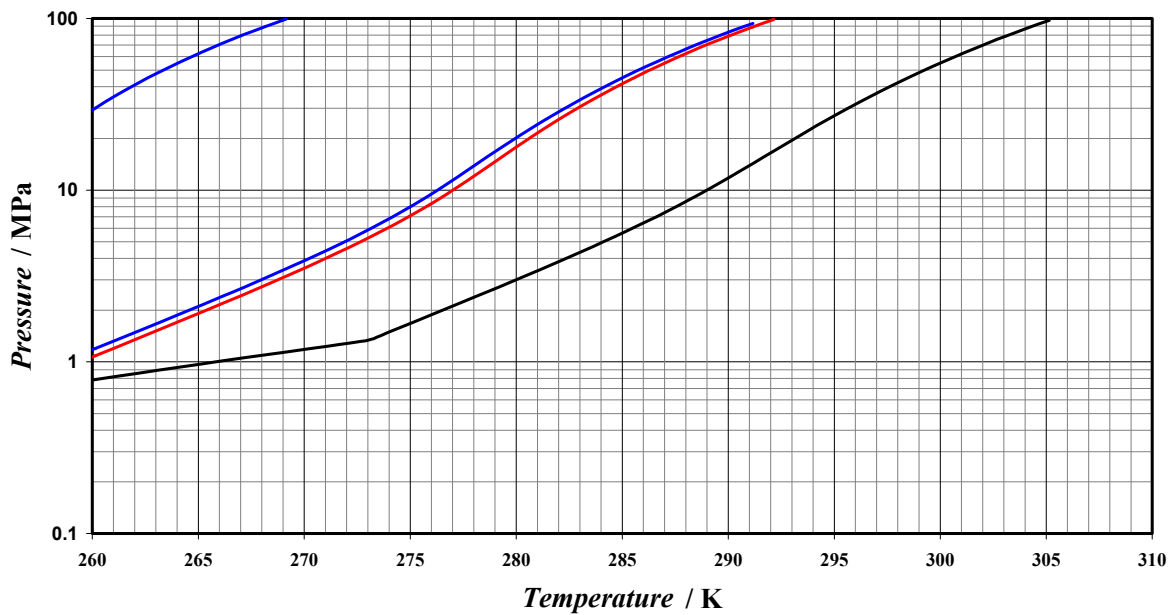
Figure 6.12: Hydrate dissociation pressures for the gas mixture in pure water, in an aqueous solution of methanol (24 and 49 wt %) and in an aqueous solution of ethylene glycol (34 wt %): black line: hydrate dissociation pressure in pure water; blue lines, hydrate dissociation pressure in the aqueous solution of methanol; red line: hydrate dissociation pressures in the aqueous solution of ethylene glycol.

Table 6.8 shows the experimental data measured for water content of the gas mixture (94% methane + 4% ethane + 2% *n*-butane), these data are also plotted along with the predictied results in Figure 6.13. This table also shows the water content values calculated by the ϕ-ϕ approach and the γ-ϕ approach (*BIPs* in Annex E). The results of both predictive methods (because the parameters are independent from these results, *BIPs* not adjusted on data of this work) are in nearly good agreement with the experimental data. It should be noted that measuring the water content in vapour phase especially at low temperatures is very difficult and the 10% uncertainty is normally acceptable. As can be seen, large deviations (>-15 % for two points) are also observed.

Temperature (K)	Pressure (MPa)	Water Content, y_{exp} ($\times 10^4$)			$(y_{exp}-y_{cal})/\Delta y_{exp}$ %	
		Exp	ϕ-ϕ approach	γ-ϕ approach	ϕ-ϕ approach	γ-ϕ approach
268.15	1.020	4.514	4.148	4.25	8	6
268.17*	6.030	0.904				
268.18*	10.058	0.588				
268.17*	17.574	0.518				
268.17*	25.049	0.422				
268.17*	34.599	0.332				
273.09	1.063	6.857	6.023	5.90	12	14
273.17*	6.012	1.090				
273.15*	10.056	0.752				
273.16*	17.542	0.662				
273.16*	25.059	0.600				
273.16*	34.610	0.501				
278.15	1.007	8.884	9.073	8.91	-2	0
278.15*	6.012	1.405				
278.15*	10.048	1.014				
278.15*	17.519	0.920				
278.16*	25.069	0.876				
278.27*	34.557	0.843				
283.14	1.018	13.715	15.010	12.41	-9	10
283.14*	5.993	2.419				
283.13*	10.007	1.648				
283.14*	17.510	1.451				
283.14*	25.067	1.355				
283.14*	34.547	1.328				
288.15	1.012	17.925	17.587	17.34	2	3
288.15	6.017	3.460	3.665	3.46	-6	0
288.15*	10.005	2.392				
288.16*	17.501	1.916				
288.16*	25.021	1.694				
288.15*	34.500	1.588				
297.93	1.010	32.050	32.219	31.87	-1	1
297.93	6.005	6.363	6.594	6.31	-4	1
297.95	10.053	4.233	4.617	4.40	-9	-4
297.95	17.543	3.015	**3.461**	**3.54**	**-15**	**-17**
297.95	25.032	2.751	3.013	2.84	-9	-3
297.94	34.514	2.580	2.693	2.56	-4	-1
303.14	1.028	38.212	42.916	42.49	-12	-11
303.12	6.036	8.450	8.813	8.48	-4	0
303.13	9.990	6.128	6.170	5.92	-1	3
303.13	17.556	4.420	4.547	4.66	-3	-5
303.13	25.168	3.788	3.920	3.85	-4	-2
303.13	34.677	3.414	3.487	3.44	-2	-1
308.12	1.029	**48.105**	**56.699**	**56.21**	-18	**-17**
308.13	6.007	10.892	11.630	11.24	-7	-3
308.13	10.044	7.722	8.026	7.75	-4	0
308.12	17.501	5.306	5.877	6.01	-11	-13
308.12	25.018	4.402	5.031	4.80	-14	-9
308.12	34.529	4.077	4.448	4.28	-9	-5
313.14	6.061	13.682	15.036	14.60	-10	-7
313.14	10.032	9.374	10.394	10.09	-11	-8
313.14	17.502	6.848	7.526	7.69	-10	-12
313.14	25.078	5.789	6.393	6.09	-10	-5
313.11	34.553	5.090	5.618	5.49	-10	-8

TABLE 6.8 – MEASURED AND CALCULATED WATER CONTENT (MOLE FRACTIONS) IN THE VAPOUR PHASE OF THE MIX1 / WATER SYSTEM. * measurement corresponding to hydrate-vapour equilibrium.
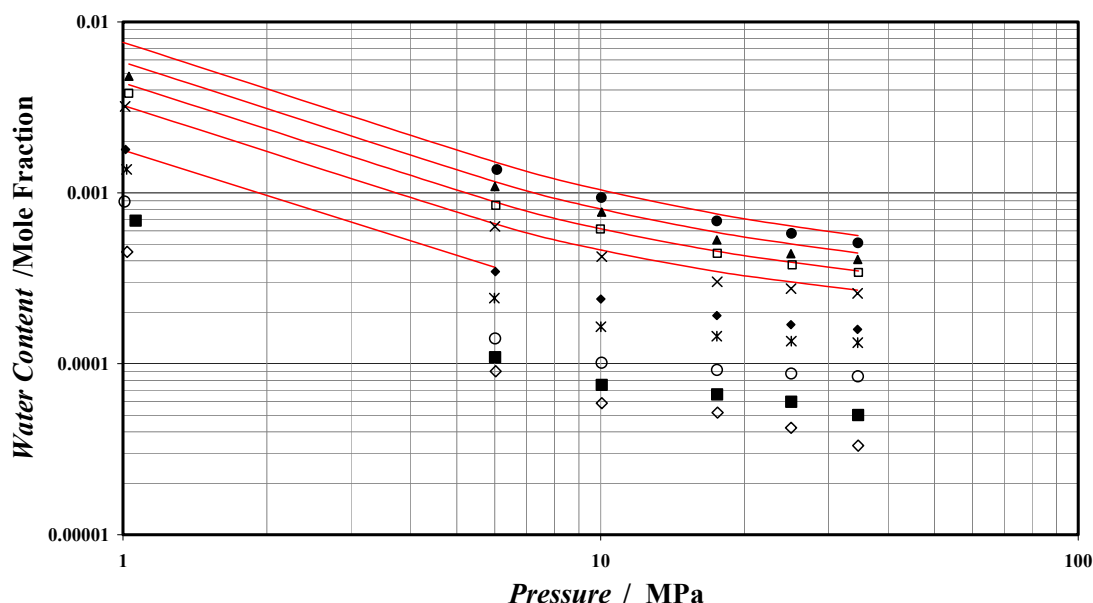
Figure 6.13: Water content in the vapour phase of the Water – MIX system. ●, 313.1 K; ▲, 308.1 K; □, 303.1 K; ✕, 297.9 K; ◆, 288.1 K; ✳, 283.1 K; ○, 278.2 K; ■, 273.2 K; ◇, 268.2 K.

The water contents in the vapour of water with -methane, -ethane and –MIX1 systems are similar, of the same order (Figure 6.14). This is quite normal as the gas mixture is mainly composed of methane (at 94 %) and thus behaves similarly to methane. For ethane as well the results are consistent as the water content has been measured at relatively low pressures (from 0.5 MPa up to the vapour pressure of ethane) and thus has a behaviour close to ideality.
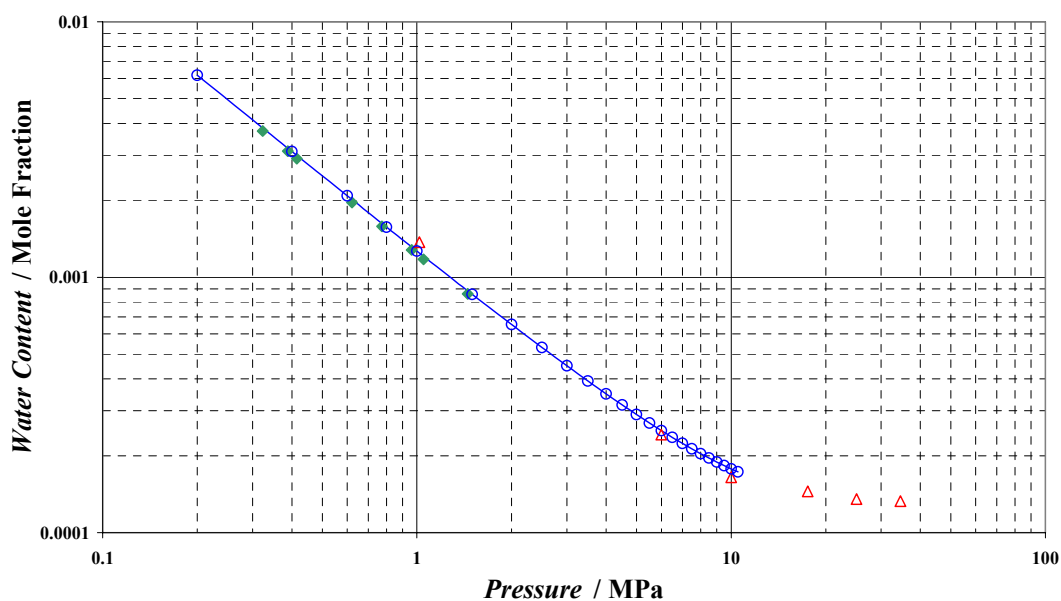
Figure 6.14: Comparison: Water Content in the Vapour Phase of the Water –Methane (○, Water content in Methane), -Ethane (◆, Water content in Ethane) and -MIX1 (△, Water content in MIX1) Systems at 283.1 K

A comparison between these new data and previously reported in the GPA research report 45 [294] at similar pressures shows that the data are in a close agreement (Figure 6.15).
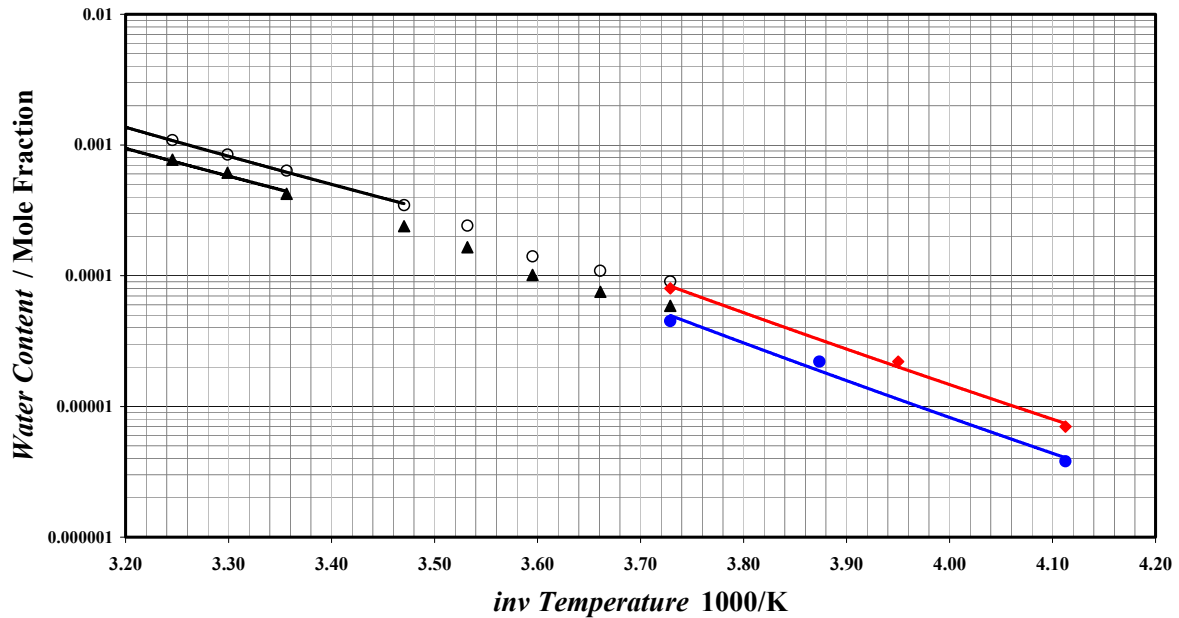
Figure 6.15: Comparison: Water Content in the Vapour Phase in VH condition
○, 6 MPa; ▲, 10 MPa; ● data from GPA RR-45 at 6.9 MPa [294]; ● data from GPA RR-45 at 10.3 MPa [294].

6.1.5 Mix1- Water-Methanol System

Water and methanol content measurements in the vapour phase have been generated from 268.15 up to 313.11 K and up to 34.5 MPa at two different composition of methanol in the aqueous phase 24 and 49 wt.% (TABLE 6.9 and Figure 6.16a). The system consisting of 24 wt % of methanol in the liquid phase (feed) presents phase equilibria near hydrate forming conditions and in hydrate conditions, in the second case studied (49 wt.% of methanol) at 273.15 and 268.15 K, only *VLE* conditions are encountered.

T /K	P /MPa	Water Content (×10³)		AD %	Methanol Content (×100)		AD %
		Experimental	Prediction		Experimental	Prediction	
268.10	6.83*	0.0669	0.0674	0.7	0.0192	0.0192	0.1
268.10	10.08*	0.0516	0.0593	15	0.0250	0.0226	9.5
268.10	16.13*	0.0472	0.0502	6.3	0.0300	0.0322	7.4
268.10	24.62*	0.0415	0.0451	8.6	0.0387	0.042	8.6
268.10	34.28*	**0.0356**	**0.0416**	**17**	0.0494	0.0485	1.8
273.10	6.13*	0.0993	0.1124	13	0.0211	0.0255	21
273.10	10.00*	0.0866	0.0840	3	0.0290	0.0353	22
273.10	10.46*	0.0850	0.0822	3.4	0.0290	0.0367	26
273.10	17.48*	0.0703	0.0680	3.2	0.0411	0.0412	0.2
273.10	17.56*	0.0706	0.0679	3.8	0.0411	0.0414	0.5
273.10	25.13*	0.0656	0.0617	5.9	0.0463	0.0509	9.9
273.10	25.16*	0.0649	0.0617	5	0.0463	0.0509	10
273.10	34.95*	0.0604	0.0567	6.2	0.0525	0.0584	11
278.10	5.93	**0.1416**	**0.1623**	**15**	0.0342	0.0328	4.1
278.10	10.01	0.1170	0.1170	0	0.0360	0.0356	1.2
278.10	17.59*	0.0966	0.0930	3.8	0.0512	0.0540	5.5
278.10	25.00*	0.0801	0.0840	4.8	0.0588	0.0741	26
278.10	34.50*	0.0746	0.0769	3.1	0.0623	0.0942	38
283.10	5.86	0.2184	0.2279	4.3	0.0447	0.0428	4.2
283.10	9.75	0.1450	0.1636	13	0.0475	0.0442	7.0
283.10	14.16	0.1261	0.1367	8.4	0.0530	0.0525	1.0
283.10	21.79	0.1183	0.1176	0.5	0.0670	0.0669	0.2
283.10	34.47	0.1073	0.1029	4.1	0.0784	0.0820	4.5
288.13	6.34	0.2964	0.2964	0.0	0.0630	0.0544	14
288.13	10.17	0.2137	0.2181	2.0	**0.0666**	**0.0558**	**16**
288.13	17.62	**0.1444**	**0.1693**	**17**	0.0720	0.0712	1
288.13	25.08	**0.1317**	**0.1504**	**14**	**0.0739**	**0.0846**	**15**
288.13	34.29	0.1280	0.1367	6.7	0.0847	0.0953	12
293.13	6.53	0.3632	0.3938	8.5	0.0713	0.0689	3.4
293.13	10.43	0.2930	0.2894	1.2	0.0765	0.0694	9.2
293.13	17.57	0.2255	0.2252	0.2	0.0850	0.0848	0.3
293.13	25.13	0.1945	0.1981	1.8	0.0893	0.0996	11
293.13	34.44	0.179	0.1790	0.0	0.0993	0.1116	12
298.15	6.29	0.5049	0.5444	7.8	0.0890	0.0876	1.6
298.15	10.06	0.3763	0.3946	4.9	0.0984	0.0849	14
298.15	16.27	0.3144	0.3067	2.5	0.1066	0.0975	8.5
298.15	25.09	0.2393	0.2591	8.3	0.1079	0.1166	8.1
298.15	34.46	0.2196	0.2328	6.0	0.1157	0.1299	12
273.10[+]	5.70	**0.0660**	**0.0886**	**34**	0.0659	0.0636	3.5
273.10[+]	10.07	0.0572	0.0628	9.7	0.0722	0.072	0.2
273.10[+]	10.13	0.0585	0.0626	7.0	0.0669	0.0723	8.1
273.10[+]	18.45	0.0507	0.0505	0.4	0.1086	0.1084	0.2
273.10[+]	25.38	0.0465	0.0465	0.0	0.1305	0.1302	0.2
273.10[+]	34.53	0.0414	0.0431	4.0	0.1331	0.1486	12
268.10[+]	6.09	0.0526	0.0590	12	0.0483	0.0482	0.2
268.10[+]	9.88*	0.0465	0.0447	3.8	0.0500	0.0567	14
268.10[+]	17.35	0.0404	0.0369	8.7	0.0980	0.0867	12
268.10[+]	25.4	0.0365	0.0337	7.6	0.1058	0.1094	3.4
268.10[+]	34.48	0.0324	0.0314	3.3	0.1217	0.1249	2.7

TABLE 6.9 – WATER AND METHANOL CONTENTS IN THE VAPOUR PHASE OF MIX1 – WATER – METHANOL SYSTEM ([+] **49wt. % of methanol in the aqueous phase instead of 24 wt. %) ***
measurement corresponding to hydrate-vapour equilibrium.

These new experimental data were compared with predictions of the HW in-house thermodynamic model. The predictions are in good agreement with the experimental data for the majority of the experiments. However, larger deviations (10-20%) between the water content measurements and the predictions are observed for 8 points, especially at high-pressure conditions. A large deviation (34%) is also observed for the point at 273.10 K and 5.7 MPa in the highest concentration of methanol is more important. The predictions for the methanol content of the vapour phase are also in relatively correct agreement (*AAD* =8%) with the experimental data. Identically, some points show larger deviations. Deviations can be

explained by the difficulties of such experiments and by the difficulties of calibrating the detector at such low water content conditions.
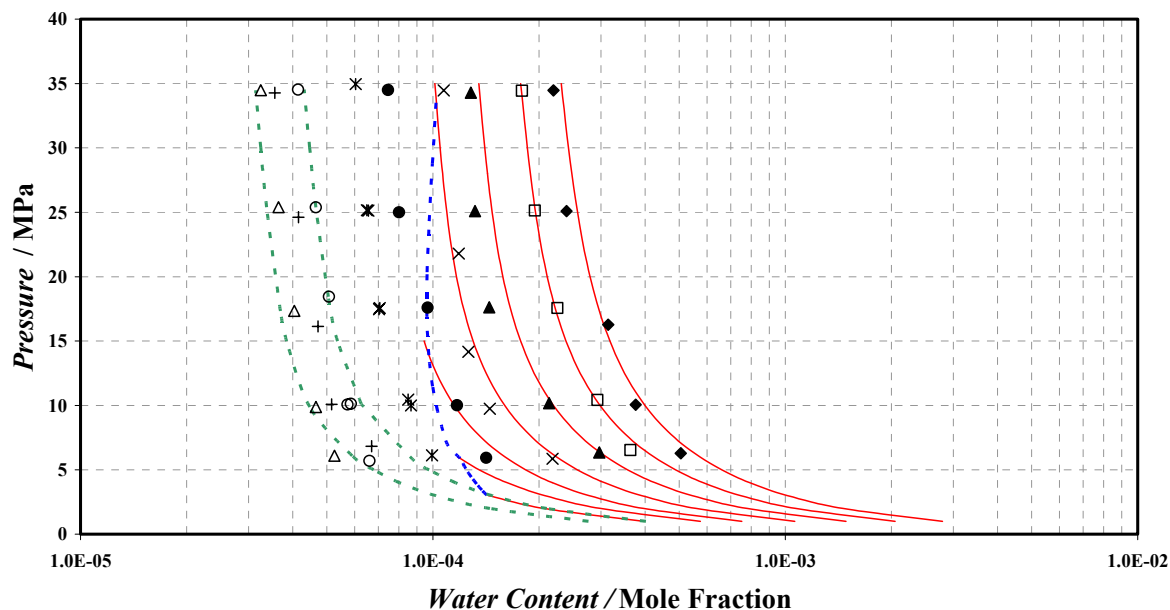
Figure 6.16a: Water content in the gas vapour phase of the MIX1- Water – X wt % Methanol system. X = 24: ◆, 298.1 K; □, 293.1 K; ▲, 288.1 K; ✕, 283.1 K; ●, 278.1 K; ✳, 273.1 K; +, 268.1 K; X = 49 : ○, 273.1* K; △, 268.1 K; Red solid line, ϕ-ϕ approach (HWHYD) at 24 wt. %; Green dashed line, ϕ-ϕ approach (HWHYD) at 49 wt.%; Blue dashed line, water content calculated at hydrate dissociation pressure.
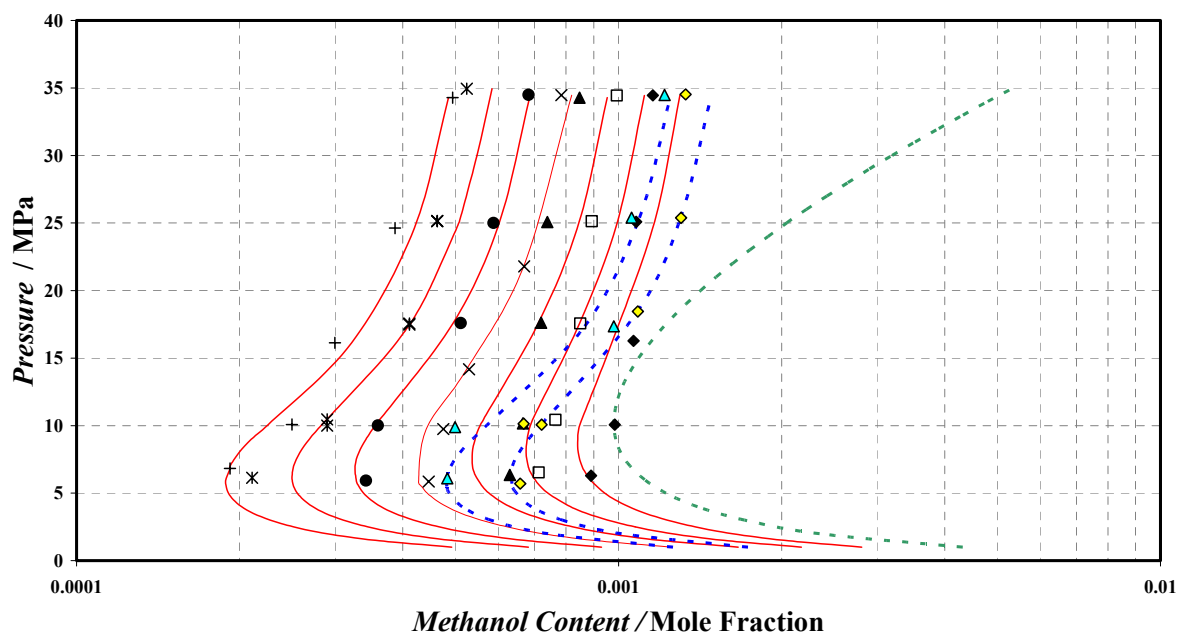
Figure 6.16b: Methanol content in the gas vapour phase of the MIX1- Water – X wt % Methanol system. X = 24: ◆, 298.1 K; □, 293.1 K; ▲, 288.1 K; ✕, 283.1 K; ●, 278.1 K; ✳, 273.1 K; +, 268.1 K; X = 49 : ○, 273.1* K; △, 268.1 K; Red solid line, ϕ-ϕ approach (HWHYD) at 24 wt. %; Blue dashed line, ϕ-ϕ approach (HWHYD) at 49 wt.%. Green dashed line, Methanol content in the vapour phase of the MIX1 – Methanol at 273.1 K (no water).

6.1.6 Mix1- Water-Ethylene Glycol System

Water content measurements in the vapour phase have been done from 268.15 to 298.13 K up to 34.5 MPa at 34 wt. % of ethylene glycol in the aqueous phase. We observe that an aqueous solution of 34 wt. % of ethylene glycol has an inhibition power similar to the 24 wt. % methanol solution (Figure 6.12). Therefore, this system presents also phase equilibria near hydrate forming conditions and in hydrate conditions. The *EG* composition in the vapour phase had not been measured and was neglected to calculate the water composition as *EG* vapour pressure of is very low and EG was undetectable through *GC*.

T /K	P /MPa	Water Content ($\times 10^3$)		*AD* %
		Experimental	*Prediction*	
298.13	6.05	0.6456	0.5617	13
298.13	10.06	0.3948	0.3949	0.0
298.13	17.58	0.2828	0.2958	-4.6
298.13	25.09	0.2353	0.2575	-9.4
298.13	34.50	0.2115	0.2306	-9.0
288.13	5.98	0.4351	0.3113	28
288.13	10.09	0.2456	0.2202	10
288.13	17.64	0.1721	0.1696	1.5
288.13	25.10	0.1544	0.1502	2.7
288.13	34.50	0.1291	0.1360	-5.3
278.10	6.02	0.2235	0.1620	27
278.10	9.10	0.1700	0.1243	27
278.10	17.47*	0.1012	0.0915	9.6
278.10	25.32*	0.0799	0.0798	0.0
278.10	34.5*	0.0718	0.0715	0.4
273.10	6.00*	0.1284	0.1140	11
273.10	9.63*	0.0871	0.0820	5.8
273.10	17.80*	0.0700	0.0681	2.8
273.10	34.50*	0.0509	0.0570	-12
268.10	6.05*	0.0802	0.0802	0.0
268.10	10.52*	0.0453	0.0587	-29
268.10	17.46*	0.0344	0.0495	-44
268.10	23.35*	0.0268	0.0460	-85
268.10	34.50*	0.0220	0.0418	-89
293.15	15.93	0.2741	0.2349	14
293.15	24.92	0.2041	0.1983	2.8
283.15	17.95	0.1413	0.1260	11

TABLE 6.10 – WATER CONTENTS IN THE VAPOUR PHASE OF MIX1 – WATER –EG SYSTEM

* measurement corresponding to hydrate-vapour equilibrium.

For mixtures with *EG*, only experimental water contents of the MIX1 (methane, ethane and *n*-butane) were determined at different temperatures and pressures using the same apparatus (no ethylene glycol was detected in the vapour phase). The experimental data were compared to predictions of the *HW* in-house thermodynamic model. The predictions are in good agreement with the experimental data for the majority of the experiments. However larger deviations (10-20%) between the water content measurements and the prediction are also observed, especially for the lowest pressure, i.e. 6 MPa. Larger deviations are also observed in the hydrate-forming zone.
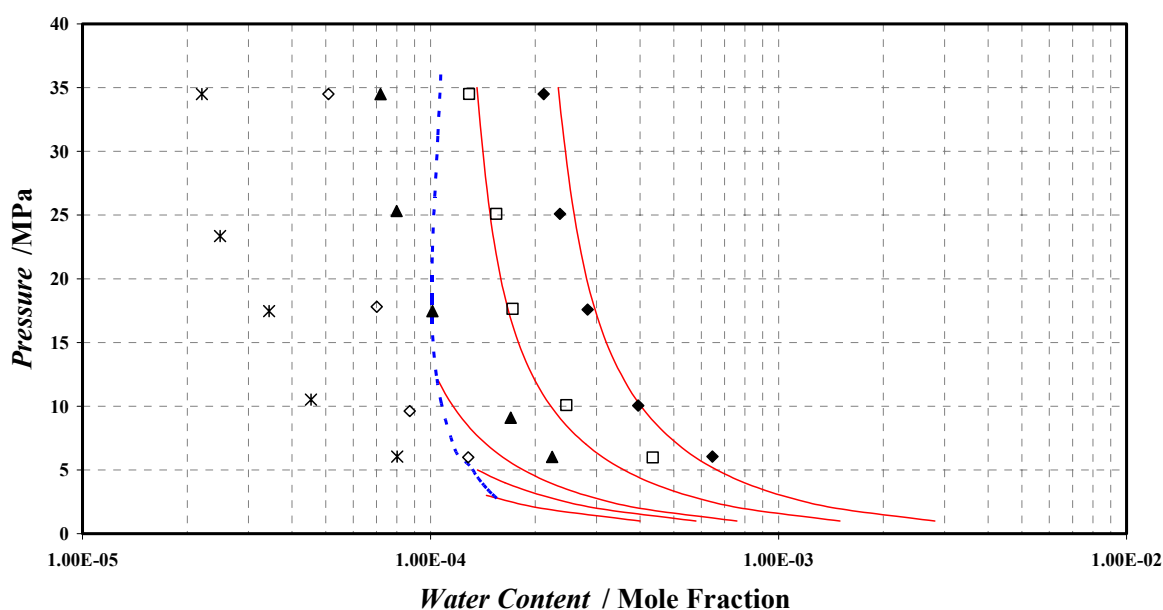
Figure 6.17: Water content in the gas phase of the MIX1- Water – Ethylene Glycol System. ◆, 298.1 K; □, 288.1 K; ▲, 278.1 K; ◇, 273.1 K; ∗, 268.1 K; Red solid line, ϕ -ϕ approach (HWHYD); Blue dashed line, water content calculated at hydrate dissociation pressure.

6.1.7   Comments and Conclusions on Water Content Measurements

Experimental results indicate that the measured water contents in the vapour of systems composed of water with: - methane, -ethane and –hydrocarbons synthetic mixture outside their respective hydrate formation region are nearly identical. However, inside the hydrate stability zone, the water contents of the mixture are lower than those of methane. The difference between the water contents of the two gases (pure methane and MIX1) increases with decreasing temperature (i.e., when the distance to the hydrate phase boundary of the

mixture becomes larger, the mixture due to the presence of n-butane forms hydrate at lower pressure than pure methane.

The water content of natural gases in equilibrium with gas hydrates is lower (typically less than 0.001 mol fraction) than the water content of natural gases in equilibrium with meta-stable liquid water and therefore difficult to measure, as hydrate formation is a time consuming process and water content of gases in the hydrate region is a strong function of composition of the feed gas. It should be pointed out that at same *PT* and in *VLE* conditions, the water content logically decreases with an increase of the inhibitor content and thus the water content of a gas vapour in equilibrium with pure water (in the liquid state) is higher than the water content in presence of an inhibitor. However at same *PT* conditions when the system is in *VH* conditions without inhibitor and in *VLE* conditions with inhibitor, the water content is higher in the second case.

6.2 Gas Solubilities in Water and Water-Inhibitor Solutions

6.2.1 Gas Solubilities in Water

6.2.1.1 Methane – Water System

The experimental and calculated gas solubility data are reported in TABLE 6.11 and plotted in Figure 6.18. The methane mole number is known within +/- 2 %. For both approaches, the *BIPs* between methane - water are adjusted directly to the measured methane solubility data (TABLE 6.11) through a Simplex algorithm using the objective function, *FOB*, displayed in eq 6.2:

$$FOB = \frac{1}{N} \sum_{1}^{N} \left| \frac{x_{i,\exp} - x_{i,cal}}{x_{i,\exp}} \right|$$

(6.2)

where *N* is the number of data points, x_{exp} is the measured solubility and x_{cal} the calculated solubility.
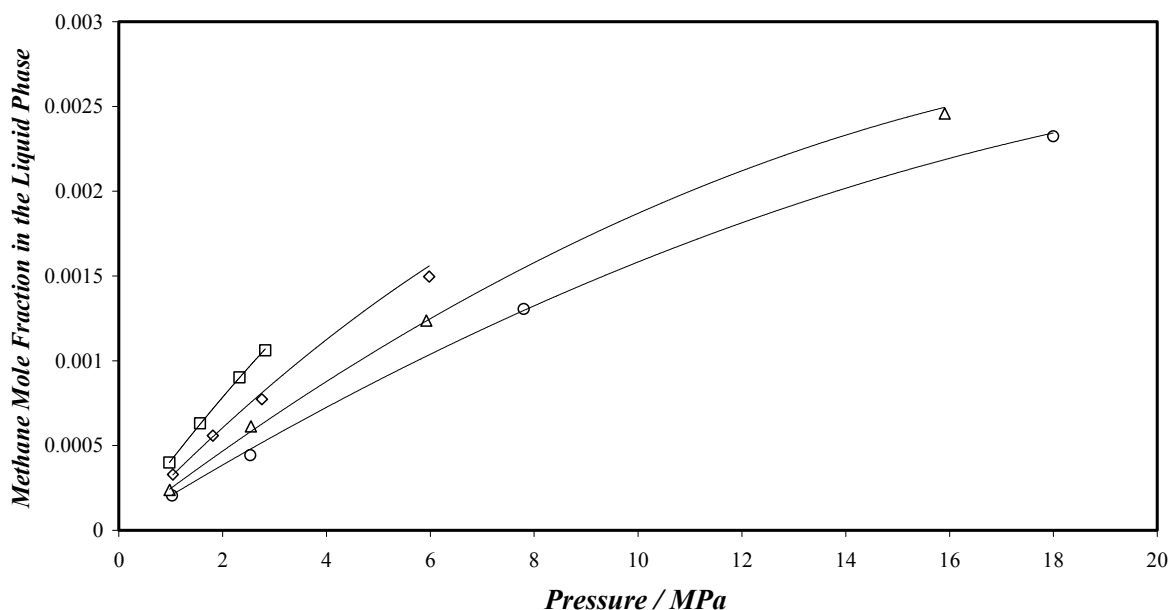
Figure 6.18: Methane mole fraction in water rich phase of the methane − water binary system as a function of pressure at various temperatures. □, 275.11 K; ◇, 283.1 K; Δ, 298.1 K; ◯, 313.1 K. Solid lines, calculated with the *VPT-EoS* and *NDD* mixing rules with parameters from TABLE E.1 (Annex E). [B5]

Our isothermal *P*, *x* data sets for the methane − water are well represented with the *VPT-EoS* and *NDD* mixing rules (*AAD* = 1.8 %). The methane solubility data of the different authors having reported such data between 274.15 and 313.2 K are plotted in Figure 6.19. At the lower temperatures (below 276 K and also around 283.15 K) and at the higher temperature (313.15 K), the model shows good agreement between the different authors, excepting for the data of *Wang et al.* [86] at 283.15 K. Solubility measurements for the 298.15 K isotherms have been more widely reported. However, some reported results show deviations between each other and with respect to the model, especially at pressures higher than 6 MPa: *Michels et al.* [68] and *Kim et al.* [87]. The data of *Yang et al.* [86] are quite dispersed at this temperature (298.15 K). The second approach using the correlation for the Henry's law proposed by *Yaws et al.* [238] (eq 6.1) and the *BIPs* listed in TABLE 6.4 predicts (independent parameters) accurately the new set of solubility data (*AAD* = 3.6 %).

T/K	P_{exp}/MPa	$x_{exp} \times 10^3$	$x_{cal} \times 10^3 (\phi - \phi)$	Deviation %	$x_{cal} \times 10^3 (\gamma - \phi)$	Deviation%
275.11	0.973	0.399	0.361	9.5	0.402	-0.6
275.11	1.565	0.631	0.567	10	0.630	0.1
275.11	2.323	0.901	0.815	9.5	0.907	1.8
275.11	2.820	1.061	0.969	8.7	1.079	-1.6
283.13	1.039	0.329	0.327	0.6	0.345	-5.0
283.12	1.810	0.558	0.553	0.9	0.584	-4.7
283.13	2.756	0.772	0.812	-5.2	0.857	-11
283.13	5.977	1.496	1.561	-4.3	1.650	-6.5
298.16	0.977	0.238	0.238	0.0	0.237	0.5
298.16	2.542	0.613	0.589	3.9	0.586	4.4
298.15	5.922	1.238	1.233	0.4	1.224	1.1
298.13	15.907	2.459	2.498	-1.6	2.481	-0.9
313.11	1.025	0.204	0.205	-0.5	0.198	-2.6
313.11	2.534	0.443	0.486	-9.7	0.471	-6.8
313.11	7.798	1.305	1.295	0.8	1.254	-6.1
313.11	17.998	2.325	2.346	-0.9	2.273	-3.7

TABLE 6.11 - EXPERIMENTAL AND CALCULATED METHANE MOLE FRACTIONS IN THE LIQUID PHASE OF THE METHANE - WATER SYSTEM [B5]
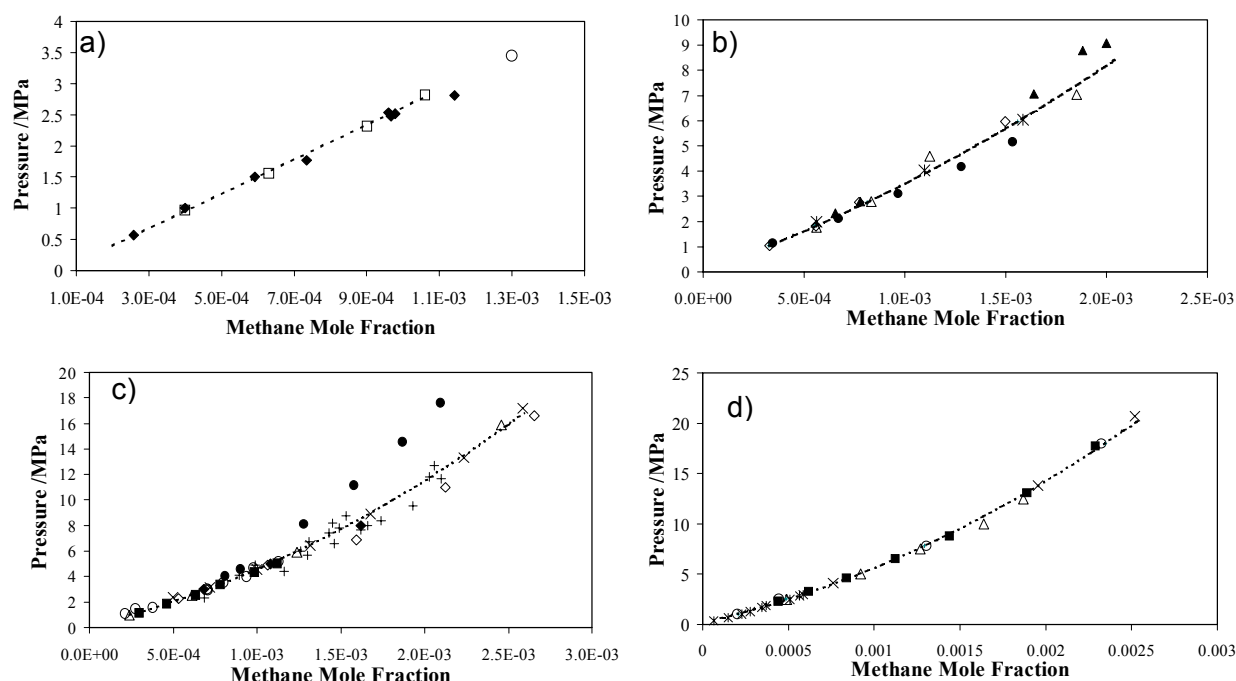
Figure 6.19: Comparison of Experimental Methane Solubilities in Water a) □, 275.11 K; O, 274.15 K from [66]; ♦, 274.29 K from [82]. b) ◇, 283.13 K; ●, 283.15 K from [84]; Δ, 283.2 K from [82]; ✳, 283.2 K from [86], ▲, 285.65 K from [82].c) Δ, 298.15 K; ×, 298.15 K from [54]; Δ, 298.15 from [78]; +, 298.1 from [83]; ●, 298.15 K from [68]; ♦ ; 298.2 K from [18]; ■, 298.15 from [80]; O, 298.15 K from [81]; ♦, 298.15 K from [80]; ◇, 298.15 K [87]; d) O, 313.11 K; ×, 310.93 from [73]; ■, 310.93 from [78]; Δ, 313.2 K from [79]; Dashed lines, calculated with the *VPT-EoS* and *NDD* mixing rules with parameters from Table E.1 (Annex E).

6.2.1.2 Ethane – Water System

The experimental and calculated gas solubility data are reported in TABLE 6.12 and are plotted in Figure 6.20. The relative uncertainty is about ± 0.9 % in mole number of ethane. As for methane, the *BIPs* between ethane - water are adjusted directly on the measured methane solubility data through a Simplex algorithm using the objective function, *FOB*, displayed in eq 6.2.
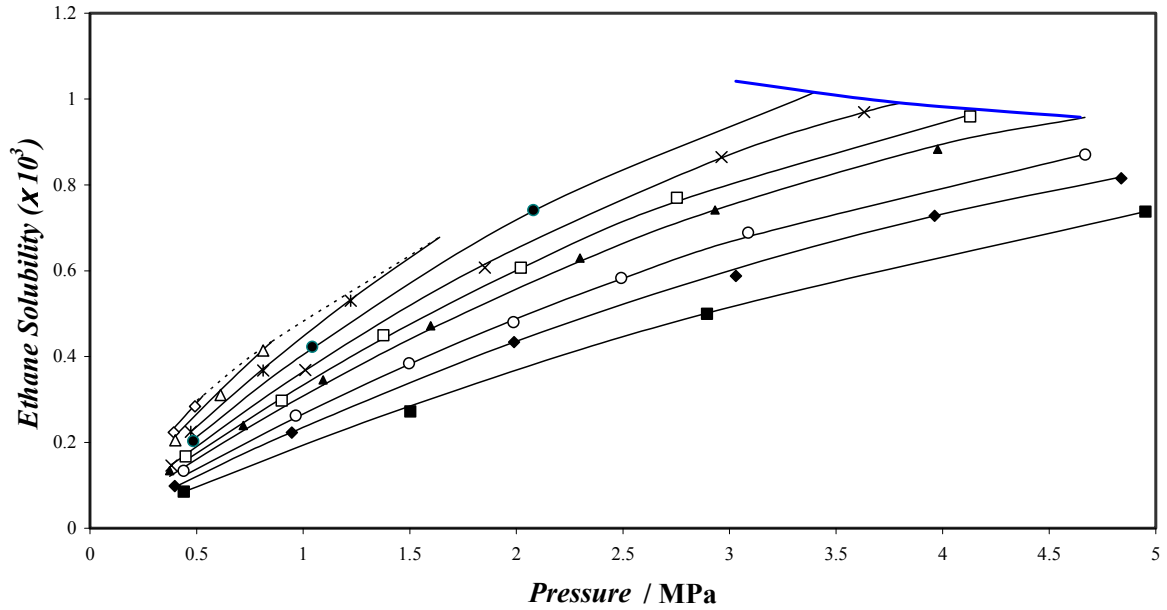
Figure 6.20: Ethane solubility in water rich as a function of pressure at various temperatures ◇, 274.3 K; Δ, 278.1 K; *, 283.1 K; ●, 288.1 K; ×, 293.3 K; □, 298.3 K; ▲, 303.2 K; ○, 313.2 K; ♦, 323.2 K; ■, 343.1 K. Solid curves, calculated with the *VPT-EoS* and *NDD* mixing rules with parameters from Table E.2. Bold solid blue curve: Ethane vapour pressure; Dashed curve: Hydrate phase boundary. [B11]

The isothermal *P*, *x* data sets for the ethane–water are well represented with the *VPT-EoS* and *NDD* mixing rules (*AAD* = 1.8 %). Some ethane solubility data reported in the literature between 293.2 and 303.2 K are plotted in Figure 6.21 and compared with these new experimental data and the calculations of the first approach. As it can be seen, the data reported by *Kim et al.* [87] are dispersed. The data reported by *Wang et al.* [86] show large deviations, especially at low temperatures and pressures. The γ-ϕ approach using eq.5.61 for the Henry's law (with *A*= 110.157; *B*=-5513.59; *C*=-35.263; *D*=0) and the *BIPs* listed in TABLE 6.4 predicts (independent parameters) accurately the new set of solubility data (*AAD* = 3.5 %).
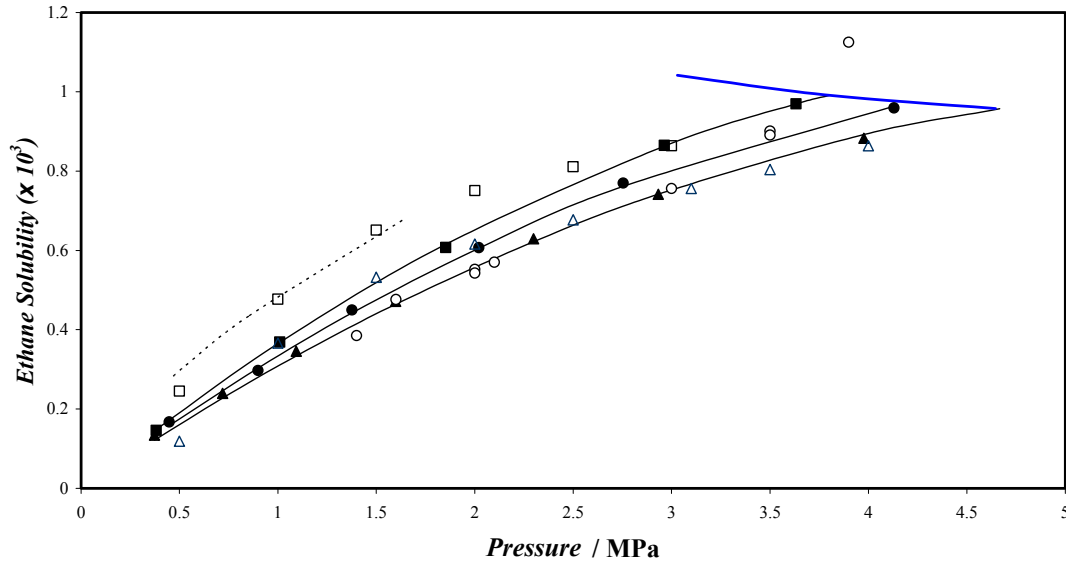
Figure 6.21: Comparison of ethane solubilities in water
□, 293.2 K, from *Wang et al.* [86]; ■, 293.31 K, This work; ○, 298.15 K, from *Kim et al.* [87]; ●, 298.3 K, This work; Δ, 303.2 K, from *Wang et al.* [86]; ▲, 303.22 K, This work. Solid curves, calculated with the *VPT-EoS* and *NDD* mixing rules with parameters from Table E.1. Bold blue solid curve: Ethane vapour pressure; Dashed curve: Hydrate phase boundary.

T/K	P_{exp}/MPa	$x_{exp} \times 10^3$	AD exp %	$x_{cal} \times 10^3 (\phi\text{-}\phi)$	Deviation %	$x_{cal} \times 10^3 (\gamma\text{-}\phi)$	Deviation %
274.26	0.393	0.2237	0.3	0.233	4.1	0.230	3.0
274.26	0.4922	0.2841	0.5	0.288	1.4	0.286	0.8
278.06	0.4004	0.205	1.3	0.216	5.2	0.210	2.7
278.04	0.6128	0.3106	2.9	0.322	3.7	0.317	2.1
278.07	0.8126	0.4143	2.5	0.416	0.5	0.414	0.1
283.12	0.473	0.225	3.6	0.225	0.1	0.218	3.3
283.1	0.8122	0.3676	1.2	0.371	1.0	0.364	1.0
283.1	1.2232	0.53	2.5	0.533	0.5	0.531	0.1
288.08	0.4844	0.203	4.7	0.207	1.8	0.199	1.8
288.08	1.0426	0.4227	4.3	0.419	1.0	0.411	2.8
288.06	2.0801	0.7411	0.7	0.739	0.3	0.753	1.6
293.33	0.382	0.1464	1.9	0.148	1.3	0.143	2.2
293.31	1.01	0.369	3.4	0.368	0.2	0.361	2.1
293.3	1.852	0.6073	4.0	0.615	1.3	0.618	1.8
293.3	2.963	0.8647	1.2	0.863	0.2	0.896	3.6
293.31	3.632	0.9696	0.2	0.970	0.0	1.029	6.2
298.3	0.4486	0.1676	0.4	0.158	5.8	0.154	7.9
298.37	0.8992	0.2972	0.5	0.303	2.0	0.299	0.5
298.35	1.377	0.4498	0.5	0.442	1.7	0.440	2.2
298.42	2.021	0.6068	1.5	0.605	0.2	0.612	0.8
298.32	2.7539	0.7699	0.3	0.762	1.1	0.782	1.6
298.31	4.1297	0.9592	2.8	0.964	0.5	1.026	6.9
303.19	0.373	0.1341	2.1	0.121	9.5	0.121	10.1
303.21	0.719	0.2396	1.1	0.227	5.1	0.227	5.4
303.21	1.093	0.346	2.7	0.334	3.5	0.335	3.3
303.22	1.598	0.4719	1.5	0.464	1.6	0.469	0.5
303.23	2.299	0.6295	1.4	0.622	1.2	0.636	1.1
303.22	2.932	0.7415	2.3	0.741	0.0	0.766	3.4
303.22	3.977	0.8827	0.6	0.892	1.1	0.938	6.3
313.17	0.439	0.1337	2.1	0.122	8.8	0.119	10.7
313.19	0.965	0.2623	0.9	0.258	1.7	0.252	4.0
313.19	1.497	0.3841	1.5	0.382	0.5	0.374	2.6
313.19	1.987	0.4799	1.4	0.485	1.1	0.477	0.7
313.19	2.492	0.583	1.6	0.581	0.4	0.572	1.9
313.19	3.088	0.6887	2.8	0.679	1.4	0.671	2.6
313.18	4.669	0.8703	2.6	0.872	0.2	0.863	0.8
323.17	0.397	0.0983	1.5	0.096	1.9	0.093	4.9
323.19	0.947	0.2231	0.9	0.224	0.4	0.214	4.2
323.19	1.989	0.4336	1.6	0.434	0.0	0.412	4.9
323.2	3.03	0.5877	2.1	0.605	2.9	0.572	2.7
323.18	3.963	0.7279	0.9	0.728	0.0	0.683	6.2
323.2	4.838	0.8154	1.9	0.818	0.3	0.759	7.0
343.08	0.44	0.0854	0.5	0.085	0.1	0.087	1.8
343.06	1.503	0.272	1.9	0.285	4.7	0.273	0.5
343.06	2.895	0.4997	0.4	0.501	0.3	0.467	6.6
343.06	4.952	0.7376	0.4	0.738	0.1	0.646	12.4

TABLE 6.12 - EXPERIMENTAL AND CALCULATED ETHANE MOLE FRACTIONS IN THE LIQUID PHASE OF THE ETHANE - WATER SYSTEM [B11]

6.2.1.3 Propane – Water System

In this work, new solubility measurements of propane in water have been generated in a wide temperature range i.e., 277.62 up to 368.16 K and up to 3.915 MPa. The relative uncertainty in the moles of nitrogen is about ± 3 %. The experimental and calculated gas solubility data are reported in TABLE 6.13 and plotted in Figure 6.22. The *BIPs* between propane - water were adjusted directly on the measured propane solubility data through a Simplex algorithm using the objective function, *FOB,* displayed in Eq. 6.2.
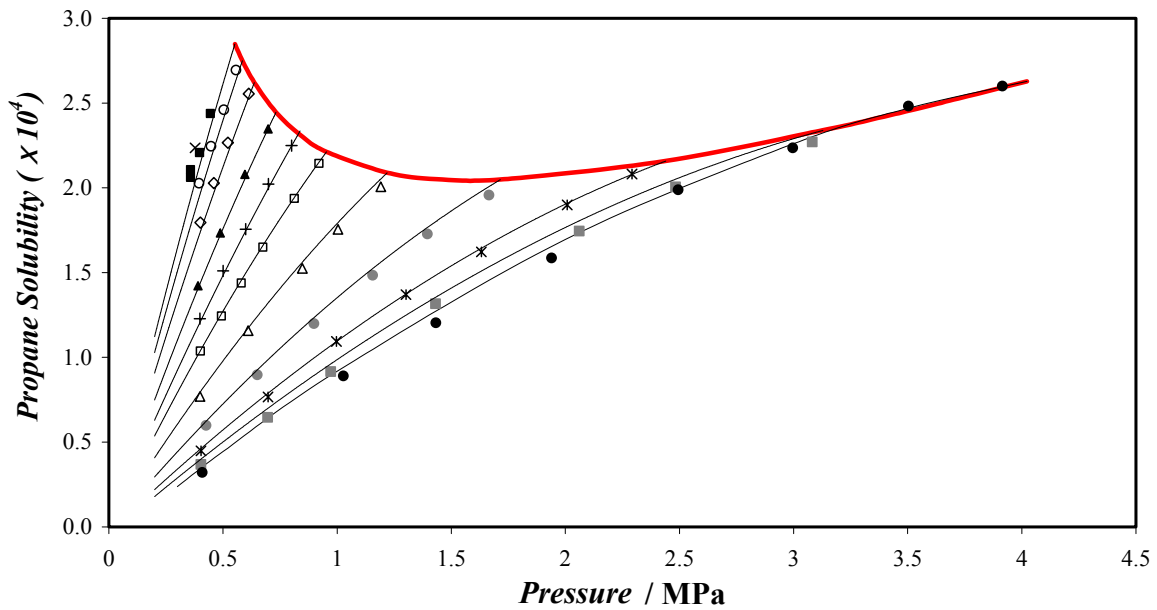
Figure 6.22: Propane mole fraction in water rich phase as a function of pressure at various temperatures. ×, 277.6 K; ■, 278,1 K; O, 280.1 K; ◇, 283.1 K; ▲, 288.1 K; +, 293.1 K; □, 298.13 K; △, 308.1 K; ●, 323.1 K; *, 338.1 K; ■, 353.2 K; ●, 368.2 K. Solid lines, calculated with the *VPT-EoS* and *NDD* mixing rules with parameters from Table E.1. Bold solid red lines: Propane solubilities at the propane vapour pressure [B10]

Our isothermal *P, x* data sets for the propane–water are well represented with the *VPT-EoS* and *NDD* mixing rules (*AAD* = 5 %). Propane solubility data reported in the literature are plotted in Figure 6.23. As it can be seem, the data reported in the literature are quite dispersed and show some strange behaviour, particularly the data at 288.71 K of *Azarnoosh and McKetta*.

The γ -ϕ approach using Eq. 6.3 for the Henry's and the *BIPs* listed in TABLE 6.4 represents accurately the new set of solubility data (*AAD* = 3.5 %).

$$\ln(H_{iw}) = 552.64799 + 0.078453\ T - 21334.4\ /\ T - -85.89736 \ln T \text{ (in } \textbf{kPa)} \qquad (6.3)$$

| T/K	P_{exp}/MPa	$x_{exp} \times 10^4$	AD exp %	$x_{cal} \times 10^4 (\phi - \phi)$	AD %	$x_{cal} \times 10^4 (\gamma - \phi)$	AD %
277.62	0.378	2.235	2.6	1.946	13	2.396	7.2
278.09	0.357	2.061	0.9	1.816	12	2.195	6.5
278.09	0.357	2.107	2.1	1.816	14	2.195	4.1
278.09	0.398	2.208	2.9	2.005	9.2	2.430	10
278.09	0.445	2.439	1.0	2.218	9.1	2.702	11
280.14	0.395	2.027	1.8	1.851	8.7	2.089	3.1
280.14	0.447	2.245	2.9	2.070	7.8	2.352	4.8
280.14	0.504	2.461	1.3	2.304	6.4	2.631	6.9
280.14	0.557	2.694	2.7	2.515	6.6	2.890	7.3
283.06	0.401	1.796	2.7	1.696	5.6	1.769	1.5
283.06	0.460	2.028	2.0	1.921	5.3	2.014	0.7
283.06	0.522	2.266	0.5	2.150	5.1	2.270	0.2
283.06	0.612	2.555	0.5	2.470	3.3	2.635	3.1
288.13	0.488	1.733	3.7	1.718	0.9	1.667	3.8
288.13	0.697	2.347	2.4	2.346	0.0	2.321	1.1
288.13	0.596	2.080	1.3	2.051	1.4	2.009	3.4
288.13	0.390	1.423	1.1	1.401	1.5	1.346	5.4
293.13	0.399	1.229	0.7	1.229	0.0	1.161	5.5
293.13	0.800	2.249	3.8	2.272	1.0	2.220	1.3
293.13	0.699	2.023	1.0	2.028	0.2	1.964	2.9
293.13	0.599	1.756	2.0	1.774	1.0	1.704	3.0
293.13	0.500	1.510	2.8	1.510	0.0	1.440	4.6
298.12	0.401	1.037	1.0	1.071	3.3	1.050	1.3
298.12	0.493	1.244	1.3	1.296	4.2	1.278	2.7
298.12	0.580	1.438	1.3	1.500	4.3	1.489	3.5
298.12	0.675	1.650	0.5	1.714	3.9	1.712	3.8
298.12	0.812	1.938	0.2	2.007	3.6	2.026	4.5
298.12	0.920	2.144	1.6	2.224	3.7	2.264	5.6
308.13	0.399	0.770	1.3	0.825	7.2	0.784	1.8
308.13	0.610	1.158	2.7	1.221	5.4	1.168	0.9
308.13	0.848	1.525	2.1	1.629	6.8	1.577	3.4
308.13	1.003	1.755	0.9	1.873	6.7	1.830	4.3
308.13	1.191	2.007	0.4	2.146	6.9	2.121	5.7
323.13	0.425	0.598	1.6	0.635	6.2	0.580	3.0
323.13	0.650	0.897	3.2	0.947	5.6	0.863	3.8
323.13	0.898	1.199	2.7	1.263	5.3	1.157	3.5
323.13	1.156	1.485	1.4	1.563	5.3	1.441	3.0
323.13	1.396	1.728	0.7	1.815	5.0	1.686	2.5
323.13	1.665	1.957	0.8	2.066	5.6	1.939	0.9
338.15	0.403	0.449	1.0	0.461	2.7	0.471	5.0
338.15	0.697	0.766	1.3	0.787	2.7	0.786	2.6
338.15	0.997	1.094	2.3	1.091	0.3	1.083	1.0
338.15	1.302	1.370	1.1	1.370	0.0	1.359	0.8
338.15	1.632	1.621	0.7	1.640	1.2	1.630	0.5
338.15	2.008	1.899	1.3	1.907	0.4	1.902	0.1
338.15	2.292	2.082	0.3	2.080	0.1	2.081	0.0
353.18	0.404	0.368	0.2	0.366	0.4	0.435	18
353.18	0.696	0.646	0.3	0.642	0.5	0.724	12
353.18	0.972	0.917	0.0	0.884	3.5	0.978	6.7
353.18	1.431	1.317	1.5	1.246	5.4	1.356	3.0
353.18	2.061	1.745	0.6	1.665	4.6	1.788	2.5
353.18	2.483	2.006	1.0	1.897	5.4	2.021	0.8
353.18	3.082	2.270	1.4	2.158	4.9	2.275	0.2
368.16	0.410	0.321	0.3	0.296	7.7	0.400	25
368.16	1.028	0.891	0.4	0.803	9.8	0.931	4.6
368.16	1.433	1.203	0.2	1.095	9.0	1.231	2.3
368.16	1.940	1.586	0.6	1.419	10	1.554	2.0
368.16	2.495	1.989	0.7	1.723	13	1.839	7.5
368.16	2.997	2.236	2.5	1.952	13	2.035	9.0
368.16	3.503	2.482	0.7	2.141	14	2.175	12.4
368.16	3.915	2.601	0.7	2.262	13	2.245	14

TABLE 6.13 - EXPERIMENTAL AND CALCULATED PROPANE MOLE FRACTIONS IN THE LIQUID PHASE OF THE PROPANE - WATER SYSTEM [B10]
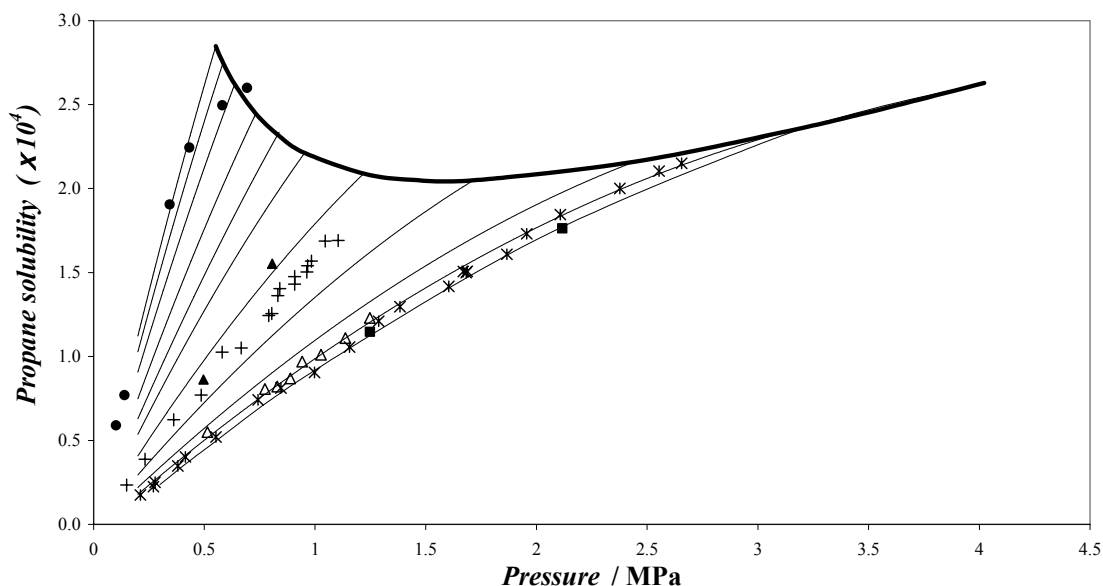
Figure 6.23: Comparison of experimental propane solubilities in water. •, 288.71 K from *Azarnoosh and McKetta* [32]; ▲, 310.93 K from *Kobayashi and Katz* [95]; +, 310.93 from *Azarnoosh and McKetta* [32]; △, 344.26 K from *Wehe and McKetta* [96]; ✳, 344.26 K from *Azarnoosh and McKetta* [32]; ■, 349.82 K from *Kobayashi and Katz* [95]. Solid lines, calculated with the *VPT-EoS* and *NDD* mixing rules at 278.09 K, 280.14 K; 283.06 K, 288.13 K, 293.13 K, 298.12 K, 308.13 K, 323.13 K, 338.15 K, 353.18 K and 368.16 K (from left to right). Bold Solid line: Propane solubility at the propane vapour pressure.

6.2.1.4 Mix1 – Water System

Solubility measurements of a gas mixture (94% methane + 4% ethane + 2% *n*-butane) in water have been generated at low and ambient temperatures. The isothermal *P*, *x* data sets for the gas mixture –water are also well represented with the *VPT-EoS* and *NDD* mixing rules (*AAD* of 1.9 % for methane solubilities, *AAD* of 4 % for ethane solubilities, *AAD* of 5 % for n-butane solubilities). An increase in *AAD* with an increase in carbon number is expected, due to low solubility of ethane and n-butane and hence the analytical work is more difficult (higher uncertainty in the calibration of the detector). The total solubility of gas in the liquid phase is slightly higher than the solubility of pure methane or pure ethane at same temperature and pressure.

T/K	P_{exp}/MPa	$x_{(1)\,exp} \times 10^3$	$x_{(1)\,prd} \times 10^3$	$\Delta x\,\%$	$x_{(2)\,exp} \times 10^4$	$x_{(2)\,prd} \times 10^4$	$\Delta x\,\%$	$x_{(3)\,exp} \times 10^5$	$x_{(3)\,prd} \times 10^5$	$\Delta x\,\%$
278.14	1.032	0.339	0.337	0.6	0.199	0.207	-4.0	0.703	0.707	-0.5
278.15	2.004	0.646	0.629	2.6	0.387	0.364	6.0	1.121	1.115	0.5
278.15	2.526	0.771	0.776	-0.6	0.433	0.434	-0.3	1.302	1.256	3.5
278.15	3.039	0.899	0.915	-1.7	0.494	0.495	-0.1	1.297	1.352	-4.3
283.16	1.038	0.300	0.306	-2.1	0.165	0.168	-1.6	0.482	0.507	-5.1
283.16	1.988	0.566	0.566	-0.0	0.285	0.294	-3.1	0.754	0.809	-7.3
283.14	0.987	0.295	0.292	0.8	0.172	0.160	6.8	0.512	0.487	4.9
283.15	2.077	0.593	0.590	0.5	0.302	0.305	-0.8	0.941	0.831	12
283.15	3.415	0.896	0.922	-2.8	0.436	0.441	-1.3	1.048	1.053	-0.4
283.14	3.413	0.891	0.921	-3.5	0.428	0.441	-3.0	1.121	1.052	6.1
283.13	6.439	1.489	1.555	-4.5	0.674	0.625	7.3	1.166	1.098	5.8
283.15	3.079	0.826	0.841	-1.8	0.385	0.411	-6.6	1.063	1.013	4.7
288.16	1.038	0.282	0.279	1.1	0.172	0.168	2.2	0.577	0.507	12
288.17	3.068	0.755	0.768	-1.8	0.399	0.430	-7.8	0.734	0.773	-5.4
298.14	14.407	2.191	2.215	-1.1	0.672	0.657	2.1			
298.14	0.994	0.218	0.228	-4.3	0.147	0.134	8.9	0.387	0.366	5.3
298.14	7.257	1.359	1.364	-0.4	0.562	0.574	-2	0.991	0.893	9.9
298.14	11.749	2.014	1.939	3.7	0.674	0.648	3.8			
298.14	2.964	0.637	0.637	-0.1	0.330	0.338	-2.4	0.811	0.773	4.7
313.12	12.624	1.817	1.748	3.8	0.586	0.594	-1.4			
313.12	7.460	1.157	1.176	-1.6	0.406	0.498	-22	0.694	0.725	-4.4

TABLE 6.14 - METHANE, ETHANE AND *N*-BUTANE MOLE FRACTIONS IN THE LIQUID PHASE OF THE GAS MIXTURE - WATER SYSTEM [B5]

6.2.1.5 Carbon Dioxide –Water System

6.2.1.5.1 Data generated with the PVT apparatus

A series of new data on the solubility of carbon dioxide in water has been generated over a wide temperature range (i.e., 274.14 up to 351.31 K). The *BIPs* between carbon dioxide - water are adjusted directly to all carbon dioxide solubility data reported in TABLE 6.15 and these new solubility measurements using the previously described procedure.
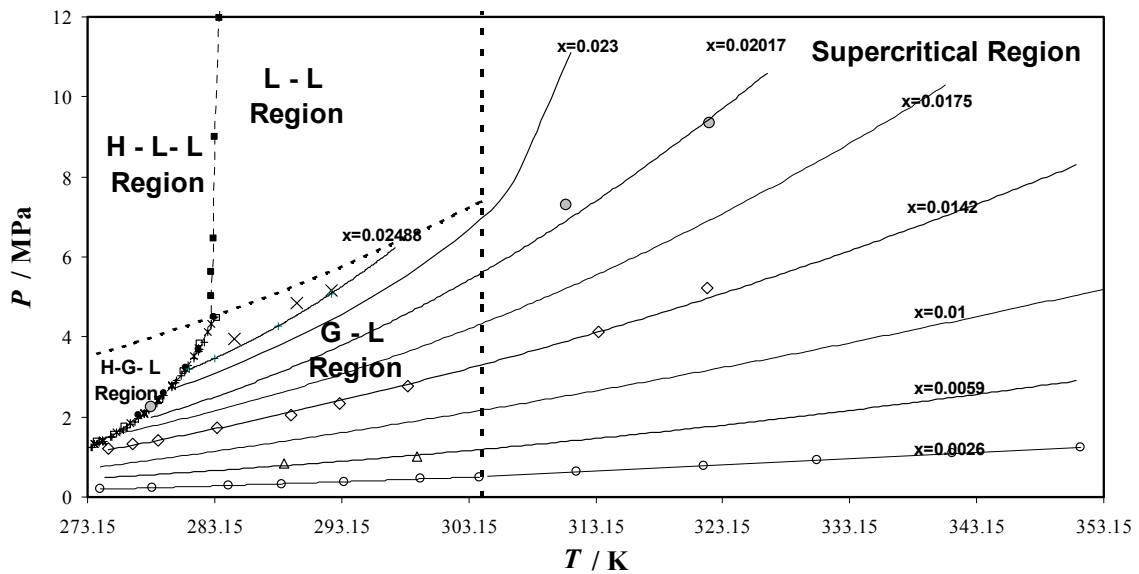
Figure 6.24: Carbon dioxide solubility data in water from 273.15 to 353.15 k generated in this work: (○) $x_{CO2}=0.00262$; (Δ) $x_{CO2}=0.0059$; (◇) $x_{CO2}=0.0142$; (●), $x_{CO2}=0.02017$; (✕) $x_{CO2}=0.02488$.

T/K	P_{exp}/MPa	$x_{exp} \times 10^3$	$x_{cal} \times 10^3 (\phi - \phi)$	Δx %	$x_{cal} \times 10^3 (\gamma - \phi)$	Δx %
274.14	0.190	2.617	2.531	3.3	2.443	6.6
278.22	0.228	2.617	2.562	2.1	2.506	4.2
284.27	0.287	2.617	2.620	-0.1	2.553	2.4
288.41	0.329	2.617	2.620	-0.1	2.552	2.5
293.34	0.385	2.617	2.631	-0.5	2.566	2.0
299.32	0.452	2.617	2.598	0.7	2.545	2.7
303.99	0.499	2.617	2.529	3.4	2.491	4.8
311.62	0.630	2.617	2.740	-4.7	2.617	0.0
321.64	0.779	2.617	2.730	-4.3	2.627	-0.4
330.60	0.913	2.617	2.697	-3.1	2.623	-0.2
341.24	1.086	2.617	2.675	-2.2	2.656	-1.5
351.31	1.243	2.617	2.630	-0.5	2.674	-2.2
288.64	0.826	5.900	6.330	-6.2	6.148	-4.2
299.06	1.008	5.900	5.654	4.2	5.525	6.3
274.83	1.201	14.200	13.769	3.0	13.809	2.8
276.74	1.327	14.200	14.092	0.8	14.077	0.9
278.74	1.426	14.200	13.986	1.5	13.978	1.6
283.38	1.732	14.200	14.330	-0.9	14.172	0.2
289.20	2.062	14.200	14.043	1.1	13.744	3.2
293.01	2.349	14.200	14.115	0.6	13.752	3.2
298.40	2.780	14.200	14.111	0.6	13.694	3.6
313.36	4.119	14.200	14.200	0.0	13.395	5.7
321.97	5.216	14.200	14.600	-2.8	13.692	3.6
310.86	7.309	20.168	21.301	-5.6	19.897	1.3
322.14	9.333	20.168	20.268	-0.5	18.794	6.8
284.73	3.938	24.880	25.750	-3.5	25.559	-2.7
289.62	4.844	24.880	25.868	-4.0	25.280	-1.6
292.35	5.172	24.880	25.193	-1.3	24.452	1.7

TABLE 6.15 - EXPERIMENTAL AND CALCULATED CARBON DIOXIDE MOLE FRACTIONS IN THE LIQUID PHASE OF THE CARBON DIOXIDE - WATER SYSTEM

The new generated solubility data sets are well represented with the *VPT-EoS* and *NDD* mixing rules (*AAD* around 2 %), with the second approach (*AAD* around 3 %) and with semi-empirical model of *Diamond and Akinfiev* [101] (*AAD* around 2 %). The *AADs* for all the references used in this work are summarized in TABLE 6.16. The overall *AADs* for the 298 selected solubility data are 2.1 and 1.8 %, respectively for this model (including 214 independent data) and the semi empirical-model exposed by *Diamond and Akinfiev* [101]

Reference	T /K	P /Mpa	N of exp. pts	AAD$^+$%	AAD*%
273.15 K < T ≤ 277.13 K					
[104]	274.15 – 276.15	0.07 – 1.42	12	1.5	0.7
[103]	273.15	1.082	1	0.1	2.8
277.13 K < T ≤ T$_c$					
[104]	278.15 – 288.15	0.83 – 2.179	42	1.1	0.9
[113]	293.15 – 303.15	0.486 – 2.986	18	3.0	3.2
[112]	298.15 – 302.55	5.07 – 5.52	2	3.1	1.9
[19]	283.15 – 298.15	1 – 5	7	2.4	2.6
[111]	298.31 – 298.57	2.7 – 5.33	7	2.9	2.5
[110]	298.15	1.11 – 5.689	18	1.4	1.8
[109]	298.15	4.955	3	3.2	3.1
[108]	298.15	4.955	4	2.4	2.2
[106-107]	291.15 – 304.19	2.53 – 5.06	5	0.9	1.5
[103]	283.15 – 303.15	0.101 – 2.027	15	0.9	1.5
[106]	303.15	0.99 – 3.891	4	2.3	2.0
T$_c$ < T ≤ 373.15 K					
[117]	304.25 – 366.45	0.69 – 20.27	13	4.6	4.7
[116]	323.15 – 373.15	10 – 60	9	5.4	2.2
[19]	323.15 – 343.15	1 – 16	16	1.7	2.5
[112]	323.15 – 373.15	1.94 – 9.12	57	2.8	1.9
[115]	323.15 – 348.15	4.955	8	1.3	1.4
[114]	373.15	4.955	3	6.5	2.8
[111]	308.15– 373.15	2.53 – 70.9	45	3.4	1.8
[110]	323.15 – 353.15	0.993 – 3.88	9	4.9	1.9
[109]	323.15 – 373.15	0.488 – 4.56	9	3.9	3.4
[106-107]	373.15	0.3 – 1.8	7	10.5	1.0
[103]	323.15 – 353.15	4 – 13.1	29	2.4	1.2

TABLE 6.16 - LIST OF RELIABLE EXPERIMENTAL DATA FOR CARBON DIOXIDE SOLUBILITY IN WATER BELOW 373.15 K [B6]
+ using *VPT- EoS* and *NDD* mixing rules
* using semi-empirical model from [101]

6.2.1.5.1 Data generated with the Static analytic apparatus

New solubility measurements of carbon dioxide in water have been generated in the 278.2 to 318.2 K temperature range for pressures up to 8 MPa. The experimental and calculated gas solubility data using the second approach are reported in TABLE 6.17 and plotted in Figure 6.25. Our isothermal *P, x* data sets for the carbon dioxide – water are well represented with the *γ - φ* model (with *BIPs* from TABLE 6.4 and using eq. 5.61 for the Henry's law with *A*=69.445, *B*=-3796.5, *C*=-21.6253 and *D*= -1.576.10^{-5}) (AAD=2.6 %). There is also a good agreement between the different authors (Figure 6.26).
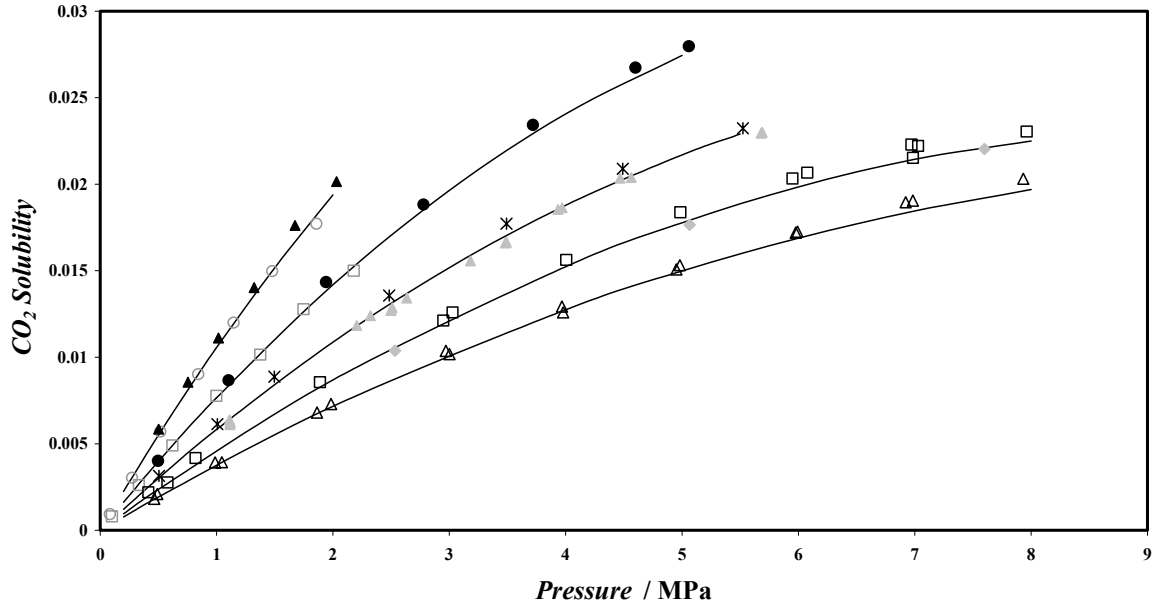
Figure 6.25: Carbon Dioxide Mole Fraction, x_1, in Water Rich Phase as a Function of Pressure at Various Temperatures. New solubility data: △, 318.2 K; □, 308.2 K; ✱, 298.2 K; ●, 288.2 K; ▲, 278.2 K; Literature data: ◆, 308.15 K from *Wiebe and Gaddy* [106-107]; ▲, 298.15 K from *Zel'vinskii* [103]; □, 288.15 K from *Anderson* [104]; ○, 278.15 K from *Anderson* [104]; Solid lines, calculated with the PR-EoS and Henry's law approach with parameters from TABLE 6.4.
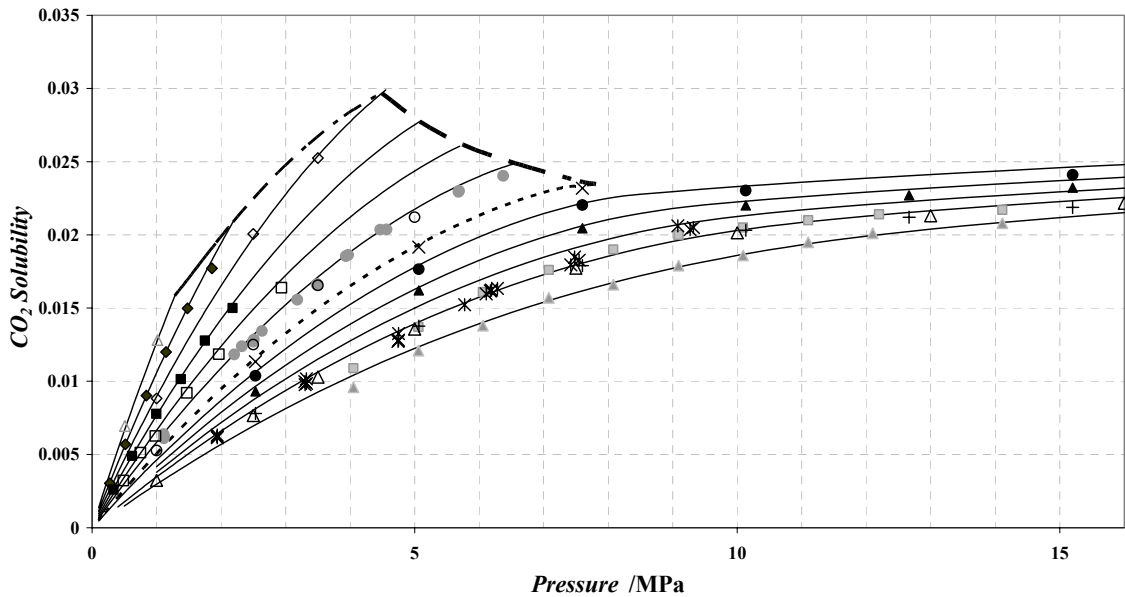
Figure 6.26: Carbon dioxide mole fraction in water rich phase as a function of pressure at various temperatures. Literature data: △, 273.15 K from *Zel'vinskii* [103]; ◆, 278.15 K from *Anderson* [104]; ◇, 283.15 K *Anderson* [104]; ■, 288.15 K from *Oleinik* [112]; □, 293.15 K from *Kritschewsky et al.* [106]; ○, 298.15 K from *Oleinik* [112]; ●, 298.15 K from *Zel'vinskii* [103]; ×, 304.19 K from *Wiebe and Gaddy* [106-107]; ●, 308.15 K from *Wiebe and Gaddy* [106-107]; ▲,313.15 K from *Wiebe and Gaddy* [106-107]; △, 323.15 K from *Oleinik* [112]; ✱, 323.15 K from *Zel'vinskii* [103]; ■, 323.15 K from *Bamberger et al.* [117]; ▲, 333.15 K from *Bamberger et al.* [117]; Solid lines, calculated with the *PR-EoS* and Henry's law approach with parameters from Table 6.4. -------, solubilities calculated at 304.21 K; — - —, solubilites calculated at hydrate dissociation pressures; ———, carbon dioxide vapour pressures.

T/K	P_{exp}/MPa	$x \times 10^2 (exp)$	$x_{prd} \times 10^2 (\gamma - \phi)$	
			Model	**AD %**
318.23	0.465	0.182	0.179	1.4
318.23	1.045	0.394	0.394	0.1
318.23	1.863	0.680	0.673	1.1
318.23	1.984	0.730	0.712	2.5
318.23	2.970	1.036	1.007	2.8
318.23	3.001	1.018	1.015	0.3
318.23	3.969	1.293	1.267	2.0
318.23	3.977	1.259	1.269	0.8
318.23	4.952	1.508	1.489	1.3
318.23	4.982	1.532	1.495	2.4
318.23	5.978	1.720	1.684	2.1
318.23	5.992	1.726	1.687	2.3
318.23	6.923	1.895	1.834	3.2
318.23	6.984	1.905	1.842	3.3
318.23	7.933	2.031	1.962	3.4
308.2	0.579	0.276	0.273	1.0
308.2	1.889	0.856	0.826	3.4
308.2	2.950	1.212	1.205	0.6
308.2	3.029	1.259	1.231	2.2
308.2	4.005	1.563	1.525	2.4
308.2	4.985	1.837	1.774	3.4
308.2	5.949	2.033	1.975	2.9
308.2	6.077	2.066	1.998	3.3
308.2	6.972	2.229	2.140	4.0
308.2	6.986	2.152	2.142	0.5
308.2	7.029	2.221	2.148	3.3
308.2	7.963	2.304	2.247	2.5
298.28	0.504	0.314	0.303	3.6
298.28	1.007	0.614	0.586	4.5
298.28	1.496	0.887	0.842	5.0
298.28	2.483	1.356	1.304	3.8
298.28	3.491	1.772	1.703	3.9
298.28	4.492	2.089	2.030	2.8
298.28	5.524	2.323	2.296	1.2
288.26	0.496	0.401	0.394	1.6
288.26	1.103	0.867	0.839	3.3
288.26	1.941	1.434	1.384	3.5
288.26	2.777	1.882	1.852	1.6
288.26	3.719	2.343	2.292	2.2
288.26	4.601	2.673	2.622	1.9
288.26	5.059	2.797	2.761	1.3
278.22	0.501	0.585	0.551	5.7
278.22	0.755	0.852	0.813	4.6
278.22	1.016	1.111	1.071	3.6
278.22	1.322	1.403	1.358	3.2
278.22	1.674	1.747	1.669	4.5
278.22	2.031	2.015	1.963	2.6

TABLE 6.17 - EXPERIMENTAL AND PREDICTED CARBON DIOXIDE MOLE FRACTIONS IN THE LIQUID PHASE OF THE CARBON DIOXIDE - WATER SYSTEM

6.2.1.6 Hydrogen Sulphide–Water System

New experimental *VLE* data of H_2S - water binary system are reported over the 298.2-338.3 K temperature range for pressures up to 4 MPa. The experimental and calculated gas solubility data are reported in TABLE 6.18 and plotted in Figure 6.27.
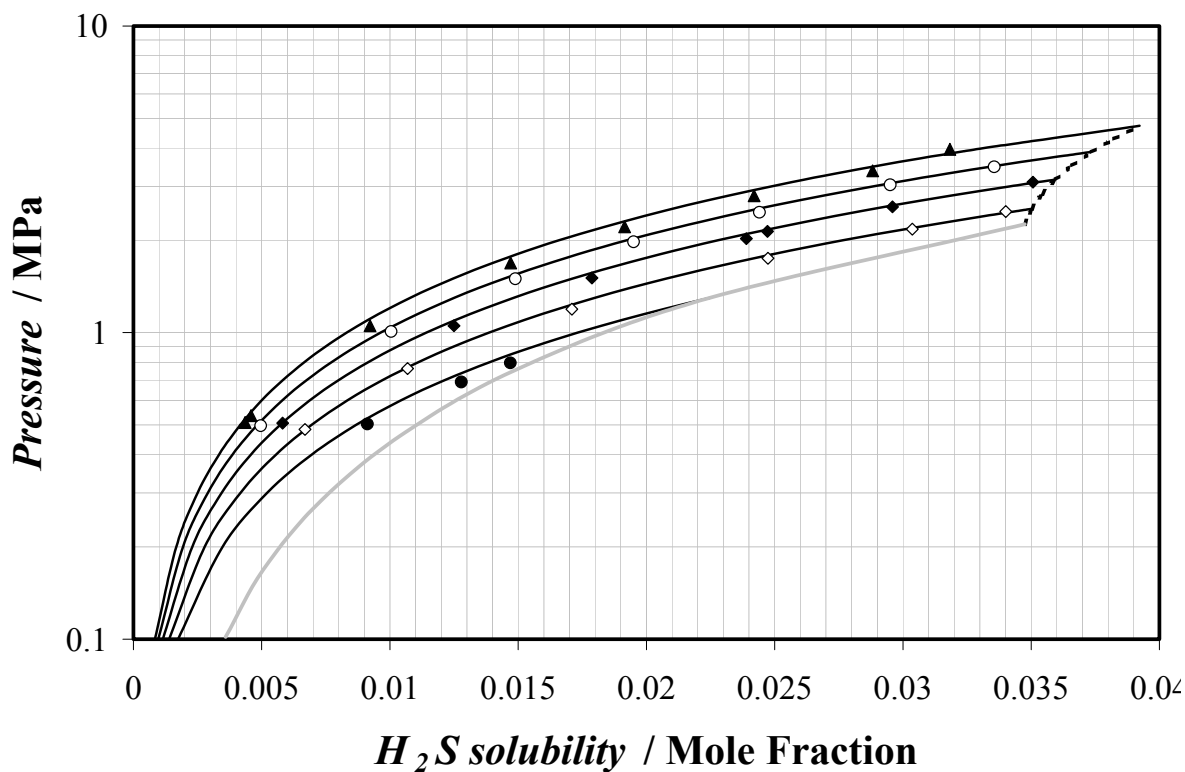
Figure 6.27: This work, H_2S solubility in water. Dashed line, hydrogen sulphide-water LL locus; Grey solid line, hydrate dissociation line; ●, 298.18 K; ◇, 308.2 K; ◆, 318 K; ○, 328.28 K; ▲, 338.34 K.

Experimental data about solubility of hydrogen sulphide in water were reported previously in TABLE 2.7; additional data have been gathered from an additional and more complete bibliographic study (TABLE 6.19). The *BIPs* between hydrogen sulphide - water are taken from TABLE 6.4 and the following parameters for the Henry's law (Eq. 5.61) *A*=84.2884, *B*=-3792.31, *C*=-29.556 and *D*= $1.072.10^{-2}$.

The new generated solubility data sets are well represented with the γ - ϕ approach (*AAD* around 1.5 %). The *AADs* for all the references used in this work are summarized in TABLE 6.19. The overall *AADs* for the selected solubility data are 3.5 % for this model (*T*<423.15 K).

Selected hydrogen sulphide solubility data reported in the literature are plotted in Figure 6.28; there is also a good agreement between the different authors and the model (Figure 6.28).

T/K	P_{exp}/MPa	$x_{exp} \times 10^3$	Model (γ - ϕ)	
			$x_{cal} \times 10^3$	AD %
298.16	0.503	9.120	9.318	2.2
298.16	0.690	12.784	12.693	0.7
298.16	0.797	14.693	14.588	0.7
308.2	0.483	6.689	7.144	6.8
308.2	0.763	10.688	11.201	4.8
308.2	1.193	17.089	17.259	1.0
308.2	1.748	24.735	24.737	0.0
308.2	2.175	30.364	30.213	0.5
308.2	2.483	34.008	33.999	0.0
318.21	0.507	5.815	6.154	5.8
318.21	1.053	12.496	12.666	1.4
318.21	1.507	17.873	17.883	0.1
318.21	2.024	23.896	23.597	1.3
318.21	2.139	24.717	24.836	0.5
318.21	2.570	29.590	29.351	0.8
318.21	3.094	35.070	34.568	1.4
328.28	0.497	4.963	5.053	1.8
328.28	1.008	10.046	10.264	2.2
328.28	1.498	14.891	15.117	1.5
328.28	1.978	19.500	19.696	1.0
328.28	2.468	24.410	24.224	0.8
328.28	3.034	29.503	29.215	1.0
328.28	3.475	33.560	32.847	2.1
338.34	0.509	4.354	4.412	1.3
338.34	0.536	4.588	4.650	1.4
338.34	1.053	9.226	9.244	0.2
338.34	1.688	14.708	14.708	0.0
338.34	2.215	19.151	19.095	0.3
338.34	2.796	24.200	23.738	1.9
338.34	3.370	28.820	28.176	2.2
338.34	3.962	31.830	31.702	0.4

TABLE 6.18 - EXPERIMENTAL AND CALCULATED H₂S MOLE FRACTIONS IN THE LIQUID PHASE OF THE H₂S–H₂O SYSTEM

Reference	T/K	P/MPa	Number of exp. Pts	AAD % [+]
Winkler (1906) [297]	273.15 – 363.15	atmospheric pressure	14	-
Kendal and Andrews (1921) [298]	298.15	atmospheric pressure	1	-
Wright and Maas (1932) [299]	278.15 - 333.15	0.04 - 0.5	52	2.5
Kiss et al. (1937) [300]	273.2 –298.1	atmospheric pressure	3	-
Selleck et al. (1952) [49]	310.93 – 444.26	0.7 –20.7	63	3.9
Pohl (1961) [301]	303.15 – 316.15	1.7	15	6.2
Kozintseva (1964) [126]	502.15 - 603.15	2.8 - 12.6	12	-
Harkness and Kelman (1967) [302]	303.15	atmospheric pressure	1	-
Burgess and Germann (1969) [48]	323.15 – 443.15	1.7 – 2.3	35	3.8
Clarke and Glew (1971) [303]	273.15 –323.15	0.05 –0.1	35	3.5
Gerrard (1972) [304]	273.15 – 293.15	atmospheric pressure	3	-
Lee and Mather (1977) [305]	283.15 –453.15	≈0.3 – 6.5	>270	3.2
Douabul and Riley (1979) [306]	275.25 – 303.07	atmospheric pressure	5	-
Gillespie et al. (1982) [19]	310.93 – 588.7	0.3 - 13.8	15	-
Barrett et al. (1988) [307]	297.15 – 367.15	atmospheric pressure	39	-
Carroll and Mather (1989) [127]	313.15 –378.15	2.8 – 9.24	5	-
Suleimenov and Krupp (1994) [308]	293.95 – 594.15	0.2 – 13.9	49	5.5
Kuranov et al. (1996) [309]	313.15	0.5 – 2.5	9	1.5

TABLE 6.19 - LIST OF EXPERIMENTAL SOLUBILITY DATA FOR THE H₂S–H₂O SYSTEM (<u>VLE CONDITIONS</u>) [+] using the γ - ϕ approach and $T < 423.15$ K.
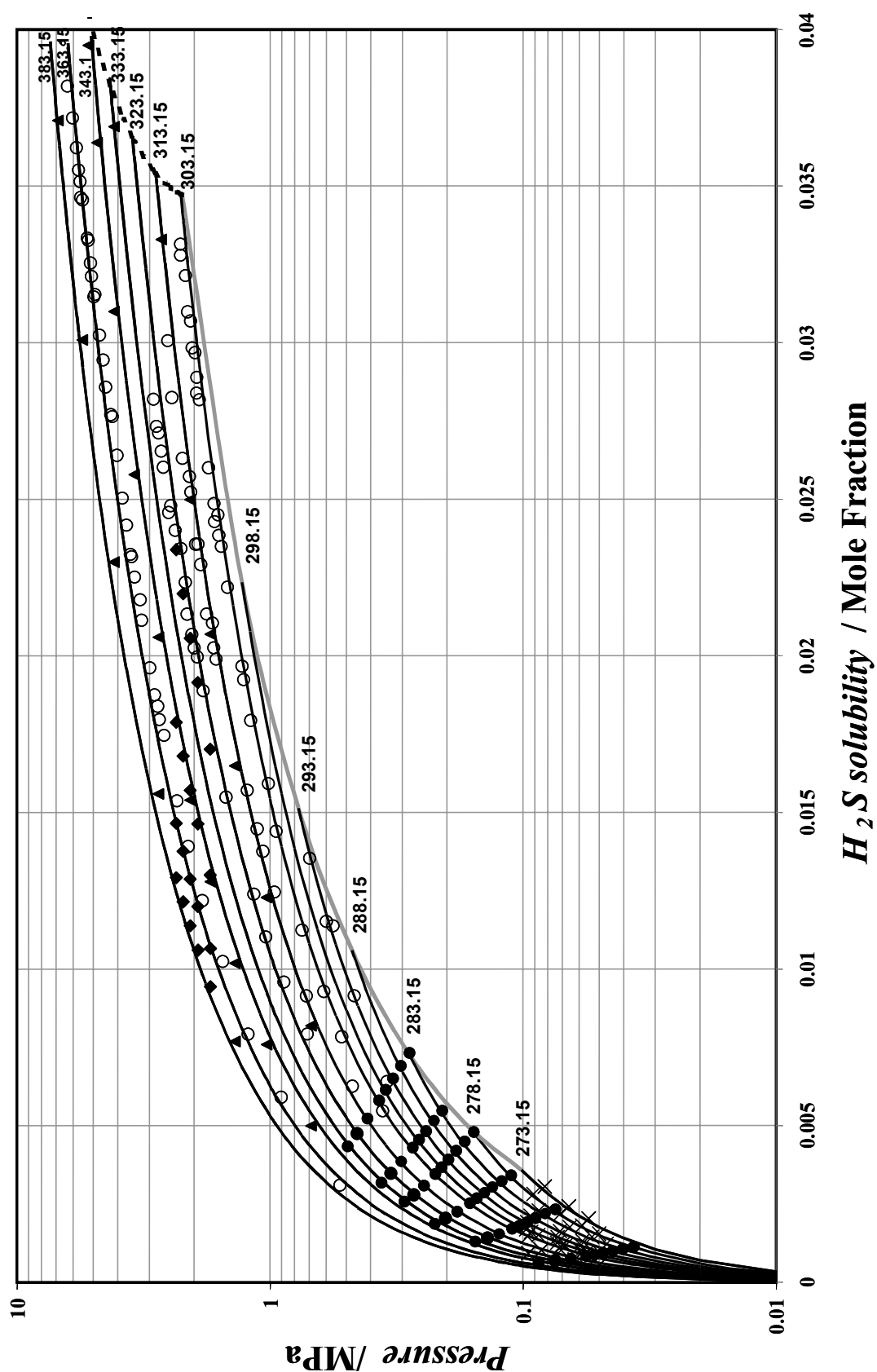
Figure 6.28: Selected literature data, H₂S solubility in water. Dashed line, hydrogen sulphide - water liquid-liquid locus; Grey solid line, hydrate dissociation line; ●, data from *Wright and Mass*; ×, data from *Clarke and Glew*; ◆, data from *Burgess and Germann*; ○, data *from Lee and Mather*; ▲, data from *Selleck et al.* **(Temperature in Kelvin)**

187

6.2.1.7 Nitrogen –Water System

New experimental solubility data of N_2 in water are reported in a wide temperature range 274.18 - 363.02 K up to 7.16 MPa. The relative uncertainty (calibration) in the moles of nitrogen is about ± 2.5 %. The experimental and calculated gas solubility data are reported in TABLE 6.16 and plotted in Figure 6.23. The adjustment procedure is the same as previously described.
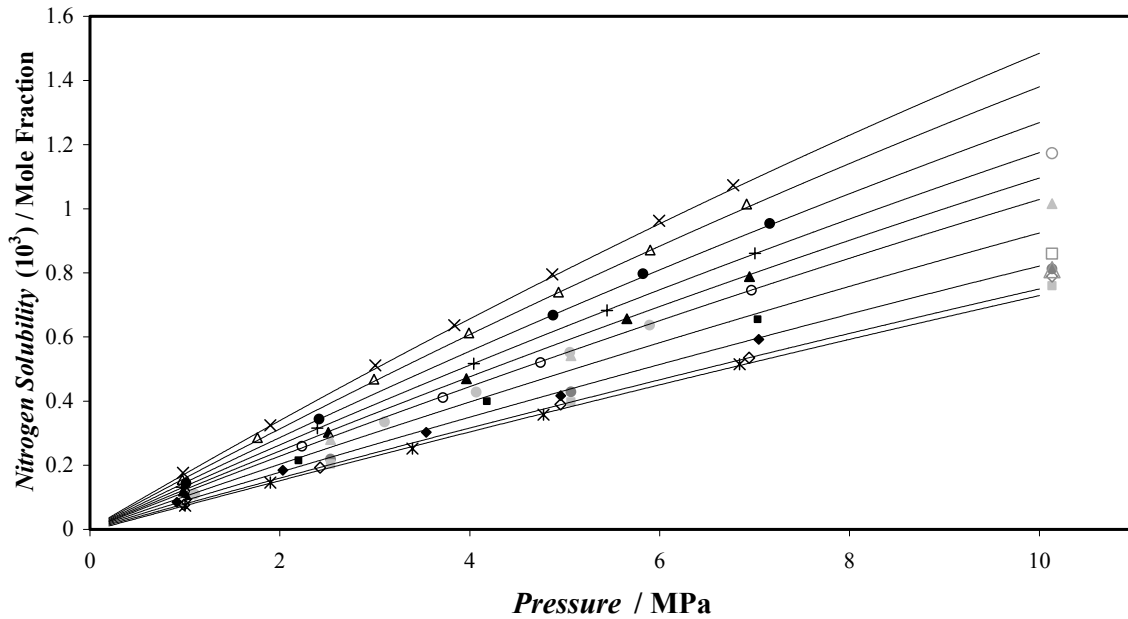
Figure 6.23: Nitrogen mole fraction in water rich phase as a function of pressure at various temperatures. New solubility data: ×, 274.2 K; △, 278.2 K; ●, 283.1 K; +, 288.1 K; ▲, 293.1 K; O, 298.1 K; ■, 308.2 K; ♦, 323.1 K; ◇, 343.0 K; ✱, 363.0 K; Literature data: ▲, 298.1 K from *Wiebe et al.* [119] ; ●, 303.1 K from *Smith et al.* [123] ; ●, 323.1 K from *Wiebe et al.* [119] ; ■, 348.1 K from *Wiebe et al.* [119] ; O, 273.1 K from *Goodmann and Krase* [118]; □, 298.1 K from *Goodmann and Krase* [118]; △, 324.6 K from *O'Sullivan et al.* [124] ; ◇, 338.1 K from *Saddington and Krase* [121]; Solid lines, calculated with the *VPT-EoS* and *NDD* mixing rules with parameters from Table E.1. [B12]

Our isothermal *P*, *x* data sets for the nitrogen–water are well represented with the *VPT-EoS* and *NDD* mixing rules (*AAD* = 1.2 %) and with the *PR-EoS* associated with Henry's law approach (Eq 6.1 with *A*=78.852; *B*=-3745; *C*=-24.8315; *D*= 0.000291) (*AAD* =1.0%). Selected nitrogen solubility data reported in the literature are plotted in Figure 6.23. There is good agreement between the different authors, with the exception of the data reported by *Goodman and Krase* [118], whose solubility data are underestimated. As it can be seen in Figure 6.23, the solubility of nitrogen follows a linear behaviour as a function of the pressure and that is why the model using the Henry's law gives accurate predictions.

T/K	P_{exp}/MPa	$x_{exp}\times10^3$	AD exp %	$x_{cal}\times10^3(\phi$ - $\phi)$	Δx %	$x_{cal}\times10^{3}(\gamma$ - $\phi)$	Δx %
274.19	0.979	0.1760	2.4	0.1704	3.2	0.1707	-0.4
274.19	1.900	0.3248	1.2	0.325	0.0	0.3259	-0.4
274.18	3.006	0.5112	1.1	0.5039	1.4	0.5058	-0.2
274.18	3.837	0.6365	1.3	0.6337	0.4	0.6366	0.0
274.19	4.868	0.7950	1.4	0.7892	0.7	0.7937	-1.1
274.21	5.993	0.9626	0.6	0.9523	1.1	0.9588	0.3
274.26	6.775	1.0733	2.2	1.0613	1.1	1.0693	-3.0
278.15	0.971	0.1552	1.4	0.1559	-0.4	0.1544	-0.4
278.21	1.763	0.2860	2.9	0.2789	2.5	0.2764	-0.6
278.19	2.990	0.4683	1.9	0.4631	1.1	0.4595	-1.6
278.19	3.990	0.6127	1.1	0.6073	0.9	0.6030	-1.9
278.16	4.934	0.7394	1.4	0.7395	0.0	0.7350	-3.3
278.05	5.900	0.8711	2.2	0.872	-0.1	0.8678	-0.5
278.17	6.916	1.0149	1.2	1.0033	1.1	0.9989	-1.6
283.12	1.012	0.1439	1.3	0.1481	-2.9	0.1450	0.7
283.13	2.413	0.3441	1.5	0.3447	-0.2	0.3378	-2.2
283.13	4.877	0.6684	0.6	0.6694	-0.1	0.6574	-3.0
283.18	5.825	0.7971	0.5	0.7868	1.3	0.7732	-1.7
283.16	7.160	0.9538	1.7	0.9479	0.6	0.9324	-1.8
288.11	0.966	0.1318	3.4	0.1299	1.4	0.1261	-2.8
288.09	2.395	0.3158	2.9	0.3149	0.3	0.3060	-2.6
288.11	4.042	0.5168	0.3	0.5178	-0.2	0.5037	-2.5
288.11	5.444	0.6829	0.3	0.6829	0.0	0.6649	-3.1
288.11	7.003	0.8609	0.2	0.8585	0.3	0.8369	-4.3
293.1	0.984	0.1195	0.9	0.1223	-2.4	0.1180	-1.2
293.08	2.511	0.3025	1.2	0.3054	-0.9	0.2949	-2.6
293.09	3.964	0.4700	2.4	0.4719	-0.4	0.4561	-3.2
293.09	5.655	0.6570	0.7	0.657	0.0	0.6358	-3.0
293.09	6.945	0.7884	0.5	0.7925	-0.5	0.7676	-2.5
298.07	1.004	0.1139	1.4	0.1164	-2.2	0.1118	-3.6
298.10	2.233	0.2590	2.3	0.2544	1.8	0.2447	-3.3
298.10	3.717	0.4111	0.7	0.4149	-0.9	0.3995	-2.8
298.08	4.745	0.5206	0.6	0.5222	-0.3	0.5032	-5.5
298.04	6.967	0.7457	0.4	0.7446	0.1	0.7185	-1.8
308.23	1.040	0.1033	1.6	0.1066	-3.2	0.1024	-0.9
308.18	2.196	0.2152	2.7	0.2222	-3.3	0.2137	-1.3
308.18	4.180	0.4000	0.5	0.4126	-3.2	0.3972	-0.7
308.19	7.032	0.6550	1.2	0.6701	-2.3	0.6464	-0.7
323.13	0.915	0.0843	0.1	0.0817	3.1	0.0796	-2.2
323.13	2.031	0.1846	1.5	0.1802	2.4	0.1756	-0.1
323.13	3.542	0.3028	2.8	0.3095	-2.2	0.3020	-0.3
323.13	4.957	0.4170	1.8	0.4266	-2.3	0.4167	-4.9
323.14	7.043	0.5926	1.8	0.5926	0.0	0.5798	-5.7
342.99	0.992	0.0771	0.7	0.0783	-1.5	0.0793	2.8
342.92	2.424	0.1929	0.7	0.1922	0.4	0.1949	0.9
342.98	4.956	0.3896	1.0	0.3854	1.1	0.3918	0.6
342.98	6.941	0.5354	1.0	0.5303	0.9	0.5402	1.0
362.90	1.001	0.0739	2.0	0.0733	0.8	n/a	-
362.90	1.900	0.1458	1.1	0.1428	2.0	n/a	-
363.00	3.396	0.2521	1.4	0.2558	-1.5	n/a	-
362.92	4.776	0.3578	1.7	0.3575	0.1	n/a	-
363.00	6.842	0.5147	1.0	0.5053	1.8	n/a	-

TABLE 6.16 - EXPERIMENTAL AND CALCULATED NITROGEN MOLE FRACTIONS IN THE LIQUID PHASE OF THE NITROGEN - WATER SYSTEM [B12]

6.2.2   Gas Solubilities in Water and Ethylene Glycol Solution

Accurate knowledge of the thermodynamic properties of the water/hydrocarbon and water-inhibitor /hydrocarbon equilibria is crucial at sub-sea pipeline conditions. The knowledge of these properties allows indeed to optimize the inhibitor quantities, and thus to prevent hydrate formation and pipeline blockage. To give a qualified estimate of the amount of gas dissolved in the liquid phase or of the amount of inhibitor needed to prevent hydrate formation, thermodynamic models are required. Accurate gas solubility data, especially near the hydrate-stability conditions, are necessary to develop and validate thermodynamic models.

The solubility of methane in pure water at low temperatures has already been the subject of a study and many other authors have investigated this system at various conditions. Solubilities of methane in pure ethylene glycol have also been reported in the literature: *Jou et al.* [295] in 1994, *Zheng et al.* [296] in 1999 and more recently by *Wang et al.* [86] in 2003. Solubility data in aqueous solution containing ethylene glycol have been scarcely investigated and have been only reported by *Wang et al.* [86] in 2003. New solubility measurements of methane in three different aqueous solution containing ethylene glycol (20, 40 and 60 wt. %) have been generated here at low and ambient temperatures.

The experimental methane solubilities data in ethylene glycol of the three different authors (*Jou et al.* [295], *Zheng et al.* [296] and *Wang et al.* [86]) are plotted in Figure 6.24. The data of *Zheng et al.* show relatively good agreement with the data of *Jou et al*. However, *Wang et al.* [86] do not show agreement with this set of data. Unfortunately *Wang et al.* [86] are the only authors having reported data solubilities of methane in *EG* solutions and thus available for comparisons. However, at high pressures the solubility data reported by *Wang et al.* in pure *EG* are curiously independent of the temperature and consequently highly doubtful. Therefore their data were not used for comparison.
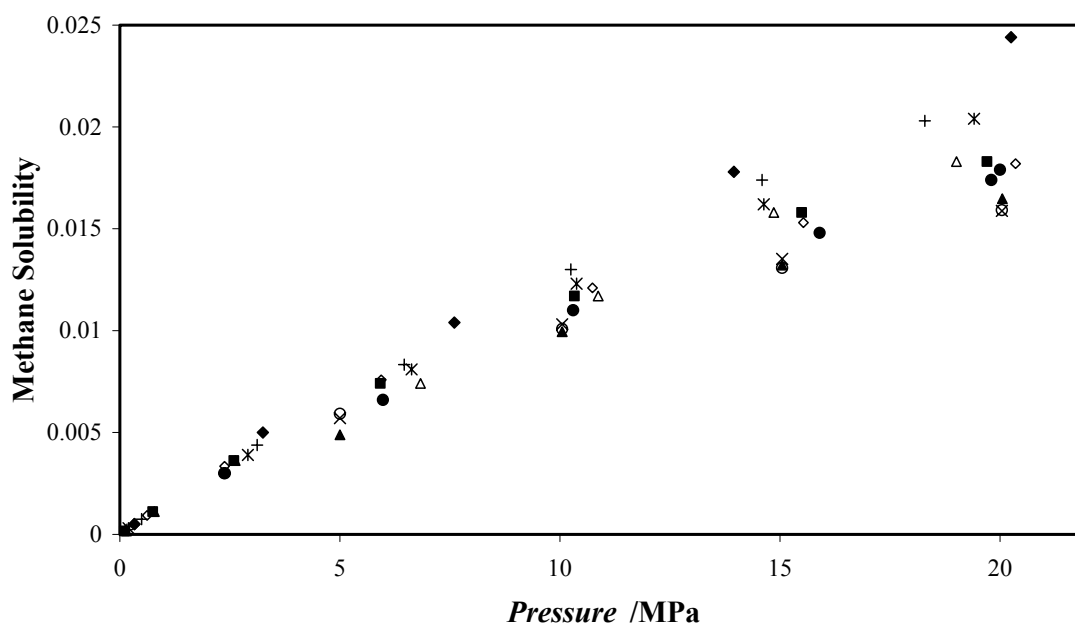
Figure 6.24: Methane mole fraction in ethylene glycol as a function of pressure at various temperatures. (♦, 398.15 K; ✱, 373.15 K; ●, 323.15 K from *Zheng et al.* [295]) ; (◇, 298.15 K; ■, 323.15 K; △, 348.15 K; +, 373.15 K from *Jou et al.* [294]) ; (▲, 283.2 K; ✕, 293.2 K; ○, 303.2 K from *Wang et al.* [86])

The experimental gas solubility data are reported in Table 6.17 for the methane – water – 20, 40 & 60 wt. % ethylene glycol systems, and plotted respectively in Figures 6.25a,b and c.
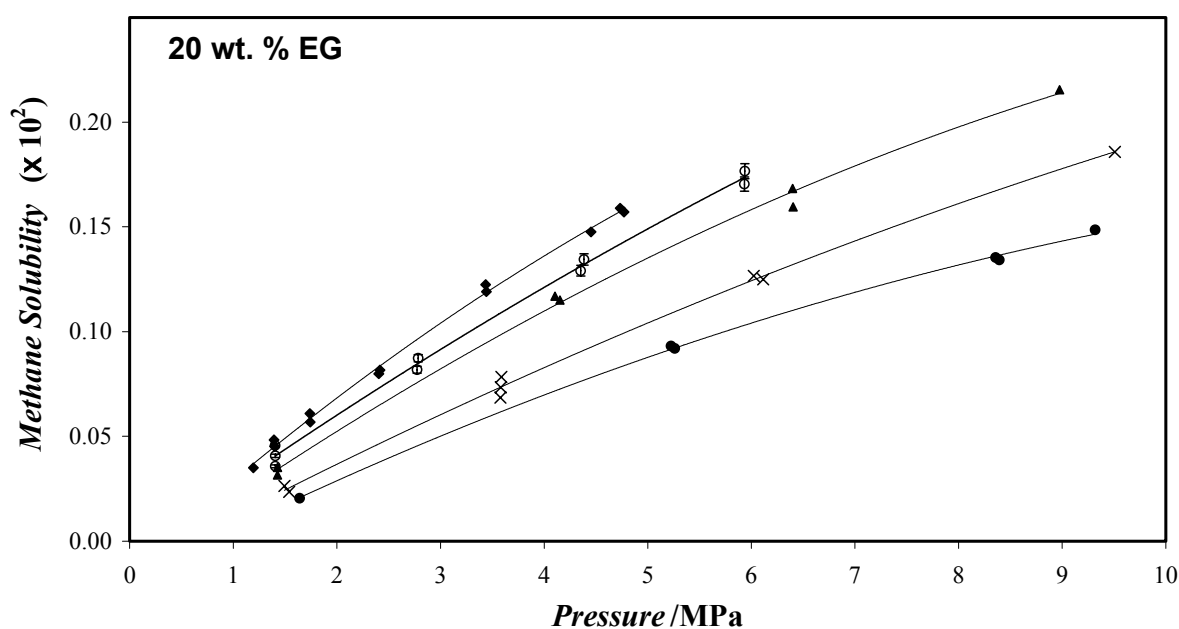
Figure 6.25a: Methane mole fraction in 20wt% ethylene glycol
◇, 273.3 K; ○, 278.2 K; ▲, 283.1 K; ✕ 297.9 K; ●, 322.7 K.
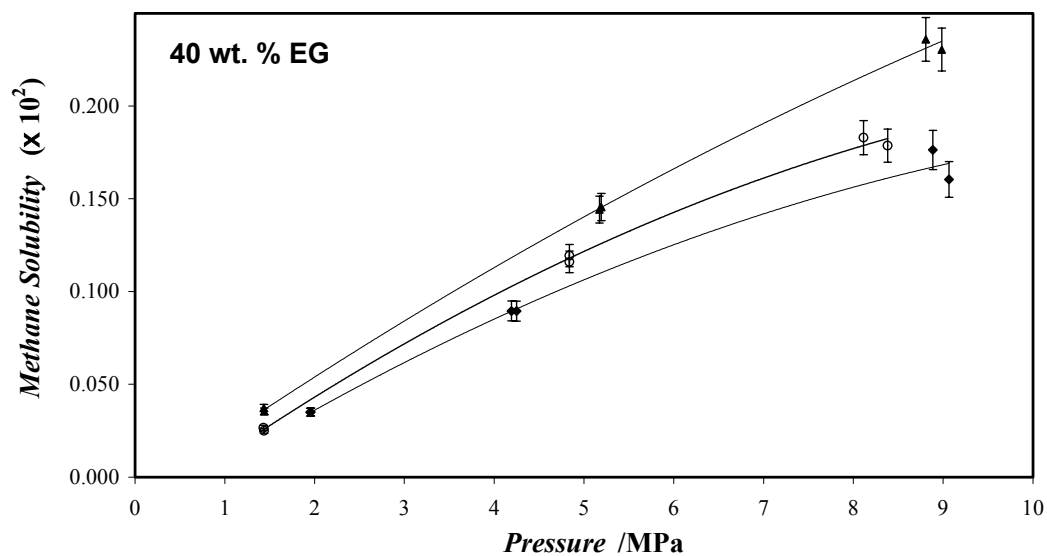
Figure 6.25b: Methane mole fraction in 40wt% ethylene glycol
▲, 273.3 K; ○, 297.3 K, ◆, 322.8 K.
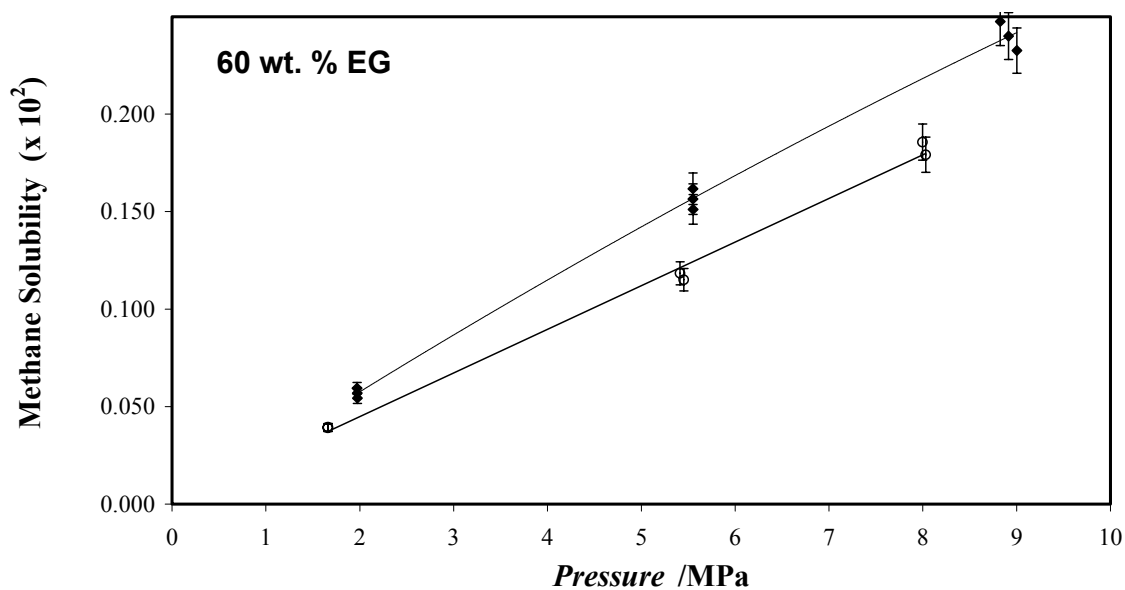
Figure 6.25c: Methane mole fraction in 60wt% ethylene glycol
◆, 273.3 K; ○, 298.1 K.

T/K	P_{exp}/MPa	$x_{exp}\times10^2$	T/K	P_{exp}/MPa	$x_{exp}\times10^2$
		20 wt. % EG			
273.30	1.195	0.035	283.05	1.426	0.032
273.28	1.394	0.048	283.05	1.427	0.035
273.28	1.398	0.045	283.07	4.105	0.117
273.28	1.738	0.061	283.07	4.152	0.115
273.28	1.743	0.057	283.08	6.399	0.168
273.28	2.404	0.080	283.09	6.404	0.160
273.28	2.416	0.082	283.09	8.974	0.216
273.28	3.436	0.123	283.07	9.167	0.219
273.28	3.443	0.119			
273.28	4.453	0.148	297.92	1.493	0.026
273.28	4.733	0.159	297.92	1.540	0.024
273.28	4.771	0.157	297.92	3.578	0.069
			297.92	3.587	0.078
278.14	1.404	0.046	297.92	3.583	0.074
278.14	1.407	0.036	297.93	6.022	0.127
273.15	1.405	0.041	297.93	6.114	0.125
278.16	2.773	0.082	297.92	9.508	0.186
278.17	2.784	0.087		9.440	0.179
278.15	4.353	0.129	297.91	9.575	0.193
278.14	4.385	0.135	297.91		
278.17	5.933	0.171	322.74	1.640	0.021
278.15	5.937	0.177	322.76	5.226	0.093
278.13	8.174	0.223	322.75	5.260	0.092
278.18	8.198	0.219	322.78	8.359	0.135
			322.72	8.392	0.134
			322.72	9.318	0.149
		40 wt. % EG			
322.73	4.249	0.090	297.96	8.113	0.183
322.76	4.193	0.090	297.93	8.381	0.179
322.76	1.958	0.040	297.96	4.839	0.119
322.74	1.951	0.040	297.94	4.837	0.116
322.74	1.951	0.040	297.94	1.431	0.027
322.74	1.951	0.035	297.94	1.436	0.025
322.76	8.885	0.176			
322.77	9.070	0.160	273.29	1.436	0.037
			273.31	1.440	0.036
			273.24	5.194	0.146
			273.29	5.172	0.144
			273.31	8.984	0.230
			273.26	8.806	0.236
		60 wt. % EG			
273.20	1.971	0.059	298.06	1.660	0.039
273.22	1.973	0.057	298.07	1.661	0.039
273.24	1.975	0.054	298.07	5.414	0.118
273.35	5.550	0.162	298.06	5.454	0.115
273.31	5.550	0.157	298.04	7.997	0.186
273.27	5.551	0.151	298.05	8.031	0.179
273.33	8.824	0.248			
273.33	8.914	0.240			
273.33	9.003	0.233			

TABLE 6.17 - EXPERIMENTAL METHANE MOLE FRACTIONS IN THE LIQUID PHASE OF THE METHANE – WATER – ETHYLENE GLYCOL SYSTEM

Correlations*

Dans ce dernier chapitre diverses corrélations et méthodes pour déterminer la teneur en eau d'un gaz en équilibre avec de l'eau seront présentées. Après avoir exposé ces méthodes, une nouvelle corrélation sera exposée pour prédire les teneurs en eau du méthane. En utilisant des facteurs correctifs, cette corrélation sera étendue aux différents composants du gaz naturels et finalement un autre facteur correctif sera introduit pour tenir compte de la présence de gaz acides.

Après avoir traité les teneurs en eau, de nouvelles corrélations pour calculer la valeur de la constante de Henry seront proposées et finalement une méthode pour calculer la solubilité de gaz dans l'eau.

* This part is a modification of reference [B9]

7   Correlations

The water content assessment by using the predictive methods is very crucial to design and select the proper conditions of natural gas facilities. It is of interest to be able to estimate water content of natural gases at given temperatures and pressures. The saturated water content of a vapour phase depends on pressure, temperature and gas feed composition. The effect of composition increases with pressure and is particularly important if the gas contains carbon dioxide and hydrogen sulphide (GPSA 1998). For lean and sweet natural gases having a gas gravity close to methane, the effect of composition can be ignored and the water content can be assumed as a function of temperature and pressure. General methods of calculation include the use of:

1) Empirical or semi – empirical correlations and charts of water content and corrections for the presence of acid gases (such as hydrogen sulphide and carbon dioxide), heavy hydrocarbons and salts.

2) Thermodynamic models.

The main advantage of empirical or semi – empirical correlations and charts is the availability of input data and the simplicity of the calculation, which can be performed. The correlations / charts have still kept their popularity among engineers in the natural gas industry. Although most available thermodynamic models could be installed on typical laptop computers, there seem to be a need for simple, yet robust, predictive methods for quick estimation of water content of natural gases.

The available correlations and charts are normally based on limited data and with limited application.   In production, transport and processing of natural gases, the available correlations / charts can predict water content of gases with enough accuracy at high temperatures. While in predicting water content at low temperature conditions, the available methods have lower accuracy and still in the light of the latest literature data, the developed correlations / charts need further verification in the range of low temperatures. In fact, during the development of the correlations / charts at that time, the experimental data describing phase equilibrium in water – hydrocarbons systems for temperatures lower than 298.15 K were not available. Due to this fact, water content for temperatures lower than 298.15 K calculated by the correlations / charts might not be accurate.

To develop new correlations / charts and to increase the accuracy of calculations, experimental data are required, which would allow to improve correlations / charts and to determine the equilibrium water content of gases. The aim of this work is to develop a semi – empirical correlation for estimating the equilibrium water content of sweet natural gases in equilibrium with liquid water and ice. Using correction factors, this approach has been extended to predict the water content in function of the gas gravity of the gas and of sour gas content.

7.1 Water Content Models and Correlations

Many thermodynamic models and correlations are available, which can calculate phase equilibrium in water – hydrocarbon systems. Thermodynamic models use different approaches in order to model liquid, ice and gas hydrates phases. For example, some thermodynamic models use activity coefficient or equation of state (EoS) approaches for modeling the aqueous phase, however other models use the Henry constant approach.

Empirical correlations and charts are more simple tools than thermodynamic based approaches and because of their ease of use, they are of interest to all engineers in petroleum industry. The original correlations / charts are only applicable to dry and sweet gases. However, the development of oil and gas fields necessitates a robust and simple method for predicting the water content in these systems. Up to now, different correlations and charts with different capabilities have been reported in order to estimate the water content / water dew point of gases. Generally, these correlations / charts have been developed for the L_w-V region and interpolating the results to the H-V and I-V regions may be questionable. In this section, a quick review is made on the most famous correlations and charts in the natural gas industry:

7.1.1 Correlation and Charts

7.1.1.1 Sweet and Dry Gas in Equilibrium with Liquid Water

- The *Ideal* model (Raoult's law) is expressed by the following expression:

$$y_w = \frac{(1-x_g)P_w^{sat}}{P} \qquad (7.1)$$

where y, x, and P are the mole fraction in the vapour phase, mole fraction in the liquid phase and pressure, respectively, and subscripts w and g relate to water and gas and the superscript *sat* relate to the saturation state. In this equation, the gas solubility in water x_g can be ignored for sweet natural gases, as hydrocarbons are very few soluble and less soluble with the increase of their molecular weight. With this assumption, the water content can be expressed by the following expression:

$$y_w = \frac{P_w^{sat}}{P} \tag{7.2}$$

The above relation assumes the water content of a gas is given by the ratio of the water vapour pressure over total pressure of the system.

A more accurate form of the *Ideal* model can be expressed by taking into account the *Poynting* correction:

$$y_w = \frac{P_w^{sat}}{P} \exp(\frac{v_w^I (P - P_w^{sat})}{RT}) \tag{7.3}$$

where v, R and T are molar volume, universal gas constant and temperature of the system, respectively and the superscript L stands for the liquid state . The *Ideal model* and its *Poynting correction* are simple tools for predicting the water content of natural gases. However, these methods can be used at low-pressures (Typically up to 1.4 MPa [10]).

- *Bukacek* [310] developed a method similar to the *ideal* model, which only requires information on the water vapour pressure and temperature and pressure of the system. This correlation (eq. 7.4) is one of the most used in the natural gas industry for calculating the water content of dry and sweet natural gases [10]:

$$y_w = 47484 \frac{P_w^{sat}}{P} + B \tag{7.4}$$

$$log(B) = \frac{-3083.87}{491.6 + t} + 6.69449 \tag{7.5}$$

where water content (y_w) and t are in *lbm/ MMscf* and temperature in °F In equation (7.5), the logarithm term is common logs (i.e., base 10). As can be seen, this correlation uses an ideal contribution and a deviation factor. The *Bukacek* correlation (Eqs. 7.4 and 7.5) is reported to

be accurate within ± 5% for temperatures between 288.15 and 511.15 K and for pressures from 0.1 to 69 MPa [10]. This accuracy is similar to experimental accuracy itself.

- *Sharma* [312] *Sharma* and *Campbell* [313] and *Campbell* [314] provided a relatively complicated method in order to calculate the equilibrium water content of sweet and sour gases in the L_W-V region. In this method, the water content is calculated through eq. 7.6:

$$y_w = k \left(\frac{f_w^{sat}}{f_{gas}} \right)^z \tag{7.6}$$

where *k, z* and *f* are respectively: a correction factor, the compressibility factor and the fugacity,. The compressibility factor z should be calculated using a suitable method. The correction factor k can be calculated from a provided figure or by the following equation:

$$k = \left(\left(\frac{P_w^{sat}}{P} \right) \left(\frac{f_w^{sat}/P_w^{sat}}{f_w/P} \right) \left(\frac{P}{P_w^{sat}} \right)^{0.0049} \right. \tag{7.7}$$

where f_w^{sat} and f_w are fugacity of water at the saturation conditions (T and P_w^{sat}) and the fugacity of water at pressure and temperature of the system (T and P). They provided a chart for calculating the fugacity of water. As mentioned before, this method is relatively complicated, however Campbell [314] mentioned that the consistency of the results from this method is high.

- *Behr* [315] proposed the following equation for pressure ranging from 1.379 to 20.679 MPa:

$$y_w = exp(A_0 + A_1(1/T)^2 + A_2(1/T)^3 + A_3(lnP) + A_4(lnP)^2 + A_5(lnP)^3 + A_6(lnP/T)^2 + A_7(lnP/T)^3) \tag{7.8}$$

where A_0 to A_7 are constants based on fitting the natural gas dew points versus the water content data of *Bukacek* [310].

- Later *Kazim* [316] proposed an analytical expression for calculating the water content of sweet natural gases:

$$y_w = A \times B^t \tag{7.9}$$

$$A = \sum_{i=1}^{4} a_i \left(\frac{p - 350}{600} \right)^{i-1} \tag{7.10}$$

$$B = \sum_{i=1}^{4} b_i \left(\frac{p - 350}{600} \right)^{i-1} \tag{7.11}$$

where p is the pressure in *psia* and a_is and b_is are constants reported in TABLE 7.1. These two correlations are similar as in which, they originate from regression methods to express the water content of natural gases as a function of temperature and pressure and require many constants, which may reduce their applications for calculating the water content of natural gases in comparison with the *Bukacek* [310] correlation.

Constants	Temperature Ranges	
	T<310.93	*310.93<T<355.37*
a_1	4.34322	10.38175
a_2	1.35912	-3.41588
a_3	-6.82391	-7.93877
a_4	3.95407	5.8495
b_1	1.03776	1.02674
b_2	-0.02865	-0.01235
b_3	0.04198	0.02323
b_4	-0.01945	-0.01155

TABLE 7.1 – CONSTANTS USED IN KAZIM EXPRESSION (EQS. 7.10 AND 7.11)

- For many years, several charts have been reported in order to calculate the equilibrium water content of gases. The most commonly used is the *McKetta – Wehe* [13] chart, which is used for sweet natural gases containing over 70% mole fraction of methane and small amounts of heavy hydrocarbons [313-314]. This chart was first published in 1948 [13] and was based on experimental data available at that time [314]. Gas Processors Association (*GPA*) and Gas Processors Supplier Association (*GPSA*) have reproduced this chart for many years. In this chart the water content of a sweet gas is plotted as a semi – logarithmic axis versus temperature at different pressures. Two correction factors have been provided in order to take into account the presence of heavy hydrocarbons in the gas phase and salts in the liquid water. In this chart, meta-stable $L_W - V$ equilibrium is assumed rather than $H - V$ equilibrium in the hydrate formation region, however the actual water content in the $H - V$ region is lower than the calculated water content by assuming $L_W - V$ equilibrium. Furthermore, reading the water content from this semi – logarithmic chart may be a little difficult, however if used with care, this chart can allow estimating the water content of sweet gases with less than 5% uncertainty [10].

- *Ning et al.* [317] proposed the following correlation based on the *McKetta – Wehe* [13] chart:

$$y_w = e^{a_0 + a_1 T + a_2 T^2} \tag{7.12}$$

For the above equation, complicated figure and table have been provided in order to calculate the pressure dependent coefficients a_0, a_1 and a_2 for pressures up to 100 MPa. It seems that this correlation is not a simple tool due to the complicated dependency of coefficients on pressure. Their correlation takes into account the effect of gas gravity by the following correction factor:

$$F_{hc} = 1.01532 + 0.011 \, (T-273.15) - 0.0182 \, SG_g - 0.0142 \, SG_g \, (T-273.15) \tag{7.13}$$

$$y_{heavy} = F_{hc} \, y_{light} \tag{7.14}$$

Where F and SG are correction factors due to presence of heavy hydrocarbons and gas gravity and subscripts hc, $heavy$ and $light$ relate to hydrocarbon, heavy and light components, respectively. However this correlation as quoted by Carroll [10] is not correct as negative correction factor are found for gas gravity below 2.

Pressure (MPa)	a_0	a_1	$a_2 \times 10^{-4}$
0.1	-30.0672	0.1634	-1.7452
0.2	-27.5786	0.1435	-1.4347
0.3	-27.8357	0.1425	-1.4216
0.4	-27.3193	0.1383	-1.3668
0.5	-26.2146	0.1309	-1.2643
0.6	-25.7488	0.1261	-1.1875
0.8	-27.2133	0.1334	-1.2884
1	-26.2406	0.1268	-1.1991
1.5	-26.129	0.1237	-1.1534
2	-24.5786	0.1133	-1.0108
3	-24.7653	0.1128	-1.0113
4	-24.7175	0.112	-1.0085
5	-26.8976	0.1232	-1.1618
6	-25.1163	0.1128	-1.0264
8	-26.0341	0.1172	-1.0912
10	-25.4407	0.1133	-1.0425
15	-22.6263	0.0973	-0.84136
20	-22.1364	0.0946	-0.81751
30	-20.4434	0.0851	-0.70353
40	-21.1259	0.0881	-0.7451
50	-20.2527	0.0834	-0.69094
60	-19.1174	0.0773	-0.61641
70	-20.5002	0.0845	-0.71151
100	-20.4974	0.0838	-0.70494

TABLE 7.2 – COEFFICIENTS USED IN NING ET AL. CORRELATION

7.1.1.2   Acid Gas in Equilibrium with Liquid Water

The above correlations / charts (except Sharma and Campbell method [312-314]) assume that the water content of dry and sweet natural gases is independent of the gas composition. However, when acid gases and heavy hydrocarbons and/or salts are present in the system, their accuracy is reduced and some corrections should be used in addition.

Both hydrogen sulphide and carbon dioxide contain more water at saturation than methane or sweet natural gas mixtures and the relative amounts vary considerably with temperature and pressure [314]. There exist some correlations for estimating water content in the presence of acid gases in the vapour phase. These correlations should be applied when the gas mixture contains more than 5% hydrogen sulphide and/ or carbon dioxide, especially at high pressures [314]. *Wiebe* and *Gaddy* [45] and *Selleck et al.* [49] reported water content of carbon dioxide and hydrogen sulphide at different temperatures and pressures, respectively. A figure for calculating the saturated water content of methane, carbon dioxide and a 95% carbon dioxide – 5% methane mixture versus pressure at 311.15 K has been reported by GPSA [13].

The *Robinson et al.* [318-320], *Maddox et al.* [321] and *Wichert – Wichert* [322] methods correct the water content of sweet and dry gases in the presence of acid gases. *Robinson et al.* [318-320] reported a series of charts to estimate the water content of sour natural gases. These charts were determined thanks to a model based on an equation of state. The authors used an equivalent mole fraction of H_2S for their charts, which is calculated by the following expression [319-320]:

$$z_{H2S}{}^{equi} = z_{H2S} + 0.75\ z_{CO2} \tag{7.15}$$

where z is the mole fraction in the natural gas, the subscripts *HC, CO$_2$* and *H$_2$S* refer to hydrocarbon, carbon dioxide and hydrogen sulphide, respectively and the superscript *equi* refers to equivalent H_2S. This method is applicable for $z_{H2S}{}^{equi} < 0.4$ (mole fraction), $283.15 < T < 450.15$ K and $2.07 < P < 69$ MPa. However, the use of these charts is a little difficult due to the interpolations needed to determine the final water content.

In *Maddox et al. correlation* [321], the water content of sour gases is calculated using the following expression:

$$y_w = y_{w,HC} \times z_{HC} + y_{w,CO2} \times z_{CO2} + y_{w,H2S} \times z_{H2S} \qquad (7.16)$$

In equation 7.16, the contribution to the sweet gas can be calculated using an appropriate correlation or chart. The acid gas contributions can be calculated by either the corresponding charts or by the corresponding equations. This correlation can be used for less than 40% acid gas components.

Wichert and *Wichert* [322] proposed a new chart based on temperature, pressure and equivalent H_2S content in order to calculate a correction factor (F_{sour}). They used definition of *Robinson et al.* [318-320] for the equivalent H_2S content. Using this correction factor, the water content of sour natural gases can be calculated by using the following expression:

$$y_{sour} = F_{sour}\, y_{sweet} \qquad (7.17)$$

In the above equation, the subscripts *sour* and *sweet* relate to the sour and sweet natural gases. The McKetta – Wehe chart is recommended to calculate y_{sweet}. This method is applicable for $z_{H2S}{}^{equi} < 0.55$ (mole fraction), $283.15 < T < 450.15$ K and $1.4 < P < 69$ MPa. This method is easier to use than the method of *Robinson et al.* [318-320], because no interpolation is necessary.

7.1.1.3   Gas in Equilibrium with Ice or Hydrate

Figure 7.1 shows a typical pressure –temperature diagram for water – hydrocarbon system. As it can be seen; the *I-V* equilibrium for dry and sweet natural gases with very low nitrogen content can be reached at relatively low-pressures. The maximum pressure at which the *I-V* equilibrium can be reached is around 2.7 MPa, which corresponds to hydrate formation for methane at 273.15 K. The *Poynting* correlation can be used for estimating the water content of dry and sweet natural gases with very low nitrogen content in equilibrium with ice. *Katz et al.* [323], *Sloan and Kobayashi* [324] also reported a chart in temperature and pressure ($254.04 < T < 273.15$ K and $0.1 < P < 2.757$ MPa) for calculating the water content of natural gases in equilibrium with ice.
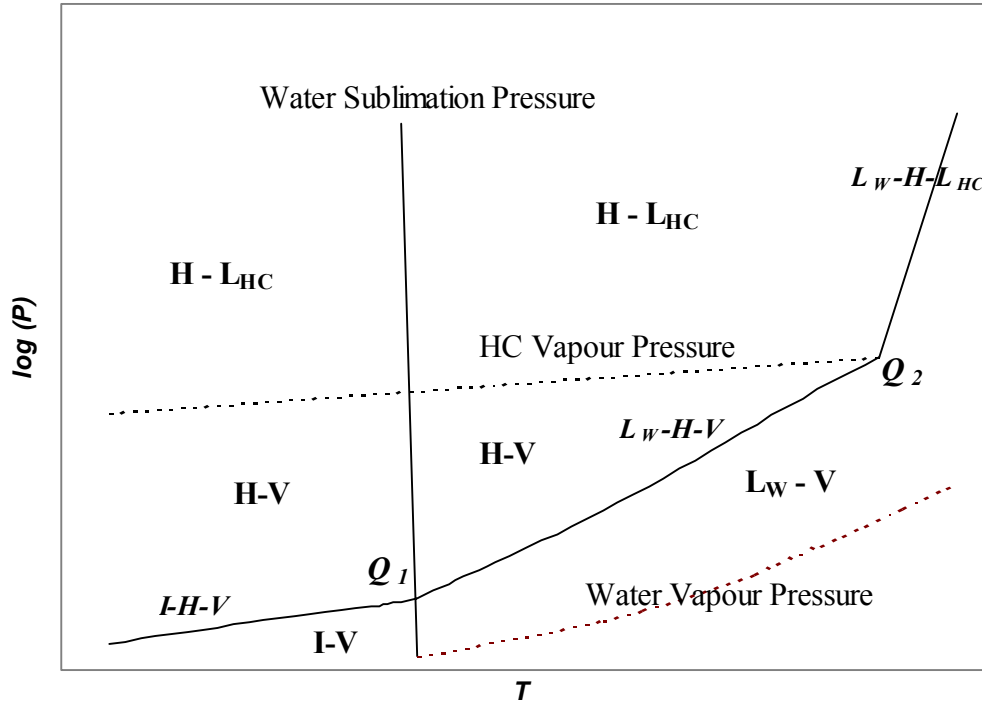
Figure 7.1: Typical pressure – temperature diagram for water – hydrocarbon systems

The water content of natural gases in equilibrium with gas hydrates is lower than the water content of natural gases in equilibrium with meta-stable liquid water and difficult to measure, as hydrate formation is a time consuming process and water content of gases in the hydrate region is a strong function of composition. On the other hand, limited experimental data have been reported in this region. Therefore, developing a relatively comprehensive correlation / chart for calculating water content of natural gases in equilibrium with gas hydrates is not easy. Few correlations for this region have been developed [321, 323]. Where experimental data is limited, utilization of a thermodynamic model can provide an estimate of water content in equilibrium with hydrates.

7.1.1.4   Comments

In addition, in many standards, the *Bukacek* [310] correlation and the *McKetta–Wehe* [13] chart are recommended to estimate the water content of sweet natural gases in equilibrium with liquid water. However, *Bukacek* [310] correlation and *McKetta–Wehe* [13] chart cannot describe real phase behavior in water – hydrocarbon systems at low temperatures, as they are based on experimental data at high temperatures. In other words, the *Bukacek* [310] correlation should be used at temperatures higher than 288.15 K [10] and the water contents obtained from the *McKetta–Wehe* [13] chart at temperatures below hydrate

formation conditions correspond to the meta-stable $L_W - V$ equilibrium rather than $H\text{-}V$ equilibrium.

7.1.2 Semi – Empirical Correlation

7.1.2.1 Approach for Sweet and Dry Gas

The vapour – liquid equilibrium (VLE) of a system is calculated, using equation 7.18:

$$f_i^V = f_i^L \qquad\qquad i = 1, N \tag{7.18}$$

where N is the number of components. The equality of fugacities can be calculated using the following relationship:

$$y_i \phi_i P = \gamma_i x_i P_i^{sat} exp \int_{P_i^{sat}}^{P} \frac{v_i^L dP}{RT} \tag{7.19}$$

This equation can be simplified using the following assumptions: in the 273.15–373.15 K temperature range and in the intermediate pressure range, liquid water is an incompressible fluid and thus a Poynting correction can be used to express the integral. At such conditions it can be assumed that the activity coefficient of water can be taken unity. Therefore, the mole fraction of water in the gas phase can be estimated, using equation 7.20:

$$y_w = \frac{(1 - x_g) P_w^{sat}}{\phi_w P} \exp(\frac{v_w^L (P - P_w^{sat})}{RT}) \tag{7.20}$$

As mentioned earlier, gas solubility (x_g) is very small compared to unity for hydrocarbons and some gases like nitrogen and also solubility of hydrocarbons in water are, in general, considerably less than water in hydrocarbons ($1\text{-}x_g \approx 1$). Therefore, the water content (y_w) is determined primarily by the fugacity coefficient of water (ϕ_w) in the gas phase. The fugacity coefficient of water (ϕ_w) may be calculated as below:

$$\phi_w = exp(BP + CP^2) \tag{7.21}$$

where B and C are temperature dependent. The following relations for B and C seem to be satisfactorily:

$$B = a + \frac{b}{T} \tag{7.22}$$

$$C = c + \frac{d}{T} \tag{7.23}$$

where a, b, c and d are constants. To estimate vapour pressure and molar volume of water in equation 7.20, the relations reported by *Daubert* and *Danner* [325] and *McCain* [311] are used, respectively:

$$P_w^{sat} = 10^{-6} exp(73.649 - 7258.2/T - 7.3037\ ln\ (T) + 4.1653 \times 10^{-6} T^2) \tag{7.24}$$

$$v_w^L = 18.015\ /\ d_w \tag{7.25}$$

$$d_w = 62.368\ /B_w \tag{7.26}$$

$$B_w = (1 + \Delta V_{wP})\ (1 + \Delta V_{wT}) \tag{7.27}$$

$$\Delta V_{wP} = -(3.58922 \times 10^{-7} + 1.95301 \times 10^{-9} t)p - (2.25341 \times 10^{-10} + 1.72834 \times 10^{-13} t)p^2 \tag{7.28}$$

$$\Delta V_{wT} = -1.0001 \times 10^{-2} + 1.33391 \times 10^{-4} t + 5.50654 \times 10^{-7} t^2 \tag{7.29}$$

where, T, t, p and P_w^{sat} are in K, ^oF, $psia$ and MPa, respectively and d_w, B_w, ΔV_{wP} and ΔV_{wT} are water density, formation volume factor, volume changes due to pressure and temperature, respectively. Equations 28 – 29 are valid at $t < 260\ ^oF$, and $p < 5000$ psia even over a wide range of salt concentrations. The saturated water content of a gas depends on pressure, temperature and composition. The effect of composition increases with pressure and is particularly important if the vapour contains carbon dioxide and/or hydrogen sulphide.

In this work, the water content data for methane, which is the main component of dry and sweet natural gases, are used for developing this approach. Data from Table F.1 are used as input for a multi-dimension regression procedure, utilizing least square optimization routines in order to minimize the average absolute deviation (*AAD*) between the experimental and calculated data. The temperature range is from 273.15 to 423.15 K, and the pressures are up to 22 MPa, respectively.

State\Parameter	Liquid	Ice
a	-0.01559551	-0.00232193
b	-1.61575838	-1.6296
c	0.00412617	0.014224
d	-1.41158956	-1.66508

TABLE 7.3 – PARAMETERS *a, b, c* AND *d* IN EQUATIONS 7.22 AND 7.23 IN FUNCTION FOR TWO WATER STATES

Agreement between the experimental and calculated data is satisfactory, with typical *AD* values between 1 % (9 % for the highest). The *AAD%* among all the experimental and calculated data is 2%. The values of the parameters of equations 7.22 and 7.23 are reported in TABLE 7.3.

As mentioned earlier, the *I-V* equilibrium for dry and sweet natural gases with very low nitrogen content can be reached at relatively low-pressures. The above approach can be used for estimating the water content of dry and sweet natural gases with very low nitrogen content in equilibrium with ice, however reliable water content data in this region are necessary in order to calculate the values of parameters *a, b, c* and *d*. In this work, the data in TABLE 7.4 are used for the *I – V* region to obtain these constants. These constants are reported in TABLE 7.3.

Reference	T / K	P / MPa	Water Content Experimental data	Water Content Estimated values	$AD / \%$
Althaus [15]	253.15	0.5	0.000213	0.000209	1.78
	258.15	0.5	0.000307	0.000335	9.13
	263.15	0.5	0.000524	0.000526	0.43
	268.15	0.5	0.000829	0.000812	2.09
	273.15	0.5	0.001235	0.001235	0.00
Kosyakov *et al.* [20]	263.15	1.013	0.000275	0.000269	2.30
	253.15	1.013	0.000107	0.000107	0.00

TABLE 7.4 – EXPERIMENTAL DATA USED FOR THE *I – V* REGION

The approach for *I - V* equilibrium can be solved using the following relations for molar volume of ice and ice sublimation pressure in equilibrium with ice [293]:

$$v_w^I = (19.655 + 0.0022364 \times (T\text{-}273.15))/10^6 \tag{7.30}$$

$$\log(P_w^{sub}) = -1033/T + 51.06 \times \log(T) - 0.09771 \times T + 7.036 \times 10^{-5} \times T^2 - 98.51 \qquad (7.31)$$

where superscript *I* and *sub* refer to ice and sublimation, respectively. In the above equations, v_w^I and P_w^{sub} are in *m³/kgmol* and *mmHg*, respectively. The logarithm term is common one (i.e., base 10).

High quantities of nitrogen in natural gases can reduce the water content and shift the hydrate phase boundaries to higher pressures. The presence of heavy hydrocarbons in natural gases increases the water content.

7.1.2.2 Gravity Correction Factor

To take into account the effect of gas composition, a correction factor has been developed, this correction allow to estimate the water content of hydrocarbon (e.g.: ethane, propane, n-butane) water binary system, as well as the water of hydrocarbon mixture up to a gas gravity around 2. This corrective factor is equal to 1 for methane, thus, the following equation is proposed:

$$C_\gamma = 1 + a_\gamma(\gamma - \gamma_M) + b_\gamma(\gamma - \gamma_M)^2 \frac{T}{T_0} + c_\gamma(\gamma - \gamma_M)^3 \left(\frac{T}{T_0}\right)^2 \qquad (7.32)$$

$$y_{corrected} = C_\gamma y_w \qquad (7.33)$$

γ is the gas gravity factor , γ_M is the methane gravity factor and T_0 is the reference temperature, which is equal to 273.15 K.

Constant	Value
a_γ	-0.013359
b_γ	-0.091676
c_γ	0.04253

TABLE 7.5 – VALUES OF CONSTANTS IN EQUATION 7.32

7.1.2.3 Acid and Sour Gas Correction Factor

Sour natural gases can contain more water than sweet natural gases. The presence of acid gases can be taken into account, using an appropriate correlation such as: *Maddox et al.* [321] or *Wichert and Wichert* [322] in addition to the new approach. To provide a quick calculation of the water content of acid gases, a correction factor based on experimental data has been developed:

$$y_{sour} = C_{acid}\, y_{sweet} \qquad (7.34)$$

with

$$C_{acid} = 1 - Z_{H_2S}^{equi}\left[a_{acid}\frac{T}{T_0} + b_{acid}\left(\frac{T}{T_0}\right)^2 + c_{acid}\left(\frac{P}{P_0}\right) + d_{acid}\left(\frac{P}{P_0}\right)^2 \right] \qquad (7.35)$$

and

$$z_{H2S}{}^{equi} = z_{H2S} + 0.75\, z_{CO2} \qquad (7.36)$$

Constant	Value
a_{acid}	0.931524
b_{acid}	-0.774631
c_{acid}	0.070257
d_{acid}	-0.000685

TABLE 7.6 – CONSTANTS *a, b* AND *c* IN EQUATION 7.35

7.1.2.4 Salt Correction Factor

Dissolved solids (salts) in the water can change water properties such as reducing the water vapour pressure and changing water density and therefore reducing the water content of natural gases. To take into account the presence of salts, the extrapolation of the salinity correction factor in *McKetta-Wehe* [13] chart to high salt concentrations is believed to underpredict the water content of a gas in equilibrium with brine. The graphical correlation of Katz *et al.* [323] for the salinity correction factor is preferred. The graphical correlation, developed from water vapour pressure depression due to the presence of salt, can be represented bt equation 7.33, [301]:

$$F_{salt} = 1 - 4.920 \times 10^{-3}\, w_{salt} - 1.7672 \times 10^{-4}\, w_{salt}{}^2 \qquad (7.33)$$

where w is the weight percent of salt in brine and subscript *salt* refers to salt.

7.1.3   Comments and discussions

As mentioned earlier, the agreements between the experimental and calculated data are satisfactory, with typical *AD* values between 0 % and 14 %. The *AAD* among all the experimental and calculated data is 2.2%. In the *I – V* region, the agreements between the experimental and calculated data are satisfactory and the *AAD* among all the experimental and calculated data is also 2.2 %.

The data generated on the water content in methane have been used as independent data to compare the predicted values and the experimental results. The agreements between the experimental and calculated data are satisfactory, and are typically of the same order as the results obtained in Table 6.1 using the PREoS.

Temperature (K)	Pressure (MPa)	Water Content, y_{exp} ($\times 10^3$)	Water Content, Calculated, y_{cal} ($\times 10^3$)	$(y_{exp}\text{-}y_{cal})/\Delta y_{exp}$ %
283.08	1.006	1.240	1.251	0.9
283.08	6.030	0.292	0.249	15
288.11	1.044	1.780	1.680	5.6
288.11	6.023	0.382	0.345	9.6
288.11	10.030	0.273	0.245	10
293.11	0.992	2.360	2.422	2.6
293.11	5.770	0.483	0.488	1.0
293.11	9.520	0.338	0.342	1.3
293.11	17.680	0.267	0.271	1.5
298.11	1.010	3.300	3.224	2.3
298.11	6.390	0.631	0.608	3.6
298.11	10.070	0.471	0.444	5.7
298.11	17.520	0.355	0.357	0.6
303.11	1.100	4.440	3.977	10
303.11	6.060	0.889	0.846	4.9
303.11	9.840	0.625	0.598	4.3
303.11	17.500	0.456	0.466	2.2
308.11	1.100	5.820	5.269	9.5
308.11	5.990	1.114	1.127	1.2
308.11	9.840	0.807	0.785	2.7
308.11	17.490	0.577	0.602	4.3
313.12	1.100	7.460	6.915	7.3
313.12	6.056	1.516	1.461	3.6
313.12	9.980	1.045	1.012	3.1
313.12	17.470	0.715	0.770	7.7
318.12	1.003	9.894	9.823	0.7
318.12	6.0170	1.985	1.901	4.2
318.12	10.010	1.326	1.301	1.9
318.12	17.500	0.890	0.975	9.6

TABLE 7.7 – MEASURED AND CALCULATED WATER CONTENT (IN MOLE FRACTION) IN THE VAPOUR PHASE OF THE METHANE/WATER SYSTEM

In Table F.2 the capabilities of this approach are tested with data from literature. As it can be observed, the predictions of this approach are in good agreement with the reported results even in the presence of heavy hydrocarbons or acid gases in natural gases. A software has been written in Delphi code to calculate the water content using this new correlation.

7.2 Gas Solubilities and Henry's Law Correlations

The Henry's constant can be calculated from various literature correlations. Some were given in the TABLE 3.5. We have decided to use the forms displayed in eq 3.74 and in eq 7.34 (from §3.1.3) to develop our Henry's correlation.

Form 1 $\qquad H_{i,w}(T) = 10^{A+B/T+C \times \log_{10}(T)+D \times T} \times 101325$ $\qquad$ (3.74)

Form 2 $\qquad H_{i,w}(T) = \exp(A + B\,T + C/T + D\,\ln(T)) \times 10^3$ $\qquad$ (7.34)

Where T is the temperature in Kelvin and H is the Henry's constant in Pa

All A, B, C, D coefficients are been adjusted with the previously generated data; the values of the coefficients are listed in TABLE 7.8.

Solute	Form	A	B	C	D	Tmin	Tmax
Methane	1	147.788	-5768.3	-52.2952	0.018616	273.15	373.15
Ethane	1	146.9014	-5768.3	-51.85925	0.01741	273.15	343.15
Propane	2	552.648	0.07845	-21334	-85.8974	273.15	368.15
n-Butane	1	146.637	-5768.3	-52.4205	0.024047	273.15	363.15
Isobutane	1	146.66	-5768.3	-52.377	0.02327	273.15	363.15
Nitrogen	1	78.852	-3745	-24.8315	0.000291	273.15	363.15
Carbon Dioxide	1	21.6215	-1499.8	-5.64947	0.0002062	273.15	373.15
Hydrogen Sulphide	1	69.445	-3796.5	-21.6253	-0.00001576	273.15	363.15

TABLE 7.8 – NEW COEFFICIENT VALUES FOR (3.72) AND NEW RANGE OF UTILIZATION

For the aqueous phase, a Henry's law approach is used to estimate the gaseous components solubility in water, as the gaseous components are at infinite dilution the asymmetric convention ($\gamma_g \to 1$ when $x_g \to 0$) is used to express the Henry's law for the gas (eq. 5.55 from §5.3)).

$$f_g^L(P,T) = H_w^L(T) \times x_g(T) \times \exp((\frac{v_g^\infty(T)}{RT})(P - P_w^{sat}))$$ (5.62)

To futher simplify the previous equation, it is chosen to express the gas solubility as a ratio of a function only depending of the pressure and the Henry value.

$$x_g(T) = \frac{\phi_g(P)}{H_w^L(T)}$$ (7.35)

where $\phi_g(P)$ is given by :

$$\phi_g(P) = A\,P + B\,P^2$$ (7.36)

Solute	A	B (×10⁸)	AAD %
Methane	0.9280	-1.7677	3.4
Ethane	0.9901	-7.2333	3.5
Propane	0.9942	-11.1810	4.6
n-Butane	0.9298	-12.6725	5.1
Isobutane	1.0441	-33.7563	3.1
Nitrogen	0.9854	-1.1073	1.0
Carbon Dioxide	0.9301	-3.1061	5.7
Hydrogen Sulphide	0.9523	-5.7155	6.5

TABLE 7.9 – COEFFICIENT VALUES FOR eq. 7.36

The *AAD* among all the experimental (generated in this work) and calculated data with this correlation are typically between 1 % and for the highest 6.5 %. Unfortunately, this approach is not extended easily to multicomponent systems.

Conclusion

8   Conclusion and Perspectives

8.1 En français

Dans les gisements, en cours de production ou dans les conduites de transport, les gaz naturels se trouvent au contact d'une phase aqueuse. En effet, l'effluent pétrolier qui sort d'un puits de production contient toujours de l'eau et des molécules hydrocarbonées légères (méthane, éthane, propane, n-butane). Sous certaines conditions de pression et de température il est possible de former des hydrates de gaz. Les conditions de formation des hydrates peuvent être réunies dans certaines conduites pétrolières et poser alors un problème de production.

Ce projet présente des mesures de teneur en eau dans différentes phases vapeur d'hydrocarbures, méthane et éthane, et dans un mélange d'hydrocarbures gazeux (méthane 94%, éthane 4%, n-butane 2%) dans des conditions proches de la formation d'hydrates (de -15 à 40 °C et jusqu'à 34 MPa). Des mesures équivalentes ont été aussi effectuées en présence d'inhibiteur thermodynamique. Des mesures de solubilités de différents gaz, méthane, éthane, propane, azote, dioxyde de carbone, sulfure d'hydrogène ont été réalisées à la suite.

Ce rapport expose la technique expérimentale mise en œuvre pour déterminer ces propriétés, ainsi que les difficultés rencontrées lors de l'étude, notamment due à l'analyse des traces d'eau. Il est connu que la détermination des traces d'eau dans les gaz est l'un des problèmes les plus difficiles de l'analyse des traces. La mise en place d'une méthode spécifique d'étalonnage de l'eau est décrite. Comme les méthodes classiques d'étalonnage ne permettent pas de travailler suffisamment précisément avec des quantités d'eau aussi faibles que celles qui doivent être analysées dans nos échantillons, il a fallu développer une technique nouvelle spécialement adaptée au problème. Cette dernière fait appel à une technique conçue au laboratoire pour la détermination de coefficients d'activité et constantes de Henry à dilution infinie : le "diluteur exponentiel".

Sur le plan de la modélisation tous les systèmes ont été traités à l'aide du logiciel qui a été développé au cours de cette thèse. Ce logiciel permet le choix de différentes équations d'état, de différentes fonctions « alpha » et de différentes approches pour calculer l'activité de l'eau en phase aqueuse. Les résultats obtenus ont été systématiquement comparés à des données de la littérature afin de valider les techniques utilisées ainsi que le modèle.

Une collaboration a été entreprise avec l'université Heriot-Watt d'Edinburgh. Cette collaboration a porté à la fois sur le travail expérimental et sur le travail de modélisation des données générées.

Plusieurs articles ont été rédigés au cours de cette thèse sur ce sujet en collaboration avec des collègues du laboratoire et l'Université d'Heriot-Watt, ainsi que sur d'autres sujets, par exemple le domaine de la réfrigération.

Une important perspective pour cette thèse serait d'étendre l'étude aux systèmes contenant du(des) sel(s) ainsi que d'examiner l'influence d'autres inhibiteurs que le méthanol ou l'éthylène glycol en particulier l'influence de l'éthanol et du triéthylène glycol utilisé aussi comme agent de déshydratation.

8.2   In English

Inside wells, natural gases normally coexist with water. The gases are in equilibrium with the sub-adjacent aquifer. Many problems are associated with the presence of water during the production, transport and processing of natural gases: water drive, water coning, which leads to decrease of the reservoir pressure, the crystallization of salt, the formation condensate phase, ice and / or gas hydrate. Accurate information on phase behavior of natural gas components and water is crucial to design and optimize operating conditions of natural gas facilities and to avoid condensate, ice and gas hydrates formation during production, transportation and processing of natural gases. On the other hand, hydrocarbon solubility in water is an important issue from an environmental aspect, due to new legislations and restrictions on the hydrocarbon content in water disposal.

Experimental data for water content of methane, ethane, and a hydrocarbon gas mixture, mix 1, (94% methane + 4% ethane + 2% n-butane) were generated in vapour liquid

conditions and vapour hydrate conditions. Similar measurements were done in presence of a thermodynamic inhibitor. Solubility measurements of various gases methane, ethane, propane, nitrogen, carbon dioxide, and hydrogen sulphide were also performed.

During the investigation, as the water content of a natural gas is very low, and thus such accurate measurements require very specialized techniques, problems have been encountered, which were related to the presence of water in the gas system at extremely low concentration. It is known that the determination of traces of water in gases is one of the most difficult problems of trace analysis. Moreover water is highly polar, therefore it adsorbs to most surfaces, normally considered to be dry and usually coated with a thin film of absorbed moisture. The report presents the different tests done to improve the quality of this research work as well as a description of the experimental apparatus and the methods that will be used to perform the desired measurements. In this work a static analytical apparatus is combined with an exponential dilutor to obtain the properties. The main difficulty is the detector calibration with water, thus different tests have been done to achieve an accurate calibration for water traces.

An in house software was developed in order to fit and model the generated data. This software allows the choice of different equations of state, alpha function, activity model…. Generated results were systematically compared with existing data to validate the experimental technique and model used in this work.

A collaboration with Heriot-Watt University has been started. Experimental and modelling works have been conducted together. As a result of the work carried out at Heriot-Watt journal publications are anticipated and it is hoped that this collaboration will be strengthening the existing contacts and providing a platform for future collaborations.

Different perspectives can be expected following the results obtained in this dissertation. One will be to generate experimental data on the distribution of other thermodynamic inhibitors in the water such as ethanol and triethylen glycol and another to generate data in presence of salt(s).

References

9 References

1. B. Tissot, Quels avenirs pour les combustibles fossiles ? Les avancées scientifiques et technologiques permettront-elles la poursuite d'un développement soutenable avec les énergies carbonées, *Earth and Planetary Sciences* 333 (2001) 787-796.

2. A Rojey, B Durand, C. Jaffrey, S. Jullian and M Valais, Le gaz naturel ; Production Traitement Transport, Publications de l'Institut Français du Pétrole, Edition Technip, 1994

3. BP Statistical Review of World Energy, June 2000.

4. BP Statistical Review of World Energy, June 2002.

5. E. D. Sloan, Clathrate hydrates of natural gases, Chemical Industries, (1990) vol 39.

6. F. Franks, Water, a Matrix of Life, 2nd edition (Royal Society of Chemistry, Cambridge, 2000).

7. C. A. Angell, Supercooled water, *Ann. Rev. Phys. Chem.* 34 (1983) 593-630.

8. P. G. Debenedetti, *Metastable Liquids. Concepts and Principles* (Princeton University Press, Princeton, 1996).

9. D. Eisenberg and W. Kauzmann, *The Structure and Properties of Water* (Clarendon, Oxford, 1996).

10. J. Carroll, Natural Gas Hydrates, A Guide for Engineers, Gulf Professional Publishing, 2003.

11. J. J. McKetta, Jr and D. L. Katz, Methane-n-butane-water system in the two and three phase regions, *Ind. Eng. Chem.* 40 (1948) 853-863.

12. P. Pendergraft, M. Marston, M. Gonzales, V. Rice and J. Erbar, Literature survey for synthetic gas component thermodynamic properties, *GPA (Tulsa Ok), RR-36* , October 1979.

13. GPA engineering Data Dook, *Published by the Gas Processor Association, 11ᵗʰ edition*, Volume 2, GPA, 1998.

14. A. Dhima, O. Noll, A. Valtz, D. Richon, 18ᵗʰ European Seminar on Applied Thermodynamics, Kutna Hora, Czech Republic (8-11ᵗʰ June 2000).

15. K. Althaus, *Foetschritts Berichte VDI*, Reihe 3, 350.(in German) GERG Technical Monograph TM14, L.R.Oellrich and K. Althaus: Relationship between water content and water dew point keeping in consideration the gas composition in the field of natural gas, Verein Deutscher Ingenieure (2001) Reihe 3- Nr. 679 (in English).

16. V. V. Ugrozov, *Zh. Fiz. Khim.* 70 (1996) 1328-1329 (in Russian).

17. C. Yokoyama, S. Wakana, G. I. Kaminishi and S. Takahashi, Vapor Liquid equilibria in the methane-diethylene glycol-water system at 298.15 and 323.15 K, *J. Chem. Eng. Data* 33 (1988) 274-276.

18. N. L Yarym-Agaev, R. P. Sinyavskaya, I. I. Koliushko and L.Ya. Levinton, *Zh. Prikl. Khim.* 58 (1985) 165-168. (In Russian)

19. P. C. Gillepsie and G. M. Wilson, Vapor Liquid and Liquid Liquid equilibria: Methane-Water; Water – Carbon - Dioxide; Water – Hydrogen Sulphide;Water – nPentane; Water – Methane - nPentane; *GPA (Tulsa Ok), RR-48* , April 1982

20. N. E. Kosyakov, B. I. Ivchenko and P. P. Krishtopa, Solubility of Moisture in Compressed Argon, Methane and Helium at Low Temperatures, *Zh. Prikl. Khim.* April, 52(4) (1979) 922-923.

21. K. Aoyagi, K. Y. Song, R. Kobayashi, E. D. Sloan and P. B. Dharmawardhana, The Water Content and Correlation of the Water Content of Methane in Equilibrium with Hydrates, (I); and the Water Content of a High Carbon Dioxide Simulated Prudhoe Bay Gas in Equilibrium with Hydrates, (II), GPA, Tulsa, Research Report 45 (1980).

22. N. E. Kosyakov, B. I. Ivchenko and P. P. Krishtopa, *Vopr Khim. Tekhnol*. 47 (1982) 33-36.

23. M. Rigby, and J. M. Prausnitz, Solubility of water in compressed nitrogen, argon and methane, *J. Phys. Chem.* 72 (1968) 330-334.

24. O. L. Culberson and J. J. Mc Ketta, Jr, Phase Equilibria in Hydrocarbon-Water Systems IV-, Vapour equilibrium constant in the methane-water and ethane-water systems, *AIME* 192 (1951) 297-300.

25. R. H. Olds, B. H. Sage and W. N. Lacey, Phase Equilibria in Hydrocarbon Systems, *Ind. Eng. Chem.* 34 (10) (1942) 1223-1227.

26. K. Y. Song, R. Kobayashi, The water content of ethane, propane and their mixtures in equilibrium with liquid water or hydrates, *Fluid Phase Equilib.* 95 (1994), 281 - 298.

27. C. R. Coan and A. D. King, Solubility of compressed carbon dioxide, nitrous oxide and ethane. Evidence of the hydratation of carbon dioxide and nitrous oxide in the gas phase, *J. Am. Chem. Soc*. 93 (1971) 1857-1862.

28. R. G. Anthony and J. J. McKetta Jr, Phase equilibrium in the ethylene-water system, *J. Chem. Eng. Data* 12 (1967), 17-20.

29. R. G. Anthony, J. J. McKetta Jr, Phase equilibrium in the ethylene–ethane–water system, *J. Chem. Eng. Data* 12 (1967), 21-28.

30. H. H. Reamer, R. H. Olds, B. H. Sage, W. N. Lacey, Phase Equilibria in Hydrocarbon Systems. Composition of a dew point gas in ethane-water system, *Ind. Eng. Chem*. 35 (1943) 790-793.

31. Klausutis, Thesis (1968) *data from DDB.*

32. R. Kobayashi and D. L. Katz, Vapor liquid equilibria for binary hydrocarbon-water systems, *Ind. Eng. Chem*. 45 (1953) 440-446.

33. A. H. Wehe and J. J. McKetta Jr, n-Butane–1-butene–water system in the three-phase region, *J. Chem. Eng. Data* 6 (1961) 167-172.

34. H. H. Reamer, B. H. Sage and W. N. Lacey, Phase Equilibria in Hydrocarbon Systems. N-Butane-water system in the two-phase region, *Ind. Eng. Chem*., 44 (1952) 609-614.

35. W.B. Brooks, G.B. Gibbs and J.J. McKetta, Jr., Mutual solubilities of light hydrocarbon-water systems, *Petrol. Refiner*. 30 (1951) 118-120.

36. H. H. Reamer, R. H. Olds, B. H. Sage and W. N. Lacey, Phase equilibria in hydrocarbon systems, *Ind. Eng. Chem*. 36 (1944) 381-383.

37. R. Dohrn, A. P. Buenz, F. Devlieghere and D. Thelen, Experimental measurements of phase equilibria for ternary and quaternary systems of glucose, water, carbon dioxide and ethanol with a novel apparatus, *Fluid Phase Equilib.* 83 (1993) 149-158.

38. R. D'Souza, J. R. Patrick and A. S. Teja, High pressure phase equilibria in the carbon dioxide – n-Hexadecane and carbon dioxide-water systems, *Can. J. Chem. Eng.* 66 (1988) 319-323.

39. J. A. Briones, J. C. Mullins, M. C. Thies and B.-U Kim, Ternary phase equilibria for acetic acid-water mixtures with supercritical carbon dioxide, *Fluid Phase Equilib.* 36 (1987) 235-246.

40. T. Nakayama, H. Sagara, K. Arai, S. Saito, High pressure liquid---liquid equilibria for the system of water, ethanol and 1,1-difluoroethane at 323.2 K, *Fluid Phase Equilib.* 38 (1987) 109-127.

41. K. Y. Song and R. Kobayashi, The Water Content of CO_2 – rich Fluids in Equilibrium with Liquid Water and/ or Hydrates, GPA, Tulsa, Research Report 99 (1986).

42. G. Mueller, E. Bender and G. Maurer, Das Dampf-Flüssigkeitsgleichgewicht des ternären Systems Ammonik-Kolhendioxid Wasser bei hohen Wassergehalten im bereich zwischen 373 und 473 K, *Ber. Bunsenges. Phys. Chem*. 92 (1988) 148-160.

43. S. Takenouchi and G. C. Kennedy, The binary system H_2O-CO_2 at high temperatures and pressures, *Am. J. Sci*. 262 (1964) 1055-1074.

44. I. P. Sidorov, Y. S. Kazarnovsky and A. M. Goldman, *Tr.Gosudarst.Nauch.-Issled.I Proekt.I nst. Azot. Prom.* 1: (1953) 48 (in Russian).

45. R. Wiebe and V. L. Gaddy, Vapor phase composition of the carbon dioxide-water mixtures at various temperatures and at pressures to 700 atm, *J. Am. Chem. Soc.* 63 (1941) 475-477.

46. A. Yu. Namiot and M. M. Bondareva, Rastvorimost' gazov v vode, Moscow: Gostekhizdat, 1959 (Quoted in ref. 19). (In Russian).

47. V. Y. Maslennikova, N. A. Vdovina and D. S. Tsiklis, *Zh. Fiz. Khim.* 45 (1971) 1354 (in Russian).

48. M. P. Burgess and R. P. Germann, Physical properties of hydrogen sulfide water mixtures, *AIChE J.* 15 (1969) 272-275

49. F. T. Selleck, L. T. Carmichael and B.H. Sage, Phase behaviour in the hydrogen sulphide water system, *Ind. Eng. Chem.* 44 (1952) 2219-2226.

50. J. Lukacs and D.B. Robinson, Water content of sour hydrocarbons system, *SPE* December (1963) 293 -297.

51. S. Huang, A.-D. Leu, H.-J. Ng and D. B. Robinson, The two phase behavior of two mixture of methane, carbon dioxide, hydrogen sulphide and water, *Fluid Phase Equilib.* 19 (1985) 21-32.

52. K. Y. Song and R. Kobayashi, Water content values of CO2-5.31 Mol Percent Methane Mixture, GPA Research Report 120, Tulsa, (1989).

53. H.-J. Ng, C.-J. Chen and H. Schroeder, Water Content of Natural Gas Systems Containing Acid Gas; GPA Research Report 174, Tulsa, January (2001).

54. O. L. Culberson and J. J. Mc Ketta, Jr, Phase Equilibria in Hydrocarbon-Water Systems III-, The solubility of methane in water at 10000 psia, *AIME* 192 (1951) 223-226.

55. R. Bunsen, Ueberdas gezsetz der Gasabsorption, *Annalen der Chemie und Pharmacie* 93 (1855) 1-50.

56. L. W. Winkler, Die Löslichkeit der Gase in Wasser, *Berliner berichte* 34 (1901) 1408-1422.

57. W. F. Claussen and M. F. Polglase, Solubilities and structures in aqueous aliphatic hydrocarbon solutions, *J. Am. Chem. Soc.* 74 (1952) 4817-4849.

58. T. J. Morisson and F. Billett, The salting out of non electolyte. Part 2. The effect of variation in non electrolyte, *J. Chem. Soc.* (1952) 3819-3822.

59. D. B. Wetlaufer, S. K. Malik, L. Stoller and R. L. Collin, Non polar group participation in the denaturation of proteins by urea and guanadium salts. Model compound studies, *J. Am. Chem. Soc.* 86 (1964) 508-514.

60. W. Y. Wen and J. H Hung, Thermodynamics of hydrocarbon gases in aqueous tetraalkyammonium salt solutions, *J. Phys. Chem.* 74 (1970) 170-180.

61. A. Ben-Naim, J. Wilf and M. Yaacobi, Hydrophobic interaction in light and heavy water, *J. Phys. Chem.* 77 (1973) 95-102.

62. A. Ben-Naim and M. Yaacobi, Effects of solutes on the strength of hydrophobic interaction and its temperature dependence, *J. Phys. Chem.* 78 (1974) 170-175.

63. S. Yamamoto and J. B. Alcauskas, Solubility of methane in distilled water and seawater, *J. Chem. Eng. Data* 21 (1976) 78-80.

64. J. A. Muccitelli and W. Y. Wen, Solubility of methane in aqueous solution of triethylenediamine, *J. Sol. Chem.* 9 (1980) 141-161.

65. T. R. Rettich, Y. P. Handa, R. Battino and E. Wilhelm, Solubility of gases in liquids. 13. High precision determination of Henry's constant for methane and ethane in liquid water at 275 to 328 K, *J. Phys. Chem.* 85 (1981) 3230-3237.

66. K. Lekvam and P. R. Bishnoi, Dissolution of methane in water at low temperatures and intermediate pressures, *Fluid Phase Equilib.* 131 (1997) 297-309.

67. P.K. Frohlich, E.J. Tauch, J.J. Hogan and A.A. Peer, Solubilities of gas in liquids at high pressure, *Ind. Eng. Chem.* 23 (1931) 548-550.

68. A. Michels, J. Gerver and A. Bijl, The influence of pressure on the solubility of gases, *Physica III*, (1936) 3819-3822.

69. O. L. Culberson, A. B. Horn and J. J. Mc Ketta, Jr, Phase Equilibria in Hydrocarbon-Water Systems: the solubility of Ethane in Water at Pressures up to 1200 Pounds per Square Inch, *AIME* 189 (1950) 1-6.

70. J. E. Davis and J. J. Mc Ketta, Jr, Solubility of methane in water, *Petrol. Refiner.* 39 (1960) 205-206.

71. J. R. Duffy, N. O. Smith and B. Nagy, Solubility of natural gases in aqueous salt solutions —1. Liquidus surfaces in the system CH_4 - H_2O – $NaCl_2$ – $CaCl_2$ at room temperature and below 1000 psia, *Geochim. Cosmochim. Acta* 24 (1961) 23-31.

72. T. D. O' Sullivan and N. O. Smith, The solubility and partial molar volume of nitrogen and methane in water and aqueous sodium chloride, *J. Phys. Chem.* 74 (1970) 1460-1466.

73. R. G. Sultanov, V. G. Skripka and A. Y. Namiot. Rastvormost metana v vode pri novysjennykh temperaturakh I davlenijakh, *Gaz. Prom.* 16 (1971) 6-7.

74. R. Amirijafari and J. Campbell, Solubility of gaseous hydrocarbure mixtures in water, *Soc. Pet. Eng. J.* February (1972) 21-27.

75. M. Sanchez and F. De Meer, Equilibrio liquido-vapor del sistema metano-agua para altas presiones y temperaturas comprendidas entre 150 y 300°C, *An. Quim.* 74 (1978) 1325-1328.

76. L. C. Price, Aqueous Solubility of Methane at elevated Pressures and Temperatures, *Am. Assoc. Pet. Geo*. Bull. 63 (1979) 1527-1533.

77. R. K. Stoessel and P. A. Byrne, Salting-out of methane in single-salt solutions at 25°C and below 800 psia, *Geochim. Cosmochim. Acta* 46 (1982) 1327-1332.

78. I. M. Abdulgatov, A. R. Bazaev and A. E. Ramazanova, Volumetric properties and virial coefficients of (water+methane), *J. Chem. Therm*. 25 (1993) 249-259.

79. S. D. Cramer, Solubility of methane in brines from 0 to 300 C, *Ind. Eng. Chem. Pr. Des. Dev*. 23 (1984) 533-538.

80. C. Yokoyama, S. Wakana, G. I. Kaminishi, and S. Takahashi, Vapor-Liquid Equilibria in the Methane-Diethylene Glycol-Water System at 298.15 and 323.15 K, *J. Chem. Eng. Data* 33 (1988) 274 -276.

81. G. J. Toplak, Solubilities of hydrocarbon gas mixtures in distilled water near hydrate forming conditions, MS thesis, University of Pittsburgh, Pittsburgh, PA.

82. Y. Wang, B. Han, H. Yan and R. Liu, Solubility of CH4 in the mixed solvent t-butyl alcohol and water, *Thermochim. Acta*. 253 (1995) 327-334.

83. K. Y. Song, G. Fneyrou, R. Martin, J. Lievois and R. Kobayashi, Solubility Measurements of Methane and Ethane in Water and near Hydrate Conditions, *Fluid Phase Equilib*. 128 (1997) 249-260.

84. S. O. Yang, S. H. Cho, H. Lee and C. S. Lee, Measurement and prediction of Phase Equilibria for methane + water in hydrate forming conditions, *Fluid Phase Equilib*. 185 (2001) 53-63.

85. P. Servio and P. Englezos, Measurement of dissolved methane in water in equilibrium with its hydrate, *J. Chem. Eng. Data* 47 (2002) 87–90.

86. L.-K. Wang, G-J. Chen, G-H. Han, X-Q. Guo and T-M. Guo, Experimental study on the solubility of natural gas components in water with or without hydrate inhibitor, *Fluid Phase Equilib*. 5180 (2003) 1–12.

87. Y. S. Kim, S. K. Ryu, S. O. Yang and C. S. Lee, Liquid Water-Hydrate Equilibrium Measurements and Unified Predictions of Hydrate-Containing Phase Equilibria for Methane, Ethane, Propane, and Their Mixtures *Ind. Eng. Chem. Res*. 42 (2003) 2409-2414.

88. R. G. Anthony and J. J. McKetta, Jr, Phase equilibrium in the ethylene-water system, *J. Chem. Eng. Data*. 12 (1967) 17-20.

89. R. G. Anthony and J. J. McKetta, Jr, Phase equilibrium in the ethylene-ethane-water system, *J. Chem. Eng. Data*. 12 (1967) 21-28.

90. O. L. Culberson and J. J. Mc Ketta, Jr, Phase Equilibria in Hydrocarbon-Water Systems II-, The solubility of ethane in water at pressures to 10000 psia, *AIME* 189 (1950) 319-322.

91. A. Danneil, K. Toedheide and E. U. Franck, Verdampfungsleichgewichte und kritische Kurven in den Systemen Äthan/Wasser und n-Butan/Wasser bei hohen Drücken, *Chem. Ing. Tech.* 39 (1967) 816-821.

92. K. A. Sparks and E. D. Sloan, Water content of NGL in presence of hydrates. Research Report (RR-71), GPA, Tulsa (1983)

93. A. Reichl, Dissertation, TU Berlin, (1996). *Data from DDB*

94. S. Umano and Y. Nakano, *Kogyo Kagaku Zasshi*. 61 (1958) 536. *Data from DDB*

95. A. Azarnoosh and J. J. McKetta, Jr, The solubility of propane in water, *Petrol. Refiner*. 37 (1958) 275-278.

96. A. H. Wehe and J. J. McKetta, Jr, Method for determining total hydrocarbons dissolved in water, *Anal. Chem.* 33(2) (1961) 291-293.

97. M. Sanchez and R. Coll, Sistema propaneo-aqua para alta pressiones y temperaturas. I. Region de dos fases, *An. Quim.* 74 (1978) 1329-1334.

98. Th. W. De Loos, A. J. M. Wijen and G. A. M. Diepen, Phase equilibria and critical phenomena in fluid (propane+water) at high pressures and temperatures, *J. Chem. Thermodyn.* 12 (1980) 193-204.

99. J. G. Le Breton and J. J. McKetta, Jr, Low-pressure solubility of n-butane in water, *Hydrocarb. Proc. & Petr. Ref.* 43(6) (1964) 136-138.

100. F.-Y. Jou and A. E. Mather, Vapor-Liquid-Liquid Locus of the System Pentane + Water, *J. Chem. Eng. Data* 45 (2000) 728-729.

101. L. W. Diamond and N. N. Akinfiev, Solubility of CO_2 in water from −1.5 to 100 °C and from 0.1 to 100 MPa: evaluation of literature data and thermodynamic modeling. *Fluid Phase Equilib.* 208 (2003) 265–290.

102. N. Spycher, K. Pruess and J. Ennis-King, CO_2 – H_2O mixtures in the geological sequestration of CO_2. I. Assessment and calculation of mutual solubilities from 12 to 100°C and up to 600 bar. *Geochim. Cosmochim. Acta* 67 (2003) 3015-3031.

103. Y. D Zel'vinskii, *Zhurn. Khim. Prom.* 14 (1937) 1250–1257 (in Russian, Cited in ref. 101).

104. G. K. Anderson, Solubility of carbon dioxide in water under incipient clathrate formation conditions. *J. Chem. Eng. Data* 47 (2002) 219–222.

105. I. R. Kritschewsky, N. M. Shaworonkoff, and V. A. Aepelbaum, *Z. Phys. Chem. A*. 175 (1935) 232–238 (Cited in ref. 101).

106. R. Wiebe and V. L. Gaddy, The solubility in water of carbon dioxide at 50, 75 and 100°C, at pressures to 700 atmospheres, *J. Am. Chem. Soc.* 61 (1939) 315–318.

107. R. Wiebe and V. L. Gaddy, The solubility in water of carbon dioxide from 12 to 40°C and at pressures to 500 atmospheres: Critical Phenomena, *J. Am. Chem. Soc.* 62 (1940) 815–817.

108. E. Bartholomé and H. Friz, *Chem. Ing. Tech.* 28 (1956) 706–708 (Cited in ref. 101).

109. J. Matous, J. Sobr, J.P. Novak and J. Pick, Solubilities of carbon dioxide in water at pressure up to 40 atm, *Collect. Czech. Chem. Commun.* 34 (1969) 3982–3985.

110. S. D. Malinin and N. I. Savelyeva, The solubility of CO_2 in NaCl and $CaCL_2$ solutions at 25, 50 and 75°C under elevated CO_2 pressures, *Geochem. Int.* 9 (1972) 410–418.

111. S. D. Malinin and N. A. Kurovskaya, Investigation of CO_2 solubility in a solution of chlorides at elevated temperatures and pressures of CO_2, *Geochem. Int.* 12 (1975) 199–201.

112. P. M. Oleinik, Method of evaluating gases in liquids and volumetric properties of solutions under pressure, *Neftepromyslovoe Delo.* (1986) (in Russian, Cited in ref. 101 and also cited by Namiot A. Y. Solubility of gases in water, Nedra, Moscow, 8 (1991) 7(in Russian)).

113. S. O. Yang, I. M. Yang, Y. S. Kim and C. S. Lee, Measurement and prediction of phase equilibria for water + CO_2 in hydrate forming conditions, *Fluid Phase Equilib.* 175 (2000) 75–89.

114. A. Zawisza and B. Malesinska, Solubility of carbon dioxide in liquid water and of water in gaseous carbon dioxide in the range 0.2 – 5 MPa and at temperatures up to 473 K. *J. Chem. Eng. Data* 26 (1981) 388–391.

115. R. A. Shagiakhmetov and A. A Tarzimanov, Deposited Document SPSTL 200 khp—D 81—1982, (1981) (Cited in ref. 101).

116. G. Müller, E. Bender and G. Maurer, Das Dampf-Flüssigkeitsgleichgewicht des ternären systems ammonik-kolhendioxid wasser bei hohen wassergehalten im bereich zwischen 373 und 473 K, *Ber. Bunsenges. Phys. Chem.* 92 (1988) 148-160.

117. A. Bamberger, G. Sieder and G. Maurer, High-pressure (vapour+liquid) equilibrium in binary mixtures of (carbon dioxide and water or acetic acid) at temperatures from 313 to 353 K, *J. Supercritical Fluids* 17 (2000) 97–110.

118. J. B. Goodman and N. W. Krase, Solubility of nitrogen in water at high pressures and temperatures, *Ind. Eng. Chem.* 23(4) (1931) 401-404.

119. R. Wiebe, V. L. Gaddy and C. Heins, Solubility of nitrogen in water at 25°C from 25 to 1000 atmospheres, *Ind. Eng. Chem.* 24 (1932) 927-930.

120. R. Wiebe, V. L. Gaddy and C. Heins, The solubility of nitrogen in water at 50.75 and 100 °C from 25 to 1000 atm, *Ind. Eng. Chem.* 55 (1933) 947-953.

121. A. W. Saddington and N. W. Krase, Vapor-liquid equilibria in the system nitrogen-water, *J. Am. Chem. Soc.* 56(2)(1934) 353-361.

122. H. A. Pray, C. E. Schweickert and B. H. Minnich, Solubility of hydrogen, oxygen, nitrogen, and helium in water, *Ind. Eng. Chem.* 44(5) (1952) 1146-1151.

123. N. O. Smith, S. Kelemen and B. Nagy, Solubility of natural gases in aqueous salt solutions—II: Nitrogen in aqueous NaCl, CaCl2, Na2SO4 and MgSO4 at room temperatures and at pressures below 1000 psia, *Geochim. Cosmochim. Acta* 26 (1962) 921-926

124. T. D. O'Sullivan, N. O.Smith and B. Nagy, Solubility of natural gases in aqueous salt solutions—III Nitrogen in aqueous NaCl at high pressures *Geochim. Cosmochim. Acta*, 30 (1966) 617-619.

125. M. Japas and E. U. Franck, High pressure phase equilibria PVT Data of the water nitrogen system to 673 K and 250 MPa, *Ber. Bensunges. Phys. Chem*. 89 (1985) 793-800.

126. T. N. Kozintseva, Solubility of hydrogen sulphide in water at elevated temperatures. *Geochem. Int.* (1964) 750–756.

127. J. J. Carroll and A. E. Mather, Phase equilibrium in the system water − hydrogen sulphide: experimental determination of the LLV locus, *Can. J. Chem. Eng.* 67 (1989) 468.

128. B. Amirijafari, Solubilty of light hydrocarbons in water under high pressures, *PhD Thesis, The U. of Oklahoma*, Norman 1969

129. R. Battino, Solubility Data Series, vol. 4, Pergamon Press, Oxford, 1980.

130. G. Fauser, *Chim. Ind.* 33 (1951) 193–204.

131. J. H. Hong, P. V. Malone, M.D. Jett and R. Kobayashi, The measurement and interpretation of the fluid-phase equilibria of a normal fluid in a hydrogen bonding solvent: the methane - methanol system, *Fluid Phase Equilib.* 38 (1987) 83–96.

132. Schneider, *Doktor–Ingenieur Dissertation*, TUB, Berlin, 1978.

133. W. Hayduk, IUPAC Solubility Data Series, vol. 9, Pergamon Press, Oxford, 1982.

134. A. S. McDaniel, The Absorption of Hydrocarbon Cases by Nonaqueous Liquids, *J. Phys. Chem.* 15 (1911) 587–610.

135. Y. H. Ma and J. P. Kohn, Multiphase and volumetric equilibria of the ethane-methanol system at temperature between –40 and 100°C, *J. Chem. Eng. Data* 9 (1964) 3–5.

136. K. Ohagaki, F. Sano and T. Katayama, Isothermal vapor-liquid equilibrium data for binary system containing ethane at high pressure, *J. Chem. Eng. Data* 21 (1976) 55–58.

137. W. Weber, *Doktor–Ingenieur Dissertation*, TUB, Berlin, 1981.

138. K. Ishihara, H. Tanaka and M. Kato, Phase equilibrium properties of ethane+methanol system at 298.15 K, *Fluid Phase Equilib.* 144 (1998) 131-136.

139. J. J. Mc Ketta, Jr and H.H. Wehe, Hydrocarbon-water correlations, in *Petroleum Production Handbook, Reservoir Engineering*, Edition Frick T.C, taylor R.W., Mc Graw Hill Book Company, New Yprk, NY, chapter 2 (1962) 1-6.

140. E. G. Hammerschmidt, Formation of gas hydrate in natural gas transmission lines, *Ind. Eng. Chem.* 26 (1934) 851-855.

141. R. M. Barrer and Av. J Edge, Gas hydrates containing argon, krypton and xenon: kinetics and energetics of formation and equilibria, *Proc. R. Soc. London*, ser. A., 300 (1967) 1-24.

142. D.R. Marschall, S. Saito and R. Kobayashi, Hydrates at high pressures. Part I. Methane-water, argon-water and nitrogen-water systems, *AlChE J.* 10 (1964) 202-205.

143. G. D. Holder, G. Corbin and K.D. Papadopoulos, thermodynamic and molecular properties of gas hydrate from mixtures containing methane, argon and krypton, *Ind. Eng. Chem. Fundam.* 19 (1980) 282-286.

144. J. L. Thakore and G. D. Holder, Solid-vapor azeotropes in hydrate forming systems, *Ind. Eng. Chem. Res.* 26 (1987) 462-469.

145. Y. P. Handa, Composition dependence of thermodynamic properties of xenon hydrate, *J. Phys. Chem.* 90 (1986) 5497-5498.

146. A. van Cleef and G. A. M Diepen, Gas hydrate of nitrogen and oxygen, *Rec. Trav. Chim.* 79 (1960) 83-86.

147. A. van Cleef and G. A. M Diepen, Gas hydrate of nitrogen and oxygen, *Rec. Trav. Chim.* 84 (1965) 1085-1093.

148. I. Ihaveri and D. B. Robinson, Hydrates in the methane-nitrogen system, *Can. J. Chem.* 43 (1965) 75-78.

149. A. H. Mohammadi, B. Tohidi and R.W. Burgass, Equilibrium Data and Thermodynamic Modeling of Nitrogen, Oxygen, and Air Clathrate Hydrates, *J. Chem. Eng. Data* 48 (2003) 612-616.

150. S. L. Miller, The occurrence of gas hydrates in the solar system, *Proc. Natl. Acad. Sci.* 47 (1961) 1798-1808.

151. C. H. Unruh and D. L. Katz, Gas-hydrate of carbon dioxide-methane mixtures, *J. Pet. Technol.* 1 (1949) 83-86.

152. D. B. Robinson and B. R. Mehta, Hydrates in the propane – carbon dioxide – water system, *J. Can. Pet. Technol.* 10 (1971) 33-35.

153. A. T. Bozzo, H. Z. Chen, J. R. Kass and A.I. Barduhn, The properties of the hydrates of chlorine and carbon dioxide, *Dessalination* 16 (1975) 303-320.

154. S. Adisasmito and E. D. Sloan, Jr, Hydrates of hydrocarbon gases containing carbon dioxide, *J. Chem. Eng. Data.* 37 (1992) 343-349.

155. W. M Deaton and E. M. Frost, Jr., Gas hydrate composition and equilibrium data, *Oil Gas J.* 45 (1946) 170-178.

156. H. O. McLeod and J. M. Campbell, Natural gas hydrates at pressures to 10 000 psia, *J. Petrol. Tech.* 13 (1961) 590-594.

157. J. L. De Roo, C. I. Peters, R. N. Liechtenthaller and G. A. M. Diepen, Occurrence of methane hydrate in saturated and unsaturated solution of sodium chloride and water independence of temperature and pressure, *AIChE J.* 29 (1983) 651-657.

158. K. Y. Song and R. Kobayashi, Final hydrate stability conditions of methane and propane in the presence of pure water and aqueous solutions of methanol and ethylene glycol, *Fluid Phase Equilib.* 47 (1989) 295-308.

159. H. H. Reamer, F. T. Selleck and B. H. Sage, Some properties of mixed paraffinic and olefinic hydrates, *J. Pet. Technol.* 195 (1952) 197-202.

160. G. D. Holder and G. C. Grigoriou, Hydrate dissociation pressures of (methane + ethane + water). Existence of locus minimum pressures, *J. Chem. Therm.* 12 (1980) 1093-1104.

161. G. D. Holder and J. H. Hand, Multiple phase equilibria in hydrates from methane, ethane, propane and water mixtures, *AIChE J.* 28 (1982) 440-447.

162. G. D. Holder and S. P. Godbole, Measurement and prediction of dissociation pressures of isobutane and propane hydrates below the ice point, *AlChE J.* 28 (1982) 931-934

163. H. Kubota, K. Shimuzu, X. Tanaka and T. Makita, Thermodynamic properties of R13, R23, R152 and propane hydrates for dessalination of seawater, *J. Chem. Eng. Jpn.* 1 (1984) 423-429.

164. I. Hayano and T. Ukida, The formation of isobutane hydrate and its thermodynamic, *J. Chem. Soc. Jpn.* 67 (1964) 997-1002.

165. O. S. Routher and A. I. Barduhn, Hydrates of iso and nornal butane and their mixtures, *Dessalination* 6 (1969) 57-73.

166. S. Saito and R. Kobayashi, Hydrates at high pressures. Part III. Methane-water, argon-water and nitrogen-water systems, *AIChE J.* 10 (1964) 202-205.

167. H. J. Ng, J. P. Petrunia and D. B. Robinson, Experimental measurement and prediction of hydrate forming conditions in the nitrogen-propane-water system, *Fluid Phase Equilib.* 1 (1977-1978) 283-291.

168. S. Adisasmito, R. J. Frank and E. D. Sloan, Jr, Hydrates of carbon dioxide and methane mixtures, *J. Chem. Eng. Data.* 36 (1991) 68-71.

169. L. J. Noaker and D. L. Katz, Gas hydrates of hydrogen sulphide-methane mixtures, *J. Pet. Technol.* 6 (1954) 135-137.

170. B. J. Wu, H. J. Ng and D. B. Robinson, Three and four-phase hydrate forming conditions in methane+isobutane+water, *J. Chem. Therm.* 8 (1976) 461-469.

171. H. J. Ng and D. B. Robinson, The role of n-butane in hydrate formation, *AIChE. J.* 22 (1976) 656-660.

172. V. T. John and G. D. Holder, Hydrates of methane+n-butane below the ice point, *J. Chem. Eng. Data.* 27 (1982) 18-21.

173. G. S. Stepanova, I. Yu. Zaitev and A.G. Burmistrov, Exploration of hydrogen sulphide-containing field of hydrocarbons, *Nedra, Moscou* (1986) (in Russian).

174. D. B. Robinson and J.M. Hutton, Hydrate formation systems containing methane, hydrogen sulphide and carbon dioxide, *J. Can. Pet. Technol.* 10 (1971) 33-35.

175. J. P. Schroeter, R. Kobayashi and M.A. Hilderbrand, Hydrate decomposition conditions in the H_2S – methane – water system, *Ind. Eng. Chem. Fundam.* 22 (1983) 361-364.

176. W. I. Wilcox, D. B. Carson and D. L. Katz, Natural gas hydrates, *Ind. Eng. Chem.* 33 (1941) 662-665.

177. R. Molinero and R. Fagegaltier, Volumetric behavior and the conditions for the formation of hydrate in natural gas rich in H_2S. *Proceedings of the IV World Petroleum Congress*, Section 11-6, Paper 6, (1956) 549-559.

178. W. R. Parrish and J. M. Prausnitz, Dissociation pressures of gas hydrate formed by gas mixture, *Ind. Eng. Chem. Process. Des. Develop.*, 11 (1972) 26-34.

179. V. I. Semin, Study of the hydrate formation conditions at the gas deposits in the north part of Tyumen province, *Development and exploration of gas and gas condensate deposits*, VNII GAS Moscou 10 (1968) 25-36. (In Russian).

180. V. A. Khoroshilov, E.B. Buckhalter and N.Ya. Zaitsev, Hydrate formation in gases from Orenburg deposit, *Gasov. Promst.* 4 (1973) 8-10. (In Russian)

181. E. V. Malenko and N. A. Gafarova, study of the conditions for the formation and degradation of the hydrates of natural gases, *Izv. Akad. Nauk Kaz. SSr Ser. Khim.* 5 (1980) 76-80. (In Russian)

182. D. B. Robinson and H. J. Ng, Hydrate formation and inhibition in gas or gas condensate streams, 36th Annual Technical Meeting of the Petroleum Society of CIM, 2-5 june (1985) Edmonton.

183. R. Kobayashi, H. J. Withrow, G. B. Williams and D. L. Katz, Gas hydrate formation with brine and ethanol solutions, Proceeding of the 30th Annual Convention, Natural Gasoline Association of America, (1951) 27-31.

184. H. J. Ng and D. B. Robinson, Hydrate formation in system containing methane, ethane, propane, carbon dioxide or hydrogen sulphide in the presence of methanol, *Fluid Phase Equilib.* 21 (1985) 145-155.

185. D. B. Robinson and H. J. Ng, Hydrate formation systems containing methane, hydrogen sulphide and carbon dioxide, *J. Can. Pet. Tecnol.* 10 (1986) 33-35.

186. H. J. Ng, C. J. Chen and T. Saeterstad, Hydrate formation and inhibition in gas condensate and hydrocarbon liquid systems. *Fluid Phase Equilib.* 36 (1987) 99-106.

187. J. L. de Roo, C. L. Peters, R. N. Lichtenthale and G. A. M. Diepen, Occurrence of methane hydrate in saturated and unsaturated solutions of sodium chloride and water in dependence of temperature and pressure, *AIChE J.* 29 (1983) 651–657.

188. S. S. S. Huang, A. D. Leu, H. J. Ng and D. B. Robinson, The phase behavior of two mixtures of methane, carbon dioxide, hydrogen sulfide, and water, *Fluid Phase Equilib.* 19 (1985) 21-32.

189. S. L. Patil, Measurement of multiphase gas hydrates phase equilibria: Effect of inhibitors and heavier hydrocarbon components, M.S. Thesis, U. Alaska, Fairbanks, AL, 1987.

190. G. R. Schneider and J. Farrar, Rsch. Dev. Rpt. No 292, *US Dept of Interior*, Jannuary (1968).

191. O. S. Rouher, The n-butane and iso- butane hydrates, M.S Thesis, U. Syracuse, June 1968.

192. S. D. Larson, Phase studies of the two-component carbon dioxide water system involving the carbon dioxide hydrate, U. Illinois (1955).

193. D. C. Bond and N.B. Russel, *Trans. AIME* 179 (1949) 192-.

194. H. J. Ng and D. B. Robinson, Equilibrium phase composition and hydrating conditions in systems containing methanol, light hydrocarbons, carbon dioxide and hydrogen sulfide, *GPA (Tulsa Ok), RR-66*, 1983.

195. H.-J. Ng and D.B. Robinson, Equilibrium phase composition and hydrating conditions in systems containing methanol, light hydrocarbons, carbon dioxide and hydrogen sulfide, *GPA (Tulsa Ok), RR-74*, 1984.

196. S. G. Paranjpe, S. L. Patil, V. A. Kamath and S. P. Godbole, Hydrate formation in crude oils and phase behavior of hydrates in mixtures of methane, propane, iso-butane and n-butane, *Third Chemical Congress of Noth America*, Toronto, Canada, June 5-10 (1987).

197. E.G. Hammerschmidt, Preventing and removing hydrates in natural gas pipe lines, *Gas Age.* April 27th 52 (1939) 66, 69, 70, 71.

198. R. B. Nielsen and R.W. Bucklin, Why not use methanol for hydrate control?, *Hydrocarbon Processing*, April 62 (1983) 71-78.

199. K. Arnold and M. Steward, Surface Production Operations, vol 2. Design of Gas-Handling Systems and Facilities, Houston, TX: Gulf Publishing (1989).

200. K. S. Pedersen, A Fredenslund and P. Thomassen, Properties of Oils and Natural Gases, Houston, TX: Gulf Publishing (1989).

201. S. Malanowski and A. Anderko, Modelling Phase Equilibria, thermodynamic background and practical tool, John Wiley & Sons, Inc (1992)

202. M. J. Assel, J. P. M. Trusler and T. F. Tsolakis, Thermodynamical properties of Fluids, Imperial College Press (1996)

203. M. Benedict, G. R. Webb and L. C. Rubin, An empirical equation for thermodynamic properties of light hydrocarbons and their mixtures, *J. Chem. Phys.* 8 (1940) 334.

204. J. D. van der Waals, Over de Continuiteit van de Gas-en Vloeistoftoestand, Doctoral Dissertation, Leyden (1873).

205. O. Riedlich and J. N. S. Kwong, On the thermodynamic of solution, V: An equation of state. Fugacities of Gaseous Solutions, *Chem. Rev.* 44 (1949) 233-244

206. G. Soave, Equilibrium Constants for Modified Redlich-Kwong Equation of State. *Chem. Eng. Sci.* 4 (1972) 1197-1203.

207. K. S. Pitzer, D. Z. Lipmann, R. F. Jr Curl, C. M. Huggins and D. E. Petersen, Compressibility factor, vapor pressure and entropy of vaporization, *J. Am. Chem. Soc.* 77 (1955) 3433.

208. D. Y. Peng and D. B. Robinson, A New two Constant Equation of State, *Ind. Eng. Chem. Fundam.* 15 (1976) 59-64.

209. G. Schmidt and H. Wenzel, A modified van der Waals type equation of state, *Chem. Eng. Sci.* 35 (1980) 1503-1512

210. G. G. Fuller, A modified Redlich-Kwong-Soave Equation of state capable of representing the liquid state, *Ind. Eng. Chem. Res.* 34(12) (1976) 4351-4363.

211. E. Usdin and J.C. McAuliffe, A one parameter family of equations of state, *Chem. Eng. Sci.* 31 (1976) 1077–1084.

212. J. J. Martin, Cubic Equations of State-Which? *Ind. Eng. Chem. Fundam.* 18 (1979) 81–97.

213. G. Heyen, A cubic equation of state with extended range of application, Chemical Engineering Thermodynamics, S. A. Newman, 1980, p 175, Ann. Arbor Science.

214. A. Harmens and H. Knapp, Three-Parameter Cubic Equation of State for Normal Substances, *Ind. Eng. Chem. Fundam.* 19 (1980) 291-294.

215. N. C. Patel and A. S. Teja, A new Cubic Equation of State for Fluids and Fluid mixtures, *Chem. Eng. Sci.* 37 (1982) 463-473.

216. J. M. Yu, Y. Adachi, B. C.-Y. Lu, in: K.C. Chao, R.L. Robinson (Eds.), Equations of State: Theories and Applications, ACS Symp. Ser. 300, ACS, Washington, DC, 1986, 537–559.

217. J. M. Yu and B.C.-Y. Lu, A three-parameter cubic equation of state for asymmetric mixture density calculations, *Fluid Phase Equilib.* 34 (1987) 1–19.

218. C. H. Twu, J. E. Coon and J. R. Cunningham, A new cubic equation of state, *Fluid Phase Equilib.* 75 (1992) 65–79.

219. A. Peneloux, E. Rauzy and R. Freze, A consistent correction for Redlich-Kwong-Soave volumes, *Fluid Phase Equilib.* 8 (1982) 7–23.

220. P. M. Mathias, T. Naheiri and E. M. Oh, A density correction for the Peng—Robinson equation of state, *Fluid Phase Equilib.* 47 (1989) 77–87.

221. W. L. Kubic, A modification of the Martin Equation of state for calculating vapour liquid equilibria, *Fluid phase Equilib.* 9 (1982) 79-97.

222. Y. Adachi, B. C.-Y. Lu and A. H. Sugie, Three parameter equation of state , *Fluid Phase Equilib.* 13 (1983) 133-142.

223. M. A. Trebble and P. R. Bishnoi, Development of a new four parameter cubic equation of state, *Fluid Phase Equilib.* 35 (1987) 1-18.

224. M. A. Trebble and P. R. Bishnoi, Accuracy and Consistency Comparison of Ten Cubic Equations of State for Polar and Non Polar Compounds, *Fluid Phase Equilib.* 29 (1986) 465-474.

225. A. Danesh, D.-H. Xu and A. C. Todd, Comparative study of cubic equations of state for predicting phase behaviour and volumetric properties of injection gas-reservoir oil system, *Fluid Phase Equilib.* 63 (1991) 259-278.

226. J. O. Valderrama, A generalized Patel-Teja equation of state for polar and non-polar fluids and their mixtures *J. Chem. Eng. Japan* 23 (1990) 87-91.

227.G. Soave, Improving the treatement of heavy hydrocarbons by the SRK EoS, *Fluid Phase Equilib.* 84 (1993) 339-342.

228. R. Stryjek, J. H. Vera, PRSV: An improved Peng Robinson equation of state for pure compounds and mixture, *Can. J. Chem. Eng.* 64 (1986) 323-333.

229. P. M. Mathias, T. W. Copeman, Extension of the Peng-Robinson Equation of State to Complex Mixtures: Evaluation of the Various Forms of the Local Composition Concept, *Fluid Phase Equilib.* 13 (1983) 91-108.

230. J. L. Daridon, B. Lagourette, H. Saint-Guirons and P. Xans, A cubic equation of state model for phase equilibrium calculation of alkane + carbon dioxide + water using a group contribution k_{ij}, *Fluid Phase Equilib.* 91 (1993) 31-54.

231. C. H. Twu, J. E. Coon, J. R. Cunningham, A new generalized alpha function for cubic equation of state. Part 1 Peng Robinson equation, *Fluid Phase Equilib.* 105 (1995) 49-59.

232. C. H. Twu, J. E. Coon, J. R. Cunningham, A new generalized alpha function for cubic equation of state. Part 2 Redlich-Kwong equation, *Fluid Phase Equilib.* 105 (1995) 61-69.

233. D. Avlonitis, A. Danesh and A. C. Todd, Prediction of VL and VLL equilibria of mixtures containing petroleum reservoir fluids and methanol with a cubic EoS, *Fluid Phase Equilib.* 94 (1994) 181-216.

234. J. M. Huron and J. Vidal, New Mixing Rules in Simple Equations of State for Representing Vapor-Liquid Equilibria of Strongly Non-Ideal Mixture, *Fluid Phase Equilib.* 3 (1979) 255-271.

235. D. S. H. Wong and S.I. Sandler, A theoretically correct mixing rule for cubic equation of state, *AIChE J.,* 38 (1992) 671-680

236. M. L. Michelsen, A modified Huron-Vidal mixing rule for cubic equations of state, *Fluid Phase Equilib.* 60 (1990) 213-219.

237. S. Dahl and M. L. Michelsen, High pressure vapor liquid equilibrium with a UNIFAC based equation of state, *AIChE J.,* 36 (1990) 1829-1836

238. C. L. Yaws, J. R. Hopper, X. Wang, A. K. Rathinsamy and R. W. Pike, Calculating Solubility & Henry's Law Constants for Gases in Water, *Chem. Eng.* June (1999) 102-105.

239. R. F. Prini and R. Crovetto, Evaluation of data on solubility of simple apolar gases in light and heavy water, *J. Phys. Chem. Ref. Data.* 18 (1989) 1231-1243.

240. C. Tsonopoulos and G. M. Wilson, High temperature mutual solubilities of hydrocarbons and water, *AIChE J.* 29 (1983) 990-999.

241. J. L. Heidman, C. Tsonopoulos, C. J. Brady and G.M. Wilson, High temperature mutual solubilities of hydrocarbons and water, *AIChE J.* 31 (1985) 376-384

242. J. Li and L. X. Nghiem, Phase equilibria of oil, gas and water/brine mixtures from a cubic equations of state and Henry's law, *Can. J. Chem. Eng.* 64 (1986) 486-496.

243. A. Saul and W. Wagner, international equation for the saturation properties of ordinary water substance, *Phys. Chem. Ref. Data*, 4 (1987) 893-901

244. H. G Rackett, Equation of state for saturated liquids, *J. Chem. Eng. Data.* 15 (1970) 514-517.

245. E. W. Lyckman, C. A. Eckert, J. M. Prausnitz, Generalized reference fugacities for phase equilibrium thermodynamic, *Chem. Eng Sc.* 20 (1965) 685-691.

246. R. A. Heidmann and J. M. Prausnitz, Equilibrium data of wet airoxidation. Water content and thermodynamic properties of saturated combustion gases, *Ind. Eng. Chem. Process Des. Dev.* 16 (1977) 375-381.

247. H. Renon and J. M. Prausnitz, Local Compositions in Thermodynamic Excess Function for Liquid Mixtures, *AIChE J.* 14 (1968) 135-144.

248. D. S. Abrams and J. M. Prausnitz, Statistical thermodynamics of liquid mixture: a new expression for the excess Gibbs energy of partly or completely miscible systems, *AIChE J.* 21 (1975) 116-128.

249. G. Maurer and J. M. Prausnitz, On the derivation and extension of the UNIQUAC equation, *Fluid Phase Equilib.* 2 (1979) 91-99.

250. A. Bondi, van der Waals volume and radii, *The Journal of Physical Chemistry*, 68 (1964) 441-451.

251. A. Bondi, Physical Properties of Molecular Crystals, Liquids and Glasses,Wiley, New-York (1968).

252. Aa. Fredenslung, R. L. Jones and J. M. Prausnitz, Group contribution. Estimation of activity coefficients for non ideal liquid mixtures, *AIChE J.* 21 (1975) 1086-1099.

253. D. B. Carson and D. L. Katz, Natural gas hydrates, Trans, *AIME,* 146 (1942) 150.

254. S. L. Mann, L. M. McClure, F. H. Poettmann and E. D. Sloan, Vapor-solid equilibrium ratio for structure I and II natural gas hydrate, Proc. 68th Ann. GPA conV., San Antonio, TX, March 13-14, (1989) 60-74.

255. D. L. Katz, Prediction of conditions for hydrate formation in natural gases, Trans, *AIME* 160 (1945) 140-144.

256. G. D. Holder, S. P. Zetts and N. Pradhan, Phase behavior in systems containing clathrate hydrates, Reviews in chemical engineering 5 (1) (1988).

257. F. Y. Makogon, Hydrates of Natural Gases, PennWell (1981) 12-13.

258. R. Kobayashi, Y. S Kyoo and E. D. Sloan, Phase Behavior of Water/Hydrocarbon Systems, Petroleum Handbook, SPE, Dallas, Richardson, TX, (1987) 13-25.

259. J. H. van Der Waals and J. C. Platteeuw, Clathrate solutions, *Adv. Chem. Phys.* 2 (1959) 2-57.

260. W. R. Parrish and J. M. Prausnitz, Dissociation pressures of gas hydrate formed by gas mixture, *Ind. Eng. Chem. Process. Des. Develop.* 11 (1972) 26-34.

261. J. Munck, S. Skjold-Jørgensen and P. Rasmussen, Computations of the formation of gas hydrates, *Chem. Eng. Sc.* 43 (1988) 2661-2672.

262. E. D. Sloan, F. M Khoury and R. Kobayashi, Water content of methane gas in equilibrium with hydrate, *Ind. Eng. Chem. Fundam.* 15 (1976) 318-323.

263. E. D. Sloan, K. A. Sparks, J. J. Johnson and M. S. Bourrie, Two-phase liquid hydrocarbon-hydrate equilibrium for ethane and propane, *Ind. Eng. Chem. Res.* 26 (1987) 1173-118.

264. H.-J. Ng and D. B. Robinson, A Method for predicting the equilibrium gas phase water content in gas-hydrate equilibrium, *Ind. Eng. Chem. Fundam.* 19 (1980) 33-36.

265. D. Avlonitis and N. Varotsis, Modelling gas hydratethermodynamic behaviour: theoretical basis and computational methods, *Fluid Phase Equilib.* 123 (1996) 107-130

266. J. B. Klauda and S. I. Sandler, A fugacity model for gas hydrate phase equilibria, *Ind. Eng. Chem. Res.* 39 (200) 3377-3386.

267. G. -J. Chen and T.-M. Guo, Thermodynamic modelling of hydrate formation based on new concepts, *Fluid Phase Equilib.* 122 (1996) 43-65.

268. G. -J. Chen and T.-M. Guo, A new approach to gas hydrate modelling, *Chem. Eng. J.* 71 (1998) 145-151.

269. M. Christov and R. Dohrn, High-pressure fluid phase Equilibria. Experimental methods and systems investigated (1994-1999), *Fluid Phase Equilib*. 202 (2002) 153-218.

270.C. Bouchot, D. Richon, Direct PVT and VLE measurements with a single equipment using a vibrating tube densimeter up to 393 K and 40 MPa: Description of the original apparatus and new data, *Ind. Eng. Chem. Res.* 37 (1998) 3295-3304.

271. C. Bouchot and D. Richon, An enhanced method to calibrate vibrating tube densimeters, *Fluid Phase Equilib*. 191 (2001) 189-208.

272. M. Meskel-Lesavre, D. Richon, H. Renon, A new variable volume cell for determining vapor-liquid equilibria and saturated liquid molar volume by the static method, Ind. *Eng. Chem. Fundam.* 20 (1981) 284-289.

273. F. Fontalba, D. Richon, H. Renon, Simultaneous determination of PVT and VLE data of binary mixtures up to 45 MPa and 433 K: a new apparatus without phase sampling and analysis, *Rev. Sci. Instrum.*55(6) (1984) 944-951.

274. D. Legret, D. Richon, H. Renon, Static still for measuring vapor liquid equilibria up to 50 bar, *Ind. Eng. Chem. Fundam.* 19 (1980) 122-126.

275. J.D. Raal, A.L. Mühlbauer, Phase Equilibria: Measurement and Computation, Taylor & Francis ed., 1997. ISBN: 156032550X.

276. P. Guilbot, A. Valtz, H. Legendre and D. Richon, Rapid on Line Sampler-Injector : a reliable tool for HT-HP Sampling and on line GC analysis, *analusis* 28 (2000) 426-431.

277. D. Legret, J. Desteve, D. Richon and H. Renon, Vapor-liquid equilibrium constants at infinite dilution determined by a gas stripping method: Ethane, Propane, n-Butane, n-Pentane in the Methane-n-Decane System, *AIChE J.* January 29 (1983) 137-143.

278. G. J. van Rossum, (ed.) *Gas Quality. Proceeding of the congress, Specification and measurement of physical and chemical properties of natural gas*, Groningen, The Netherlands, 22-25 April 1986. Amsterdam: Elsevier Science Publishers B.V.

279. A. Duswalt and W. Brandt, Carbon-Hydrogen determination by gas chromatography *Analytical Chemistry* 1960, 32, 272-274.

280. O. E. Sundberg and C. Maresh, Application of gas chromatography to micro determination of carbon and hydrogen , *Analytical Chemistry*, 32 (1960) 274-277.

281. H. S. Knight and F. T. Weiss, Determination of traces of water in hydrocarbons, *Analytical Chemistry*, 34 (1962) 749-571.

282. A. Goldup and M. T. Westaway, M. T., Determination of trace quantities of water in hydrocarbons, *Analytical Chemistry*, 38 (1966) 1657-1661.

283. R. Kaiser, Wasserbestimmung bis 10^{-9} Gew. %, *Chromatographia*, 2 (1969) 453-461

284. G. M. Neumann, Gas Chromatographische Bestimmung von Wasser, *Z. Anal. Chem*, 244 (1969) 302-305.

285. S. Latif and J. K. Haken, Trace water analysis in gases using reaction gas chromatography, *Journal of Chromatography*, 258 (1983) 233-237.

286. D. Tianhui, L. Baoq, Z. Hongyi and L. Yanfang, Determination of trace amounts of water in high-purity silane, arsine and phosphine by gas chromatography, *Analyst* 117 (1992) 1577-1579.

287. S. Yajima, K. Shiba, M. Handa and Y. Takahashi, The determination of water by gas chromatography, *Bull. Chem. Soc. Jap.* 37 (1974) 800-804.

288. V. C. Y. Kong,; F. R. Foukles, D. W. Kirk and J. T. Hinatsu, Development of hydrogen storage for fuel cell generators, *Int. Jour. Hyd. En.* 24 (1999) 665-675.

289. R. C. Reid, J. M. Prausnitz and B. E. Poling, *The Properties of Gases and Liquids*, 4th ed., McGraw-Hill New York (1988).

290. E. R. Åberg and A. G. Gustavsson, Design and Evaluation of Modified Simplex Methods, *Analytica Chimica Acta* 144 *(*1982) 39-53.

291. D. Avlonitis, Thermodynamics of Gas Hydrate Equilibria; Ph.D. Thesis, Heriot-Watt University, 1992.

292. B. Tohidi, R. W. Burgass, A. Danesh and A. C. Todd, Hydrate inhibition effect of produced water, Part 1. Ethane and propane simple gas hydrates, *SPE 26701, Proceedings of the SPE Offshore Europe 93 Conference* (1993) 255-264.

293. B. Tohidi-Kalorazi, Gas Hydrate Equilibria in the Presence of Electrolyte Solutions; Ph.D. Thesis, Heriot-Watt University, 1995.

294. GPA RR 45 The Water Content and Correlation of the Water Content of Methane in Equilibrium with Hydrates, (I); and the Water Content of a High Carbon Dioxide Simulated Prudhoe Bay Gas in Equilibrium with Hydrates, (II)

295. F.-Y. Jou, F. D. Otto and A. E. Mather, Solubility of Methane in Glycols at Elevated Pressures, *Can. J. Chem. Eng.* 72 (1994)130-133.

296. D-Q. Zheng, W-D. Wei and T-M. Guo, Solubility study of methane, carbon dioxide and nitrogen in ethylene glycol at elevated temperatures and pressures, *Fluid Phase Equilib.* 155 (1999) 277–286.

297. L.W. Winkler, Gesetzmäßigkeitbei der Absorption der gase in Flüssigkeiten, *Z. Phys. Chem.* 55 (1906) 344-354.

298. J. Kendal and J. C. Andrews, The solubilities of acids in aqueous solutions of other acids, *J. Am. Chem. Soc.* 43 (1921) 1545-1560.

299. R.H. Wright and O. Maas, The solubility of hydrogen sulphide in water from the vapor pressures of the solutions, *Can. J. Res.* 6 (1932) 94–101.

300. A.V. Kiss, I. Lajtai and G. Thury, Über die Löslichkeit von Gasen in Wasser – Nichtelektrolytgemischen, *Z. Anorg. Allg. Chem.* 233 (1937) 346-352.

301. H.A. Pohl, Thermodynamics of the hydrogen sulfide -water system relevant to the dual temperature process for the production of heavy water, *J. Chem. Eng. Data* 6(4) (1961) 515-521.

302. A. C. Harkness and B. A. Kelman, Solubility of methylmercaptan in water, *TAPPI* 50 (1967) 13.

303. E. C. W. Clarke and D. N.Glew, Aqueous non electrolyte solutions. Part VIII. Deuterium and hydrogen sulfide solubilities in deuterium oxide and water, *Can. J. Chem. Eng.* 49 (1971) 691-698.

304. W.Gerrard, Solubility of hydrogen sulphide, dimethyl ether, methyl chloride and sulphur dioxide in liquids. The prediction of solubility of all gases. *J. Appl. Chem. Biothechnol.* 22 (1972) 623-650.

305. J.I. Lee and A. E.Mather, Solubility of hydrogen sulphide in water, *Ber. Besunges. Phys.* 81 (1977) 1021-1023.

306. A. A.Douabul and J. P. Riley, The solubility of gases in distilled water and seawater -V. Hydrogen sulphide, *Deep-sea research* 26A (1979) 259-272.

307. T.J. Barrett, G.M. Anderson and J. Lugowski, The solubility of hydrogen sulphide in 0-5m NaCL solutions at 25-95 C and one atmosphere, *Geochimica et Cosmochemica Acta,* 52 (1988) 807-811.

308. O.M. Suleimenov and R. E. Krupp, Solubility of hydrogen sulphide in pure water and in NaCl solutions from 20 to 320 C and at saturation pressures, *Geochemica et Cosmochemica Acta* 58(11) (1994) 2433-2444.

309. G. Kuranov, B. Rumpf, N. A. Smirnova and G. Maurer, Solubility of single carbon dioxide and hydrogen sulphide in aqueous solutions of N Methyldiethanolamine in the temperature range 313 -413 K at pressure up to 5 MPa, *Ind. Eng Chem. Res.* 35 (1996) 1959-1966.

310. R. F. Bukacek, Equilibrium Moisture Content of Natural Gases, Institute of Gas Technology (1955) Research Bulletin 8. .

311. W. D. McCain Jr., The Properties of Petroleum Fluids, second edition, Penn well Publishing Company, Tulsa, Oklahoma (1990).

312. S. C. Sharma, Equilibrium water content of gaseous mixtures, PhD thesis, The University of Oklahoma (1969).

313. S. C. Sharma and J.M.Campbell, Predict natural-gas water content with total gas usage, *Oil & Gas J.* (4 Aug 1969) 67 (31), 136-137.

314. Gas Conditioning and Processing, Volume 1: The Basic Principles, J.M. Campbell, Campbell Petroleum Series, Oklahoma (1994).

315. W. R. Behr, Correlation eases absorber-equilibrium-line calculations for TEG-natural gas dehydration, *Oil & Gas Journal* (7 Nov 1983) 96-98.

316. F. M. A. Kazim, Quickly calculate the water content of natural gas, *Hydrocarbon Processing* (March 1996) 105-108.

317. Y. Ning, H. Zhang, and G. Zhou, Mathematical simulation and program for water content chart of natural gas, *Chem. Eng. Oil Gas* 29 (2000) 75-77 (in Chinese, Quoted ref. 10).

318. J. N. Robinson, R. G. Moore, R. A. Heidemann and E. Wichert, Estimation of the Water Content of Sour Natural Gases, *SPE J.* (August 1977) 281-286.

319. J. N. Robinson, R. G. Moore, R. A. Heidemann and E. Wichert, Charts help estimate H2O content of sour gases, *Oil & Gas J.* 76(5) (1978) 76-78.

320. J. N. Robinson, R. G. Moore, R. A. Heidemann and E. Wichert, Estimation of the Water Content of Sour Natural Gas, Laurance Reid Gas Conditioning Conference, Norman, OK (1980).

321. R. N. Maddox, L.L. Lilly, M. Moshfeghian and E. Elizondo, Estimating Water Content of Sour Natural Gas Mixtures, Laurance Reid Gas Conditioning Conference, Norman, OK, (March 1988).

322. G.C. Wichert and E. Wichert, Chart estimates water content of sour natural gas, *Oil & Gas J.* 90(13) (1993) 61-64.

323. D. L Katz, D. Cornell, R. Kobayashi and F. H. Poettmann, Handbook of Natural Gas Engineering, McGraw-Hill Book Company (1959).

324. Petroleum Engineering Handbook, E.D. Sloan and R. Kobayashi, Chapter 25: "Phase Behavior of Water/Hydrocarbon Systems," Society of Peroleum Engineers, Richardson, Texas (1987).

325. T. E. Daubert and R. P. Danner, DIPPR Data Compilation Tables of Properties of Pure Compounds; AIChE, New York, 1985.

326. A. A. Elgibaly and A. M. Elkamel Daubert, A new correlation for predicting hydrate formation conditions for various gas mixtures and inhibitors, *Fluid Phase Equilib.* 152 (1998) 23–42.

Appendices

Appendix A: PROPERTIES OF SELECTED PURE COMPOUNDS

Component	Pc (Pa)	Tc(K)	ω	V_c	C_1 (SRK)	C_2 (SRK)	C_3 (SRK)	C_1 (PR)	C_2 (PR)	C_3(PR)
Hydrogen	1296960	33.19	-0.2160	0.64147	0.161	-0.225	-0.232	0.0949	-0.2751	-0.0293
Methane	4600155	190.564	0.0110	0.0992	0.549	-0.409	0.603	0.4157	-0.1727	0.3484
Oxygen	5080435.5	154.58	0.0222	0.0734	0.545	-0.235	0.292	0.4129	-0.0171	0.0917
Nitrogen	3394387.5	126.2	0.0377	0.08921	0.584	-0.396	0.736	0.4483	-0.1568	0.4687
Ethylene	5041628.025	282.35	0.0865	0.131	0.652	-0.315	0.563	0.5120	-0.0871	0.3490
Hydrogen Sulphide	8936865	373.53	0.0942	0.0985	0.641	-0.183	0.513	0.5074	0.0076	0.3423
Ethane	4883865	305.32	0.0995	0.1479	0.711	-0.573	0.894	0.5312	-0.0618	0.2142
Propane	4245517.5	369.95	0.1523	0.203	0.775	-0.476	0.815	0.6001	-0.0063	0.1739
Isobutane	3639594	408.8	0.1808	0.263	0.807	-0.432	0.910	0.6524	-0.1494	0.5992
n-Butane	3799687.5	425.15	0.2002	0.255	0.823	-0.267	0.402	0.6773	-0.0811	0.2985
Cyclohexane	4073001.6	553.58	0.2096	0.308	0.860	-0.566	1.3751	0.6836	-0.0887	0.5495
Benzene	4895000.6	562.05	0.2103	0.256	0.840	-0.389	0.917	0.7012	-0.2521	0.9761
Carbon Dioxide	7377000	304.21	0.2236	0.094	0.867	-0.674	2.471	0.7046	-0.3149	1.8908
Isopentane	3381002.5	460.43	0.2275	0.306	0.876	-0.386	0.660	0.7235	-0.1661	0.5149
Neopentane	3195700	433.8	0.306	0.306	0.845	-0.619	1.419	0.683	-0.2541	0.8793
Pentane	3369056.25	469.7	0.2515	0.304	0.901	-0.305	0.542	0.7629	-0.2243	0.6695
Ammonia	11287600	405.65	0.2526	0.07247	0.916	-0.369	0.417	0.7483	-0.0254	0.0014
Toluene	4107999.2	591.75	0.2640	0.316	0.923	-0.301	0.494	0.7617	-0.0420	0.2707
Hexane	3014418.75	507.4	0.3013	0.371	1.005	-0.591	1.203	0.8703	-0.5880	1.5039
Acetone	4701003.8	508.2	0.3065	0.209	0.993	-0.322	0.265	0.8210	0.0064	-0.0900
Water	22055007.45	647.13	0.3449	0.05595	1.095	-0.678	0.700	0.9193	-0.3320	0.3172
Heptane	2740000.3	540.2	0.3495	0.428	1.036	-0.258	0.488	0.8776	-0.0307	0.3019
Octane	2490001.1	568.7	0.3996	0.486	1.150	-0.587	1.096	0.9583	-0.1341	0.4867
Methanol	8096000	512.60	0.559	0.118	1.43506	-0.8410	0.5013	1.2317	-0.3907	-0.0516
Ethanol	6383000	516.20	0.635	0.167	1.42132	0.2341	-1.4189	1.2156	0.6616	-1.9362
Ethylene Glycol	7701000	645	0.4868	0.186	0.993707	1.7551	-2.8989	0.8183	2.0229	-3.1677
Diethylene Glycol	4770000	753	1.301	0.316	1.46273	-0.6922	1.7390	1.2574	-0.2465	1.1384
Triethylene Glycol	3300100	797	1.3863	0.443	1.89525	-2.5462	3.7892	1.6604	-1.9303	2.9140

Appendix B: PUBLISHED PAPERS AND PROJECTS DONE DURING THE PhD

[B1] A. Chapoy, C. Coquelet, D. Richon, Solubility Measurement and Modeling of Water in the Gas Phase of the Methane/Water Binary System at Temperatures from 283.15 to 318.15 K and Pressures up to 35 MPa. *Fluid Phase Equilibria*, 214 (1) (2003), 101-117.

[B2] A. Chapoy, C. Coquelet, D. Richon, Measurement of the Water Solubility in the Gas Phase of the Ethane + Water Binary System near Hydrate forming Conditions. *J. Chem. Eng. Data*, 48 (2003), 957-966.

[B3] A. Chapoy, C. Coquelet, D. Richon, Development of a new alpha function for the Peng-Robinson equation of state: Comparative study of alpha function models for pure compound and water – gas system, *Int. J. of Therm.* 25 (1) (2004) 133-157.

[B4] F. Rivollet, A. Chapoy, C. Coquelet, D. Richon, Vapor Liquid Equilibrium for the Carbon Dioxide (CO2) + Difluoromethane (R32) at Temperatures from 283.12 to 343.25 K and Pressures up to 7.46 MPa, *Fluid Phase Equilib.* 218 (2004) 95–101.

[B5] A. Chapoy, A. H. Mohammadi, D. Richon, B. Tohidi, Gas Solubility Measurement and Modeling for Methane – Water and Methane – Ethane – n-Butane - Water Systems near Hydrate Forming Conditions, *Fluid Phase Equilib.* 220 (2004) 113-121.

[B6] A. Chapoy, A. H. Mohammadi, A. Chareton, D. Richon, B. Tohidi, Measurement and Modeling of Gas Solubility and Literature Review of the Properties for the Carbon Dioxide - Water System, *Ind. Eng. Chem.* 43 (2004) 1794-1802.

[B7] A. H. Mohammadi, A. Chapoy, D. Richon, B. Tohidi, Experimental Measurement and Thermodynamic Modeling of Water Content in Methane and Ethane Systems. *Ind. Eng. Chem.* 43 (2004) 7148-7162.

[B8] A. Chapoy, A. H. Mohammadi, R. W. Anderson, D. Richon, B. Tohidi, Vapor-Liquid Equilibria in Methane-Water-Ethylene Glycol System. *In preparation*.

[B9] A. H. Mohammadi, A. Chapoy, D. Richon, B. Tohidi, A Simple Approach for Estimating the Water Content of Dry and Sweet Natural Gases, *Ind. Eng. Chem.* 43 (2004) 7137-7147.

[B10] A. Chapoy, S. Mokraoui, A. Valtz, D. Richon, A. H. Mohammadi B. Tohidi, Vapor-Liquid Equilibria for Propane-Water System from 277.62 to 368.16 K, *Fluid Phase Equilibria* 226 (2004) 213-220.

[B11] A. H. Mohammadi, A. Chapoy, D. Richon, B. Tohidi, Measurements and Thermodynamic Modeling of Vapor-Liquid Equilibria in Ethane –Water Systems from 274.26 to 343.08 K, *Ind. Eng. Chem.* 43 (2004) 5418-5424.

[B12] A. Chapoy, D. Richon, A. H. Mohammadi B. Tohidi, Gas Solubility Measurement and Modeling for Nitrogen + Water System from 274.18 K to 363.02 K, *J. Chem. Eng. Data* 49 (2004) 1110 -1115.

[B13] A. Valtz, A. Chapoy, C. Coquelet, P. Paricaud and D. Richon, Vapour - Liquid Equilibria in the Carbon Dioxide – Water System, Measurement and Modelling from 278.2 to 318.2 K, *Fluid Phase Equilibria* 226 (2004) 333-344.

[B14] A. Chapoy, A. H. Mohammadi, D. Richon, B. Tohidi, Water Content Measurement and Modelling for Methane – Water and Methane – Ethane – n-Butane - Water Systems using a New Sampling Device, submitted to *J. Chem. Eng. Data* (2004).

[B15] A. Chapoy, A. H. Mohammadi, D. Richon, B. Tohidi, Water Content Measurement and Modeling in the Nitrogen + Water System, *J. Chem. Eng. Data* (2005) in press.

[B16] A. Chapoy, A. H. Mohammadi, B. Tohidi, A. Valtz, D. Richon, Vapour - Liquid Equilibria and Literature Review of the Properties for the Hydrogen Sulphide – Water System from 273.15 to 403.15 K., *in preparation*, 2005.

And projects from the Gas Processor Association
    GPA project 987: Water and Inhibitor Distribution in Gas Production Systems
    GPA project 021: Solubility of Amine in Hydrocarbon Liquid

Appendix C: THERMODYNAMIC RELATIONS FOR FUGACITY COEFFICIENT CALCULATIONS USING RK, RKS OR PR-EOS.

1. Pure Compounds.

The following general form can be used for expressing any cubic equation of state:

$$p = \frac{RT}{v-b} - \frac{a}{(v-br_1)(v-br_2)}$$

(C.1)

with r_1=0, r_2=-1 for Soave or *Redlich and Kwong* and $r_1 = -1-\sqrt{2}$, $r_1 = -1+\sqrt{2}$ for *Peng and Robinson*.

The fugacity coefficient can be expressed as:

$$\ln(\Phi) = Z - 1 - \ln\left(\frac{p(v-b)}{RT}\right) + \frac{a}{bRT}\frac{1}{r_1-r_2}\ln\left(\frac{v-br_1}{v-br_2}\right)$$

(C.2)

2. Mixtures.

The fugacity coefficient for component *i* in a mixture can be expressed as:

$$\ln(\Phi_i) = \ln\left(\frac{v}{v-b}\right) - \ln(Z) + \frac{bB_i}{v-b} + \frac{A_i - \frac{a}{b}B_i}{bRT}\frac{1}{r_1-r_2}\ln\left(\frac{v-br_1}{v-br_2}\right)$$
$$+ \frac{aB_i}{bRT}\frac{1}{r_2-r_1}\left(\frac{r_1}{v-br_1} - \frac{r_2}{v-br_2}\right)$$

(C.3)

where

$$B_i = \frac{\partial nb}{\partial n_i}$$

(C.4)

$$A_i = \frac{1}{n}\frac{\partial n^2 a}{\partial n_i}$$

(C.5)

The *a* and *b* parameters and their derivation are calculated from the applied mixing rules.

3. Parameter derivations

The derivation of the different parameters for different mixing rules are:

- Classical mixing rules:

$$A_i = 2\sum_i x_i a_{ij} \tag{C.6}$$

$$B_i = b_i \tag{C.7}$$

- *Huron Vidal* mixing rules:

$$A_i = \frac{a}{b}b_i + b\left(\frac{a_i}{b_i} + CRT\ln(\gamma_i)\right) \tag{C.8}$$

$$B_i = b_i \tag{C.9}$$

$$C = \frac{(r_1 - r_2)}{\ln\left(\dfrac{1 - r_1}{1 - r_2}\right)} \tag{C.10}$$

- *Wong-Sandler* mixing rules:

$$D = \frac{1}{RT}\sum_i\left(CRTx_i\ln(\gamma_i) + x_i\frac{a_i}{b_i}\right) \tag{C.11}$$

$$Q = \sum_i\sum_j x_i x_j\left(b - \frac{a}{RT}\right)_{ij} \tag{C.12}$$

$$D_i = \frac{\partial nD}{\partial n_i} = \frac{1}{RT}\left(CRT\ln(\gamma_i) + \frac{a_i}{b_i}\right) \tag{C.13}$$

$$Q_i = \frac{1}{n}\frac{\partial n^2 D}{\partial n_i} = 2\sum_i x_i\left(b - \frac{a}{RT}\right)_{ij} \tag{C.14}$$

$$B_i = \frac{1}{1-D}Q_i - \frac{nQ}{(1-D)^2}(1 - D_i) \tag{C.15}$$

$$A_i = RT(DB_i + bD_i) \tag{C.16}$$

$$C = \frac{(r_1 - r_2)}{\ln\left(\dfrac{1 - r_1}{1 - r_2}\right)} \tag{C.17}$$

- *MHV1* and *PSRK* mixing rules:

$$A_i = \frac{a}{b}b_i + b\left(\frac{a_i}{b_i} + \frac{RT}{q_1}\ln(\gamma_i) - \frac{RT}{q_1}\left(\ln\left(\frac{b_i}{b}\right) + 1 - \frac{b_i}{b}\right)\right) \tag{C.18}$$

$$B_i = b_i \tag{C.19}$$

- *MHV2* mixing rules:

$$\alpha = \frac{a}{bRT} \tag{C.20}$$

$$A_i = \frac{a}{b}b_i + \frac{q_2\alpha^2 + q_1\alpha_i + q_2\alpha_i^2 + \ln(\gamma_i) + \ln\left(\frac{b}{b_i}\right) + 1 - \frac{b_i}{b}}{2q_2\alpha + q_1} \tag{C.21}$$

$$B_i = b_i \tag{C.22}$$

Appendix D: CALCULATION OF FUGACITY COEFFICIENT USING AN EoS AND THE NDD MIXING RULES.

The following general form can be used for expressing any cubic equation of state:

$$P = \frac{RT}{v-b} - \frac{a}{v^2 + uv - w^2}$$
(D.1)

The fugacity coefficient for component i in a mixture can be expressed as:

$$\ln \phi_i = -\ln(Z-B) + \frac{B_i'B}{Z-B} + \frac{A}{\sqrt{U^2+4W^2}}\left[A_i' - \frac{U_i'U^2 + 4W_i'W^2}{U^2+4W^2}\right] \times$$

$$\ln\left[\frac{2Z+U-\sqrt{U^2+4W^2}}{2Z+U+\sqrt{U^2+4W^2}}\right] - A\left[\frac{2(2Z+U)W_i'W^2 + (UZ-2W^2)U_i'U}{(Z^2+UZ-W^2)(U^2+4W^2)}\right]$$
(D.2)

where:

$$A = \frac{Pa}{(RT)^2} , \qquad\qquad B = \frac{Pb}{RT}$$
(D.3, D.4)

$$U = \frac{Pu}{RT} , \qquad\qquad W = \frac{Pw}{RT}$$
(D.5, D.6)

$$Z = \frac{Pv}{RT}$$
(D.7)

and:

$$A_i' = \frac{1}{na}\left[\frac{\partial(n^2a)}{\partial n_i}\right]_{T,n_{j\neq i}} , \qquad B_i' = \frac{1}{b}\left[\frac{\partial(nb)}{\partial n_i}\right]_{T,n_{j\neq i}}$$
(D.8, D.9)

$$U_i' = \frac{1}{u}\left[\frac{\partial(nu)}{\partial n_i}\right]_{T,n_{j\neq i}} , \qquad W_i' = \frac{1}{w}\left[\frac{\partial(nw)}{\partial n_i}\right]_{T,n_{j\neq i}}$$
(D.10, D.11)

The compressibility factor Z is given by the following dimensionless equation:

$$Z^3 - (1+B-U)Z^2 + (A-BU-U-W^2)Z - (AB-BW^2-W^2) = 0$$
(D.12)

Appendix E: BIPS FOR THE VPT EOS

Component	Water		
	$k_{i,j}$	$l_{i,j}^{0}$	$l_{i,j}^{1} \times 10^{4}$
Methane[+]	0 .5044	1.8302	51.72
Methane*	0.4969	1.8332	58.13
Ethane	0.54421	1.5629	32.227
Propane	0.65117	1.8137	37.709
n-Butane	0.5800	1.6885	33.57
i-Butane	0.5863	1.7863	37.40
n-Pentane	0.5525	1.6188	23.72
Carbon Dioxide[+]	0.19314	0.72280	26.928
Carbon Dioxide[#]	0.16860	0.67136	26.433
Carbon Dioxide[§]	0.19650	0.72320	23.740
Hydrogen Sulphide	0.1382	0.3809	13.24
Nitrogen	0.4788	2.6576	65.102
Methanol	-0.0789	-0.0149	0

[+]for 277.13 < T ≤ 313.11 K *for 273.15 < T ≤ 277.13 K
[#]for 277.13 < T ≤ 304.2 K   [§] Supercritical conditions

TABLE E.2 - BIPS OF WATER FOR VPT EOS AND NDD MIXING RULES

Component	Methanol		
	$k_{i,j}$	$l_{i,j}^{0}$	$l_{i,j}^{1} \times 10^{4}$
Methane	0.2538	0.7319	6.88
Ethane	0.0137	0.0519	21.7
Propane	0.0278	0.0779	0
n-Butane	0.1465	0.2917	0
i-Butane	0.1233	0.3029	17.6
n-Pentane	0.2528	0.7908	58.28
Carbon Dioxide	0.0510	0.0700	11.56
Hydrogen Sulphide	0.0694	0.1133	0
Nitrogen	0.2484	1.0440	7.22
Methanol	-	-	-
Ethanol	-	-	-
Water	-0.0789	0.0835	0

TABLE E.2 - BIPS OF METHANOL FOR VPT EOS AND NDD MIXING RULES

Appendix F: DATA USED FOR THE WATER CONTENT CORRELATION

T /K	P /MPa	γ	Water Content Experimental	Water Content Correlation	AD %	Water Content Bukacek	AD %
ALTHAUS, K (1999) [15]							
288.15	1.000	0.554	1.75E-03	1.75E-03	0.5	1.82E-03	4.2
283.15	1.000	0.554	1.26E-03	1.26E-03	0.1	1.32E-03	4.4
283.15	1.500	0.554	8.51E-04	8.51E-04	0.7	9.11E-04	7.0
283.15	4.000	0.554	3.57E-04	3.57E-04	2.1	3.99E-04	11.9
283.15	6.000	0.554	2.51E-04	2.51E-04	0.0	2.97E-04	18.4
288.15	1.500	0.554	1.18E-03	1.18E-03	0.8	1.25E-03	6.3
288.15	4.000	0.554	4.85E-04	4.85E-04	0.1	5.44E-04	12.2
288.15	6.000	0.554	3.50E-04	3.50E-04	0.8	4.02E-04	14.9
288.15	8.000	0.554	2.84E-04	2.84E-04	1.0	3.31E-04	16.6
288.15	10.000	0.554	2.44E-04	2.44E-04	0.0	2.88E-04	18.2
293.15	4.000	0.554	6.65E-04	6.65E-04	0.3	7.34E-04	10.3
293.15	6.000	0.554	4.70E-04	4.70E-04	0.8	5.39E-04	14.6
293.15	8.000	0.554	3.86E-04	3.86E-04	0.9	4.41E-04	14.3
293.15	10.000	0.554	3.32E-04	3.32E-04	0.4	3.83E-04	15.3
278.15	0.500	0.554	1.75E-03	1.75E-03	1.1	1.82E-03	3.7
278.15	1.500	0.554	6.16E-04	6.16E-04	1.2	6.53E-04	6.0
278.15	4.000	0.554	2.50E-04	2.50E-04	0.4	2.90E-04	16.0
273.15	0.500	0.554	1.23E-03	1.23E-03	0.7	1.28E-03	3.7
273.15	1.500	0.554	4.26E-04	4.26E-04	0.1	4.62E-04	8.5
		NG3					
288.15	1.500	0.628	1.15E-03	1.19E-03	4.0	1.25E-03	9.46
288.15	6.000	0.628	3.26E-04	3.47E-04	6.4	4.02E-04	23.2
288.15	10.000	0.628	2.30E-04	2.46E-04	7.0	2.88E-04	25.5
283.15	1.500	0.628	8.26E-04	8.58E-04	4.0	9.11E-04	10.3
283.15	6.000	0.628	2.33E-04	2.51E-04	7.8	2.97E-04	27.5
278.15	0.500	0.628	1.72E-03	1.78E-03	3.2	1.82E-03	5.5
278.15	1.500	0.628	5.89E-04	6.10E-04	3.5	6.53E-04	10.9
278.15	4.000	0.628	2.27E-04	2.49E-04	9.8	2.90E-04	27.9
		NG1					
288.15	1.500	0.565	1.16E-03	1.19E-03	25	1.25E-03	8.2
288.15	6.000	0.565	3.56E-04	3.46E-04	2.6	4.02E-04	13.0
288.15	10.000	0.565	2.50E-04	2.45E-04	1.8	2.88E-04	15.6
283.15	1.500	0.565	8.42E-04	8.56E-04	1.6	9.11E-04	8.1
283.15	6.000	0.565	2.51E-04	2.50E-04	03	2.97E-04	18.3
278.15	0.500	0.565	1.68E-03	1.77E-03	5.5	1.82E-03	8.2
278.15	1.500	0.565	6.05E-04	6.08E-04	0.5	6.53E-04	8.0
278.15	4.000	0.565	2.58E-04	2.48E-04	4.0	2.90E-04	12.2
278.15	6.000	0.565	1.77E-04	1.79E-04	1.0	2.17E-04	22.8
		NG2					
293.15	6.000	0.598	4.65E-04	4.74E-04	1.8	5.39E-04	15.8
293.15	10.000	0.598	3.26E-04	3.33E-04	2.2	3.83E-04	17.5
288.15	1.500	0.598	1.16E-03	1.19E-03	2.2	1.25E-03	7.7
288.15	4.000	0.598	4.68E-04	4.84E-04	3.5	5.44E-04	16.4
288.15	6.000	0.598	3.56E-04	3.47E-04	2.6	4.02E-04	12.9
288.15	8.000	0.598	2.72E-04	2.82E-04	3.4	3.31E-04	21.6
283.15	1.500	0.598	8.42E-04	8.57E-04	1.8	9.11E-04	8.1
283.15	6.000	0.598	2.51E-04	2.51E-04	0.1	2.97E-04	18.3
278.15	0.500	0.598	1.68E-03	1.77E-03	5.7	1.82E-03	8.2
278.15	1.500	0.598	6.05E-04	6.09E-04	0.7	6.53E-04	8.0
278.15	4.000	0.598	2.58E-04	2.49E-04	3.8	2.90E-04	12.2
278.15	6.000	0.598	1.77E-04	1.79E-04	1.2	2.17E-04	22.8
		NG4					
293.15	6.000	0.633	4.70E-04	4.74E-04	1.0	5.39E-04	14.6
293.15	8.000	0.633	3.62E-04	3.84E-04	6.0	4.41E-04	21.8
288.15	1.500	0.633	1.17E-03	1.19E-03	1.7	1.25E-03	7.1
288.15	4.000	0.633	4.85E-04	4.85E-04	0.0	5.44E-04	12.2
288.15	6.000	0.633	3.48E-04	3.47E-04	0.2	4.02E-04	15.5
283.15	1.500	0.633	8.50E-04	8.59E-04	1.0	9.11E-04	7.2
283.15	4.000	0.633	3.30E-04	3.50E-04	6.1	3.99E-04	21.1
278.15	0.500	0.633	1.71E-03	1.78E-03	3.9	1.82E-03	6.2
278.15	1.500	0.633	5.91E-04	6.10E-04	3.2	6.53E-04	10.5
		NG5					
288.15	1.500	0.667	1.17E-03	1.19E-03	2.1	1.25E-03	7.4

288.15	6.000	0.667	3.35E-04	3.48E-04	3.7	4.02E-04	20.0
288.15	10.000	0.667	2.44E-04	2.46E-04	0.8	2.88E-04	18.1
283.15	1.500	0.667	8.36E-04	8.59E-04	2.8	9.11E-04	8.9
283.15	6.000	0.667	2.37E-04	2.51E-04	6.3	2.97E-04	25.6
278.15	0.500	0.667	1.69E-03	1.78E-03	5.2	1.82E-03	7.4
278.15	1.500	0.667	5.82E-04	6.11E-04	4.9	6.53E-04	12.2
		NG6					
288.15	1.500	0.640	1.16E-03	1.19E-03	2.5	1.25E-03	7.9
288.15	6.000	0.640	3.49E-04	3.48E-04	0.3	4.02E-04	15.3
288.15	10.000	0.640	2.47E-04	2.46E-04	0.5	2.88E-04	16.7
283.15	1.500	0.640	8.55E-04	8.59E-04	0.5	9.11E-04	6.6
283.15	6.000	0.640	2.51E-04	2.51E-04	0.3	2.97E-04	18.5
278.15	0.500	0.640	1.72E-03	1.78E-03	3.1	1.82E-03	5.4
278.15	1.500	0.640	6.03E-04	6.10E-04	1.2	6.53E-04	8.3
278.15	4.000	0.640	2.40E-04	2.49E-04	3.6	2.90E-04	20.6
		NG7					
278.15	0.5	0.811	1.76E-03	1.81E-03	3.0	1.86E-03	5.7
288.15*	4.000	0.569	4.94E-04	4.83E-04	2.1	5.44E-04	10.3
288.15*	6.000	0.569	3.52E-04	3.46E-04	1.6	4.02E-04	14.2
278.15*	1.500	0.569	6.12E-04	6.08E-04	0.6	6.53E-04	6.8

Rigby and Prausnitz (1968) [23]

298.15	2.354	0.554	1.48E-03	1.45E-03	2.3	1.53E-03	3.4
298.15	3.051	0.554	1.18E-03	1.14E-03	3.0	1.23E-03	4.3
298.15	4.055	0.554	9.15E-04	8.86E-04	3.2	9.68E-04	5.8
323.15	2.975	0.554	4.47E-03	4.51E-03	0.9	4.67E-03	4.4
323.15	4.775	0.554	2.92E-03	2.96E-03	1.3	3.11E-03	6.3
323.15	6.728	0.554	2.19E-03	2.22E-03	1.6	2.36E-03	7.8
348.15	3.121	0.554	1.34E-02	1.34E-02	0.1	1.36E-02	1.5
348.15	5.473	0.554	8.03E-03	8.10E-03	0.8	8.29E-03	3.3
348.15	6.727	0.554	6.71E-03	6.78E-03	1.0	6.98E-03	4.0
373.15	5.741	0.554	1.99E-02	2.01E-02	1.0	2.03E-02	2.0
373.15	7.189	0.554	1.64E-02	1.65E-02	0.4	1.68E-02	2.1
373.15	9.347	0.554	1.31E-02	1.31E-02	0.0	1.35E-02	3.1

Yokoama et al. (1988) [17]

298.15	3.000	0.554	1.18E-03	1.16E-03	2.0	1.24E-03	5.3
298.15	5.000	0.554	7.41E-04	7.41E-04	0.0	8.21E-04	10.7
323.15	3.000	0.554	4.48E-03	4.48E-03	0.0	4.64E-03	3.5
323.15	5.000	0.554	2.79E-03	2.84E-03	1.9	2.99E-03	7.2
323.15	8.000	0.554	2.11E-03	1.93E-03	8.3	2.06E-03	2.2

Gillepsie and Wilson (1982) [19]

323.15	1.379	0.554	9.64E-03	9.31E-03	3.4	9.48E-03	1.7
323.15	6.205	0.554	2.45E-03	2.37E-03	3.2	2.51E-03	2.4
323.15	13.790	0.554	1.36E-03	1.32E-03	2.7	1.42E-03	4.1
348.15	1.379	0.554	2.94E-02	2.90E-02	1.1	2.92E-02	0.5
348.15	6.205	0.554	7.10E-03	7.26E-03	2.3	7.46E-03	5.1
348.15	13.790	0.554	3.66E-03	3.81E-03	4.0	4.05E-03	10.5

Kosyakov et al. (1982) [22]

273.16	1.010	0.554	6.47E-04	6.24E-04	3.6	6.60E-04	2.0
273.16	2.030	0.554	3.40E-04	3.21E-04	5.6	3.56E-04	4.8
283.16	2.030	0.554	6.40E-04	6.45E-04	0.7	6.98E-04	9.0
283.16	4.050	0.554	3.46E-04	3.46E-04	0.0	3.96E-04	14.4
283.16	6.080	0.554	2.20E-04	2.49E-04	13.0	2.95E-04	33.9

Olds et al. (1942) [25]

377.59	2.987	0.554	4.28E-02	4.26E-02	0.5	4.27E-02	0.5
377.59	9.316	0.554	1.55E-02	1.53E-02	1.2	1.57E-02	1.8
377.59	6.591	0.554	2.07E-02	2.07E-02	0.1	2.10E-02	1.4
377.59	13.810	0.554	1.12E-02	1.08E-02	3.9	1.16E-02	3.5
344.26	2.672	0.554	1.34E-02	1.31E-02	1.6	1.33E-02	0.1
344.26	6.289	0.554	6.42E-03	6.11E-03	4.9	6.30E-03	1.9
344.26	9.645	0.554	4.50E-03	4.30E-03	4.5	4.49E-03	0.2
310.93	13.485	0.554	6.70E-04	7.43E-04	10.8	8.08E-04	20.5
310.93	13.716	0.554	6.70E-04	7.36E-04	9.8	7.99E-04	19.3

TABLE F.1 – DATA USED FOR THE CORRELATION (eq. 7.34)

T /K	P /MPa	γ	γ Correction	Z_{H2S}^{equi}	Water Content Experimental	Water Content Correlation	AD %
all: *Song and Kobayashi (1989)* [52]
288.71	5.721	1.4681	0.9431	0.710	6.17E-04	5.45E-04	11.6
294.26	6.204	1.4681	0.9430	0.710	8.15E-04	7.34E-04	9.9
300.15	6.204	1.4681	0.9428	0.710	1.02E-03	1.022E-03	0.6
305.15	6.204	1.4681	0.9427	0.710	1.29E-03	1.34E-03	3.6
306.09	6.204	1.4681	0.9427	0.710	1.36E-03	1.40E-03	3.2
307.15	7.582	1.4681	0.9427	0.710	1.33E-03	1.40E-03	5.1
316.15	6.204	1.4681	0.9426	0.710	2.20E-03	2.32E-03	5.8
316.15	7.582	1.4681	0.9426	0.710	2.03E-03	2.18E-03	7.4
323.15	6.204	1.4681	0.9426	0.710	2.99E-03	3.22E-03	7.7
323.15	7.582	1.4681	0.9426	0.710	2.74E-03	3.01E-03	9.7
323.15	13.786	1.4681	0.9426	0.710	3.44E-03	3.29E-03	4.3
316.48	13.786	1.4681	0.9426	0.710	3.13E-03	2.49E-03	20.4
310.93	13.786	1.4681	0.9427	0.710	3.01E-03	1.95E-03	35.1
300.15	6.207	1.4681	0.9428	0.710	1.02E-03	1.022E-03	0.0
305.15	6.207	1.4681	0.9427	0.710	1.30E-03	1.34E-03	3.0
306.09	6.207	1.4681	0.9427	0.710	1.37E-03	1.40E-03	2.6
316.15	6.207	1.4681	0.9426	0.710	2.21E-03	2.32E-03	4.9
323.15	6.207	1.4681	0.9426	0.710	3.02E-03	3.22E-03	6.8
302.73	7.586	1.4681	0.9428	0.710	1.23E-03	1.11E-03	10.0
304.76	7.586	1.4681	0.9427	0.710	1.25E-03	1.24E-03	0.8
307.15	7.586	1.4681	0.9427	0.710	1.34E-03	1.40E-03	4.6
316.15	7.586	1.4681	0.9426	0.710	2.04E-03	2.18E-03	6.6
323.15	7.586	1.4681	0.9426	0.710	2.76E-03	3.01E-03	8.9
323.15	10.345	1.4681	0.9426	0.710	2.97E-03	2.93E-03	1.3
323.15	13.793	1.4681	0.9426	0.710	3.47E-03	3.29E-03	5.0
316.48	13.793	1.4681	0.9426	0.710	3.15E-03	2.49E-03	21.0
all: *Althaus (1999)* [15]
278.50	0.500	0.8107	0.9912	0.188	1.76E-03	1.86E-03	5.7
all: *Engineering Databook Eleventh Edition-SI (1998)* [13]
311.15	13.800	0.6601	0.9975	0.083	8.08E-04	8.22E-04	1.7
344.15	6.900	0.6601	0.9974	0.083	5.67E-03	5.84E-03	3.1
311.15	13.800	0.7470	0.9939	0.150	8.08E-04	8.76E-04	8.4
344.15	6.900	0.7470	0.9936	0.150	5.59E-03	5.99E-03	7.0
327.15	10.300	0.6037	0.9991	0.080	2.21E-03	2.08E-03	6.0
344.15	9.430	0.7251	0.9947	0.275	4.90E-03	5.19E-03	5.8
344.15	6.900	0.6597	0.9974	0.170	5.79E-03	6.06E-03	4.7
311.15	7.600	1.1954	0.9630	0.550	1.61E-03	1.53E-03	5.6
323.15	13.800	1.4681	0.9426	0.710	3.27E-03	3.29E-03	0.6
all: *Ng et al. (2001)* [53]
322.04	1.379	0.8101	0.9905	0.203	1.11E-02	8.93E-03	19.4
322.04	10.342	0.8101	0.9905	0.203	2.23E-03	1.77E-03	20.4
366.48	1.379	0.8101	0.9898	0.203	5.93E-02	5.85E-02	1.4
366.48	10.342	0.8101	0.9898	0.203	1.12E-02	1.08E-02	3.5
322.04	1.379	1.1011	0.9700	0.488	1.15E-02	9.06E-03	21.3
322.04	10.342	1.1011	0.9700	0.488	2.58E-03	2.23E-03	13.6
366.48	1.379	1.1011	0.9684	0.488	6.40E-02	5.64E-02	11.8
366.48	10.342	1.1011	0.9684	0.488	1.27E-02	1.26E-02	0.9
322.04	1.379	1.3921	0.9477	0.772	1.16E-02	9.17E-03	20.7
366.48	1.379	1.3921	0.9475	0.772	5.99E-02	5.45E-02	9.1
366.48	10.342	1.3921	0.9475	0.772	1.52E-02	1.52E-02	0.5
366.48	1.379	1.0497	0.9725	0.525	6.50E-02	5.66E-02	13.0
366.48	10.342	1.0497	0.9725	0.525	1.27E-02	1.30E-02	1.8
322.04	1.379	1.3107	0.9536	0.831	1.31E-02	9.30E-03	28.8
366.48	1.379	1.3107	0.9526	0.831	6.14E-02	5.46E-02	11.0
366.48	10.342	1.3107	0.9526	0.831	1.54E-02	1.61E-02	5.0
322.04	1.379	0.7673	0.9928	0.234	8.17E-03	8.99E-03	10.1
322.04	10.342	0.7673	0.9928	0.234	1.73E-03	1.82E-03	5.3
322.04	27.579	0.7673	0.9928	0.234	1.57E-03	1.64E-03	4.8
366.48	1.379	0.7673	0.9923	0.234	5.97E-02	5.85E-02	1.9
366.48	10.342	0.7673	0.9923	0.234	1.04E-02	1.10E-02	5.3
322.04	10.342	0.9983	0.9779	0.563	2.68E-03	2.43E-03	9.4
366.48	1.379	0.9983	0.9765	0.563	6.33E-02	5.67E-02	10.4
366.48	10.342	0.9983	0.9765	0.563	1.43E-02	1.34E-02	6.7
322.04	1.379	1.2293	0.9599	0.891	9.44E-03	9.44E-03	0.0
366.48	1.379	1.2293	0.9585	0.891	6.27E-02	5.48E-02	12.6

366.48	10.342	1.2293	0.9585	0.891	1.91E-02	1.71E-02	10.3
322.04	1.379	0.7608	0.9931	0.203	8.74E-03	8.96E-03	2.5
322.04	10.342	0.7608	0.9931	0.203	1.87E-03	1.78E-03	5.1
322.04	20.684	0.7608	0.9931	0.203	1.65E-03	1.45E-03	11.8
322.04	34.474	0.7608	0.9931	0.203	1.46E-03	1.76E-03	20.0
366.48	10.342	0.7608	0.9926	0.203	1.05E-02	1.08E-02	2.7
366.48	20.684	0.7608	0.9926	0.203	6.11E-03	7.33E-03	19.9
322.04	1.379	0.7180	0.9952	0.234	9.37E-03	9.01E-03	3.8
322.04	10.342	0.7180	0.9952	0.234	1.81E-03	1.82E-03	0.5
322.04	20.684	0.7180	0.9952	0.234	1.76E-03	1.53E-03	12.9

Lukacs and Robinson (1963) [50]

344.26	9.618	0.6535	0.9976	0.160	4.75E-03	4.80E-03	1.1
344.26	6.964	0.6597	0.9974	0.170	6.16E-03	6.05E-03	1.8
344.26	4.213	0.6722	0.9969	0.190	9.30E-03	9.05E-03	2.7
344.26	2.468	0.6846	0.9964	0.210	1.50E-02	1.44E-02	3.7
344.26	9.598	0.7251	0.9947	0.275	5.20E-03	5.16E-03	0.8
344.26	6.378	0.7344	0.9942	0.290	6.90E-03	6.75E-03	2.1

McKetta and Katz (1948) [11]

310.93	20.657	0.9425	0.9823	0.000	6.50E-04	6.60E-04	1.6
310.93	20.657	1.8765	0.9273	0.000	6.39E-04	6.23E-04	2.4
310.93	13.776	0.9447	0.9821	0.000	8.04E-04	7.42E-04	7.8
344.26	20.808	1.0914	0.9699	0.000	2.74E-03	2.63E-03	4.1
344.26	14.120	1.0911	0.9699	0.000	3.28E-03	3.26E-03	0.6
344.26	20.326	0.8517	0.9876	0.000	2.70E-03	2.71E-03	0.2
344.26	13.707	0.8445	0.9880	0.000	3.39E-03	3.38E-03	0.2
344.26	20.670	1.7299	0.9344	0.000	2.54E-03	2.54E-03	0.0
344.26	13.721	1.7344	0.9343	0.000	3.16E-03	3.20E-03	1.2
377.59	20.670	1.2926	0.9537	0.000	7.95E-03	7.89E-03	0.7
377.59	13.783	1.2882	0.9540	0.000	1.06E-02	1.09E-02	2.9
377.59	20.657	1.8747	0.9485	0.000	7.18E-03	7.85E-03	9.4

TABLE F.2 - WATER CONTENT PREDICTION FOR ACID GASES (eq. 7.34)

Appendix G: ARTIFICIAL NEURAL NETWORK FOR GAS HYDRATE

PREDICTIONS

The purpose of this annex is to propose the use of a neural network model for predicting hydrate formation conditions for various pure gases, gas mixtures, and different inhibitors and salts. Such an approach has already attended by *Elgibaly and Elkamel* in 1998 [326]. To have the most accurate results they used network with 16 input variables (*T*, gas composition, inhibitor composition….), 50 neurons in the hidden layer and one output (*P*). Their model correlated the experimental data (2389 data) with an average error of 19 %.

It is chosen to use a similar approach. However the number of input variables and their choice is different, a single hidden network with 19 input variables is chosen and 35 neurons in the hidden layer:
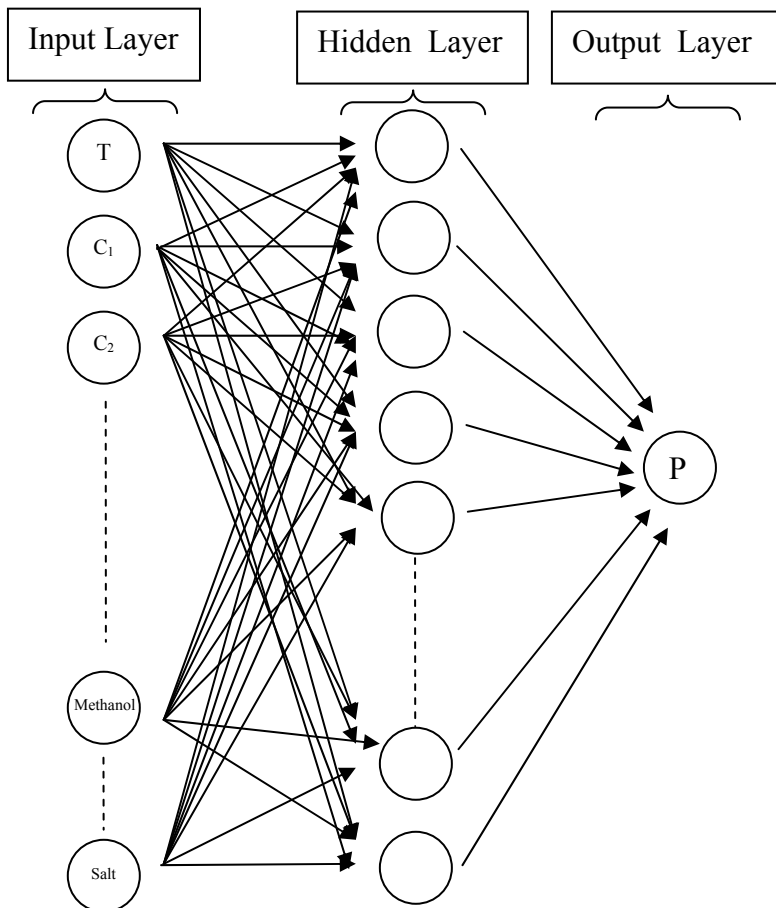
1- T: temperature (between 240 K up to 303 K)
2- Choice of structure I or II

Gas Feed
3- Methane composition (from 0 to 100 %)
4- Ethane composition (from 0 to 100 %)
5- Propane composition (from 0 to 100 %)
6- i-Butane composition (from 0 to 100 %)
7- n-Butane composition (from 0 to 40 %)
8- i-Pentane composition (from 0 to 20 %)
9- n-Pentane composition (from 0 to 10 %)
10- C6+ composition (from 0 to 3 %)
11- Carbon dioxide composition (from 0 to 100 %)
12- Hydrogen sulphide composition (from 0 to 100 %)
13- Nitrogen composition (from 0 to 100 %)

Liquid Feed
14- Methanol composition (from 0 to 51 % mole fraction)
15- Ethanol composition (from 0 to 66 % mole fraction)
16- Ethylene glycol composition (from 0 to 25 % mole fraction)
17- Diethylene glycol composition (from 0 to 10 % mole fraction)
18- Triethylene glycol composition (from 0 to 15 % mole fraction)
19- Salt composition (from 0 to 10 % mass in the liquid)

The model was trained using 3296 data gathered from the literature. The model correlated the experimental data with an average error of 4 %. The predictions are compared to existing correlations and also to real experimental data (independent from the tuned data). The neural network model enables the user to accurately predict hydrate formation conditions for a given gas mixture (TABLE G.1). A good accuracy is even obtained for high concentration of thermodynamic inhibitors (Figure G.3 and Figure G.4)
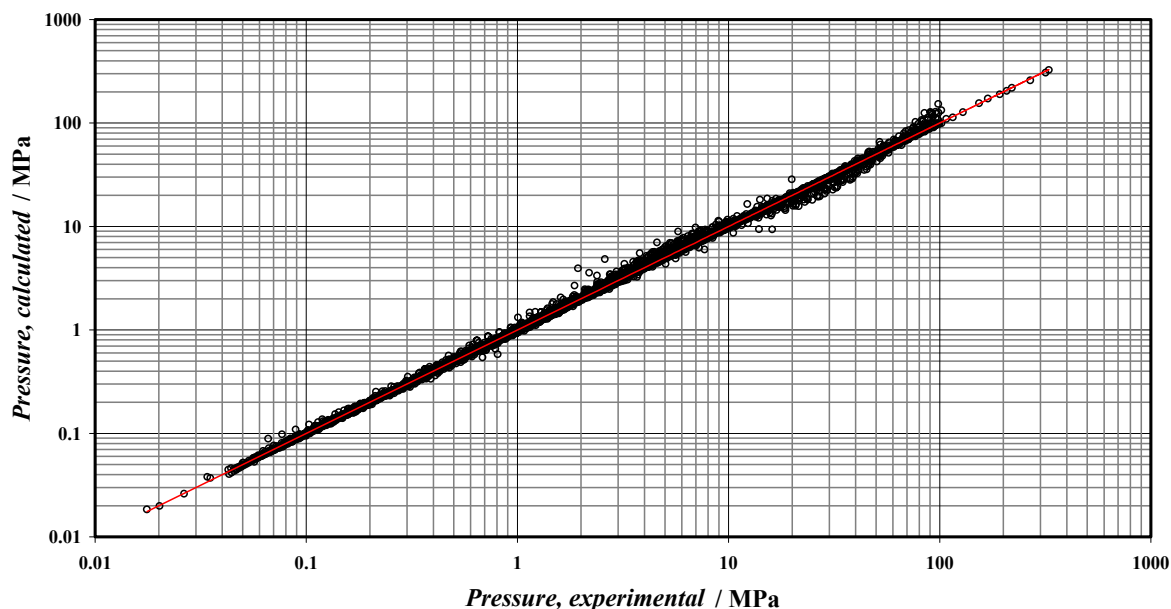

Figure G.1: Comparison between experimental and calculated hydrate dissociation pressures.
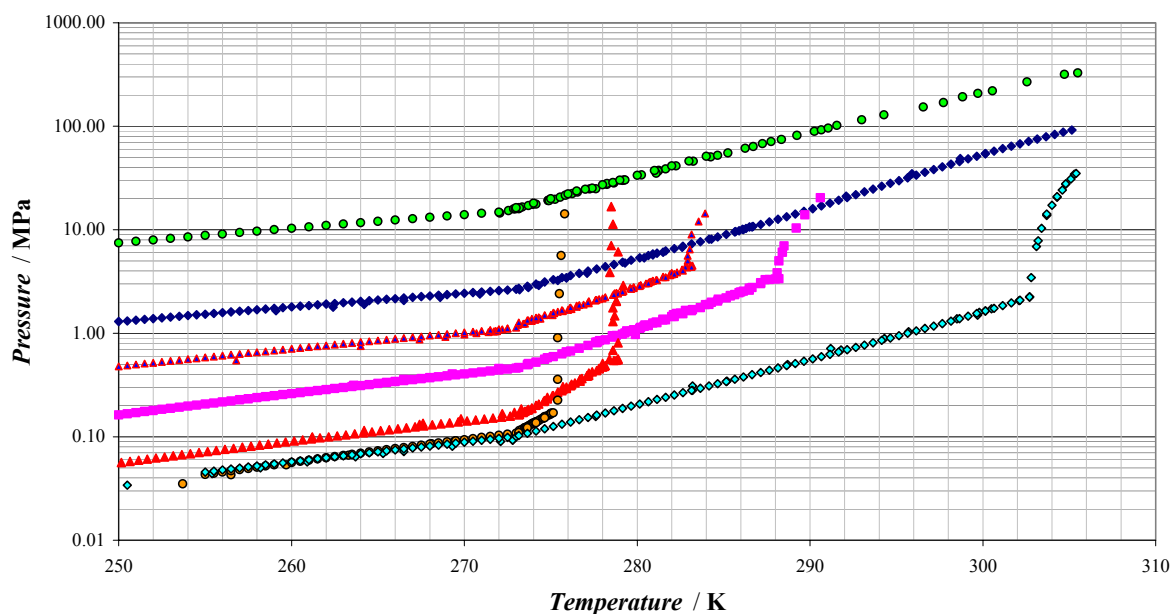
Figure G.2: Pure compound hydrate dissociation pressure (from top to bottom: nitrogen, methane, ethane, propane, carbon dioxide, hydrogen sulphide (light blue) and i-butane (orange))
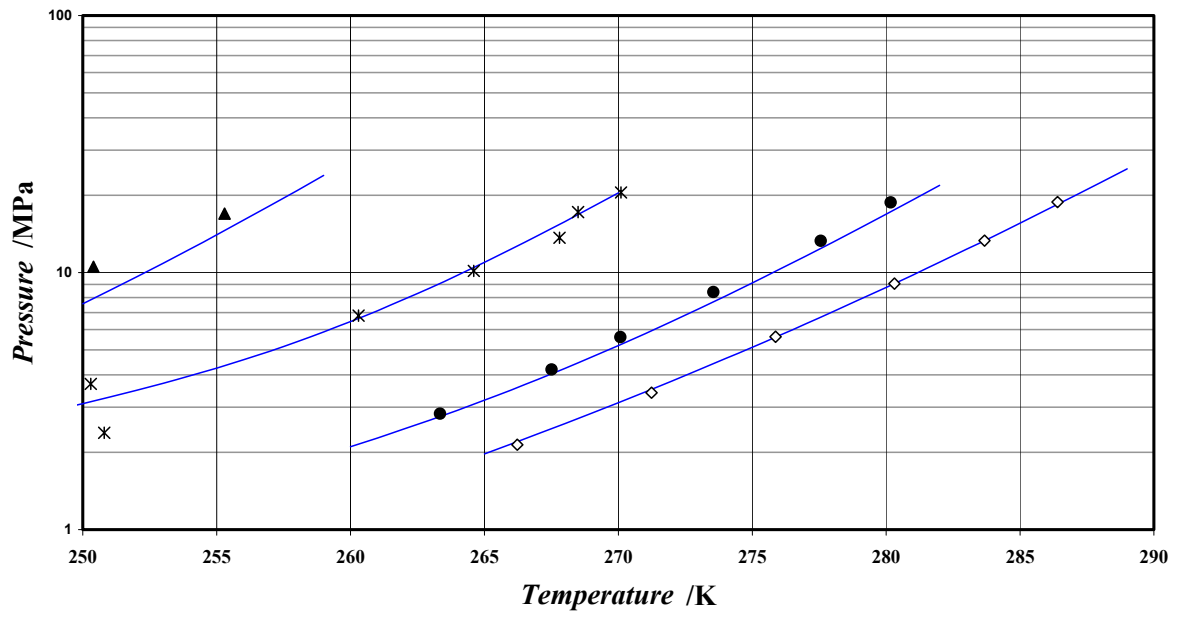
Figure G.3: Methane hydrate dissociation pressure in presence of methanol: ◇, 10 wt. % [184]; ● 20 wt. % [184];✱ 35 wt. % [185];▲ 50 wt. % [185].
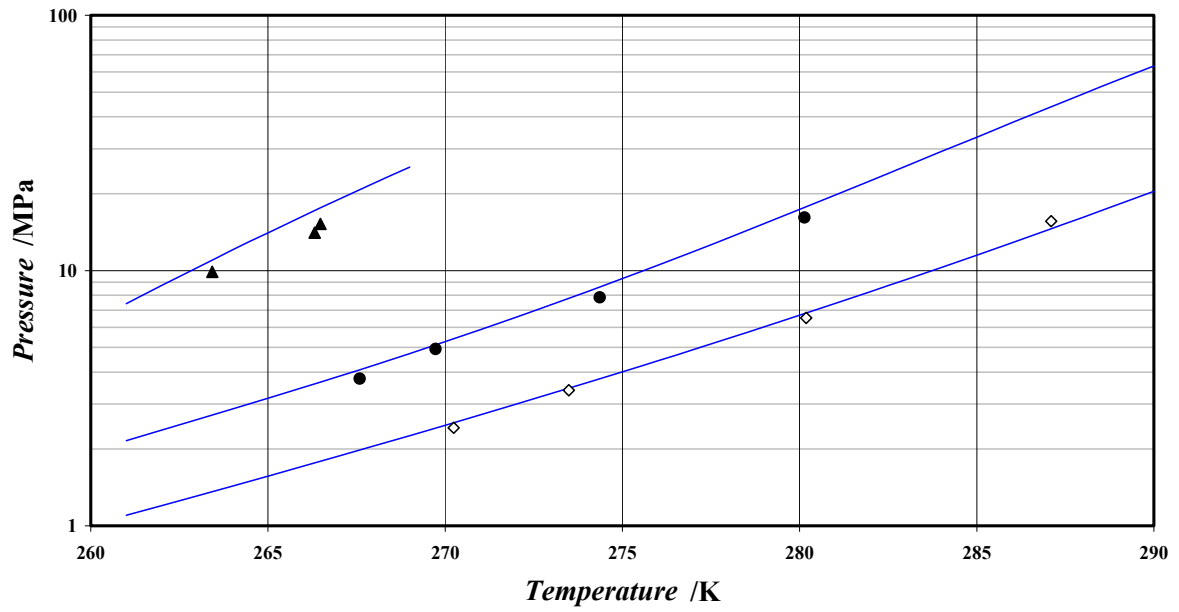

Figure G.4: Methane hydrate dissociation pressure in presence of ethylene glycol: ◇, 10 wt. % [185]; ● 30 wt. % [185]; ▲ 50 wt. % [185].

T / K	Mol %CH$_4$	P$_{exp}$ /MPa	P$_{cal}$ /MPa	Deviation %
Methane - ethane from [160]				
283.9	1.6	1.81	1.82	-0.6
285.7	1.6	2.31	2.42	-4.8
286.6	1.6	2.71	2.83	-4.4
287.8	1.6	3.08	3.51	-14
279.4	4.7	0.99	0.98	1.0
281.5	4.7	1.34	1.27	5.2
283.3	4.7	1.71	1.64	4.1
285.3	4.7	2.17	2.22	-2.3
286.4	4.7	2.51	2.66	-6.0
287.6	4.7	2.99	3.29	-10
281.6	17.7	1.42	1.34	5.6
283.3	17.7	1.77	1.68	5.1
284.8	17.7	2.14	2.08	2.8
286.2	17.7	2.66	2.57	3.4
287.0	17.7	3.00	2.92	2.7
Methane - propane from [155]				
274.8	36.2	0.272	0.28	-2.9
277.6	36.2	0.436	0.42	3.7
280.4	36.2	0.687	0.65	5.4

TABLE G.1 – EXPERIMENTAL AND CALCULATED HYDRATE DISSOCIATION PRESSURES
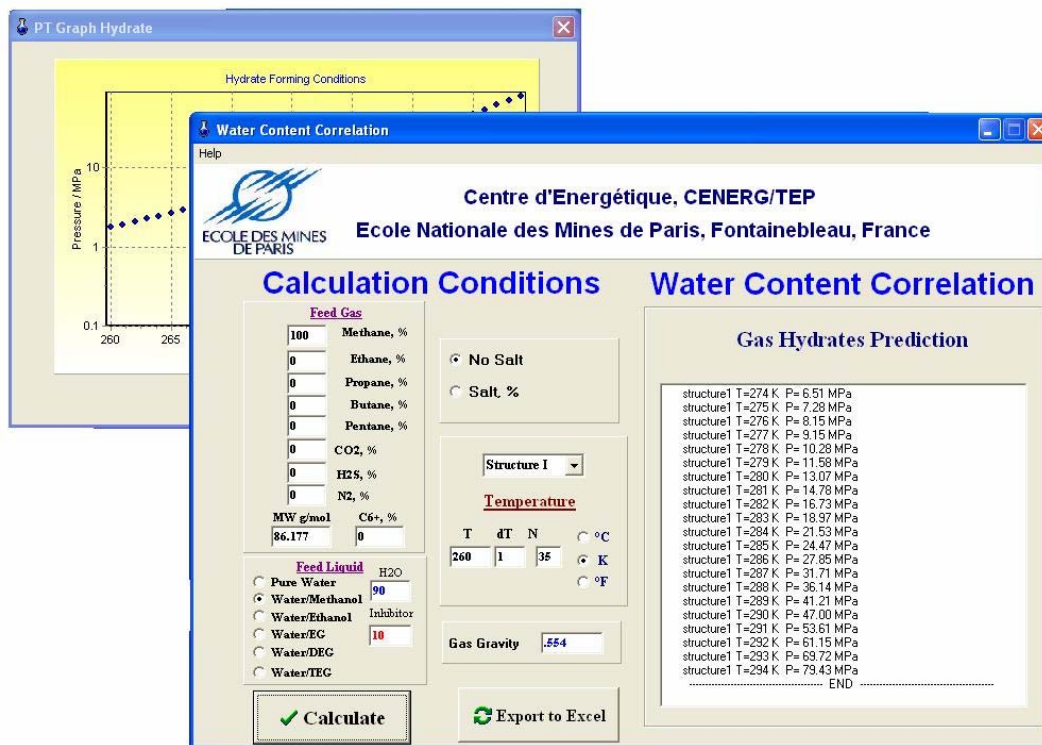
ETUDE DES EQUILIBRES EAU, HYDROCARBURES ET GAZ ACIDES DANS LE CADRE DES SYSTEMES DE PRODUCTION DE GAZ

Résumé

Dans les gisements, en cours de production ou dans les conduites de transport, les gaz naturels se trouvent fréquemment au contact d'une phase aqueuse. Les conditions sont telles que les pressions peuvent atteindre de très haute valeur dans une large gamme de températures. La connaissance du comportement des systèmes "eau-hydrocarbures" est donc essentielle à la profession profession pétrolière ainsi que celles des systèmes "eau-hydrocarbures-inhibiteur thermodynamique " pour lesquelles les données sont rares.

Des mesures de teneur en eau ont été réalisées dans les phases vapeurs de différents systèmes d'hydrocarbures: méthane et éthane, et dans un mélange d'hydrocarbures gazeux (méthane 94%, éthane 4%, n-butane 2%) dans des conditions proches de la formation d'hydrates (de 258.15 à 313.15 K et jusqu'à 34.5 MPa) en présence ou non d'inhibiteurs tels que le méthanol ou l'éthylène glycol. Des mesures de solubilités de gaz des principaux constituants du gaz naturel ont été effectuées dans une large gamme de pressions et de températures. Ces mesures ont été effectuées avec deux techniques expérimentales, une technique statique-analytique avec échantillonnage de phases et une technique synthétique avec cellule à volume variable.

Pour réaliser le traitement des données un logiciel a été développé, ce logiciel a permis l'ajustement et le traitement des résultats expérimentaux.

Mots clés: *Equilibres Vapeur-liquide, hydrate, méthane, éthane, propane, n-butane, eau, dioxyde de carbone, sulfure d'hydrogène, azote modélisation, teneur en eau, solubilité de gaz.*

PHASE BEHAVIOUR IN WATER/HYDROCARBON SYSTEMS IN GAS PRODUCTION SYSTEM

Abstract

Inside wells, natural gases frequently coexist with water. The gases are in equilibrium with the sub-adjacent aquifer. Many problems are associated with the presence of water during the production, transport and processing of natural gases. Accurate knowledge of the thermodynamic properties of the water/hydrocarbon and water-inhibitor/hydrocarbon equilibria near the hydrate forming conditions, at sub-sea pipeline conditions and during the transport is crucial for the petroleum industry.

An apparatus based on a static–analytic method combined with a dilutor apparatus to calibrate the gas chromatograph (GC) detectors with water was used to measure the water content of binary systems (i.e.: water –methane, ethane- water, nitrogen –water…) as well of a synthetic hydrocarbon gas mixture (i.e.: 94% methane, 4% ethane and 2% n-butane) with and without inhibitor. This same apparatus was also used generate data of methane, ethane, propane, n-butane and nitrogen solubility in water and also the solubilities of a synthetic mixture in water.

In-house software has been developed in order to fit and model the experimental data.

Keywords: *Vapour-liquid Equilibria, gas hydrate, water, methane, ethane, propane, n-butane, carbon dioxide, hydrogen sulphide, nitrogen, modelling, water content, gas solubilities.*